

LEACHING OF CATIONS DURING DISPLACEMENT BY ACID  
SOLUTIONS THROUGH COLUMNS OF CECIL SOIL

BY

KO-HUI LIU

A DISSERTATION PRESENTED TO THE GRADUATE SCHOOL  
OF THE UNIVERSITY OF FLORIDA IN  
PARTIAL FULFILLMENT OF THE REQUIREMENTS  
FOR THE DEGREE OF DOCTOR OF PHILOSOPHY

UNIVERSITY OF FLORIDA

1987

To My Parents

## ACKNOWLEDGEMENT

The author wishes to express her sincere appreciation to Dr. R. S. Mansell, chairman of the graduate supervisory committee, for guidance, valuable discussions, and suggestions throughout her entire course of study.

Sincere appreciations are also extended to Drs. E. A. Hanlon, C. C. Hsu, W. W. McFee, and R. D. Rhue for their valuable discussions and helpful suggestions made during this work and their review of the manuscript.

Special appreciation is expressed to Dr. S. A. Bloom, Scientific Programmer, for assistance and counsel in plotting graphs, to Dr. C. C. Hsu for generously lending the LSODE subroutine and to a friend, Mr. Fang-Yin Lee, for providing x-ray analyses for each of the soil samples.

This research was supported in part by the U.S. Environmental Protection Agency under Project A0457-06, entitled "Effects of Acid Deposition on Ion Mobilities in Selected Soils". Partial support by the Soil Science Department is also greatly appreciated.

Deepest gratitude is expressed to the author's parents for their support and to her husband Ming-Hsiung for his understanding, consideration, and encouragement.

## TABLE OF CONTENTS

	Page
ACKNOWLEDGEMENTS.....	iii
LIST OF TABLES.....	vii
LIST OF FIGURES.....	x
ABSTRACT.....	xv
 CHAPTER	
I     INTRODUCTION .....	1
Description of Problem .....	1
Hypotheses .....	2
Objectives .....	3
 II    MODEL SIMULATIONS OF BINARY CATION EXCHANGE AND TRANSPORT IN COLUMNS OF CECIL SOIL.....	5
Introduction .....	5
Theory .....	9
Transport Equation .....	9
Equation for Instantaneous Cation Exchange .....	11
Transport with Ion Exchange .....	15
A Galerkin Finite-Element Numerical Method...	18
Finite-Element Method .....	18
Interpolation Function .....	19
Method of Weighted Residuals .....	23
Computational Methods .....	25
Material and Methods .....	28
Soil .....	28
Column Experiment .....	31
Cation Exchange Isotherms from Soil Columns .....	34
Results and Discussion .....	34
Soil Properties .....	34
Verification of the Numerical Model .....	36
Exchange Isotherm Curves for Columns of Cecil Soil .....	38
Exchange Selectivity Coefficients (Ks) for Soil Columns .....	43
Model Sensitivity Analysis .....	46
Conclusions .....	73

III	CATION LEACHING DURING CONTINUOUS DISPLACEMENT BY AQUEOUS HYDROCHLORIC ACID SOLUTION THROUGH COLUMNS OF CECIL SOIL .....	75
	Introduction .....	75
	Basic Theory .....	77
	Surfaces of Soil Particles .....	77
	Cation Exchange Equilibria .....	78
	Effects of Acidification .....	79
	Materials and Methods .....	80
	Physical and Chemical Properties of Soil...	80
	X-Ray Diffraction .....	81
	Column Preparation and Displacement Procedure .....	82
	Dissection of Soil Columns, Extraction, and Chemical Analysis .....	83
	Results and Discussion .....	85
	Concentrations and pH of Column Effluent ..	87
	Concentrations of Cations in Solution and Exchange Phases .....	101
	Estimated Selectivity Coefficients of Ion Pairs .....	106
	Charge Balance of Major Cations for Topsoil and Subsoil .....	114
	Conclusions.....	119
IV	CATION LEACHING DURING CONTINUOUS DISPLACEMENT BY HYDROCHLORIC ACID SOLUTION THROUGH COLUMNS OF CHEMICALLY-PRETREATED CECIL SOIL .....	123
	Introduction .....	123
	Cation Exchange Reaction .....	124
	Saturation Mechanisms for Soil Exchange Sites with a Single Cation Species .....	124
	Mechanisms of $H^+$ Replacement of Exchangeable Cations on Soil Exchange Sites .....	126
	Materials and Methods .....	128
	Preparation of Pretreated Soil .....	128
	Soil Column Preparation and Procedure for Displacing HCl Solutions through Columns.	130
	Method for Dissection, Extraction and Chemical Analysis of Soil Columns .....	132
	Results and Discussion .....	133
	Exchange Sites for Chemically Pretreated Soil .....	138
	Effluent pH for Treated Soil Columns.....	138
	Cation Concentrations in Effluent from Treated Soil Columns .....	139
	Cation Concentrations in Effluent from Chemically Pretreated Mixed Soil Columns.	154
	Concentrations of $Al^{3+}$ in Effluent from Mixed Soil Columns .....	165
	Concentrations of Cations in Solution and	

	Exchange Phases for Treated and Mixed Soil Columns after Application of 25 Pore Volumes of HCl Solution .....	165
	Charge Balance Using All Major Cations for Treated and Mixed Soil Columns .....	190
	Conclusions .....	203
V	SUMMARY AND CONCLUSIONS .....	206
	Summary .....	206
	Conclusions .....	212
	REFERENCES .....	215
	BIOGRAPHICAL SKETCH .....	221

## LIST OF TABLES

Table	Page
2-1 Soil parameters used in column experiments .....	35
2-2 Properties of Cecil topsoil and subsoil .....	35
2-3 Concentrations of cations in solution and exchange phases for topsoil after miscible displacement with 4.5 pore volumes .....	44
2-4 Concentrations of cations in solution and exchange phases for subsoil after miscible displacement with 3.6 pore volumes .....	45
3-1 Physical and chemical parameters for Cecil topsoil and subsoil columns .....	85
3-2 Initial concentrations of exchangeable cations, pH, and CEC for Cecil topsoil and subsoil .....	86
3-3 Concentrations of cations in solution and exchange phases for topsoil after leaching with pH 3.9 solution .....	102
3-4 Concentrations of cations in solution and exchange phases for topsoil after leaching with pH 4.9 solution .....	103
3-5 Concentrations of cations in solution and exchange phases for subsoil after leaching with pH 3.9 HCl solution .....	104
3-6 Concentrations of cations in solution and exchange phases for subsoil after leaching with pH 4.9 HCl solution .....	105
3-7 Topsoil selectivity coefficients as determined after leaching with pH 3.9 HCl solution .....	108
3-8 Topsoil selectivity coefficients as determined after leaching with pH 4.9 HCl solution .....	109
3-9 Subsoil selectivity coefficients as determined after leaching with pH 3.9 HCl solution .....	110
3-10 Subsoil selectivity coefficients as determined	

	after leaching with pH 4.9 HCl solution .....	111
3-11	Mass balance of cations for columns of topsoil ...	117
3-12	Mass balance of cations for columns of subsoil ...	118
4-1	Concentrations of exchangeable cations for nontreated topsoil and subsoil .....	134
4-2	Soil parameters for chemically pretreated topsoil columns after leaching with HCl solutions .....	134
4-3	Soil parameters for chemically pretreated subsoil columns after leaching with HCl solutions .....	135
4-4	Soil parameters for mixed soil columns after leaching with HCl solutions .....	136
4-5	Concentrations of exchangeable cations for pretreated and mixed topsoil and subsoil .....	137
4-6	Concentrations of cations in solution and exchange phases for K-subsoil after leaching with pH 3.9 HCl solution .....	168
4-7	Concentrations of cations in solution and exchange phases for K-subsoil after leaching with pH 4.9 HCl solution .....	169
4-8	Concentrations of cations in solution and exchange phases for Ca-subsoil after leaching with pH 3.9 HCl solution .....	171
4-9	Concentrations of cations in solution and exchange phases for Ca-subsoil after leaching with pH 4.9 HCl solution .....	172
4-10	Concentrations of cations in solution and exchange phases for Mg-subsoil after leaching with pH 3.9 HCl solution .....	174
4-11	Concentrations of cations in solution and exchange phases for Mg-subsoil after leaching with pH 4.9 HCl solution .....	175
4-12	Concentrations of cations in solution and exchange phases for Ca-topsoil after leaching with pH 3.9 HCl solution .....	177
4-13	Concentrations of cations in solution and exchange phases for Ca-topsoil after leaching with pH 4.9 HCl solution .....	178
4-14	Concentrations of cations in solution and	

	exchange phases for K-topsoil after leaching with pH 3.9 HCl solution.....	180
4-15	Concentrations of cations in solution and exchange phases for K-topsoil after leaching with pH 4.9 HCl solution.....	181
4-16	Concentrations of cations in solution and exchange phases for Mg-topsoil after leaching with pH 3.9 HCl solution.....	183
4-17	Concentrations of cations in solution and exchange phases for Mg-topsoil after leaching with pH 4.9 HCl solution.....	184
4-18	Concentrations of cations in solution and exchange phases for mixed-cation subsoil after leaching with pH 3.9 HCl solution.....	186
4-19	Concentrations of cations in solution and exchange phases for mixed-cation subsoil after leaching with pH 4.9 HCl solution.....	187
4-20	Concentrations of cations in solution and exchange phases for mixed-cation topsoil after leaching with pH 3.9 HCl solution.....	188
4-21	Concentrations of cations in solution and exchange phases for mixed-cation topsoil after leaching with pH 4.9 HCl solution.....	189
4-22	Charge balance of cations for columns of Ca-topsoil.....	191
4-23	Charge balance of cations for columns of K-topsoil.....	192
4-24	Charge balance of cations for columns of Mg-topsoil.....	193
4-25	Charge balance of cations for columns of Ca-subsoil.....	194
4-26	Charge balance of cations for columns of K-subsoil.....	195
4-27	Charge balance of cations for columns of Mg-subsoil.....	196
4-28	Charge balance of cations for columns of mixed-cation subsoil.....	201
4-29	Charge balance of cations for columns of mixed-cation topsoil.....	202

## LIST OF FIGURES

Figure		Page
2-1	Numerical and analytical solutions obtained using topsoil parameters for the case where the binary exchange selectivity coefficient equals zero .....	39
2-2	Numerical and analytical solutions obtained using topsoil parameters for the case where the exchange selectivity coefficient equals unity..	40
2-3	Mg <sup>2+</sup> exchange isotherm curve obtained from the topsoil column after miscible displacement with 4.5 pore volumes.....	41
2-4	Mg <sup>2+</sup> exchange isotherm curve obtained from the subsoil column after miscible displacement with 3.6 pore volumes.....	42
2-5	Experimental distributions of Mg <sup>2+</sup> concentrations in the solution phase of the topsoil column after miscible displacement with 4.5 pore volumes, along with calculated results obtained using three values for the dispersion coefficient.....	47
2-6	Experimental distributions of Mg <sup>2+</sup> concentrations in the solution phase of the subsoil column after miscible displacement with 3.6 pore volumes, along with calculated results obtained using three values for the dispersion coefficient.....	48
2-7	Experimental distributions of Mg <sup>2+</sup> concentrations in the solution phase of the topsoil column after miscible displacement with 4.5 pore volumes, along with calculated results obtained using three values for volumetric water content.....	50
2-8	Experimental distributions of Mg <sup>2+</sup> concentrations in the solution phase of the subsoil column after miscible displacement with 3.6 pore volumes, along with calculated results obtained using three values for the volumetric water content.....	51
2-9	Experimental and simulated distributions of Mg <sup>2+</sup> concentrations for three values of bulk density for the topsoil column after miscible displacement with 4.5 pore volumes.....	53

2-10	Experimental and simulated distributions of $Mg^{2+}$ concentrations for three values of bulk density for the subsoil column after miscible displacement with 3.6 pore volumes.....	54
2-11	Experimental distributions of $Mg^{2+}$ concentrations for the topsoil column after miscible displacement with 4.5 pore volumes, along with simulation results for three values of the selectivity coefficient .....	56
2-12	Experimental distributions of $Mg^{2+}$ concentrations for the subsoil column after miscible displacement with 3.6 pore volumes, along with simulated results for three values of the selectivity coefficient .....	57
2-13	Experimental distributions of $Mg^{2+}$ concentrations for the topsoil column after miscible displacement with 4.5 pore volumes, along with simulation results for two values of the cation exchange capacity .....	59
2-14	Experimental distributions of $Mg^{2+}$ concentrations for the subsoil column after miscible displacement with 3.6 pore volumes, along with simulation results for two values of the cation exchange capacity .....	60
2-15	Calculated and experimental distributions of $Mg^{2+}$ concentrations in the solution phase for the subsoil column after miscible displacement with 3.6 pore volumes .....	63
2-16	Calculated and experimental distributions of $Mg^{2+}$ concentrations in the exchange phase for the subsoil column after miscible displacement with 3.6 pore volumes.....	64
2-17	Calculated and experimental distributions of $Mg^{2+}$ concentrations in the solution phase for the topsoil column after miscible displacement with 4.5 pore volumes .....	65
2-18	Calculated and experimental distributions of $Mg^{2+}$ concentrations in the exchange phase for the topsoil column after miscible displacement with 4.5 pore volumes.....	66
2-19	Calculated and experimental distributions of $Mg^{2+}$ concentrations in the solution phase for the topsoil column after miscible displacement with 4.5 pore volumes.....	68
2-20	Calculated and experimental distributions of $Mg^{2+}$ concentrations in the exchange phase for the topsoil column after miscible displacement with 4.5 pore volumes .....	69

2-21	Simulation results and experimental data for distributions of $Mg^{2+}$ concentrations in the solution phase for the subsoil column after miscible displacement with 3.6 pore volumes.....	70
2-22	Simulation results and experimental data for distributions of $Mg^{2+}$ concentrations in the exchange phase for the subsoil column after miscible displacement with 3.6 pore volumes.....	71
2-23	Effluent pH values for the topsoil and subsoil columns .....	72
3-1	Breakthrough curves for pH in the effluent from Cecil topsoil columns which had received two input HCl solutions with different values of pH.....	88
3-2	Breakthrough curves for cation concentrations in the effluent from Cecil topsoil columns which had received pH 3.9 input HCl solution.....	89
3-3	The effect of input solution pH upon the breakthrough curves of $K^+$ from Cecil topsoil columns....	91
3-4	The effect of input solution pH upon the breakthrough curves of summed concentrations of $Ca^{2+}$ , $Mg^{2+}$ , $K^+$ , and $Na^+$ in effluent from topsoil columns.	92
3-5	The effect of input solution pH upon the breakthrough curves of $Al^{3+}$ from Cecil topsoil columns.....	93
3-6	Breakthrough curves for pH in the effluent from Cecil subsoil columns which received two input HCl solutions with different values of pH.....	94
3-7	Breakthrough curves for cations in the effluent from Cecil subsoil columns which received pH 4.9 input HCl solution.....	96
3-8	The effect of input solution pH upon the breakthrough curves of $Ca^{2+}$ from Cecil subsoil columns .	97
3-9	The effect of input solution pH upon the breakthrough curves of summed concentrations of $Ca^{2+}$ , $Mg^{2+}$ , $K^+$ , and $Na^+$ in effluent from subsoil columns.	98
3-10	The effect of input solution pH upon the breakthrough curves of $Al^{3+}$ from Cecil subsoil columns .	99
4-1	Breakthrough curves for pH in the effluent from Ca-topsoil columns which received input HCl	

	solutions with two different pH values .....	140
4-2	Breakthrough curves for pH in the effluent from Ca-subsoil columns which received input HCl solutions with two different pH values.....	141
4-3	Breakthrough curves of $K^+$ from K-topsoil columns which received input HCl solutions with two different pH values .....	144
4-4	Breakthrough curves of $Ca^{2+}$ from Ca-topsoil columns which received input HCl solutions with two different pH values.....	145
4-5	Breakthrough curves of $Mg^{2+}$ from Mg-topsoil columns which received input HCl solutions with two different pH values .....	146
4-6	Breakthrough curves of $K^+$ from K-subsoil columns which received input HCl solutions with two different pH values .....	147
4-7	Breakthrough curves of $Ca^{2+}$ from Ca-subsoil columns which received input HCl solutions with two different pH values .....	148
4-8	Breakthrough curves of $Mg^{2+}$ from Mg-subsoil columns which received input HCl solutions with two different pH values .....	149
4-9	Breakthrough curves of $Al^{3+}$ from K-subsoil columns which received input HCl solutions with two different pH values .....	151
4-10	Breakthrough curves of $Al^{3+}$ from Ca-subsoil columns which received input HCl solutions with two different pH values .....	152
4-11	Breakthrough curves of $Al^{3+}$ from Mg-subsoil columns which received input HCl solutions with two different pH values .....	153
4-12	Breakthrough curves of $Al^{3+}$ from K-topsoil columns which received input HCl solutions with two different pH values .....	155
4-13	Breakthrough curves of $Al^{3+}$ from Ca-topsoil columns which received input HCl solutions with two different pH values .....	156
4-14	Breakthrough curves of $Al^{3+}$ from Mg-topsoil columns which received input HCl solutions with two different pH values .....	157

4-15	Breakthrough curves of cations in the effluent from a mixed-cation topsoil column which received pH 3.9 input HCl solution .....	158
4-16	Breakthrough curves of cations in the effluent from a mixed-cation subsoil column which received pH 3.9 input HCl solution .....	159
4-17	Breakthrough curves of $K^+$ from mixed-cation topsoil columns which received input HCl solutions with two different pH values .....	161
4-18	Breakthrough curves of $Ca^{2+}$ from mixed-cation topsoil columns which received input HCl solutions with two different pH values .....	162
4-19	Breakthrough curves of $K^+$ from mixed-cation subsoil columns which received input HCl solutions with two different pH values .....	163
4-20	Breakthrough curves of $Mg^{2+}$ from mixed-cation subsoil columns which received input HCl solutions with two different pH values .....	164
4-21	Breakthrough curves of $Al^{3+}$ from mixed-cation topsoil columns which received input HCl solutions with two different pH values .....	166
4-22	Breakthrough curves of $Al^{3+}$ from mixed-cation subsoil columns which received input HCl solutions with two different pH values .....	167

Abstract of Dissertation Presented to the Graduate School  
of the University of Florida in Partial Fulfillment of the  
Requirements for the Degree of Doctor of Philosophy

LEACHING OF CATIONS DURING DISPLACEMENT BY ACID  
SOLUTIONS THROUGH COLUMNS OF CECIL SOIL

By

KO-HUI LIU

August, 1987

Chairman: R.S. Mansell  
Major Department: Soil Science

Cation transport under conditions of steady liquid flow was investigated, using columns filled with water-saturated Cecil (Typic Hapludult) topsoil and subsoil. Initially the soils were saturated with  $\text{Ca}^{2+}$ , using  $\text{CaCl}_2$  solution, which was then miscibly displaced by  $\text{MgCl}_2$  solution.

A Galerkin finite-element method with cubic-spline shape functions was used to numerically solve the equation for one-dimensional transport and binary exchange of cations in the Cecil soil columns. The numerical model was verified by assuming that the solute was non-reactive solute or that paired cations had no preference for soil exchange sites.

Cation exchange capacity (CEC) was shown to be the most sensitive input parameter when the model was used to simulate cation transport in the soil columns. Increase of CEC increased retardation of cation movement. Relatively

small values of CEC gave reasonable predictions for the cation distributions in the soil columns.

Dilute HCl solutions with a pH of 3.9 and 4.9 were applied at  $1.0 \text{ cm h}^{-1}$  Darcy flux to columns of air-dry soils to simulate the effects of acid rain upon leaching of soil cations. Soil columns were prepared using Cecil topsoil and subsoil initially saturated separately with  $\text{K}^+$ ,  $\text{Ca}^{2+}$ , and  $\text{Mg}^{2+}$ , also using untreated and mixed-cation soils. "Mixed-cation" soils were obtained by mixing equal masses of  $\text{K}^+$ -,  $\text{Ca}^{2+}$ -, and  $\text{Mg}^{2+}$ - saturated soils.

The initial effluent samples from acid-treated soil columns were high in basic and acidic cation concentrations and low in pH. Dramatic decreases in cation concentrations and increases in pH were observed with increasing volume of effluent up to about 3 to 5 pore volumes. Between 5 to 30 pore volumes of effluent, pH was in the range from 6.0 to 6.5, and cation concentrations decreased gradually. Soil base saturation in the columns was drastically reduced after acid application, especially for columns receiving pH 3.9 acid solution. Experimental results from the leaching experiments indicated that total quantities of cations removed by the acid at pH 3.9 were 1.2 to 2.0 times more than those at pH 4.9.

## CHAPTER I INTRODUCTION

### Description of Problem

During recent decades, the environmental impact of acid precipitation has become a major concern in many industrialized countries. Concerns about possible harmful effects on soil, vegetation and surface-water supplies have resulted in intensive research in this area. The most serious effects of acid deposition upon forest soils are commonly thought to be the potentials for accelerating cation leaching, for increasing soil acidity, and hence for decreasing forest productivity. Acidification of surface waters resulting in the release of toxic aluminum ions ( $\text{Al}^{3+}$ ) from sediments in lakes and streams is harmful to aquatic ecology (Hutchinson and Havas, 1980).

During rain events, rainwater which does not run off the surface or undergo evapotranspiration infiltrates into the soil profile. As the soil water moves by mass flow, hydrodynamic dispersion mixes the native soil solution with the incoming rainwater. Ion species moving with the soil solution may undergo ion-exchange with counter ions initially present on the soil exchange phase. In addition to ion exchange phenomena, the presence of  $\text{H}^+$  in the rainwater results in secondary reactions such as acid

dissolution of sesquioxides and clay minerals to yield  $\text{Al}^{3+}$  ions.

To understand the mechanisms of ion movement during acid-rain deposition in forest soils, the interaction between rainwater and soil must be carefully examined. In particular, ion-exchange processes are of great importance (Wiklander, 1975).

### Hypotheses

The working hypothesis for this research is that acid precipitation increases nutrient leaching from forest soils in direct proportion to the  $\text{H}^+$  concentration of incoming rainwater. Direct sampling of soil and soil solution at specific forest sites to determine changes in ionic composition of soil exchange and solution phases is very time-consuming and expensive. More importantly, forest soils also commonly generate  $\text{H}^+$  ions (Mollitor and Raynal, 1982, Reuss and Johnson, 1985) due to biological processes.

A need exists to provide foresters and soil scientists with predictive tools for describing the leaching of nutrient cations, such as  $\text{Ca}^{2+}$ ,  $\text{Mg}^{2+}$ ,  $\text{K}^+$ , etc., through soil profiles. The usefulness of such predictive tools for planning purposes should include assessment of the benefits and consequences of forest management and fertilizing. Furthermore, such a tool could provide information help in controlling groundwater quality. Predicting changes in ionic composition of the soil solution and exchange phases

as acid solution infiltrates soil is central to evaluating acid-rain effects upon forest soils. Predictions based upon established soil physical-chemical methods would be the most reliable method of evaluating long-term effects of acid rain on soil (Reuss, 1983).

### Objectives

The ion-exchange process is one of the most important soil chemical processes which influences cation leaching during infiltration of acid rain into soil. Thus, a computer model solely based on binary ion-exchange equilibrium and saturated steady water flow was developed for predicting the movement of cation species in soil. The response of cation leaching to input acid solution at two different pH values was determined using columns of Cecil soil (Typic Hapludult).

There are three objectives in this study. The first objective was to evaluate a numerical model by simulating binary cation exchange and transport during miscible displacement of electrolyte solutions through columns of Cecil soil. The second objective was to experimentally determine effects upon cation leaching of applying artificial acid-rain solutions (hydrochloric acid) to columns of Cecil soil. The third objective was to determine the leaching effect of applied artificial acid-rain solutions (hydrochloric acid) to columns of Cecil soil pretreated to saturate exchange sites with specific cation

species. The format for this dissertation follows the sequence of stated objectives.

## CHAPTER II MODEL SIMULATION OF BINARY CATION EXCHANGE AND TRANSPORT IN COLUMNS OF CECIL SOIL

### Introduction

The exchange of cations between exchange and solution phases in a soil system is an important phenomenon which greatly influences nutrient movement in soil, leaching of cations by acid-rain infiltration, reclamation of salt-affected soil, contaminant migration, and other processes. Ion transport in packed exchanger beds and in soil columns has been investigated for many decades and several approaches have been used to model the ion-exchange process. Thomas (1944) developed an equation applicable to cation transport in columns of synthetic ion exchanger, assuming that the exchange mechanism obeyed reversible, second-order, reaction kinetics. Rible and Davis (1955) used chromatographic theory of ion exchange to investigate cation exchange and transport in soil columns, but neglected the effect of hydrodynamic dispersion during transport. Assuming chemical equilibrium between cations in solution and on the exchange phase, Lapidus and Amundson (1952) proposed a model for ion transport such that exchange followed a linear isotherm, with hydrodynamic dispersion

then resulting in mixing of displacing and displaced solutions in the porous media. In some investigations (Lai and Jurinak, 1971; Reiniger and Bolt, 1972; Persaud and Wierenga, 1982), empirical equations have been fitted to measured adsorption data in order to obtain adsorption isotherms for incorporation into the transport equation. Ion chromatography theory is based upon differences of ionic migration rates for different ions in a packed bed. In modeling, the movement of these ionic species is based upon the principle of conservation of mass. In multicomponent chromatography theory (Bolt 1967; Helfferich and Klein, 1970), where the local equilibrium condition is also assumed, the exchange relationship between any two given ion species in the system can be described by a Vanselow selectivity coefficient. This coefficient is valid when ionic strength and ion-pair corrections are made for cation activities in the solution phase (Babcock and Schulz 1963; van Beek and Bolt, 1973). Therefore, quantitative relationships between the equilibrium constants for ion exchange, concentrations, and valences of each pair of ions can be obtained. Using multicomponent chromatography, Rubin and James (1973) proposed a general mathematical form for transport and exchange for each of several ion species by using a generalized Vanselow selectivity function. The model was later used successfully to describe the processes of exchange and transport for three major cations ( $\text{Ca}^{2+}$ ,  $\text{Mg}^{2+}$ ,  $\text{Na}^{+}$ ) in an aquifer system (Valocchi et al., 1981). In

that study, cation-exchange reactions were assumed to be controlled by local equilibrium, the soil column was assumed to be water saturated, water flow was assumed to be one-dimensional and steady, and exchange selectivity coefficients for each pair of ion species were assumed to be constant. Although the model successfully described the movement of several major cations, the selectivity coefficients for binary pairs of ions are not constant in soil but are known to vary as the solution composition changes (Sposito, 1981; Mansell et al., 1986).

The convection-dispersion transport model for cations in porous media is governed by a system of nonlinear partial differential equations which can be solved by employing different numerical techniques with the aid of a digital computer. Lai and Jurinak (1971) used a finite-difference method and a single-component exchange isotherm to model cation adsorption in soil. They found, for the  $\text{Ca}^{2+} \rightarrow \text{Mg}^{2+}$  binary reaction (i.e. exchange sites initially occupied with  $\text{Mg}^{2+}$  and displacement by  $\text{Ca}^{2+}$ ), the use of a nonlinear exchange function demonstrated good agreement between computed and experimental results. Rubin and James (1973) later formulated the governing transport equation for multi-ion species in one-dimensional space by applying the Galerkin finite-element method with linear-basis shape functions over the space domain. The resulting system of nonlinear ordinary differential equations was solved using Crank-Nicholson method and predictor-corrector

approximations. Their numerical simulations included homovalent binary cation exchange with different values for the cation exchange capacity and dispersion coefficient parameters. Valocchi et al. (1981) extended this technique to a two-dimensional (axially symmetric) model with the use of isoparametric quadrilateral elements in order to solve a ground-water contamination problem for an aquifer. They concluded that, for a binary system, ion concentration profiles consist of a single advancing exchange front while, for a ternary system, two fronts may be separated by a plateau zone. These phenomena were actually observed in their field simulation of  $\text{Na}^+$ ,  $\text{Mg}^{2+}$  and  $\text{Ca}^{2+}$  breakthrough curves for well-water downstream from an injection well. Jennings et al. (1982) followed the approach of Rubin and James (1973) and applied equilibrium interaction chemistry (speciation, etc.) independently of the convective-dispersive transport equation. A set of algebraic chemistry equations was coupled to the mass transport equation and a numerical solution was obtained by the Galerkin finite-element method applied over the space domain. A backward finite-difference approximation was used for the time derivative, and a surface complexation sorption model allowed the consideration of complex metal and ligand species at soil surfaces. The sorption reaction was assumed to occur under instantaneous equilibrium conditions. Using concepts from multispecies ion chromatography as given by Valocchi et al. (1981), and mobile-immobile water theory as

given by van Genuchten and Wierenga (1976), Mansell et al. (1986) constructed a numerical model to simulate the leaching of cations in soil columns. The mathematical solution was numerically approximated using a Crank-Nicholson finite-difference technique, and cation transport was observed to be best simulated when selectivity coefficients were given as functions of the equivalent fractions of specific cations in the solution phase.

The first objective of this investigation was to develop a finite-element computer model capable of simulating exchange and transport of multiple species of cations in soil columns. This computer model could then be used by the soil scientists or foresters as a basic working tool for predicting the movement of cations in soil. A second objective was to experimentally determine selectivity coefficients from cation concentrations in solution phase and on exchange sites for soil columns. A third objective was to evaluate the model as a means to simulate binary ion exchange and transport in columns of Cecil soil by comparing simulated with experimental data.

### Theory

#### Transport Equation

The general form of the differential equation used to describe one-dimensional, convective-dispersive transport of each cation species  $i$  in uniform porous medium or soil under steady water-flow conditions may be written as

$$\frac{\partial C_i}{\partial t} + \frac{\sigma}{\theta} \frac{\partial \bar{C}_i}{\partial t} = D \frac{\partial^2 C_i}{\partial x^2} - v \frac{\partial C_i}{\partial x} \quad i=1,2,\dots,n \quad [2-1]$$

where  $C_i(x,t)$  (mmole(+)  $L^{-1}$ ) is the aqueous-phase concentration of species  $i$ ,  $\bar{C}_i$  (mmole(+)  $Kg^{-1}$ ) is the adsorbed-phase (exchange) concentration,  $D$  ( $m^2 h^{-1}$ ) is the dispersion coefficient,  $v$  ( $m h^{-1}$ ) is the average pore-water velocity,  $\sigma$  ( $Mg m^{-3}$ ) is the dry-soil bulk density,  $\theta$  ( $m^3 m^{-3}$ ) is the volumetric water content,  $x$  (m) is distance (downward) in the soil, and  $t$  (h) is time. The second term on the left-hand side of equation [2-1] describes the time rate of change of the exchange-phase concentration for ion species  $i$ . If  $n$  cation species are considered,  $n$  equations having the form of equation [2-1] must be solved simultaneously subject to the following initial and boundary conditions:

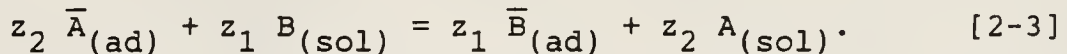
$$\begin{aligned} t = 0 \text{ and } x \geq 0 & \quad C_i = C_{ib} \\ t \geq 0 \text{ and } x = 0 & \quad vC_{if} = -D \frac{\partial C_i}{\partial x} + v C_i \\ t \geq 0 \text{ and } x = L & \quad \frac{\partial C_i}{\partial x} = 0 \end{aligned} \quad [2-2]$$

where  $C_{ib}$  (mmole(+)  $L^{-1}$ ) is the initial concentration of each species  $i$  in the porous medium and  $C_{if}$  is the input solution concentration for ion species  $i$ . Before solving equation [2-1] subject to auxiliary equations [2-2], the time rate of change of the adsorbed concentration ( $\bar{C}_i$ ) in equation [2-1] with respect to  $C_i$  should be obtained as a functional

relationship between  $C_i$  and  $\bar{C}_i$ . Details of this analysis for  $C_i$  are given in the next section.

#### Equation for Instantaneous Cation Exchange

The reversible, equilibrium-controlled cation-exchange reaction involving ion species A with valence  $z_1$  and ion species B with valence  $z_2$  can be expressed as



The preference for soil exchange sites for competing cations can be expressed in quantitative terms by the law of mass action (Helfferich, 1962) as

$$K = \frac{[\bar{B}]^{z_1} [A]^{z_2}}{[\bar{A}]^{z_2} [B]^{z_1}}, \quad [2-4]$$

where  $[\bar{A}]$  and  $[\bar{B}]$  denote activities of cation A and B adsorbed onto soil exchange sites, respectively;  $[A]$  and  $[B]$  denote activities of cations A and B in solution, respectively; and  $K$  is the thermodynamic exchange constant which is an indicator of the affinity of exchange sites for ion B relative to affinity for ion A.

If  $\bar{M}_A$  and  $\bar{M}_B$  are given in units of mole per kg on the exchange phase of ion species A and B, respectively, mole fractions for ion species A and B are defined as

$$\bar{M}_A^* = \frac{\bar{M}_A}{\bar{M}_T},$$

$$\text{and } \bar{M}_B^* = \frac{\bar{M}_B}{\bar{M}_T}, \quad [2-5]$$

where  $\bar{M}_T$  represents the sum of  $\bar{M}_A$  and  $\bar{M}_B$  (mole per kg) of the soil. The relationship between activities and mole fractions for ion species in the exchange phase is given by Sposito (1981) as

$$\begin{aligned} [\bar{A}] &= \mu_A \bar{M}_A^* ; \\ [\bar{B}] &= \mu_B \bar{M}_B^* ; \end{aligned} \quad [2-6]$$

where  $\mu_A$  and  $\mu_B$  are activity coefficients for cations A and B on the exchange phase, and  $\bar{M}_A^*$  and  $\bar{M}_B^*$  are mole fractions for cations A and B on the exchange phase, respectively.

The relationship between activities and concentrations for the solution phase is given by Sposito (1981) as

$$\begin{aligned} [A] &= r_A M_A ; \\ [B] &= r_B M_B ; \end{aligned} \quad [2-7]$$

where  $r_A$  and  $r_B$  are ion activity coefficients for cations A and B in the solution phase and  $M_A$  and  $M_B$  are molar concentrations for cations A and B in the solution phase. Substitution of equations [2-6] and [2-7] into equation [2-8] yields

$$K = \frac{(\mu_B \bar{M}_B^*)^{z_1} (r_A M_A)^{z_2}}{(\mu_A \bar{M}_A^*)^{z_2} (r_B M_B)^{z_1}} . \quad [2-8]$$

The activity coefficients  $r_A$  and  $r_B$  for the solution phase may be calculated from the extended Debye-Huckel equation as functions of ionic strength (I) as

$$r_i = \exp \left[ \frac{-0.5085 z_i^2 \sqrt{I}}{1 + 0.328 a_i \sqrt{I}} \right] , \quad [2-9]$$

where  $z_i$  is the valence of cation  $i$  ( $i = A$ , or  $i = B$ ),  $a_i$  is the ion-size parameter for ion A or B, and  $I = 0.5 \sum (C_i z_i^2)$ . Equation (2-3) then can be rewritten as

$$K = \frac{[\bar{B}]^{z_1} (r_A M_A)^{z_2}}{[\bar{A}]^{z_2} (r_B M_B)^{z_1}} . \quad [2-10]$$

When an exchange reaction is reversible, it is useful to measure the Vanselow selectivity coefficient ( $K_v$ ) as a function of the exchange composition. Any variation in  $K_v$  is related directly to that of the activity coefficient of the components of the exchange phase.  $K_v$  is defined by Sposito (1981) as

$$K_v = \frac{\mu_A^{z_2}}{\mu_B^{z_1}} K , \quad [2-11]$$

In equation [2-11] the exchange-phase activity coefficients are generally not known for soils. However, the thermodynamic formulations of Gaines and Thomas (1953) can be used for calculation of the equilibrium constant and exchange-phase activity coefficients, yielding

$$\ln K = \int_0^1 \ln K_v d\bar{C}_B . \quad [2-12]$$

An equilibrium-controlled cation exchange reaction is defined as follows (Helfferich, 1962; Bolt, 1967):

$$z_2 C_1 + z_1 \bar{C}_2 = z_1 C_2 + z_2 \bar{C}_1 , \quad [2-13]$$

where 1 and 2 are exchanging species with  $z_1$  and  $z_2$  valences, respectively. Concentrations (mmole(+)  $\text{kg}^{-1}$  soil) of each exchange species are given as  $\bar{C}_i$ , and concentrations (mmole(+)  $\text{L}^{-1}$ ) of dissolved species are given as  $C_i$ . Therefore, an ion-exchange selectivity coefficient  $K_s$  can be defined as

$$K_s = \left[ \frac{\bar{C}_1^*}{C_1} \right]^{z_2} \left[ \frac{C_2}{\bar{C}_2^*} \right]^{z_1} . \quad [2-14]$$

where

$$\bar{C}_i^* = \frac{\bar{C}_i}{\bar{C}_i + \bar{C}_j} \quad i, j = 1 \text{ or } 2$$

and  $\bar{C}_i^*$  is called the equivalent fraction of ion  $i$  on the exchange phase.

This form is reasonably suited to describe the ion-exchange phenomenon. The magnitude of  $K_s$  changes with the cation concentrations in the solution phase and also with the equivalent fractions of individual ions on the exchange

sites (Helfferich, 1962; Cho, 1985). The value of  $\bar{C}_T$  is assumed to be constant for a given soil material. For numerical simulations in this work the magnitude of  $K_s$  was assumed to be constant (Valocchi et al., 1981) during the ion exchange transport process.

#### Transport with Ion Exchange

For the case of binary cation exchange and steady water flow, the convective-dispersive mass-transport equation [2-1] can be explicitly written as

$$\frac{\partial C_1}{\partial t} + \frac{\sigma}{\theta} \frac{\partial \bar{C}_1}{\partial t} = D \frac{\partial^2 C_1}{\partial x^2} - v \frac{\partial C_1}{\partial x} , \quad [2-15]$$

and

$$\frac{\partial C_2}{\partial t} + \frac{\sigma}{\theta} \frac{\partial \bar{C}_2}{\partial t} = D \frac{\partial^2 C_2}{\partial x^2} - v \frac{\partial C_2}{\partial x} . \quad [2-16]$$

Equations [2-14] and [2-15] are coupled through additional equations for the time rate of change of adsorbed-phase terms (the second terms on the left-hand sides of equations [2-15] and [2-16]) to specifically describe the cation-exchange process. If one assumes the soil cation exchange capacity  $\bar{C}_T$  to be time invariant at any given location in the soil, it can be expressed as the local sum of the concentrations of cations in the exchange phase as

$$\bar{C}_T = \bar{C}_1 + \bar{C}_2 , \quad [2-17]$$

and the total solution-phase concentration  $C_T$  at any given time and distance is the sum of the concentrations of ion species present in the solution phase

$$C_T = C_1 + C_2 . \quad [2-18]$$

If one further considers the simplified case where the (input) solution has the same total normality  $C_T$  as the native solution ( $C_T$  is constant), an explicit form for the exchange isotherm can be obtained by substituting equations [2-17] and [2-18] into equation [2-14]. This yields

$$\bar{C}_1 = \frac{\bar{C}_T}{1 + \Gamma} , \quad [2-19]$$

where  $\Gamma = \alpha / \beta$ ,  $\alpha = C_T - C_1$ , and  $\beta = K_S^{1/z_1} C_1^{z_2/z_1}$ .

This simplification reduces the binary-exchange problem to a single-species exchange problem (Rubin and James, 1973; Valocchi et al., 1981). If we define a parameter  $F$  as

$$F = \frac{\partial \bar{C}_1}{\partial C_1} = \frac{\tau}{\epsilon^2} , \quad [2-20]$$

where  $\tau = C_T K_S^{1/z_1} \bar{C}_T$ , and  $\epsilon = C_T + (K_S^{1/z_1} - 1)C_1$ , the chain rule may be used to obtain

$$\frac{\partial \bar{C}_1}{\partial t} = \frac{\partial \bar{C}_1}{\partial C_1} \frac{\partial C_1}{\partial t} = F \frac{\partial C_1}{\partial t} . \quad [2-20]$$

Therefore, using equations [2-14], [2-20] and [2-21], equations [2-15] and [2-16] can be combined to give one equation with one dependent variable  $C_1$  as given by

$$\left(1 + \frac{\sigma}{\Theta} F\right) \frac{\partial C_1}{\partial t} = D \frac{\partial^2 C_1}{\partial x^2} - v \frac{\partial C_1}{\partial x} \quad [2-22]$$

The term  $R = 1 + (\sigma/\Theta)F$  is referred to as the retardation function for transport of ion 1 through the soil. For binary nonpreferential ( $K_s = 1$ ) homovalent exchange  $F = \bar{C}_T / C_T$  and  $R = 1 + (\sigma/\Theta) (\bar{C}_T / C_T)$ , so that, for constant cation exchange capacity, retardation of cation transport tends to increase as  $C_T$  decreases towards small values such as those that normally occur in rain water. Also, for this case, cation retardation can be expected to be greatest in soils with highest values for  $\bar{C}_T$  and with highest soil-to-solution ratios ( $\sigma/\Theta$ ). Appropriate initial and boundary conditions for equation [2-22] are

$$t = 0 \quad x \geq 0 \quad C_1 = C_{1i} \quad [2-23a]$$

$$t \geq 0 \quad x = 0 \quad v C_{1f} = -D \frac{\partial C_1}{\partial x} + v C_1 \quad \text{and}$$

$$t \geq 0 \quad x = L \quad \frac{\partial C_1}{\partial x} = 0 \quad [2-23b]$$

Partial differential equations given as [2-22] and [2-23] constitute a mathematical description of cation transport and exchange in a soil column of finite length  $L$  during steady water flow, they were solved in this research by use of a Galerkin finite-element method. For simplicity, concentration  $C_1$  for ion species 1 is denoted by  $C$  throughout the remainder of the dissertation. Subscript or

superscript notation for C was only used for formulation purposes in the finite-element method.

### A Galerkin Finite-Element Numerical Method

#### Finite-Element Method

Finite-element methods typically incorporate an approximating integral equation to replace the original governing partial differential equation (Pinder and Gray, 1977). Variational and weighted-residual techniques are two methods most commonly used to obtain the approximate integral equation. The Galerkin finite-element weighted-residual method has been widely used for the mass-transport equation (Price et al., 1968; Pinder, 1973) and is the method used here. In the finite-element method, the domain of interest is discretized into a number of subdomains called elements. In this study, a line-segment element was used and a cubic-spline function was chosen as the interpolation function. For the Galerkin approximation, consider a linear differential operator of the form

$$L(\tilde{u}) = 0 \quad \text{on domain } D. \quad [2-24]$$

To solve  $u$ , a trial function  $\tilde{u}(x,t)$  is assumed which is composed of a linear combination of approximation functions containing time-dependent, undetermined coefficients  $G_j(t)$  and specified-shape functions  $N_j(x)$  that satisfy the given boundary condition of the problem. The trial function can be expressed as

$$u(x,t) \approx \tilde{u}(x,t) = \sum_{j=1}^N G_j(t) N_j(x). \quad [2-24]$$

where  $n$  denotes the number of nodal points.

Substituting the trial function  $\tilde{u}$  into the linear differential operator  $L$  for the exact solution  $u$  will result in a residual  $R(x,t)$  as defined by

$$R(x,t) = L(\tilde{u}) = L \left( \left[ \sum_{j=1}^N G_j(t) N_j(x) \right] \right) \neq 0 . \quad [2-26]$$

This residual is forced to zero in an average sense over the entire domain  $D$  through the selection of undetermined coefficients  $G_j(t)$ . The  $G_j(t)$  values are calculated by setting the weighted integral of the residual to zero. In the Galerkin finite-element, weighted-residual method, the shape functions are used as the weighting functions and the resulting integral form is:

$$\int_D R(x,t) N_i(x) dx = 0 . \quad [2-27]$$

### Interpolation Function

The use of cubic-spline functions as interpolation functions in the finite-element method has been successfully applied in solving boundary-layer flow problems (Hsu, 1976; Hsu and Liakopoulos, 1981). In the present study, the unknown function  $C(x,t)$  at a given depth in a soil column (profile) is represented by classical cubic splines. Since classical cubic-spline interpolation functions provide expression of  $C(x,t)$  as continuous functions with continuous first and second derivatives, classical cubic-spline

functions possess a number of desirable optimal properties (Ahlberg et al., 1967).

For a selected soil column of length  $L$ , suppose that the space interval  $0 < x < L$  is properly discretized into  $n$  interconnected elements with  $n+1$  nodal points at  $0 = x_1 < x_2 < x_3 < \dots < x_{n+1} = L$ , where values of  $C(x_j, t)$  and its derivatives with respect to  $x$  at nodal point  $j$  are defined as

$$\begin{aligned} C(x_j, t) &= C_j(t) , \\ C_j'(t) &= \left. \frac{\partial C}{\partial x} \right|_{x_j} , \\ \text{and } C_j''(t) &= \left. \frac{\partial^2 C}{\partial x^2} \right|_{x_j} . \end{aligned} \quad [2-28]$$

For the  $i$ th element, one defines the element size  $h_i$  as  $h_i = x_{i+1} - x_i$  and the local coordinate  $z$  as  $z = x - x_i$  with  $0 < z < h_i$ . One further expresses the cubic polynomial function approximating  $C(x, t)$  in the  $i$ th element as  $g(z, t)$ . If  $g(z, t)$  is made to satisfy the conditions

$$\begin{aligned} g_i(0, t) &= C_i(t) , \\ g_i(h, t) &= C_{i+1}(t) , \\ g_i''(0, t) &= C_i''(t) , \end{aligned} \quad [2-29]$$

$$\text{and } g_{i+1}''(h, t) = C_{i+1}''(t) ,$$

$g(z, t)$  is given by

$$g_i(z, t) = - \frac{z(z-h_i)(z-2h_i)}{6h_i} C_i''(t) - \frac{z-h_i}{h_i} C_i(t)$$

$$+ \frac{z(z-h_i)(z+h_i)}{6h_i} C_{i+1}''(t) + \frac{z}{h_i} C_{i+1}'(t) . \quad [2-30]$$

The requirement of slope continuity at nodes is further imposed as

$$\begin{aligned} g'_i(h_i) &= g'_{i+1}(0) , \\ g'_1(0) &= C'_1(t) , \end{aligned} \quad [2-31]$$

and  $g'_n(h_n) = C'_{n+1}(t) .$

The following system of  $n+1$  equations is thus obtained

$$\begin{aligned} \frac{h_1}{3} C_1'' + \frac{h_1}{6} C_2'' &= -\frac{C_1}{h_1} + \frac{C_2}{h_2} - C_1' , \\ \frac{h_j}{6} C_j'' + \frac{(h_j+h_{j+1})}{3} C_{j+1}'' - \frac{h_{j+1}}{6} C_{j+2}'' &= \\ &\frac{C_j}{h_j} - \left( \frac{1}{h_j} + \frac{1}{h_{j+1}} \right) C_{j+1} + \frac{1}{h_{j+1}} C_{j+2} \\ \frac{h_n}{6} C_n'' + \frac{h_n}{3} C_{n+1}'' &= \frac{C_n}{h_n} - \frac{C_{n+1}}{h_n} + C_{n+1}' . \end{aligned} \quad [2-32]$$

The system of equations given as equation (2-31) can be written in matrix form simply as

$$[A] \{C''_i\} = [B] \{C_i\} + \{S\} . \quad [2-33]$$

where  $[A]$  and  $[B]$  are nonsingular, symmetric, tridiagonal  $(n+1)$ -by- $(n+1)$  constant matrices, and

$$\begin{aligned} \{C''_i\}^T &= [C_1'', C_2'', \dots, C_{n+1}''] , \\ \{C_i\}^T &= [C_1, C_2, \dots, C_{n+1}] , \end{aligned} \quad [2-34]$$

$$\text{and } \{ S \}^T = [ -C_1', 0, \dots, 0, C_{n+1}' ] .$$

Consequently, one has

$$\{ C''_i \} = [ A ]^{-1} [ B ] \{ C_i \} + [ A ]^{-1} \{ S \} . \quad [2-35]$$

Alternatively, in component form

$$C''_i(x,t) = \sum_{j=1}^{n+1} \alpha_{i,j} C_j(t) - 6\beta_{i,1} C'_1(t) + 6\beta_{i,n+1} C'_{n+1}(t) .$$

$$\text{where } [ \alpha_{i,j} ] = [ A ]^{-1} [ B ] \quad [2-36]$$

$$\text{and } [ \beta_{i,j} ] = [ A ]^{-1}$$

Substituting equation (2-35) into equation (2-29), the cubic polynomial approximating function  $g(z,t)$  for  $C(x,t)$  in the  $i$ th element, in polynomial of degree three in  $z$ , is given by the following formula:

$$g_i(z,t) = \sum_{j=1}^{n+1} a_{i,j}(z) C_j(t) + b_{i,1}(z) C'_1(t) + b_{i,n+1}(z) C'_{n+1}(t)$$

$$\text{where} \quad [2-37]$$

$$a_{i,j}(z) = -\alpha_{i,j} \frac{z^3 - 3z^2 + 2zh_i^2}{6h_i} + \alpha_{i+1,j} \frac{z^3 - zh_i^2}{6h_i} - \delta_{i,j} \frac{z - h_i}{h_i} + \delta_{i+1,j} \frac{z}{h_i} , \quad [2-38]$$

$$b_{i,1}(z) = \beta_{i,1} \frac{z^3 - 3z^2 h_i + 2zh_i^2}{h_i} - \beta_{i+1,1} \frac{z^3 - zh_i^2}{h_i} ,$$

and

$$b_{i,n+1}(z) = -\beta_{i,n+1} \frac{z^3 - 3z^2 h_i + 2zh_i^2}{h_i} + \beta_{i+1,n+1} \frac{z^3 - zh_i^2}{h_i} .$$

in which  $\delta$  is the Kronecker's delta. Therefore the cubic

polynomial  $g(z,t)$ , approximating  $C(x,t)$  in the  $i$ th element, is a linear function of all the nodal values of  $C(x,t)$  and the slopes at extreme nodes. The resulting trial function  $\tilde{C}(x,t)$  of classical cubic spline approximation for the function  $C(x,t)$  at a specific length of soil column (profile) is given by

$$\tilde{C}(x,t) = \sum_{j=1}^n \delta_i g_j(x,t) \quad \text{where } \delta_i = \begin{cases} 1 & \text{for } x_i < x < x_{i+1} \\ 0 & \text{otherwise.} \end{cases} \quad [2-39]$$

It is obvious that cubic spline function  $\tilde{C}(x,t)$  agrees with  $C(x,t)$  at nodes and is twice continuously differentiable in the interval of interest.

#### Method of Weighted Residuals

Substituting the boundary conditions of equation [2-23] into equation [2-37], the approximation function  $g(z,t)$  becomes:

$$g_i(z,t) = \sum_{j=1}^{n+1} a_{i,j}(z) C_j(t) + b_{i,1} \frac{v}{D} (C_1 - C_f) . \quad [2-40]$$

Therefore, the unknown coefficients to be determined are  $C_1, C_2, C_3, \dots, C_{n+1}$ . Substituting equation [2-40] into equation [2-39] yields

$$\tilde{C}(x,t) = \sum_{j=1}^{n+1} N_j(z) C_j(t) + B_1(z) \frac{v}{D} C_f , \quad [2-41]$$

where

$$N_1 = \sum_{i=1}^n \delta_i a_{i,1}(z) + \frac{v}{D} \sum_{i=1}^n \delta_i b_{i,1}(z) ,$$

$$N_j = \sum_{i=1}^n \delta_i a_{i,j}(z) \quad j=2,3,\dots,n+1 \quad ,$$

$$\text{and} \quad B_1 = \sum_{i=1}^n \delta_i b_{i,1}(z) \quad .$$

For the initial boundary-value problem given by equation [2-22] that satisfies the boundary condition [2-23b], the trial solution can be written as

$$C(x,t) \approx \tilde{C}(x,t) = \sum_{j=1}^{n+1} N_j(z) C_j(t) + B_1(z) \frac{v}{D} C_f \quad .$$

$$j=1,2,\dots,n+1 \quad [2-42]$$

Substituting equation [2-42] into equation [2-22] and applying the method of weighted residuals one obtains

$$\int_0^L N_m(x) \left[ \left(1 + \frac{\sigma}{\Theta} F\right) \frac{\partial \tilde{C}}{\partial t} - D \frac{\partial^2 \tilde{C}}{\partial x^2} + v \frac{\partial \tilde{C}}{\partial x} \right] dx = 0 \quad .$$

$$[2-43]$$

Equation [2-42] can be explicitly rewritten as

$$\begin{aligned} & \int_0^L \left(1 + \frac{\sigma}{\Theta} F\right) N_m(x) \left[ \sum_{j=1}^{n+1} N_j(z) \frac{\partial C_j}{\partial t} + \frac{v}{D} B_1(z) \frac{\partial C_f}{\partial t} \right] dx \\ &= \int_0^L N_m \left[ \sum_{j=1}^{n+1} D \frac{\partial^2 N_j}{\partial x^2} C_j(t) + D C_f \frac{\partial^2 B_1(z)}{\partial x^2} \right] dx \\ &- \int_0^L N_m \left[ \sum_{j=1}^{n+1} v \frac{\partial N_j}{\partial x} C_j(t) + v C_f \frac{\partial B_1(z)}{\partial x} \right] dx \quad , [2-44] \end{aligned}$$

where  $N_m$  are weighting functions. Since there are  $n+1$  unknown nodal values for the dependent variable  $C(x,t)$ , a set of  $n+1$  weighting functions must be chosen for  $N_j$ . Therefore, using Galerkin's method, the weighting functions

are chosen to be the interpolation (shape) functions of the assumed solution, such as

$$N_m = N_j . \quad [2-45]$$

### Computational Method

After rearranging, equation [2-44] becomes

$$[Q] \left\{ \frac{\partial C_j(t)}{\partial t} \right\} = ([R] - [U]) \{C_j(t)\} + (\{V\} - \{S\}) C_f , \quad [2-46]$$

where:

$$[Q] = \int_0^L \left( 1 + \frac{\sigma}{\Theta} F \right) N_m(z) \sum_{j=1}^{n+1} N_j(z) dx ,$$

$$[R] = D \int_0^L N_m(z) \sum_{j=1}^{n+1} \frac{\partial^2 N_j(z)}{\partial x^2} dx ,$$

$$[U] = v \int_0^L N_m(z) \sum_{j=1}^{n+1} \frac{\partial N_j(z)}{\partial x} dx ,$$

$$\{V\} = D \int_0^L N_m(z) \frac{\partial^2 B_1(z)}{\partial x^2} dx , \quad [2-47]$$

$$\text{and } \{S\} = v \int_0^L N_m(z) \frac{\partial B_1(z)}{\partial x} dx .$$

In equation [2-46], undetermined coefficients  $C_j(x,t)$  do not appear explicitly but are embedded in the function  $F$ . This nonlinear term is linearized by employing the previous time-step solution of  $C_j^*(x,t)$  into the  $F$  term for manipulation. For example, if we consider  $m = 2, 3, \dots, n+1$ , the matrix coefficients at the left-hand side of equation [2-37] can be written as

$$Q_{m,j} \frac{\partial C_j(t)}{\partial t} = \sum_{j=2}^{n+1} \int_0^h a_{m,i}(z) \left( 1 + \frac{\sigma}{\Theta} \frac{\eta}{(C_T + W)^2} \right) \sum_{i=1}^{n+1} a_{i,j} dz \frac{\partial C_j(t)}{\partial t}, \quad [2-48]$$

where  $\eta = C_T K_S \bar{C}_T$ ,

$$\text{and } W = C_T + (K_S - 1) \left( \sum_{i=1}^{n+1} \delta_i \sum_{j=1}^{n+1} a_{i,j} C_j^* + \sum_{i=1}^{n+1} \delta_i b_{i,1} (-C_f q/D) \right)$$

For the right-hand side of equation [2-46], the matrix coefficients are given as:

$$R_{m,j} = D \left( \sum_{j=2}^{n+1} \left( \sum_{i=1}^{n+1} \int_0^h a_{m,i}(z) a_{i,j}''(z) dz \right) \right), \quad [2-49]$$

$$U_{m,j} = v \left( \sum_{j=2}^{n+1} \left( \sum_{i=1}^{n+1} \int_0^h a_{m,i}(z) a_{i,j}'(z) dz \right) \right), \quad [2-50]$$

$$V_{m,1} = -q C_f \left( \sum_{j=2}^{n+1} \left( \sum_{i=1}^{n+1} \int_0^h a_{m,i}(z) b_{i,1}''(z) dz \right) \right), \quad [2-51]$$

and

$$S_{m,1} = v \left( \sum_{j=2}^{n+1} \left( \sum_{i=1}^{n+1} \int_0^h a_{m,i}(z) b_{i,1}'(z) \left( -\frac{q}{D} C_f \right) dz \right) \right). \quad [2-52]$$

In the process of numerical integration, the definite integral is given by equations [2-48] through [2-52]. Since these equations are very complex, an explicit expression can not be obtained. However, this integral can be effectively

evaluated by using Gaussian-Legendre quadrature formula (Krylov, 1962)

$$\int_{-1}^1 F(\varphi) d\varphi \approx \sum_{m=1}^M A_m^{(M)} F(\varphi_m)^{(M)} \quad [2-53]$$

where  $A_m^{(M)}$  and  $\varphi_m^{(M)}$  are the set of weighting coefficients and roots associated with M-th degree Legendre polynomials. The quadrature formula is exact if  $F(\varphi)$  is a polynomial of degree less than or equal to  $2M-1$ . In the present work,  $m=4$  was used. In applying equation [2-53] to the equations [2-48] through [2-52] one must first transform the interval  $[0, h_i]$  onto  $[-1, 1]$ . This can be accomplished by the transformation

$$w = \frac{h_i}{2} (1 + \varphi) \quad [2-54]$$

The system of equations [2-46] is large and 'stiff'. This is typical for the system of ordinary differential equations arising from the application of the method of lines to partial differential equations (Hindmarsh, 1981). In solving the system of ordinary differential equations, if the magnitude of eigenvalues cover a wide range, an undesirably small time-step size is required. A problem of this type is called 'stiff'. A computer model for simulating convective-dispersive ion exchange/transport consists of 28 elements with this proposed method, giving rise to 29 ordinary differential equations to be solved simultaneously. Due to the presence of stiffness, conventional numerical integration of the equations [2-46]

becomes inefficient and a method that is more suitable for stiff equations should be employed. The LSODE solver developed by A. C. Hindmarsh at the Lawrence Livermore National Laboratory was used in this study as a part of the main subroutine throughout the program. The LSODE subroutine (Hindmarsh, 1980, 1983) is capable of solving systems of ordinary differential equations of the form

$$\frac{dy}{dt} = f(t,y) \quad , \quad [2-55]$$

and  $y(t,0) = f_0$

where  $y$ ,  $f$ , and  $f_0$  are vectors of length  $N$ .

In the computation, the spatial discretization was made to give a small element-size in the immediate vicinity of the inlet boundary, and gradually coarser elements were used for increasing distances from the inlet. Element sizes were obtained by trial and error in order to provide solutions without oscillations. Mass-balance error was not allowed to exceed 2% in a given simulation. A small initial time step ( $5 * 10^{-10}$  sec) was used for generating stable solutions, after which larger time steps (300 sec) were used. All computations were performed with the IFAS computer network on a VAX 11/750 computer at the University of Florida. Double-precision arithmetic was used in all computations.

### Material and Methods

#### Soil

The Cecil (Typic Hapludult) soil used in this study was obtained from a forest site located at Clemson University in

Clemson, South Carolina. The exact location of the site was reported earlier by Dr. V. L. Quisenberry (Cassel, 1985) from the Agronomy Department of Clemson University. Reported texture of the Cecil soil profile varied from site to site, with the clay content of the Ap horizon ranging from 6 to 38 percent depending upon the amount of subsoil mixing which had occurred subsequent to soil erosion. Clay content in the B horizon ranged from 42 to 72 percent (Cassel, 1985). In situ values of unsaturated hydraulic conductivity reported (Cassel, 1985) for the 0-30 cm depth ranged from  $1.70 \times 10^{-4}$  to  $4.51 \times 10^{-2}$  cm h<sup>-1</sup>, whereas those for the 30-60 cm depth ranged from  $4.32 \times 10^{-4}$  to  $4.6 \times 10^{-1}$  cm h<sup>-1</sup>, respectively. In situ values of soil water content for the 0-30 cm depth ranged from 0.275 to 0.495 cm<sup>3</sup> cm<sup>-3</sup>, whereas values ranged from 0.409 to 0.560 cm<sup>3</sup> cm<sup>-3</sup> for the 30-60 cm depth (Cassel, 1985). Typic Hapludult soils are freely drained with great or moderate depth to hard rock, have an ochric epipedon that is not both thick and sandy, and have a loamy or clayey particle-size class in an argillic horizon.

Cecil topsoil and subsoil bulk samples for this research were obtained from the 0-30 and 30-60 cm depths, respectively, of the profile. The soil was air-dried, passed through a 2-mm sieve, and stored in covered plastic buckets.

Values of pH for the soil samples were determined in a soil:water suspension (1:1 soil:water) using a glass

electrode. Organic matter content was determined by the Walkley-Black method (Allison, 1965). Particle-size distribution was determined by the pipette method (Day, 1965).

Exchangeable cation concentrations were determined using neutral 1 M  $\text{NH}_4\text{OAc}$ , by placing 5-g of 2-mm air-dried soil in duplicate 50-ml centrifuge tubes, and adding 25 ml of 1 M  $\text{NH}_4\text{OAc}$  to each. All tubes were stoppered and shaken for 30 minutes. The tubes were then placed in a centrifuge and spun at 2000 rpm for 10 minutes, with number 42 Whatman filter paper being used to collect the supernatant in a 50-ml volumetric flask. The same procedure was repeated and finally the solution was brought to a volume of 50 ml with 1 M  $\text{NH}_4\text{OAc}$  (Thomas, 1982).

Exchangeable  $\text{Al}^{3+}$  was determined by 1 M  $\text{KCl}$  extraction of 10-g of air-dried soil in duplicate 50-ml volumetric flasks, using 25 ml of 1 M  $\text{KCl}$ . The soil and  $\text{KCl}$  were mixed, allowed to stand for 30 minutes, and then transferred to Buchner funnels fitted with number 42 Whatman filter paper mounted on 250-ml vacuum flasks. An additional 125 ml of  $\text{KCl}$  was added in 25-ml increments to give a final volume of 150 ml (Thomas, 1982).

Total potential acidity as determined by  $\text{BaCl}_2$ -TEA extraction was obtained by placing 10-g soil samples in duplicate 50-ml volumetric flasks. To each flask, 25 ml of buffer solution was added, mixed well with the soil sample, and allowed to stand for 1 hour. It was then transferred to

a 5.5-cm diameter Buchner funnel fitted with Whatman number 42 filter paper. Three 25-ml volumes of buffer solution were then added to the suspension. These additions were followed with 100 ml of replacement solution to give a final volume of 200 ml. Also, a blank solution was prepared from 100 ml of buffer solution and 100 ml of replacing solution. Two drops of bromocresol green indicator and 10 drops of the mixed indicator were added. Finally, the solution was titrated with 0.2 M HCl to a repeatable endpoint in the visual color range from green to purple. The same procedure, using the same endpoint, was used for soil leachates (Thomas, 1982).

#### Column Experiment

The cylindrical container for soil columns used in this investigation was constructed by stacking 20 lathe-cut plexiglass rings with  $3.75 \times 10^{-2}$  m inside diameter and 0.01-m length each. At the top and bottom of the soil columns endplates consisting of a fixed, thin-plastic disc with small holes evenly distributed over the surface were placed in contact with the soil. On the opposite side of each endplate two outlets were designed, one for inflow or outflow purposes and a second for flushing the solution, if necessary. The cylindrical rings were held together by carefully wrapping water-proof, acid-resistant electric tape around the circumference. A check for water leakage was made prior to packing soil into each column.

Two columns designated topsoil and subsoil were prepared carefully by uniformly packing air-dried Cecil topsoil and Cecil subsoil, respectively. Soil columns were positioned vertically and placed between two wooden boards supported by threaded steel rods to hold the soil and rings in place. A Rainin model Rabbit<sup>tm</sup> peristaltic pump was used to introduce solutions at predetermined and calibrated rates into the bottom of these columns. Effluent from the top of the column was collected by an ISCO model 430 fraction collector. Soil columns were initially saturated with 0.01 mmole(+)  $\text{CaCl}_2$  from the bottom of the columns. Periodic checks for  $\text{Ca}^{2+}$  concentration in the effluent were made, until steady state was reached with respect to  $\text{Ca}^{2+}$  concentrations of input and output solutions. Soil exchange sites were then assumed to be saturated with  $\text{Ca}^{2+}$ . Miscible displacement was initiated by adding a 0.01 mmole(+)  $\text{L}^{-1}$   $\text{MgCl}_2$  exchanging solution into the bottom at constant flux. When predetermined total amounts of exchanging solution had been added to a given column, the flow was terminated. The pore volume for each soil column was obtained as the weight difference between wet and air-dried soil columns obtained before and after each experiment. Pore-volume corrections were made for the volume of entrapped solution inside the two endplates. The columns were equilibrated overnight before being dissected to ensure that soil exchange and solution phases were of equilibrium. A centrifuge method was used to separate the soil-solution phase from the

adsorbed phase for each section of every soil column. For the centrifuge method, two different sizes of centrifuge tube are required. A small hole was made at the bottom of the smaller tubes (0.015-m diameter) and a number 42 Whatman filter paper was cut and placed over that hole. Each column section of soil was carefully transferred into a prenumbered small centrifuge tube. Then, each small tube was placed into a corresponding prenumbered larger centrifuge tube (0.025-m diameter). A glass bead was placed between the small and large tubes. After balancing pairs of tubes within the centrifuge, they were spun at 4000 rpm for 30 minutes. Moist soil samples were quantitatively removed and weighed. Weights of air-dry soil were also recorded. Each dried sample was then ground and passed through a 2-mm sieve. The exchanger phase concentrations of cations were obtained by the forementioned extraction method. A correction was made for concentrations of cations in residual solution in the exchange phase of the soil sample.

In addition, one topsoil column and one subsoil column were prepared to permit determination of solute dispersion coefficients (D). Soil columns were set up vertically for flow experiments. A peristaltic pump was calibrated and used to introduce distilled water into the bottom of each soil column. After one day of leaching, a check for zero  $\text{Cl}^-$  concentration was obtained, and the distilled water was changed to 0.001 M KCl input solution. The effluent was fractionally collected, and the experiments were terminated

once the  $\text{Cl}^-$  concentration of the effluent had reached that of the input concentration. The  $\text{Cl}^-$  dispersion-coefficient values were obtained by using the resulting  $\text{Cl}^-$  breakthrough curves and a least-squares fitting procedure (van Genuchten, 1981) was used to fit an analytical solution (Brenner, 1962; van Genuchten and Alves, 1982) to experimental breakthrough data.

#### Cation-Exchange Isotherms from Soil Columns

The cation exchange isotherm for  $\text{Mg}^{2+} \rightarrow \text{Ca}^{2+}$  exchange was obtained from columns of Cecil topsoil and subsoil, respectively. Concentrations of  $\text{Ca}^{2+}$  and  $\text{Mg}^{2+}$  in solution and exchange phases as obtained by the centrifuge method were used to determine the exchange isotherms. Tables 2-2 and 2-3 present concentrations of cations in the two phases for Cecil topsoil and subsoil, respectively. CEC values for each specific depth were obtained by taking the sum of the basic and acidic cations. An average CEC value for the whole column was used in this calculation. Total solution concentrations of cations were assumed to have similar magnitudes as those of the input solution. Concentrations of  $\text{Ca}^{2+}$  and  $\text{Mg}^{2+}$  were determined using an atomic absorption spectrophotometer (Perkin Elmer model 460).

### Results and Discussion

#### Soil Properties

Soil parameters used in the column experiments are presented in Table 2-1. General soil properties, such as

soil pH, particle size distribution, clay content, and cation exchange capacity, are presented in Table 2-2.

Table 2-1 Soil parameters used in the column experiments

Parameter	Topsoil	Subsoil
Darcy velocity ( $M H^{-1}$ )	$1.11 \times 10^{-2}$	$1.08 \times 10^{-2}$
Dispersion coeff. ( $M^2 H^{-1}$ )	$3.03 \times 10^{-4}$	$1.85 \times 10^{-4}$
Bulk density ( $Mg M^{-3}$ )	1.64	1.42
Volumetric water content ( $M^3 M^{-3}$ )	0.37	0.46
Bulk volume of soil (L)	$2.21 \times 10^{-1}$	$2.21 \times 10^{-1}$
Column length (M)	$20.05 \times 10^{-2}$	$20.05 \times 10^{-2}$
Total concentration (MMOLE(+) $L^{-1}$ )	0.01	0.01
Porosity	0.38	0.46
Pore volume (L)	$81.97 \times 10^{-3}$	$101.47 \times 10^{-3}$
Total number of pore volumes collected	4.50	3.62
Cation exchange capacity (MMOLE(+) $Kg^{-1}$ soil)	10.6	17.0
Selectivity coeff. ( $K_{Mg \rightarrow Ca}$ )	0.225	0.798

Table 2-2 Properties of Cecil topsoil and subsoil

	Topsoil	Subsoil
pH(1:1)	4.46	4.80
Sand(%)	76.90	61.60
Silt(%)	14.00	13.70
Clay(%)	9.10	24.70
O.M.(%)	1.60	1.04
CEC from $NH_4OAc+KCl$ (mmole(+) $Kg^{-1}$ soil)	17.00	27.00
CEC from $NH_4OAc+BaCl_2-TEA$ (mmole(+) $Kg^{-1}$ soil)	54.00	70.00
Soil texture	Sandy loam	Sandy clay loam
Clay minerals	Interlayered-hydroxy Vermiculite, Kaolinite, Quartz.	Interlayered-hydroxy Vermiculite, Kaolinite, Gibbsite, Quartz.
Amorphous	Al, Fe hydrous oxides	Al, Fe hydrous oxides

The two different CEC values for the Cecil soil resulted from the two extraction methods used for exchangeable acidity. Exchangeable acidity as determined by  $\text{BaCl}_2$ -TEA extraction has more practical utility for calcareous than for acid soils (Thomas and Hargrove, 1984), and KCl extraction is reflects the immediate need for lime (Thomas, 1982). Thomas (1982) suggests that the best method for determining exchangeable acidity for acid soils is to use a neutral, unbuffered salt to remove the acidity at the pH of the salt solution-soil mixture.

Clay content of the Cecil subsoil was 2.7 times greater than that for the topsoil, but organic matter content of the topsoil was only 1.6 times greater than that for the subsoil. The ratio of subsoil to topsoil CEC values was somewhat less (1.3 to 1.6) than the 2.7 ratio for clay contents. The higher clay content in the subsoil did, however, result in a higher CEC and volumetric water content for the subsoil. The texture of the topsoil was sandy loam as compared to sandy clay loam for the subsoil. The type of clay minerals in the topsoil and subsoil indicates that both soils were highly weathered and had electrostatic charge sites which were predominately pH-dependent charge surfaces.

#### Verification of the Numerical Model

Predictive accuracy of the computer program for the numerical solution to the convective-dispersive ion-transport equation was evaluated for a simple problem of transport of a conservative solute (i.e. where  $K_s = 0$ ) for

which an analytical solution was available, by comparing the model simulation with the analytical solution. Assuming that the retardation factor  $R = (1 + (\sigma/\theta)F) = 1$  and that the selectivity coefficient  $K_s = 0$ , the appropriate transport equation for this problem is:

$$R \frac{\partial C}{\partial t} = D \frac{\partial^2 C}{\partial x^2} - v \frac{\partial C}{\partial x} \quad , \quad [2-56]$$

where the following initial and boundary conditions were assumed:

$$C(x, 0) = C_i \quad ,$$

$$-D \frac{\partial C}{\partial x} + vC \bigg|_{x=0} = vC_0 \bigg|_{x=0} \quad , \quad 0 \leq t \leq t_0 \quad ,$$

$$\text{and} \quad \frac{\partial C}{\partial x} \bigg|_{x=L} = 0 \quad . \quad [2-57]$$

$$C_i = 0.000001 \text{ mmole(+) } L^{-1}$$

and  $C_0 = 0.01 \text{ mmole(+) } L^{-1}$  were used as chosen values.

Brenner (1962) has given an analytical solution to this boundary-value problem as:

$$\begin{aligned} \frac{C - C_i}{C_0 - C_i} &= \frac{1}{2} \operatorname{erfc}\left(\frac{\eta}{u}\right) + \frac{\tau}{2} \exp\left(-\frac{\eta}{u}\right)^2 \\ &+ \frac{1}{2} \left(1 + \alpha + \frac{\beta}{R}\right) \exp(\alpha) \operatorname{erfc}\left(\frac{Rx + vt}{u}\right) \\ &+ \tau \left(1 + \frac{p}{2} - \frac{\alpha}{4} + \frac{\beta}{4R}\right) \exp\left(p - \frac{R}{4Dt} \Phi^2\right) \end{aligned}$$

$$-\left[2p - \alpha + \frac{3}{2} \frac{\beta}{R} + \left(\frac{v}{2D} \Phi\right)^2\right] \exp(p) \operatorname{erfc}\left(\frac{R(2L-x)+vt}{u}\right) . \quad [2-58]$$

where

$$\Phi = (2L-x+vt/R), \quad u = 2(DRt)^{1/2},$$

$$\tau = (4v^2t/\pi DR)^{1/2}, \quad \beta = v^2t/D,$$

$$\text{and} \quad \alpha = vx/D, \quad p = vL/D, \quad \eta = Rx - vt .$$

The numerical solution was obtained using the Cecil topsoil parameters presented in Table 2-1. The result is shown in Fig. 2-1 for the case  $K_s = 0$  and  $R = 1$ . Nonpreferential ion exchange with selectivity coefficient  $K_s = 1$  and  $R = (1+(\sigma \bar{C}_T)/(\Theta C_T))$  was also performed and is given in Fig. 2-2. Excellent agreement between numerical and analytical solutions demonstrates that the computer program functioned as designed for the case of transport of inert solutes as well as for the case of non-preferentially reactive cations.

#### Exchange Isotherm Curves for Columns of Cecil Soil

The  $Mg^{2+}$  exchange isotherms for  $Mg^{2+} \rightarrow Ca^{2+}$  binary exchange on Cecil topsoil and subsoil are shown in Figs. 2-3 and 2-4, respectively. The magnitude of  $K_{Mg-Ca}$  indicates the relative preference of exchange sites for the  $Ca^{2+}$  and  $Mg^{2+}$  species. The shape of experimental isotherms for the Cecil soil was concave relative to the diagonal (for normalized plots of equivalent fractions of  $Mg^{2+}$  in the exchange phase plotted versus equivalent fractions of  $Mg^{2+}$

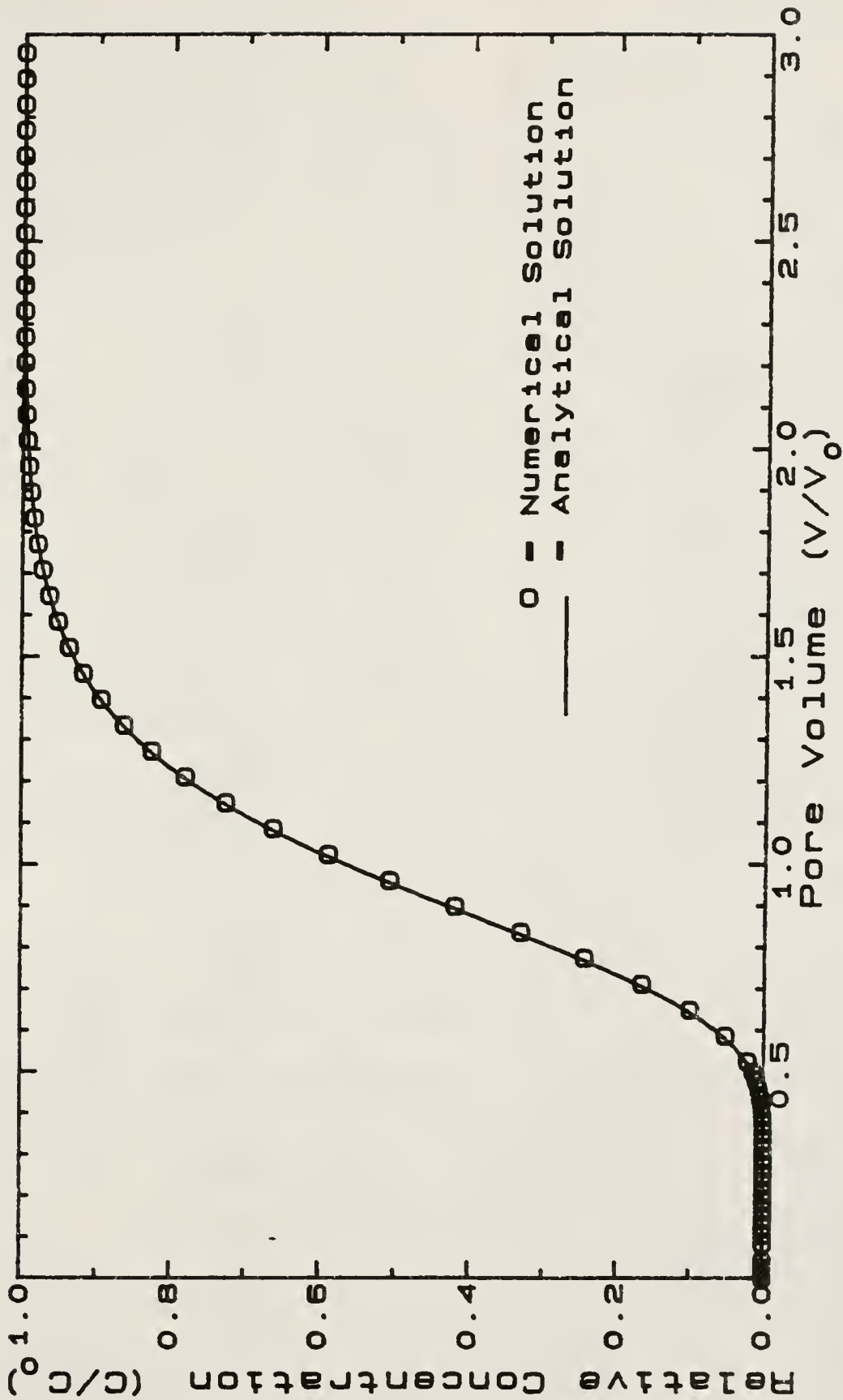


Figure 2-1 Numerical and analytical solutions obtained using topsoil parameters for the case where the binary exchange selectivity coefficient equals zero.

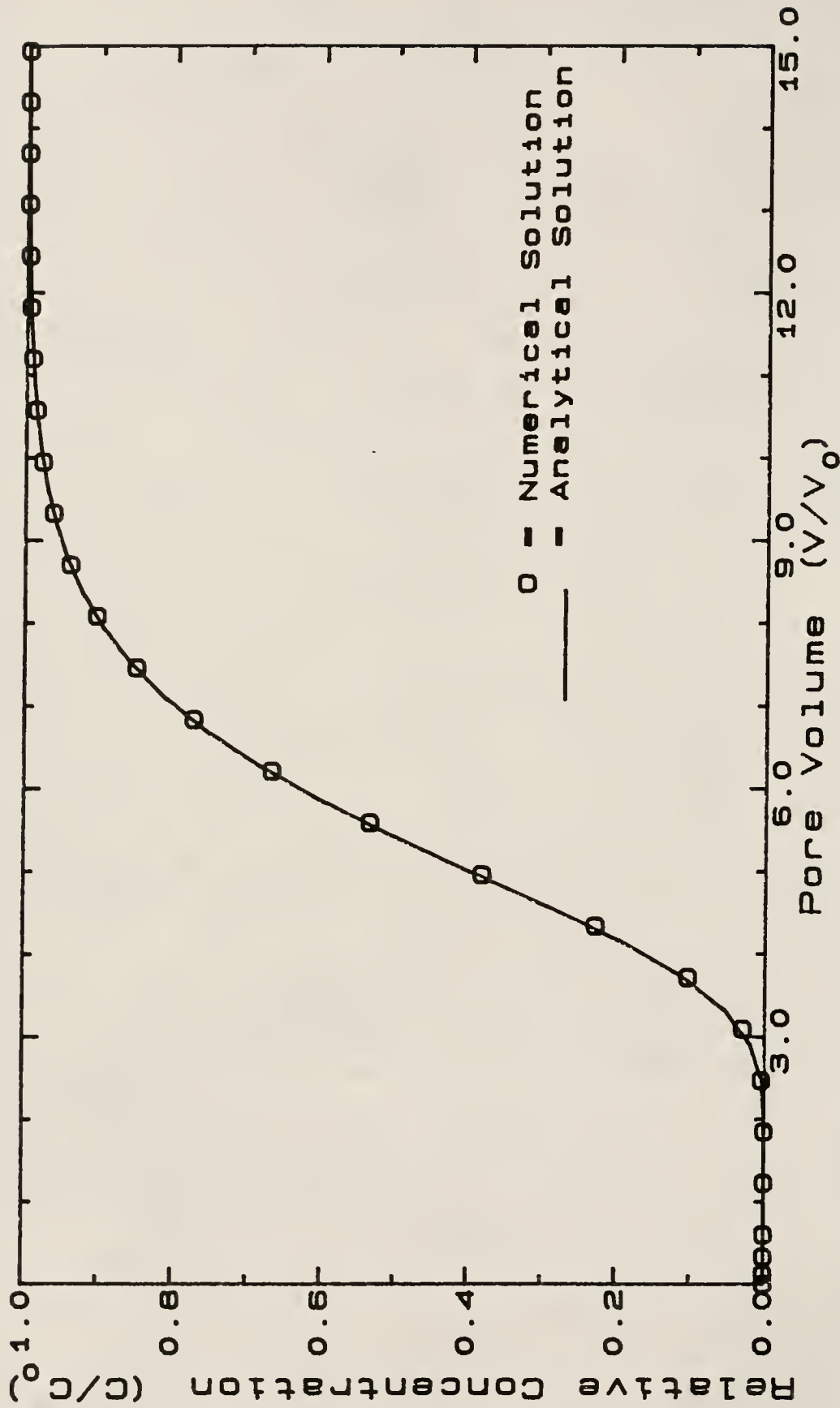


Figure 2-2 Numerical and analytical solutions obtained using topsoil parameters for the case where the exchange selectivity coefficient equals unity.

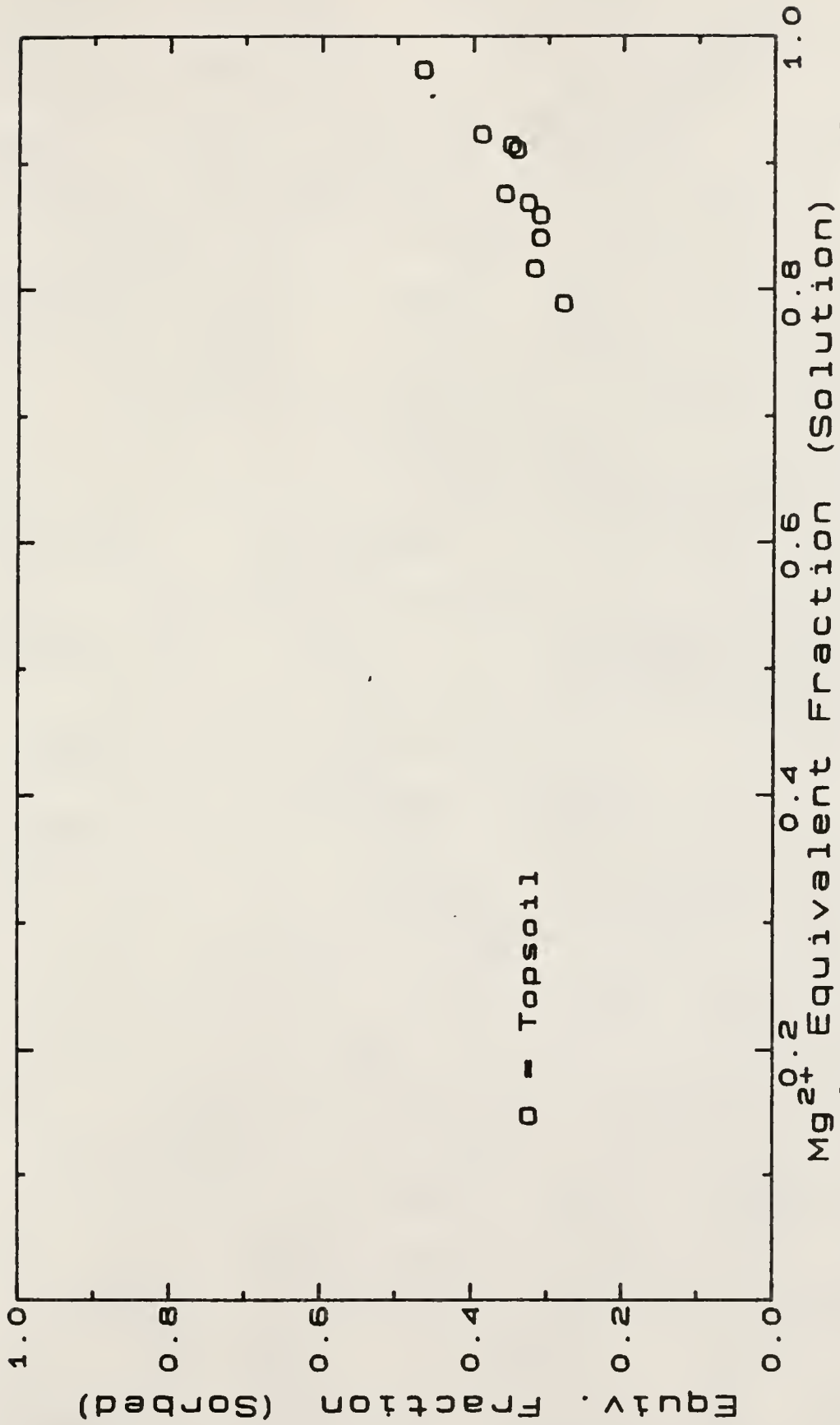


Figure 2-3  $Mg^{2+}$  exchange isotherm curve obtained from the topsoil column after miscible displacement with 4.5 pore volumes.

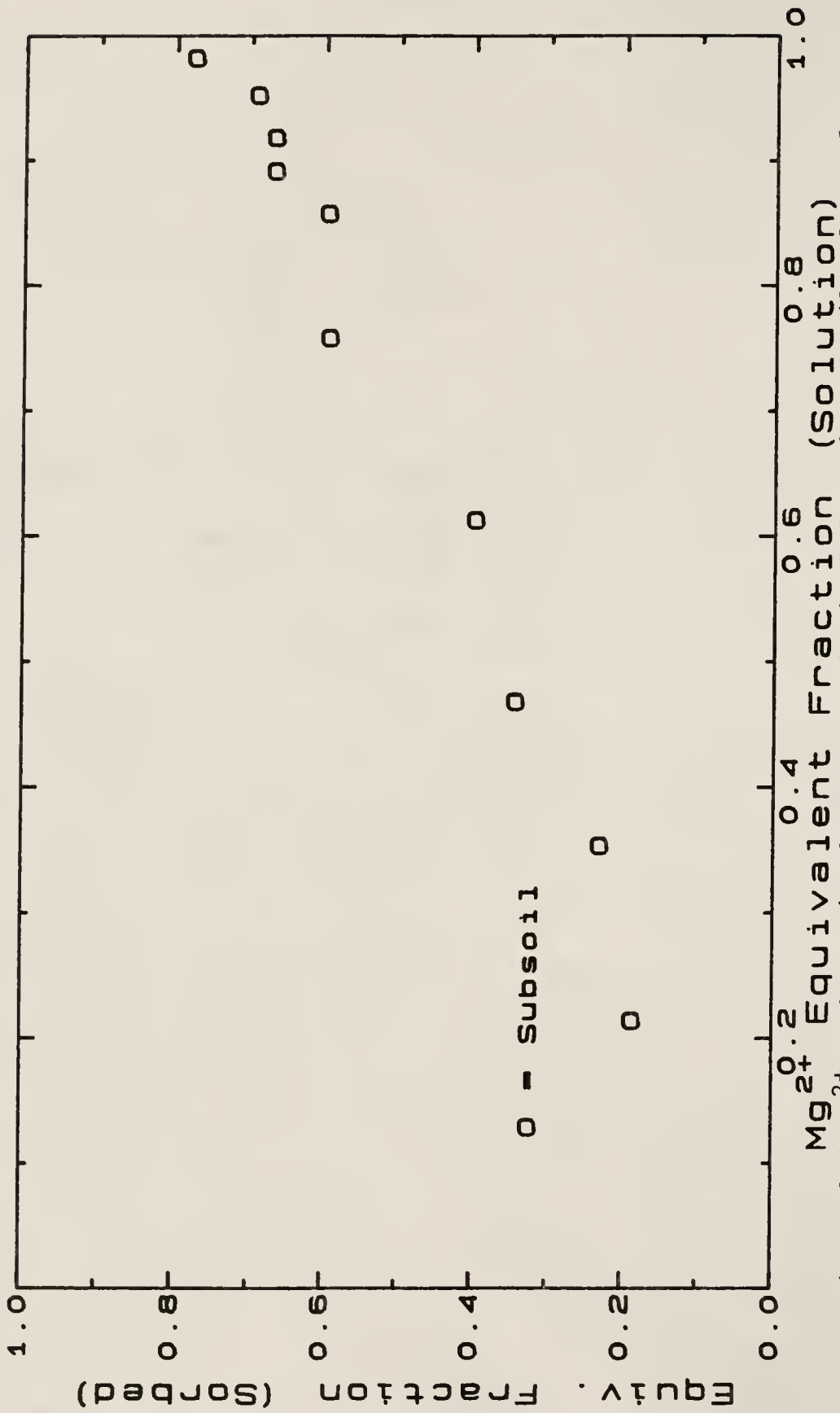


Figure 2-4  $Mg^{2+}$  exchange isotherm curve obtained from the subsoil column after miscible displacement with 3.6 pore volumes.

in the solution phase). The selectivity coefficients for  $\text{Mg}^{2+} \rightarrow \text{Ca}^{2+}$  exchange are considerably less than unity at all values of solution concentration, implying that exchange sites in Cecil topsoil and subsoil preferred  $\text{Ca}^{2+}$  over  $\text{Mg}^{2+}$ . The observed effect was greater for subsoil than for topsoil, however. After displacing 4.5 pore volumes of effluent through the topsoil,  $\text{Mg}^{2+}$  occupied 30% to 60% of the cation exchange capacity throughout the column. After displacing 3.6 pore volume of effluent through the subsoil, however,  $\text{Mg}^{2+}$  occupied from 15% to 80% of the cation exchange capacity. The average of the total solution cation concentrations in both the topsoil and subsoil columns was about 3% less than the  $C_T$  value (Tables 2-3 and 2-4). This 3% may represent the  $\text{H}^+$  concentration in the solution phase. The average of the total cation content on the exchange sites of topsoil and subsoil columns was about 37% less than the corresponding  $\bar{C}_T$  value (Tables 2-3 and 2-4). The displacing cation  $\text{Ca}^{2+}$ , although initially saturating the soil exchange sites, due to the unknown masking effects of interlayer-hydroxy vermiculite ( $\text{M}^+(\text{Mg},\text{Fe})_3(\text{Si},\text{Al})_4\text{O}_{10}(\text{OH})_2$ ) could become a non-exchange cation.

#### Exchange selectivity Coefficients ( $K_s$ ) for Soil Columns

From the soil-column experiments, concentrations of cations in the solution and exchange phases are given in Tables 2-3 and 2-4 for Cecil topsoil and subsoil, respectively. The selectivity coefficients ( $K_{\text{Mg-Ca}}$ ) were obtained by using equation [2-14]. The cation exchange

Table 2-3 Concentrations of cations in solution and exchange phases for topsoil after miscible displacement with 4.5 pore volume

Depth (cm)	Ca	Mg	K	Na	Al	Sum
	Solution phase					
	mmole(+) L <sup>-1</sup>					
1	0.224	9.050	0.231	0.348	0.014	9.867
2	0.188	9.150	0.174	0.459	0.016	9.987
3	0.184	8.990	0.143	0.414	0.016	9.747
4	0.211	8.670	0.127	0.470	0.016	9.494
5	0.319	8.560	0.311	0.599	0.013	9.802
6	0.259	8.590	0.127	0.459	0.016	9.451
7	0.323	8.780	0.341	0.517	0.013	9.974
8	0.419	8.160	0.272	0.334	0.012	9.197
9	0.511	11.900	0.409	0.487	0.013	13.320
10	0.387	8.560	0.262	0.431	0.012	9.652
11	0.547	8.330	0.346	0.894	0.013	10.130
12	0.459	8.230	0.272	0.424	0.012	9.397
13	0.487	8.230	0.270	0.327	0.012	9.326
14	0.523	7.900	0.256	0.410	0.013	9.102
15	0.607	8.030	0.256	0.435	0.013	9.341
16	0.675	7.670	0.260	0.348	0.013	8.966
17	0.705	7.960	0.274	0.485	0.019	9.443
18	0.799	8.070	0.327	0.434	0.017	9.647
19	0.898	7.340	0.149	0.334	0.017	8.738
20	0.978	7.410	0.258	0.431	0.016	9.093

Depth (cm)	Ca	Mg	K	Na	Average	9.684
	Exchange phase				Al	Sum
	mmole(+) kg <sup>-1</sup> soil					
1	0.609	6.580	0.125	0.265	*	*
2	0.614	4.940	0.146	0.257	4.280	10.237
3	0.544	4.860	0.113	0.261	*	*
4	0.564	4.120	0.107	0.265	5.592	10.648
5	0.584	3.950	0.133	0.270	*	*
6	0.659	3.700	0.113	0.261	5.792	10.525
7	0.589	3.460	0.105	0.270	*	*
8	0.664	3.460	0.125	0.257	5.859	10.365
9	0.709	3.790	0.110	0.257	*	*
10	0.828	3.620	0.128	0.261	5.826	10.663
11	0.813	3.540	0.194	0.287	*	*
12	0.973	3.790	0.141	0.278	5.992	11.174
13	0.913	3.540	0.164	0.270	*	*
14	0.938	3.290	0.153	0.287	5.603	10.271
15	1.060	3.790	0.166	0.261	*	*
16	1.070	3.370	0.189	0.278	5.692	10.599
17	1.100	3.210	0.248	0.270	*	*
18	1.140	3.290	0.177	0.283	5.647	10.537
19	1.270	3.290	0.215	0.278	*	*
20	1.500	2.960	0.205	0.287	6.014	10.966

* undetermined	Average	10.598
----------------	---------	--------

Table 2-4 Concentrations of cations in solution and exchange phases for subsoil after miscible displacement with 3.6 pore volumes

Depth (cm)	Ca	Mg	K	Na	Al	Sum
	Solution phase					
	mmole(+) L <sup>-1</sup>					
1	0.188	9.420	0.143	0.470	0.064	10.285
2	0.148	9.510	0.190	0.518	0.060	10.426
3	0.148	9.250	0.176	0.511	0.056	10.141
4	0.144	9.220	0.135	0.483	0.055	10.037
5	0.212	8.950	0.205	0.435	0.052	9.854
6	0.244	8.890	0.203	0.424	0.051	9.812
7	0.224	8.490	0.131	0.477	0.049	9.371
8	0.299	8.630	0.137	0.497	0.048	9.611
9	0.435	8.760	0.174	0.351	0.044	9.764
10	0.667	8.300	0.258	0.407	0.042	9.674
11	0.853	8.110	0.240	0.370	0.040	9.613
12	1.600	7.340	0.184	0.306	0.039	9.469
13	2.110	7.180	0.209	0.282	0.019	9.800
14	3.450	5.930	0.276	0.337	0.024	10.017
15	3.730	5.730	0.143	0.157	0.024	9.784
16	4.420	4.530	0.171	0.157	0.021	9.299
17	5.140	3.790	0.258	0.209	0.022	9.419
18	5.360	3.420	0.194	0.170	0.020	9.164
19	5.540	3.620	0.269	0.235	0.020	9.684
20	6.560	2.070	0.371	0.365	0.016	9.382

Depth (cm)	Ca	Mg	K	Na	Average Al	9.731 Sum
	Exchange phase					
	mmole(+) Kg <sup>-1</sup>					
1	0.609	13.700	0.177	0.235	*	*
2	0.509	13.000	0.184	0.226	1.993	15.912
3	0.489	12.100	0.197	0.243	*	*
4	0.549	11.600	0.258	0.243	4.663	17.313
5	0.499	11.300	0.230	0.226	*	*
6	0.589	11.200	0.235	0.226	4.974	17.224
7	0.599	10.900	0.238	0.235	*	*
8	0.793	11.200	0.287	0.243	4.396	16.919
9	0.913	10.000	0.317	0.243	*	*
10	1.300	10.500	0.333	0.235	4.072	16.440
11	1.200	9.960	0.243	0.226	*	*
12	2.590	9.710	0.266	0.226	4.264	17.056
13	3.540	7.570	0.261	0.252	*	*
14	4.340	6.670	0.304	0.243	4.266	15.824
15	6.090	5.760	0.279	0.235	*	*
16	4.740	7.160	0.289	0.261	4.511	16.961
17	8.280	4.530	0.312	0.217	*	*
18	8.930	3.870	0.327	0.226	4.534	17.887
19	9.430	3.130	0.404	0.243	*	*
20	10.300	2.470	0.476	0.235	5.190	18.671

\* undetermined

Average 17.020

capacity was approximated as being the average sum of the concentrations of  $\text{Ca}^{2+}$ ,  $\text{Mg}^{2+}$ ,  $\text{K}^+$ ,  $\text{Na}^+$ , and  $\text{Al}^{3+}$  in the exchange phase. Since 5 species were involved, the equivalent fractions of  $\text{Ca}^{2+}$  and  $\text{Mg}^{2+}$  did not sum to unity. Thus, values obtained for Ks were approximated. Values for  $K_{\text{Mg-Ca}}$  varied with depth since solution and exchange phases of cation concentrations varied and ranged from 0 to 1. In order to simplify model simulation,  $K_{\text{Mg-Ca}}$  was assumed constant, and the input value for  $K_{\text{Mg-Ca}}$  was obtained by taking the mean of  $K_{\text{Mg-Ca}}$  obtained for all depths for the Cecil topsoil and subsoil columns, respectively. The magnitude for  $K_{\text{Mg-Ca}}$  was 0.225 for Cecil topsoil, and 0.798 for Cecil subsoil, indicating that  $\text{Ca}^{2+}$  was preferred over  $\text{Mg}^{2+}$  by both topsoil and subsoil but that  $\text{Mg}^{2+}$  was preferred more by subsoil exchange sites than by topsoil exchange sites.

#### Model Sensitivity Analysis

A sensitivity analysis for dispersion coefficient (D), volumetric water content ( $\theta$ ), bulk density ( $\sigma$ ), selectivity coefficient ( $K_{\text{Mg-Ca}}$ ), and cation exchange capacity ( $\bar{C}_T$ ) was performed for the numerical model with respect to the experimental data from the soil columns.

Dispersion coefficient. Figures 2-5 and 2-6 present predicted and observed distributions for  $\text{Mg}^{2+}$  concentrations in the soil solution phase with column depth where a sensitivity analysis was performed for the dispersion coefficient (D) for both topsoil and subsoil. Dispersion

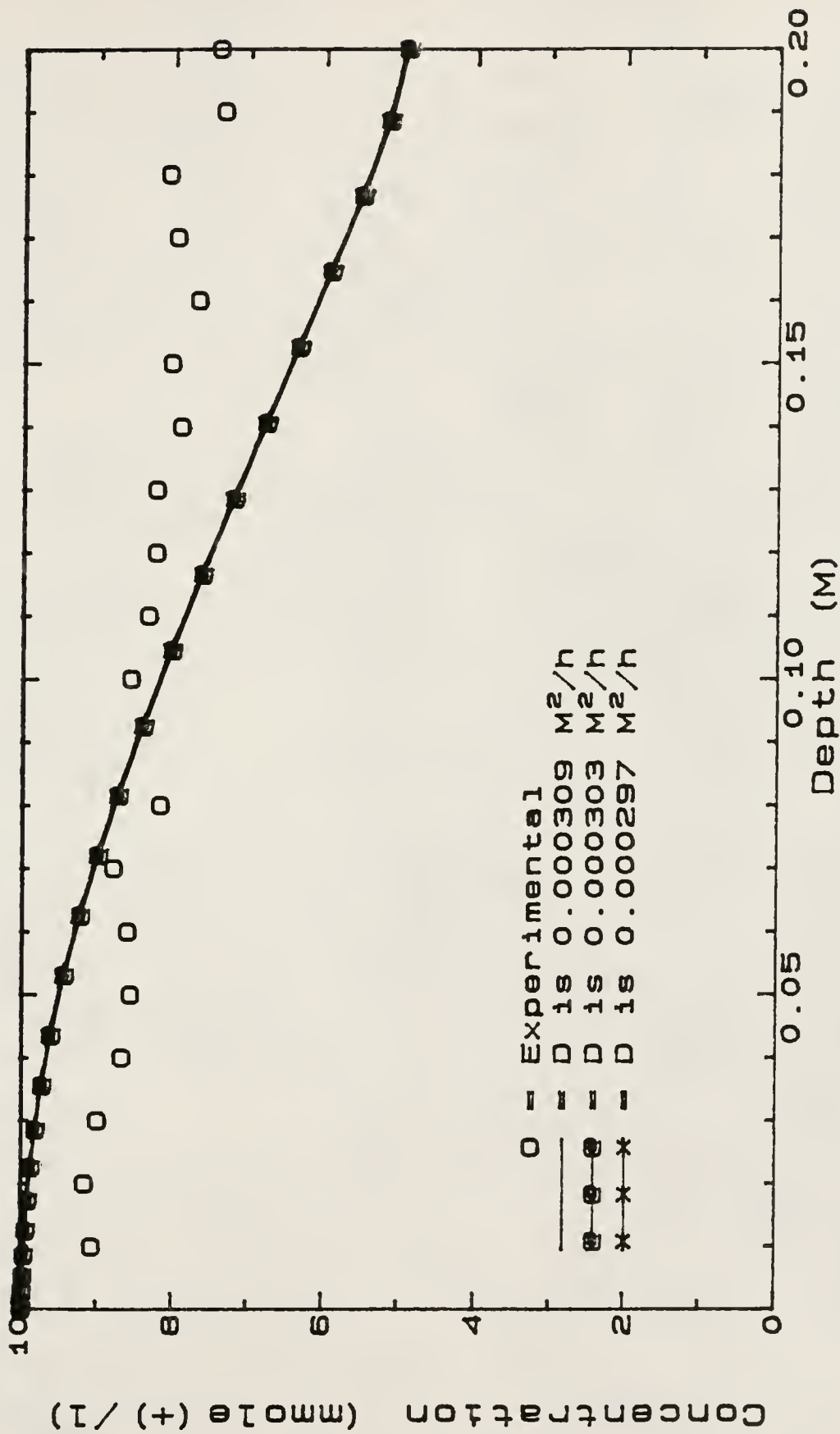


Figure 2-5 Experimental distributions of  $Mg^{2+}$  concentrations in the solution phase of the topsoil column after miscible displacement with 4.5 pore volumes, along with calculated results obtained using three values for the dispersion coefficient.

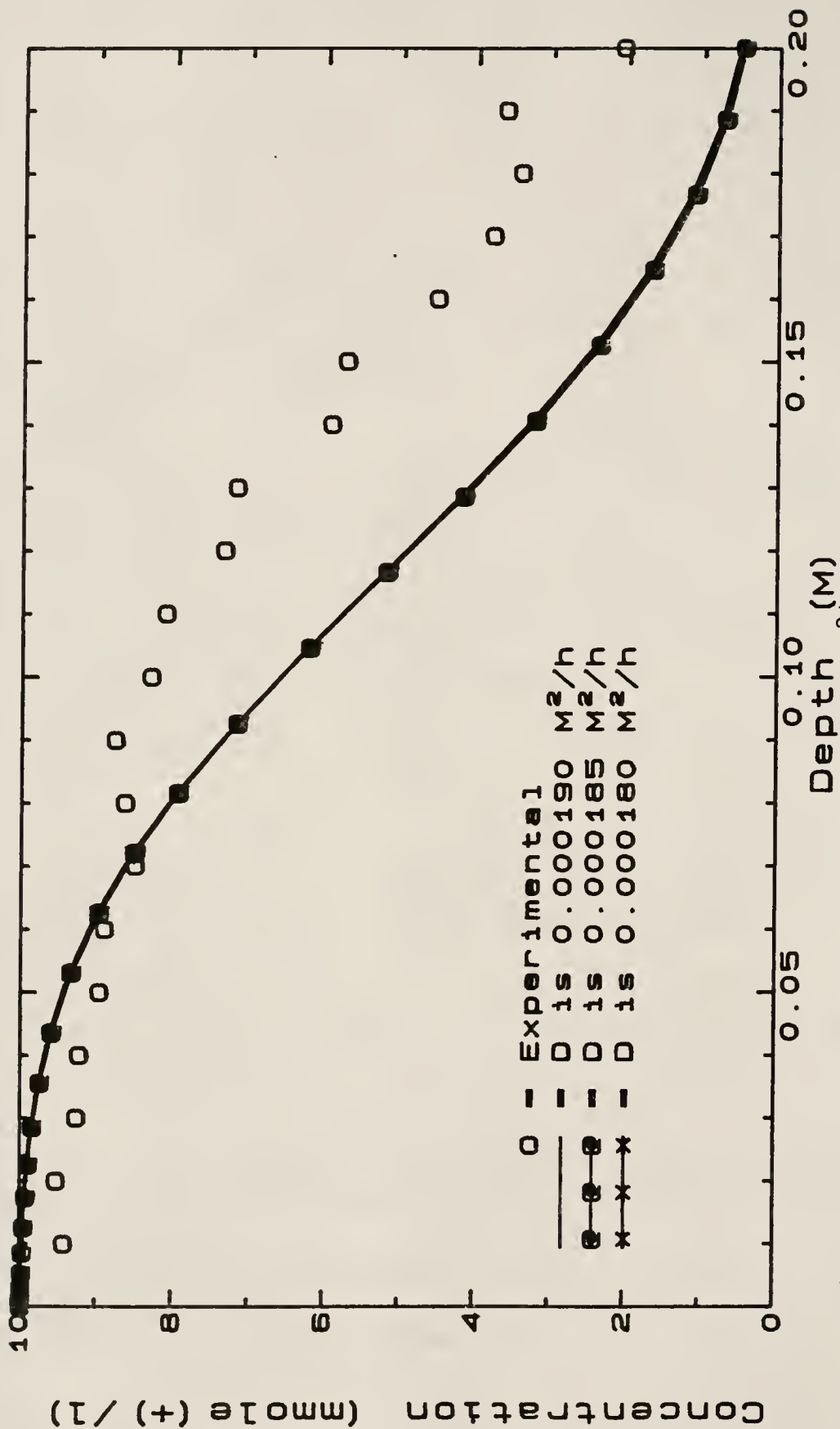


Figure 2-6 Experimental distributions of  $Mg^{2+}$  concentrations in the solution phase of the subsoil column after miscible displacement with 3.6 pore volumes, along with calculated results obtained using three values for the dispersion coefficient.

coefficients (D) of  $1.85 \times 10^{-4}$  and  $3.03 \times 10^{-4} \text{ m}^2/\text{h}$  were obtained from experimental  $\text{Cl}^-$  breakthrough curves for subsoil and topsoil columns, respectively. Values of the dispersion coefficient that had  $\pm 2\%$  deviation from experimental dispersion coefficients were used in model simulations for both topsoil and subsoil. Experimental and simulated cation-concentration distributions for D values of  $3.09 \times 10^{-4}$ ,  $3.06 \times 10^{-4}$  and  $3.03 \times 10^{-4} \text{ M}^2 \text{ h}^{-1}$  for the topsoil column are presented in Fig. 2-5. Experimental and simulated cation-concentration distributions for D values of  $1.90 \times 10^{-4}$ ,  $1.85 \times 10^{-4}$ , and  $1.80 \times 10^{-4} \text{ M}^2 \text{ h}^{-1}$  for the subsoil column are presented in Fig. 2-6. For both topsoil and subsoil columns, the effect of  $\pm 2\%$  variation in D upon predicted profiles of  $\text{Mg}^{2+}$  in the solution phase was extremely small. This analysis revealed that the model is relatively insensitive to small changes in values of D.

In these simulations, the effect of the dispersion coefficient upon distributions of  $\text{Mg}^{2+}$  concentration in the soil was apparently slight due to the fact that the dispersion coefficient is independent from the cation-retardation factor R.

Volumetric water content. Predicted and observed distributions of  $\text{Mg}^{2+}$  concentration in the solution phase with column depth are presented in Figs. 2-7 (topsoil) and 2-8 (subsoil), where a sensitivity analysis was performed with respect to the volumetric water content ( $\theta$ ). Average volumetric water contents obtained experimentally from

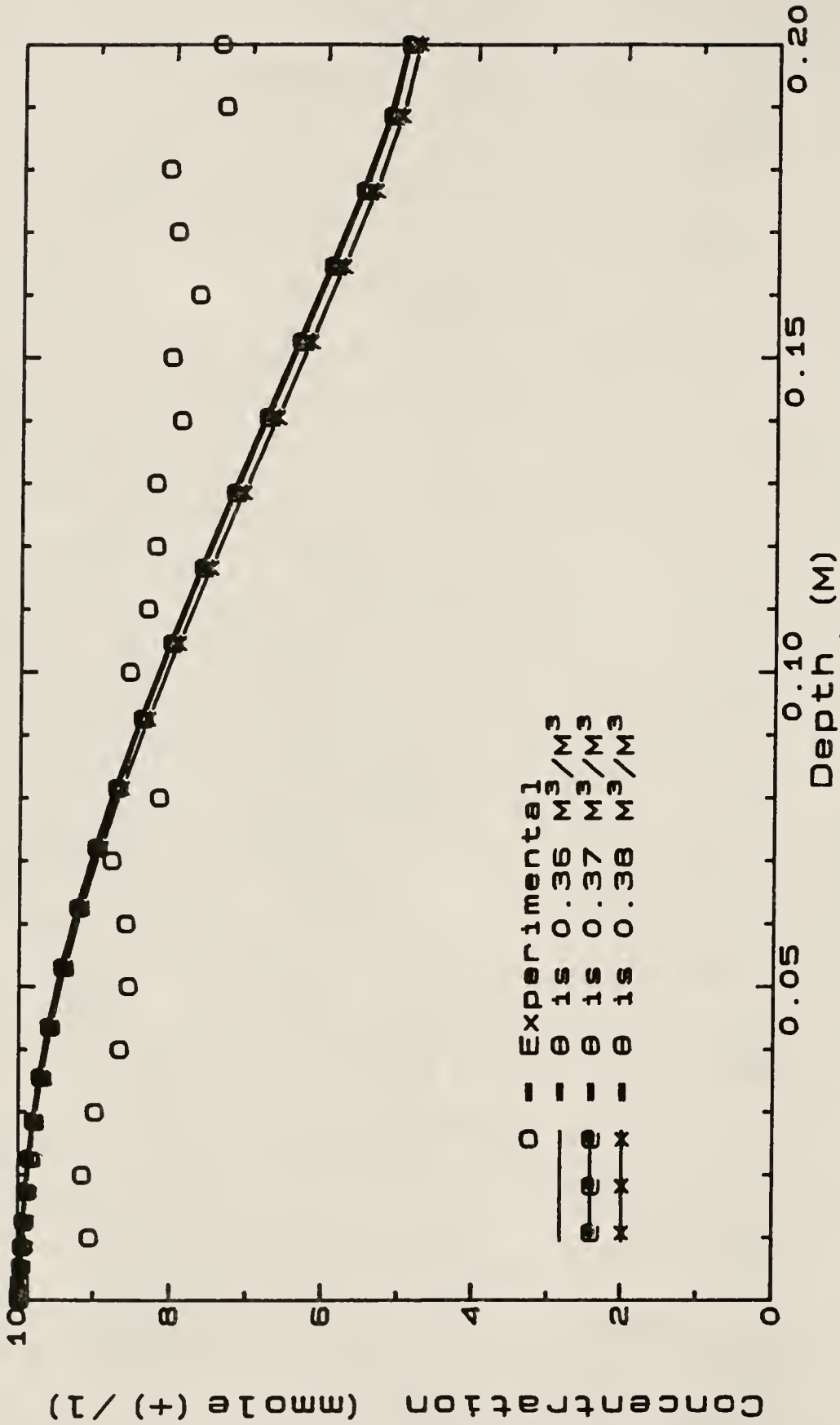


Figure 2-7 Experimental distributions of  $Mg^{2+}$  concentrations in the solution phase of the topsoil column after miscible displacement with 4.5 pore volumes, along with calculated results obtained using three values for volumetric water content.

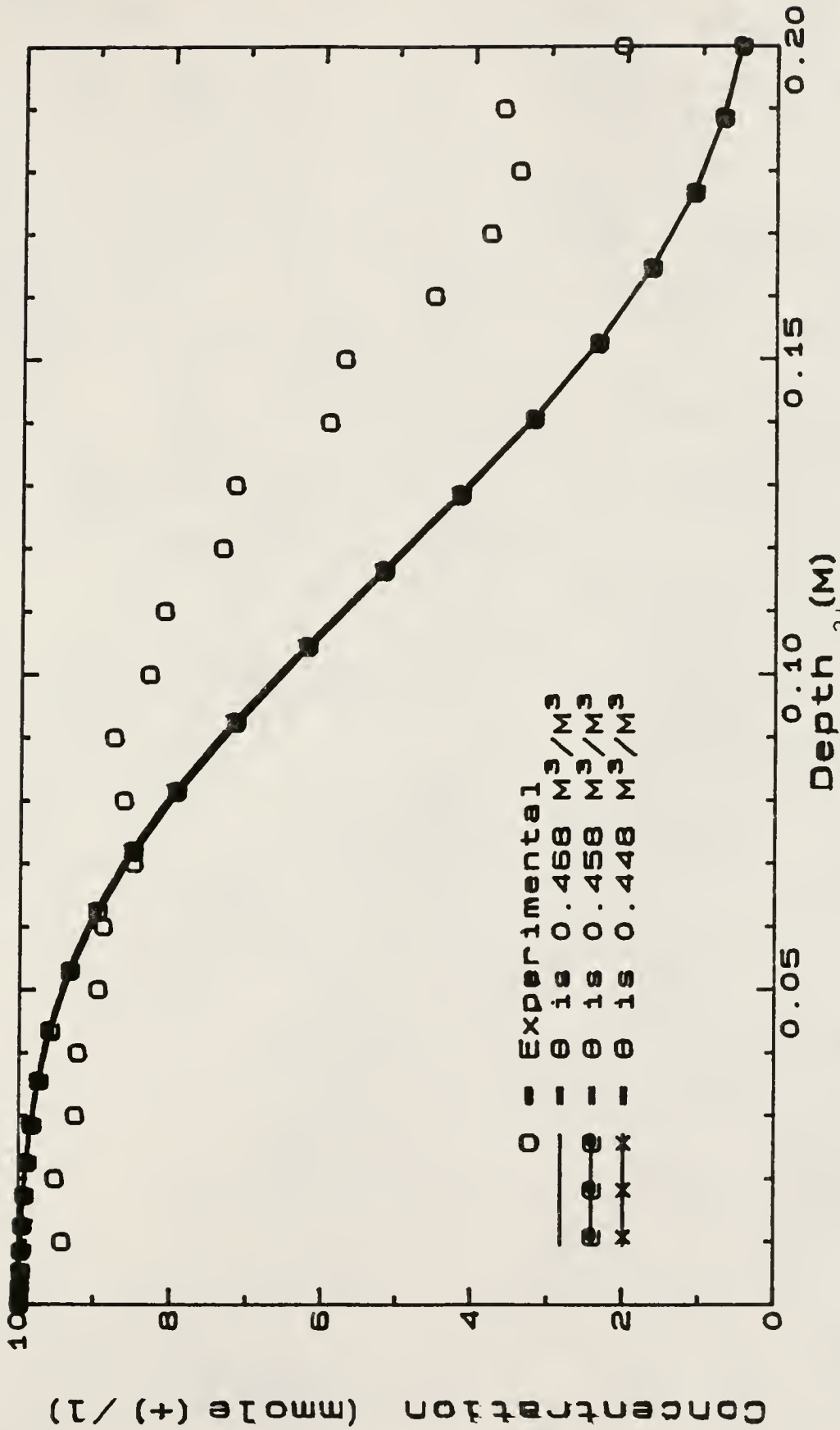


Figure 2-8 Experimental distributions of  $\text{Mg}^{2+}$  concentrations in the solution phase of the subsoil column after miscible displacement with 3.6 pore volumes, along with calculated results obtained using three values for the volumetric water content.

column experiments were  $0.370$  and  $0.458 \text{ M}^3 \text{ M}^{-3}$  for topsoil and subsoil, respectively. A range of volumetric water-content values of  $\pm 2\%$  deviation from the experimental data, such as  $0.360$  and  $0.380 \text{ M}^3 \text{ M}^{-3}$  for topsoil and  $0.468$  and  $0.448 \text{ M}^3 \text{ M}^{-3}$  for subsoil, respectively, was tested to determine the sensitivity of  $\theta$  as an input parameter to the model. Results show that the effect of variations in  $\theta$  on prediction of  $\text{Mg}^{2+}$  concentration was small for topsoil and had essentially no effect for subsoil. The effect of  $\theta$  is shown by the term  $\sigma/\theta$  (the soil-to-solution ratio) in the cation-retardation factor ( $R$ ). The smaller values of  $\theta$  give the higher ratios of  $\sigma/\theta$  and the most retarded cation movement.

Bulk density. Computed and observed depth distributions of  $\text{Mg}^{2+}$  concentration in the solution phase are given in Figs. 2-9 and 2-10, where a sensitivity analysis was performed for bulk density ( $\sigma$ ). Experimental bulk density values obtained from the column experiment were  $1.64$  and  $1.42 \text{ Mg M}^{-3}$  for topsoil and subsoil, respectively. Values with  $\pm 2\%$  deviation from the experimental data gave values of  $1.67$  and  $1.61 \text{ Mg M}^{-3}$  and  $1.45$  and  $1.39 \text{ Mg M}^{-3}$  for use in the sensitivity analysis, respectively. The effect of  $\sigma$  occurs through the ratio  $\sigma/\theta$  in  $R$ . The sensitivity analysis revealed that even slight changes in values for  $\sigma$  could substantially influence simulated cation concentrations.

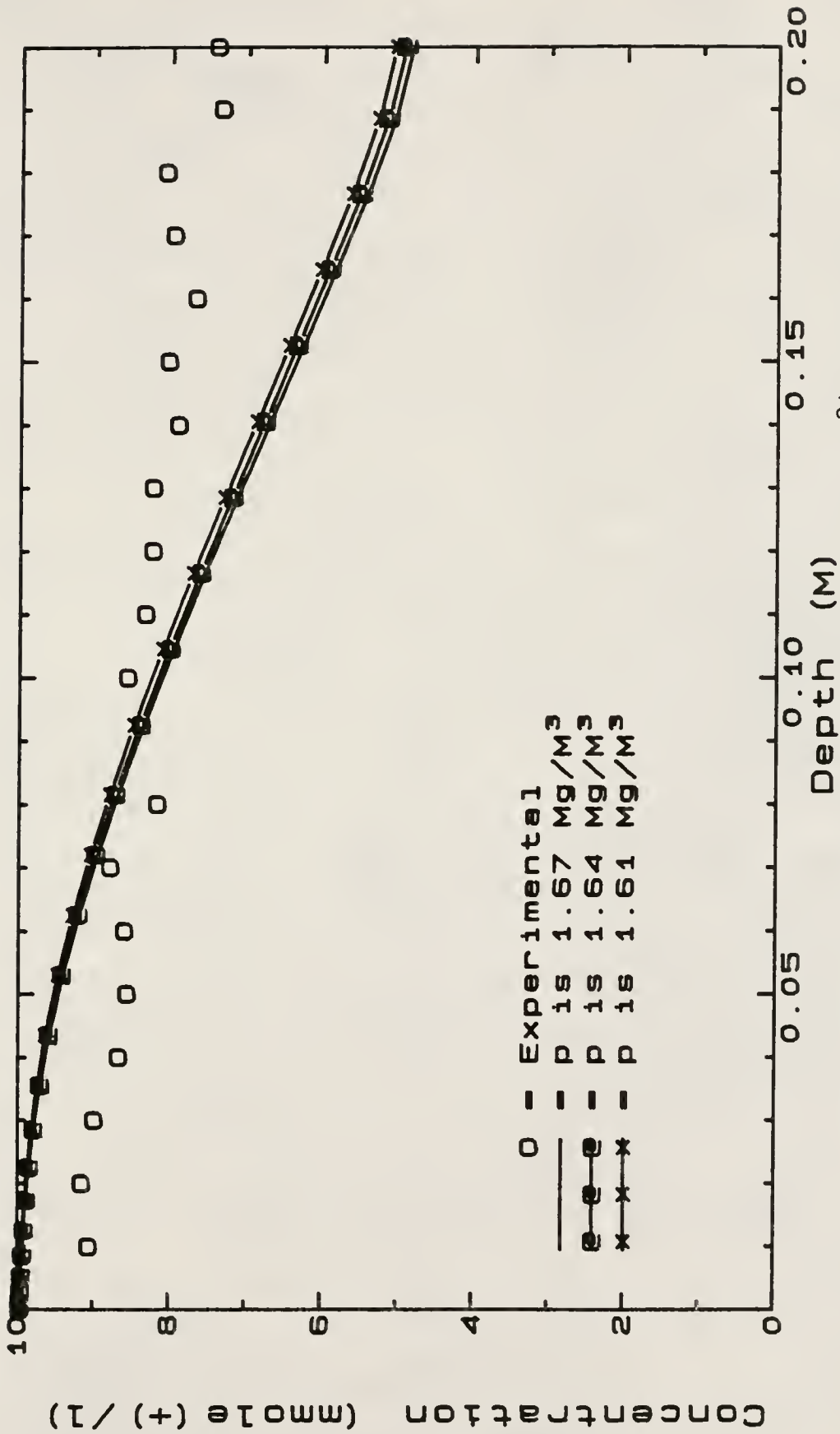


Figure 2-9 Experimental and simulated distributions of  $Mg^{2+}$  concentrations for three values of bulk density for the topsoil column after miscible displacement with 4.5 pore volumes.

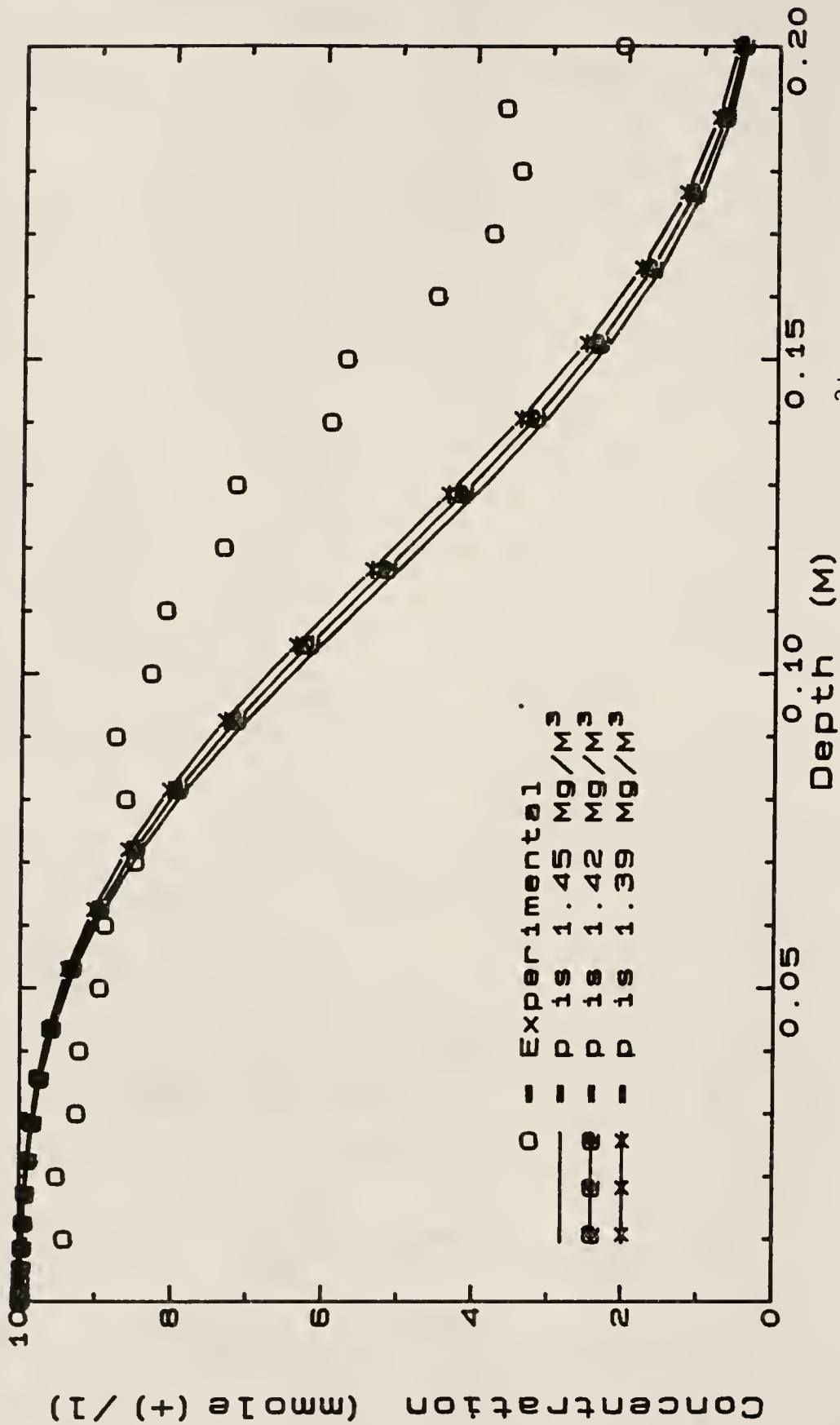


Figure 2-10 Experimental and simulated distributions of  $Mg^{2+}$  concentrations for three values of bulk density for the subsoil column after miscible displacement with 3.6 pore volumes.

Selectivity coefficient. Figs. 2-11 and 2-12 present simulated and observed distributions for  $\text{Mg}^{2+}$  in the solution phase with depth for topsoil and subsoil columns, respectively. The approximate selectivity coefficients ( $K_{\text{Mg-Ca}}$ ) obtained from column experiments were 0.225 and 0.798 for topsoil and subsoil, respectively. A deviation of  $\pm 2\%$  from these experimental values were used in simulations to determine sensitivity to this input parameter. These values were 0.230 and 0.220 for topsoil and 0.782 and 0.814 for subsoil, respectively. The effect of  $K_{\text{Mg-Ca}}$  upon the simulation of  $\text{Mg}^{2+}$  concentration distributions in the solution phase was minor for both topsoil and subsoil. Although the selectivity coefficient occurs within the cation retardation factor  $R$ , sensitivity analysis showed that slight changes in  $K_{\text{Mg-Ca}}$  had little effect upon the  $\text{Mg}^{2+}$ -concentration profile distribution.

Cation exchange capacity. Sensitivity of the model to change in cation exchange capacity ( $\bar{C}_T$  or CEC) was examined by using two values of CEC in separate simulations. Values of the CEC of 70 and 54 mmole(+)  $\text{Kg}^{-1}$  soil were obtained experimentally from the buffered 1 M  $\text{NH}_4\text{OAc}$  plus  $\text{BaCl}_2$ -TEA method, whereas values of 27 and 17 mmole(+)  $\text{Kg}^{-1}$  were obtained from the buffered 1 M  $\text{NH}_4\text{OAc}$  plus unbuffered 1 M  $\text{KCl}$  method, for original subsoil and topsoil, respectively. CEC values of 17.0 and 10.6 mmole(+)  $\text{Kg}^{-1}$  soil were the mean CEC values obtained from all dissected soil sections (Tables 2-3 and 2-4) in columns of subsoil and topsoil,

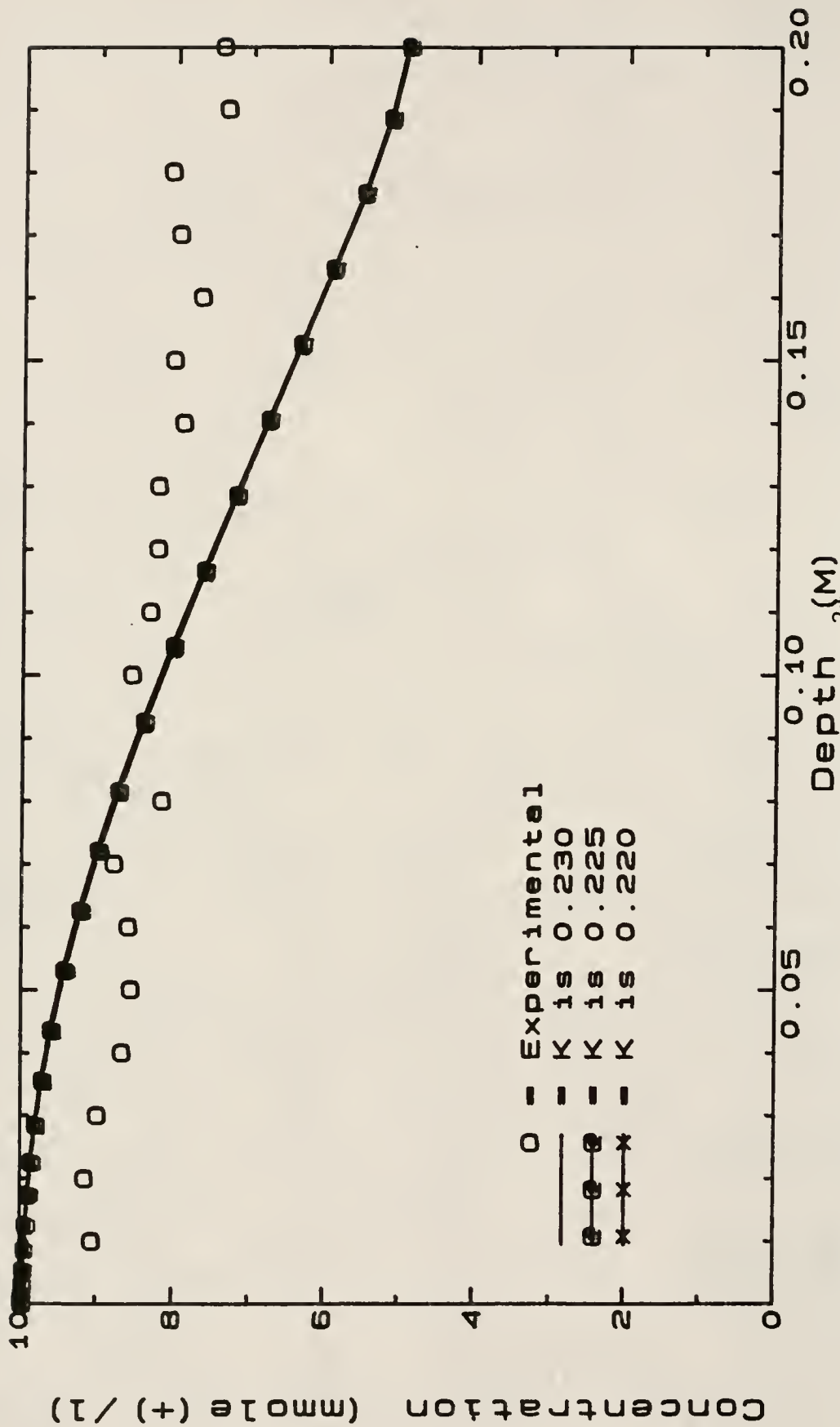


Figure 2-11 Experimental distributions of  $Mg^{2+}$  concentrations for the topsoil column after miscible displacement with 4.5 pore volumes, along with simulation results for three values of the selectivity coefficient.

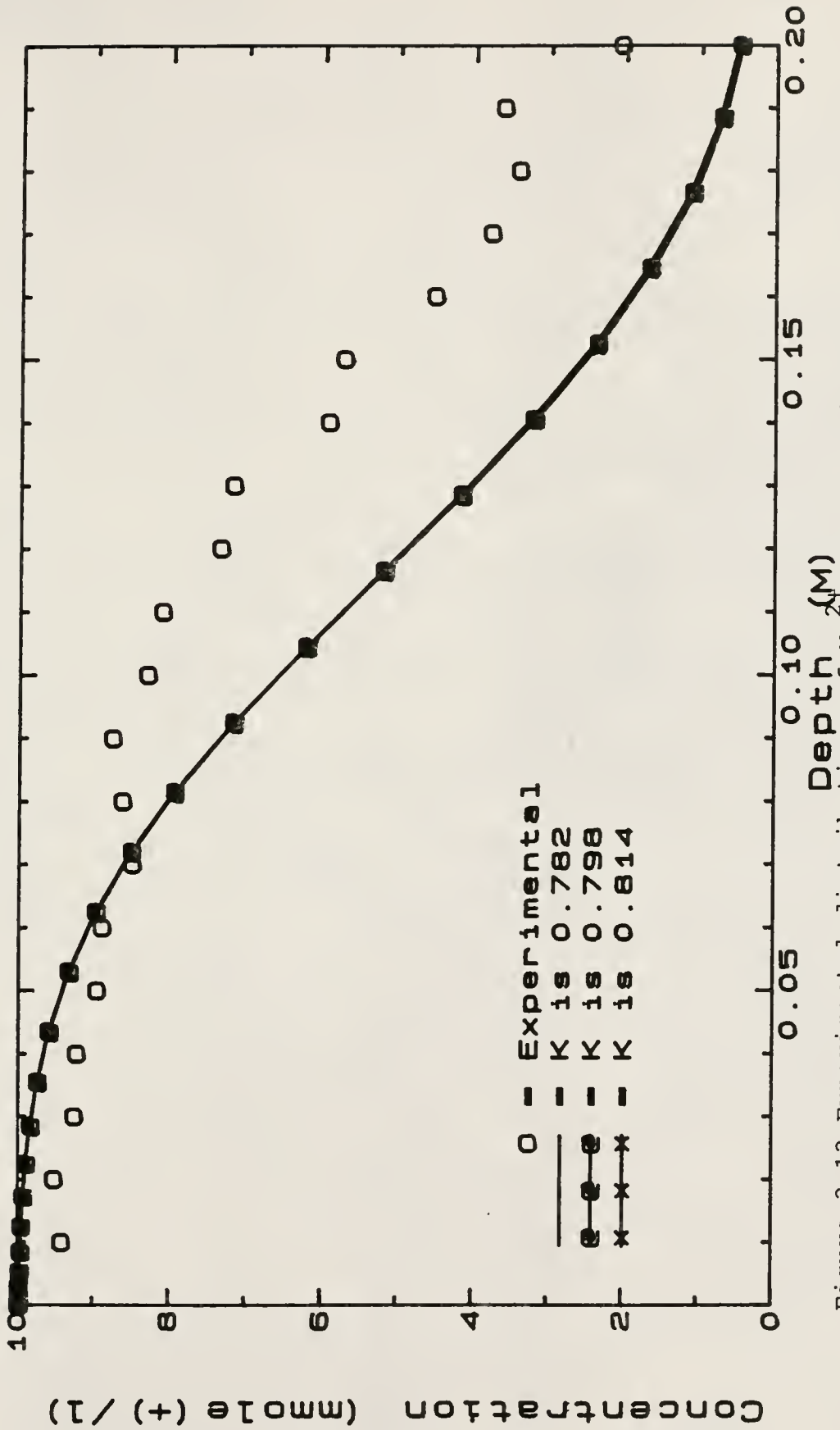


Figure 2-12 Experimental distributions of  $Mg^{2+}$  concentrations for the subsoil column after miscible displacement with 3.6 pore volumes, along with simulated results for three values of the selectivity coefficient.

respectively. The CEC for each section was obtained by extraction with buffered 1 M  $\text{NH}_4\text{OAc}$  plus unbuffered 1 M  $\text{KCl}$ , and then summing exchange-phase concentrations for  $\text{Ca}^{2+}$ ,  $\text{Mg}^{2+}$ ,  $\text{K}^+$ ,  $\text{Na}^+$  and  $\text{Al}^{3+}$ . The CEC for the last set of sections obtained from the soil column were used to represent the CEC for experimental columns of subsoil and topsoil, respectively. Column effluent pH values were below pH 4.5 for both columns (Fig. 2-23). This acidity could be coming from  $\text{Al}^{3+}$  which underwent exchange with  $\text{Ca}^{2+}$  and  $\text{Mg}^{2+}$ . The pH values of the input solutions were 5.5 for  $\text{CaCl}_2$  and 5.7 for  $\text{MgCl}_2$ .

Figures 2-13 and 2-14 demonstrate the dramatic model sensitivity to the cation exchange capacity parameter. The cation exchange capacity values used were 10.6 and 54.0  $\text{mmole}(+) \text{Kg}^{-1}$  soil for topsoil, and 17.0 and 70.0  $\text{mmole}(+) \text{Kg}^{-1}$  soil for subsoil, respectively. A large increase in CEC value the simulated movement of the  $\text{Mg}^{2+}$  front to be retarded during miscible displacement relative to the experimental data. This effect was greatest for the finer-textured Cecil subsoil.

Calculated and observed data did not coincide exactly for either the topsoil or subsoil columns. Overall, model-simulated curves for distributions of solution-phase concentrations of  $\text{Mg}^{2+}$  with depth best described experimental data when the smaller of the cation exchange capacity values were used. This result was as expected,

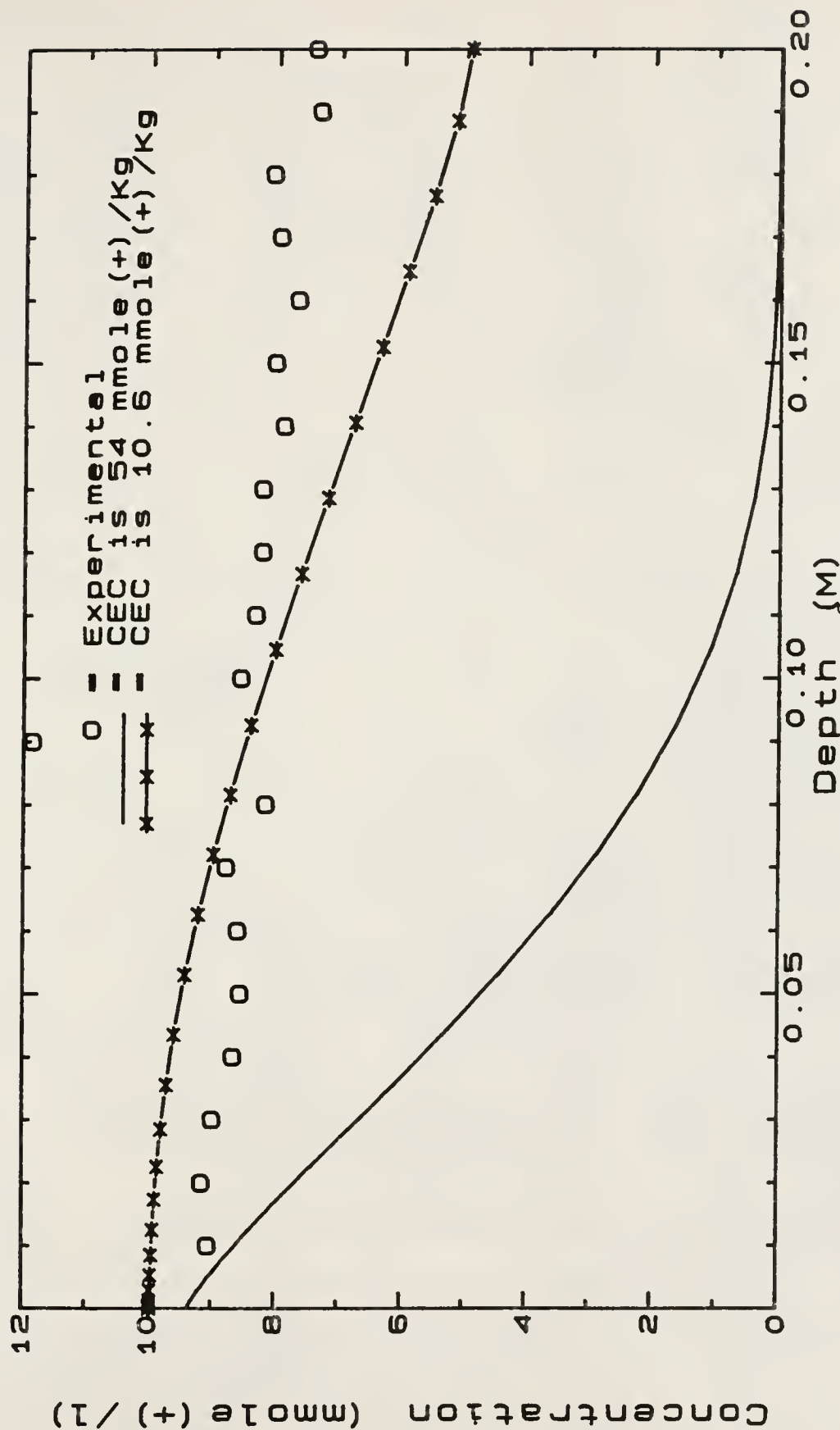


Figure 2-13 Experimental distributions of  $Mg^{2+}$  concentrations for the topsoil column after miscible displacement with 4.5 pore volumes, along with simulation results for two values of the cation exchange capacity.

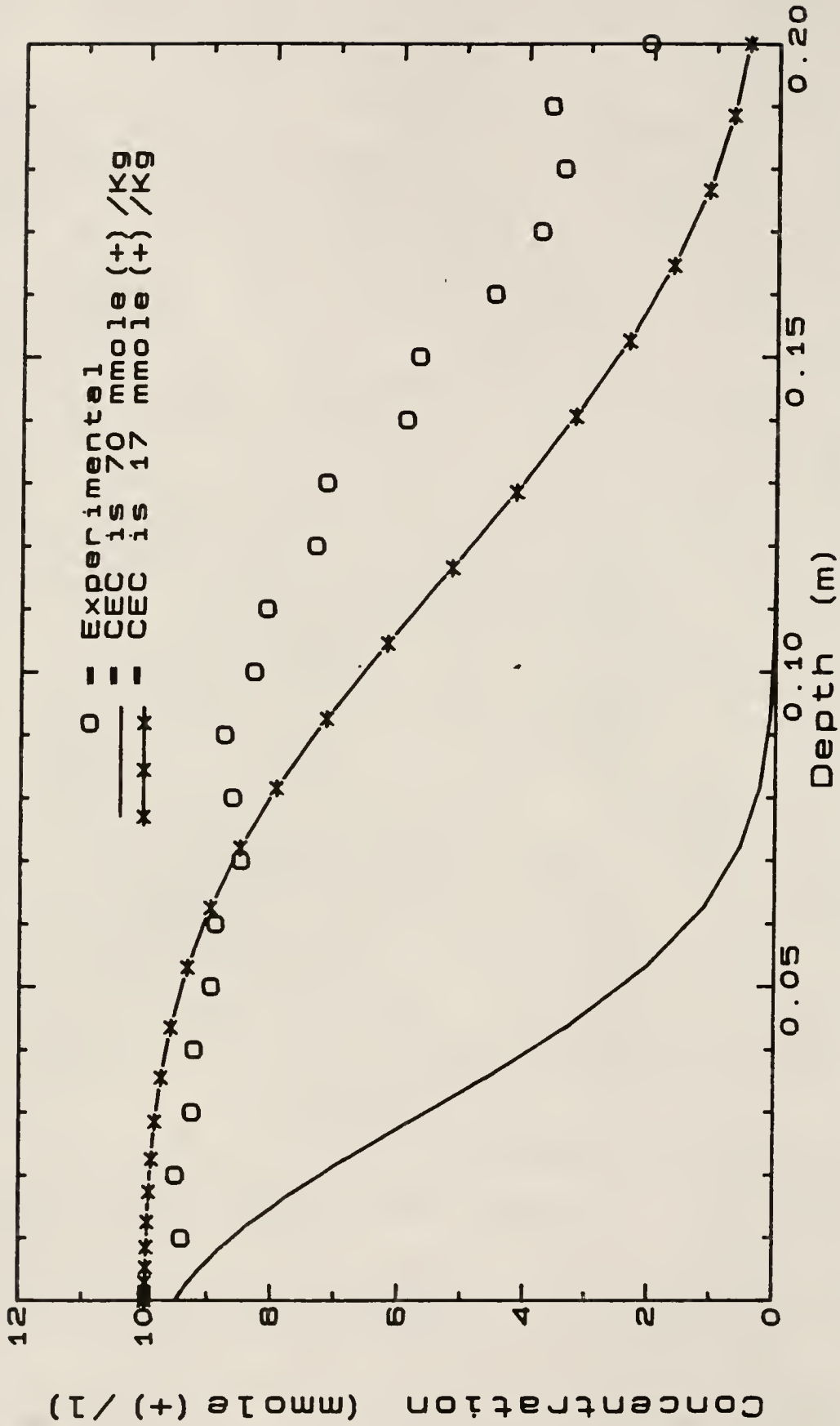


Figure 2-14 Experimental distributions of  $Mg^{2+}$  concentrations for the subsoil column after miscible displacement with 3.6 pore volumes, along with simulation results for two values of the cation exchange capacity.

since retardation  $R$  is a function of both  $\bar{C}_T$  and  $C_T$ . Therefore, using large values of CEC in the simulation would tend to retard cation movement.

Discrepancies observed between predicted and observed distributions of  $Mg^{2+}$  concentration using CEC values of 10.6 and 17.0 mmole(+)  $Kg^{-1}$  soil for topsoil and subsoil columns, respectively, were attributed to several factors. First, certain of the model assumptions were not strictly met. Careful examination of the soil system reveals that a contradiction occurs between some of the assumptions and reality. The cation exchange capacity was not constant but actually varied from point to point along the soil column as shown in Tables 2-3 and 2-4. At any given point, the extent that a specific ion could occupy soil exchange sites would also be affected by the presence of other ion species in the system. Exchangeable  $Al^{3+}$  comprised about 25% and 50% of total exchangeable cations for Cecil subsoil and topsoil, respectively, after leaching with  $MgCl_2$ . This probably means that  $Ca^{2+}$  occupied only 50-75% of the exchange sites initially, which is considerably less than 100% as assumed for the model. Experimental conditions involved  $Ca^{2+}$ ,  $Mg^{2+}$ ,  $Al^{3+}$ ,  $K^+$ ,  $Na^+$  and  $H^+$ , whereas the model assumptions only allowed for  $Ca^{2+}$  and  $Mg^{2+}$ . Model simulations performed here did not sufficiently account for this discrepancy.

Two other sets of cation exchange capacity values were calculated for Cecil topsoil and subsoil. The reason for

using these two additional sets of CEC values was to determine if exclusion of exchangeable  $\text{Al}^{3+}$  from the CEC, or if exclusion of all of the existing cations species except  $\text{Ca}^{2+}$  and  $\text{Mg}^{2+}$ , would improve simulated results. First, modified cation-exchange capacity values were obtained by summing the exchange phase concentrations of all cations species except  $\text{Al}^{3+}$  over all depths as given in Tables 2-3 and 2-4, and then taking means for topsoil and subsoil, respectively. Magnitudes for subsoil and topsoil were 12.73 and 4.97 mmole(+)  $\text{Kg}^{-1}$  soil, respectively. Using these modified cation exchange capacity values, calculated results for  $\text{Mg}^{2+}$  concentration distributions in solution and adsorbed phases are given in Figs. 2-15 and 2-16 for subsoil and in Figs. 2-17 and 2-18 for topsoil, respectively. Agreement between simulated and experimental data was better for the subsoil than for the topsoil. Simulations for  $\text{Mg}^{2+}$  concentrations in the topsoil showed an overestimation of  $\text{Mg}^{2+}$  concentrations in both the solution and exchange phases.

The second method for obtaining a better estimation of cation exchange capacity values was obtained by summing the exchange-phase concentrations of  $\text{Ca}^{2+}$  and  $\text{Mg}^{2+}$  for all depths (Tables 2-3 and 2-4) and then taking the mean for topsoil and subsoil, respectively. Magnitudes of CEC for subsoil and topsoil were 12.1 and 4.7 mmole(+)  $\text{Kg}^{-1}$  soil, respectively. Based upon these second modified CEC values, predicted results for distributions of  $\text{Mg}^{2+}$  concentrations

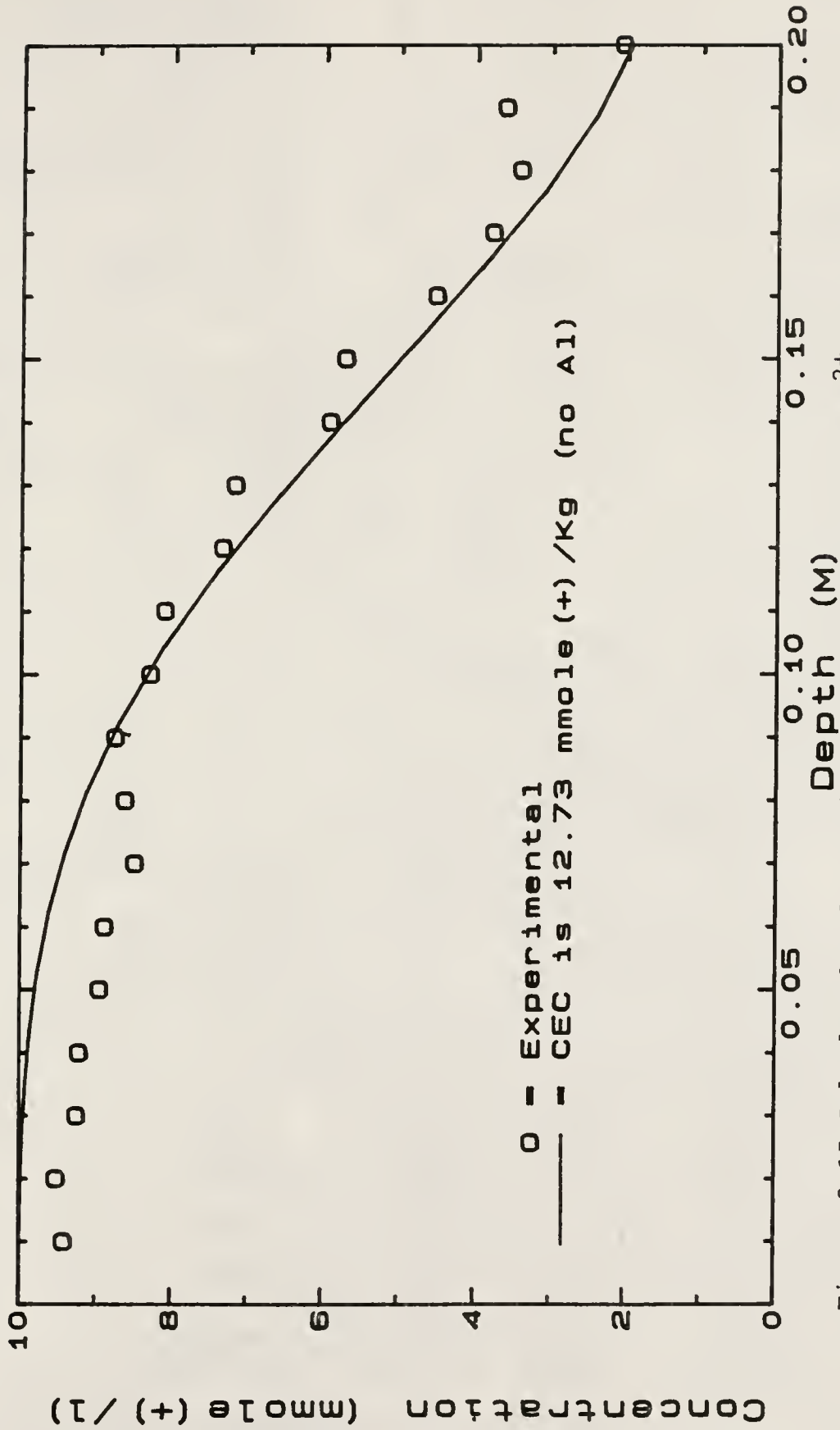


Figure 2-15 Calculated and experimental distributions of  $Mg^{2+}$  concentrations in the solution phase for the subsoil column after miscible displacement with 3.6 pore volumes.

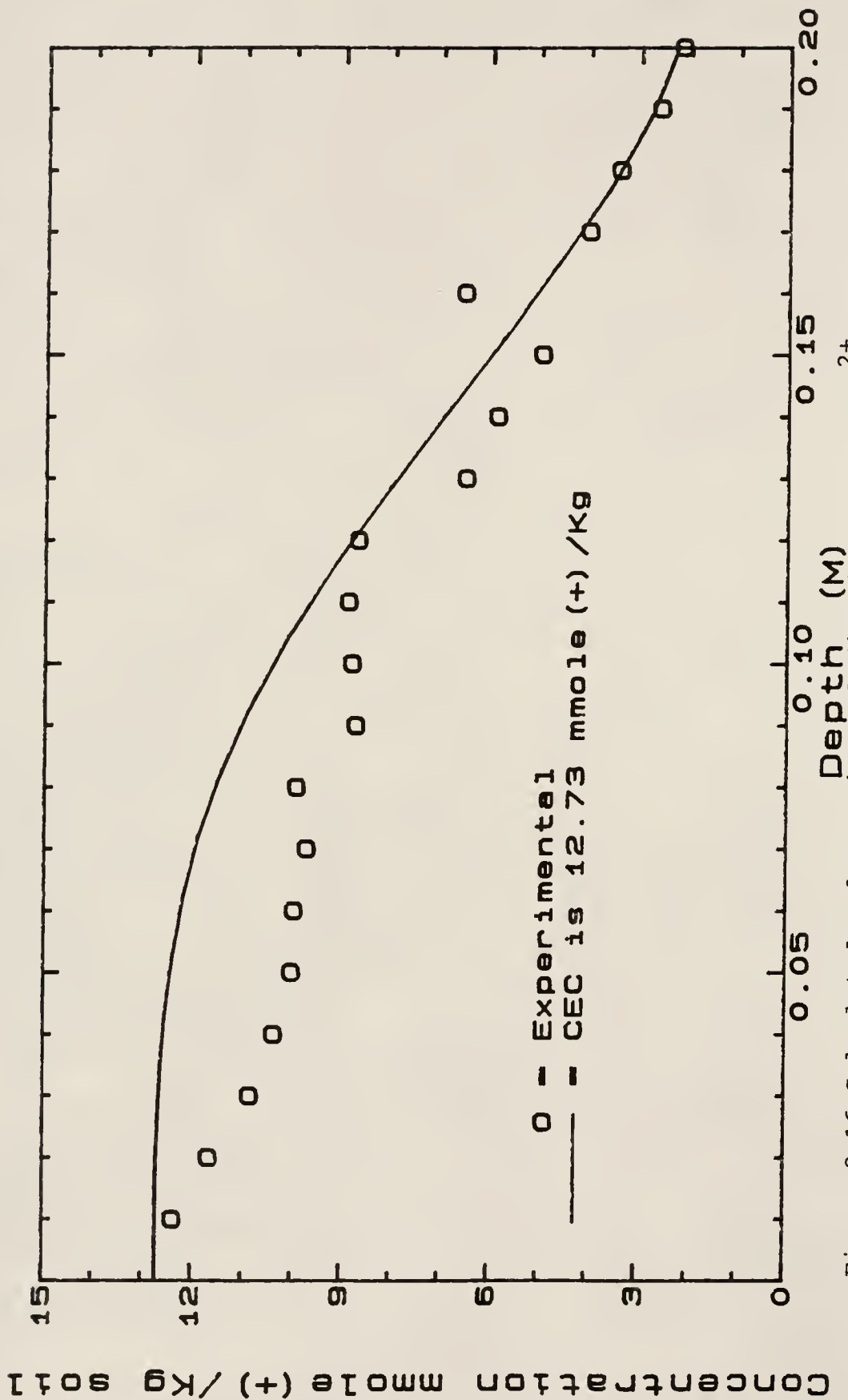


Figure 2-16 Calculated and experimental distributions of  $Mg^{2+}$  concentrations in the exchange phase for the subsoil column after miscible displacement with 3.6 pore volumes.

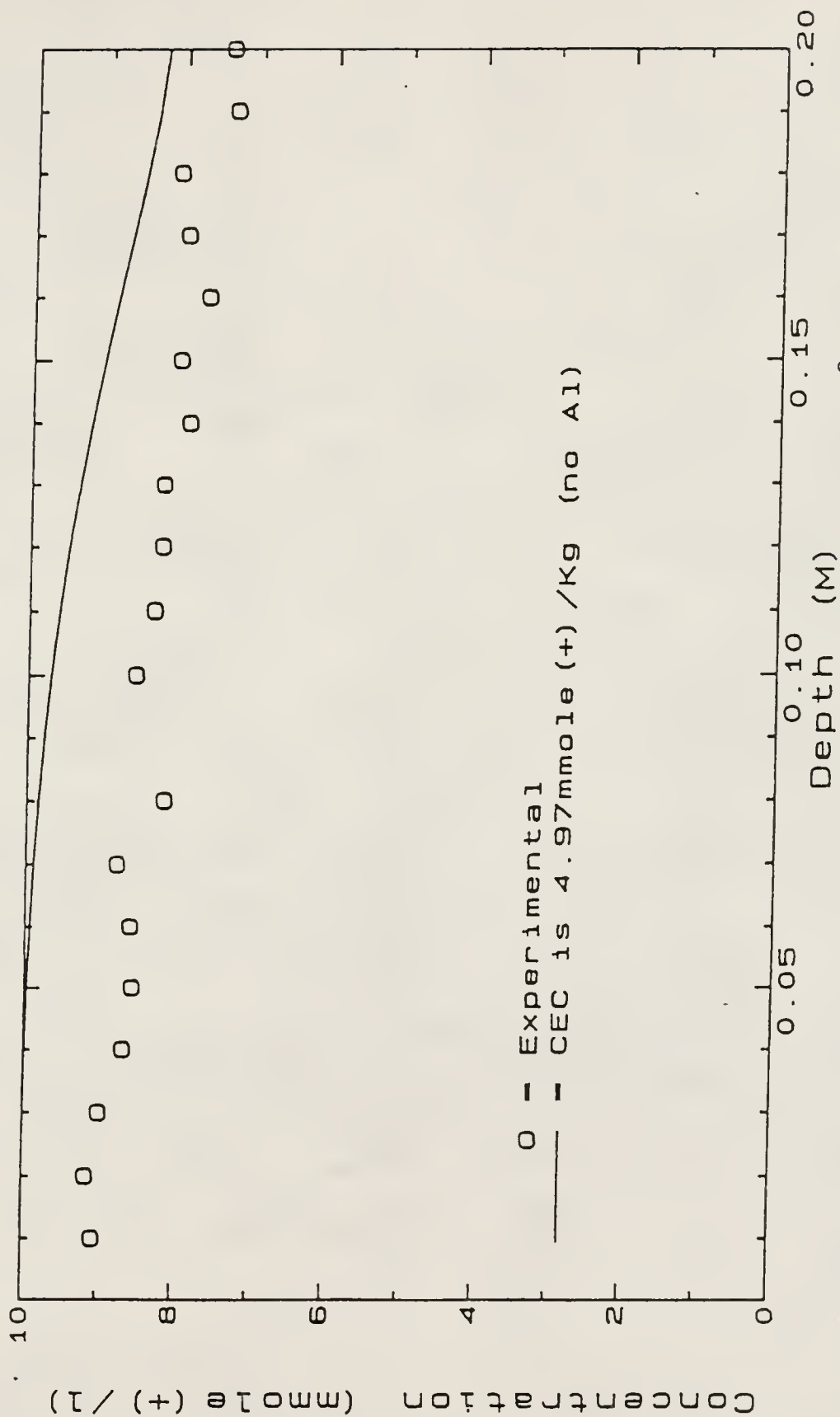


Figure 2-17 Calculated and experimental distributions of  $Mg^{2+}$  concentrations in the solution phase for the topsoil column after miscible displacement with 4.5 pore volumes.

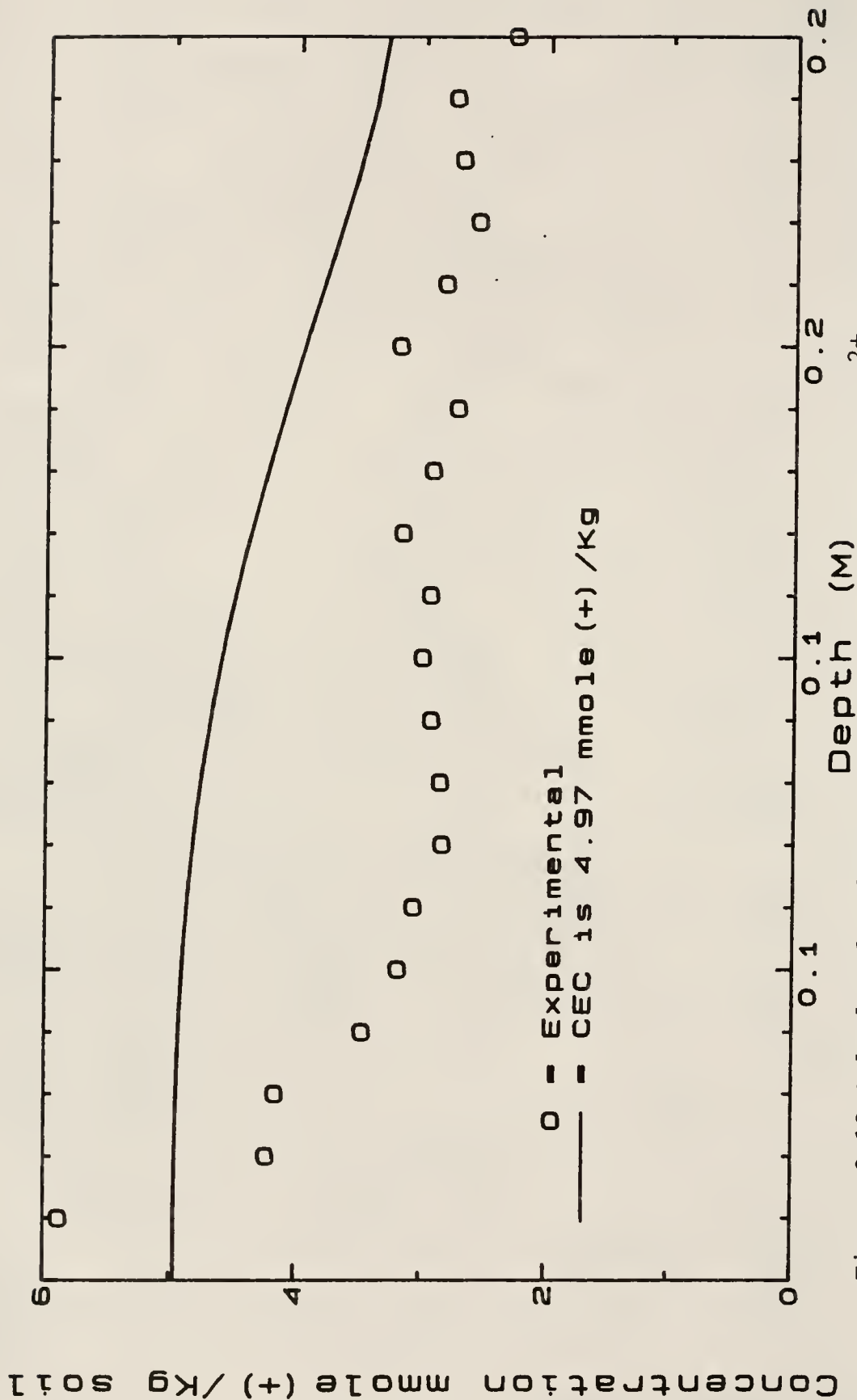


Figure 2-18 Calculated and experimental distributions of  $Mg^{2+}$  concentrations in the exchange phase for the topsoil column after miscible displacement with 4.5 pore volumes.

in solution and exchange phases are given in Figs. 2-19 and 2-20 for topsoil and in Figs. 2-21 and 2-22 for subsoil, respectively. Simulated results for the subsoil were greatly improved as compared to the case where  $\text{Al}^{3+}$  was not included among the exchangeable cations. Simulated results for topsoil better approximated the observed data, but an overestimation for concentrations in both the solution and exchange phases was observed. Careful examination of constituent cations located on exchange sites of the topsoil revealed that  $\text{Al}^{3+}$  was the dominant cation species, comprising about 50% of the total exchangeable cations. Cation concentrations in the exchange phase for the topsoil decreased in the order  $\text{Al}^{3+} > \text{Mg}^{2+} > \text{Ca}^{2+} > \text{Na}^+ > \text{K}^+$ . The topsoil column was obviously no longer dominated by  $\text{Mg}^{2+}$ . For the subsoil column, however, the order was  $\text{Mg}^{2+} > \text{Al}^{3+} > \text{Ca}^{2+} > \text{K}^+ \approx \text{Na}^+$ . This phenomenon can be attributed to the topsoil containing more interlayer-hydroxy vermiculites than the subsoil. Displacing salt solution through either topsoil or subsoil resulted in the exchange of  $\text{Ca}^{2+}$  or  $\text{Mg}^{2+}$  with  $\text{Al}^{3+}$ . Additional acidity (Fig. 2-23) would be caused by the hydrolysis of  $\text{Al}^{3+}$ , which would tend to induce further mineral dissolution. The subsequent further production of  $\text{Al}^{3+}$  would then compete with divalent  $\text{Ca}^{2+}$  and  $\text{Mg}^{2+}$  for soil exchange sites. The result would be a higher saturation of exchange sites with  $\text{Al}^{3+}$ .

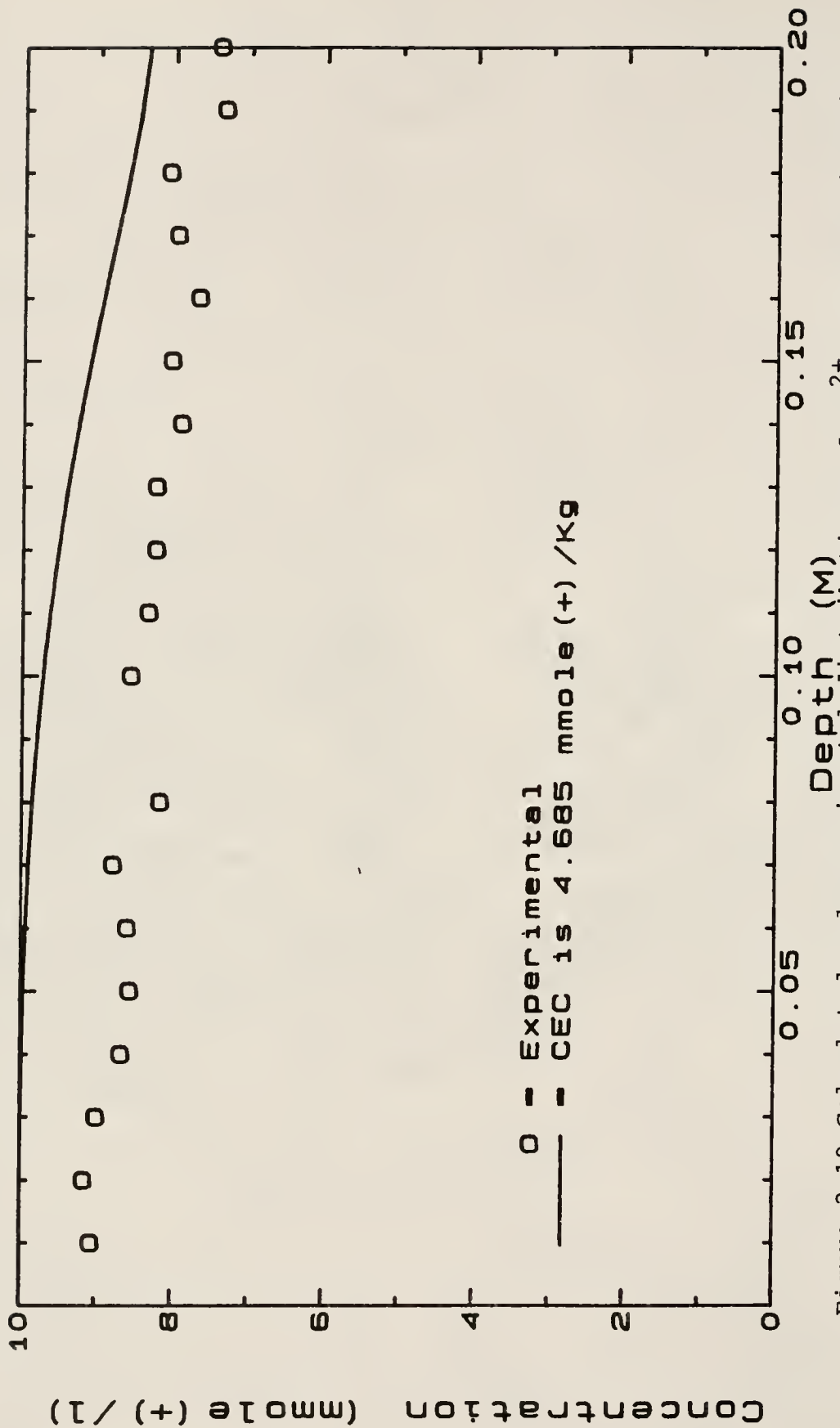


Figure 2-19 Calculated and experimental distributions of  $Mg^{2+}$  concentrations in the solution phase for the topsoil column after miscible displacement with 4.5 pore volumes.

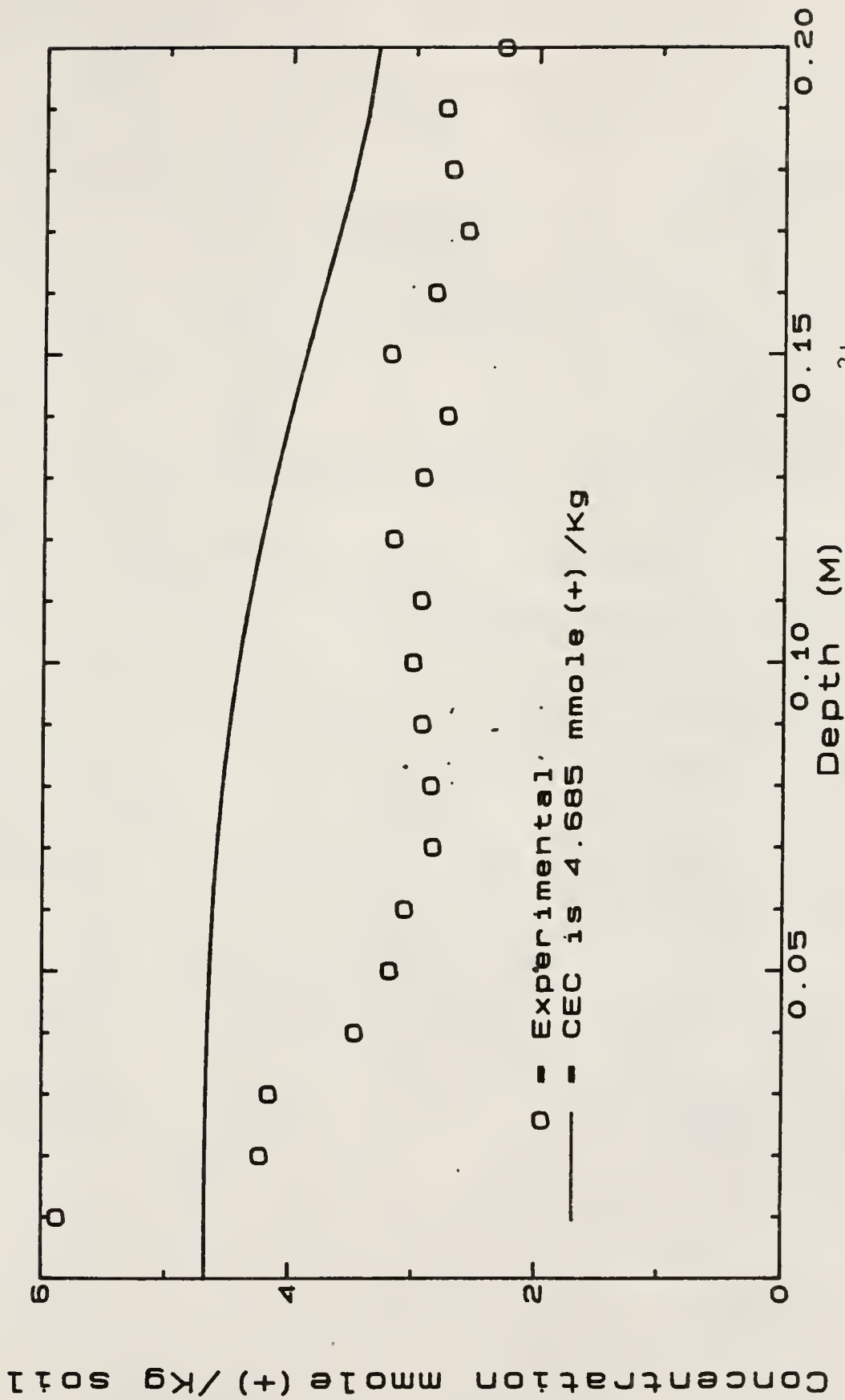


Figure 2-20 Calculated and experimental distributions of  $Mg^{2+}$  concentrations in the exchange phase for the topsoil column after miscible displacement with 4.5 pore volumes.

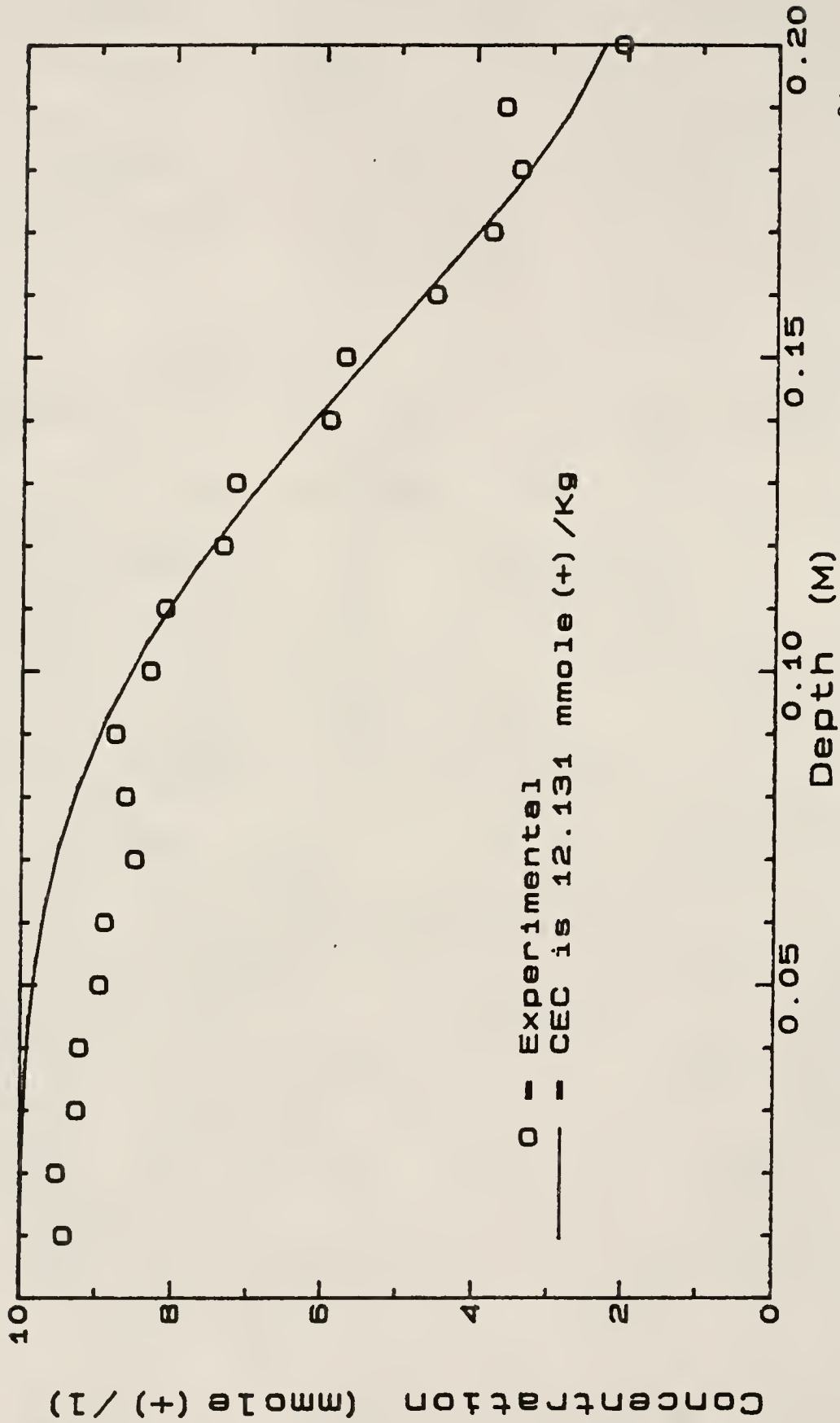


Figure 2-21 Simulation results and experimental data for distributions of  $Mg^{2+}$  concentrations in the solution phase for the subsoil column after miscible displacement with 3.6 pore volumes.

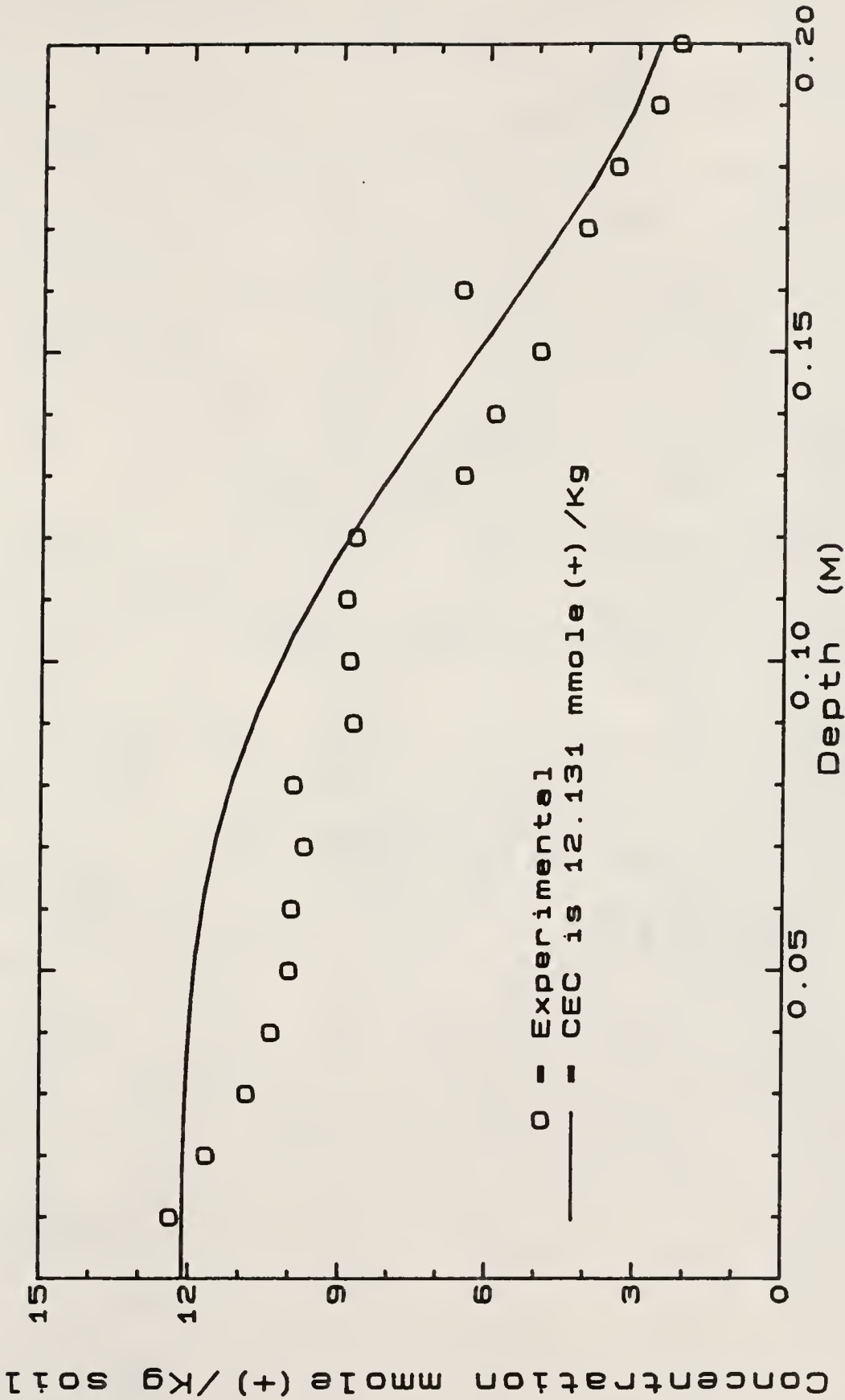


Figure 2-22 Simulation results and experimental data for distributions of  $Mg^{2+}$  concentrations in the exchange phase for the subsoil column after miscible displacement with 3.6 pore volumes.

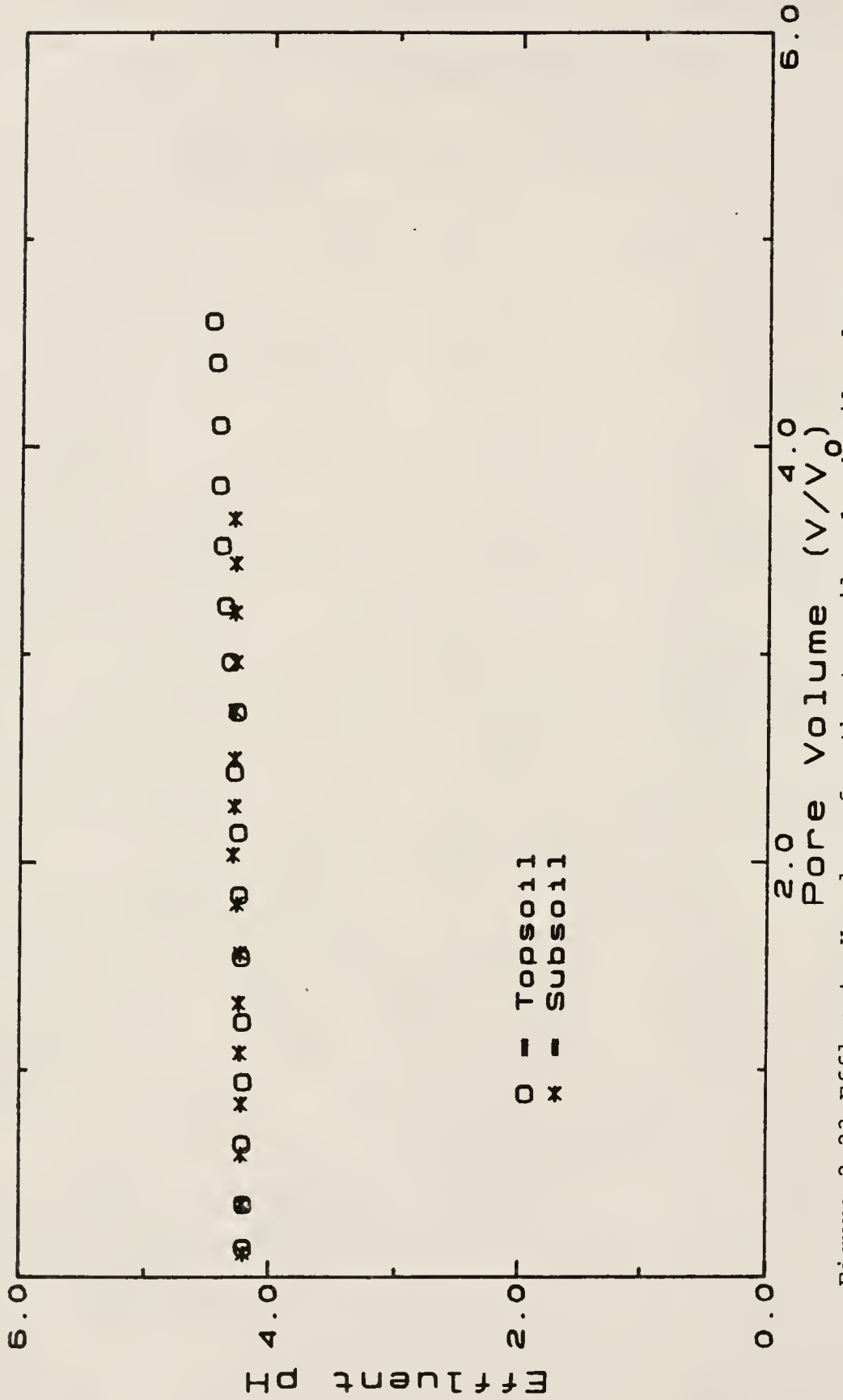


Figure 2-23 Effluent pH values for the topsoil and subsoil columns.

### Conclusions

The principal minerals in the Cecil topsoil and subsoil are kaolinite, interlayer-hydroxy vermiculite and quartz. Gibbsite was also found in the subsoil. This highly weathered acid soil also contains amorphous materials in the form of Al and Fe oxides. The clay content in the subsoil is almost three-fold greater than for the topsoil, and organic matter in the topsoil is 1.6 times greater than for the subsoil.

Exchange isotherms for  $Mg^{2+} \rightarrow Ca^{2+}$  reaction in Cecil soil were concave in shape for both soils, indicating that  $Ca^{2+}$  was adsorbed preferentially to  $Mg^{2+}$  on the soil exchange sites. This result was as expected.

Excellent agreement between numerical and analytical solutions demonstrated that the computer program for convective-dispersive transport of two ion species functioned as designed for the cases of both non-reactive and reactive solute species.

Results from sensitivity analysis showed that the model-simulation results were essentially insensitive to small changes in the dispersion coefficient and selectivity coefficient. The dispersion coefficient was apparently independent from the cation retardation factor  $R$ , although the selectivity coefficient is actually embedded in the retardation factor. The volumetric water content and soil bulk density both showed slight effects upon model-predicted results, which can be explained by the inclusion in  $R$  by the

soil-to-solution ratio  $\sigma/\theta$ . The exact magnitude of  $R$  could not be obtained, since  $R$  involved unknown concentration variables. The cation exchange capacity is the most critical input parameter to the simulation. This is a result of the cation retardation function  $R = (1+(\sigma/\theta)F)$ , where the function  $F$  in equation [2-20] is a function of  $\bar{C}_T$ . Therefore, cation movement undergoes greater retardation in soil with a larger value of CEC (and thus a larger value of  $R$ ) than in soil with a small CEC.

CHAPTER III  
CATION LEACHING DURING CONTINUOUS DISPLACEMENT  
BY AQUEOUS HYDROCHLORIC ACID SOLUTION  
THROUGH COLUMNS OF CECIL SOIL

Introduction

Acid rain is commonly considered to be a serious environmental problem for industrialized nations. In particular, soil scientists are concerned that acid atmospheric inputs could accelerate cation (examples:  $\text{Ca}^{2+}$ ,  $\text{Mg}^{2+}$ ,  $\text{K}^{+}$ , etc.) leaching from the soil profile. Nutrient deficiency accelerated by leaching of cations and mobilization of toxic  $\text{Al}^{+3}$  in the soil solution may lead to eventual decline in productivity of certain soils. Since agricultural soils routinely receive limestone and fertilizer as a crop-management aid, whereas forest soils do not, scientists are generally more concerned about effects of acid precipitation upon forest soils than upon agricultural soils. Acid rain in the forms of  $\text{H}_2\text{SO}_4$  or  $\text{HNO}_3$  may affect the status of forest nutrients such as  $\text{Ca}^{2+}$  and  $\text{Mg}^{2+}$ , either positively or negatively. This phenomenon has been extensively investigated by Abrahamsen (1980). In cases where nutrient cations are abundant and S and N concentrations are at plant-deficiency levels in the soil, moderate inputs of acid rain may actually cause increased forest growth. At the other extreme, however, where soil

sites have adequate N and S concentrations but are deficient in nutrient cations, acid rain in sufficient amounts may decrease productivity (Johnson et al., 1982).

In all cases, anions associated with acid inputs or present in the soil must be mobile in the soil solution if basic cations are to be transported through the soil profile. That is, cations cannot leach from soil without an equivalent concentration of accompanying anions in solution. Immobilization of anions can effectively prevent cation leaching; therefore, the entire process of soil leaching is strongly dependent on the input solution or on the internal production of mobile anions (Johnson and Cole, 1980).

However, anion-leaching theory has been questioned by Krug and Frink (1983). They point out that some of the factors commonly considered to make soils susceptible to acidification by acid rain are the same as those which acidify soil through natural processes. Reuss (1983) used cation-exchange equilibrium to predict the leaching of  $\text{Ca}^{2+}$  and  $\text{Al}^{3+}$  following the application of  $\text{H}_2\text{SO}_4$  to soil. Cosby et al. (1985a) presented an equilibrium model which included equilibrium soil-solution cation exchange, inorganic aluminum reactions and dissolved inorganic reactions. The model demonstrated the interaction of soil chemical processes as a key to controlling stream water chemistry. A mathematical model which used quantitative descriptions of soil chemical processes to estimate long-term chemical changes that occur in the soil, soil water and surface water

of catchments in response to changes in acid deposition was proposed by Cosby et al. (1985b). Due to the lack of long-term records of catchment-water quality, however, results obtained from their model need further verification.

Any criteria used for assessing soil sensitivity to cation leaching by acid rain should include cation-exchange capacity (CEC), base saturation and mobilized  $\text{Al}^{3+}$ , pH and carbonate content (McFee, 1980). Critical properties, such as CEC and cation-selectivity coefficients, are especially needed in the investigation of effects of acid deposition upon soils.

The first objective of this study was to determine the influence of input solution pH upon leaching of basic cations during continuous displacement by aqueous HCl solutions through hand-packed columns of Cecil topsoil and subsoil. The second objective was to determine the influence of input solution pH upon distributions of cation concentrations in soil columns after leaching experiments, and the third objective was to use cation concentrations in the solution and exchange phases to calculate binary selectivity coefficients for ion-pairs.

### Basic Theory

#### Surfaces of Soil Particles

Constant electrostatic surface charge for a clay mineral is derived from isomorphous substitution of  $\text{Si}^{4+}$  by  $\text{Al}^{3+}$  or of  $\text{Mg}^{2+}$  for  $\text{Al}^{3+}$  within the crystalline structure. Mica and related 2:1 lattice-type minerals, smectites,

vermiculites and interstratified forms of these minerals typically have constant surface charge regardless of solution concentration or pH (Gast, 1977). Colloids with constant surface potential and variable surface charge are in turn commonly found in soils which are extensively weathered and dominated by sesquioxides of Fe and Al or 1:1 kaolinitic minerals. The surface charge density for colloids of this type varies with pH and salt concentration (Keng and Uehara, 1974). Soil organic matter also has pH-dependent charge, arising from dissociation of phenolic OH and carboxylic groups.

#### Cation-Exchange Equilibria

The exchange reaction between an exchange-phase cation 1 with valence  $z_1$  and a cation 2 of valence  $z_2$  in solution can be described by the equation

$$z_2 C_1 + z_1 \bar{C}_2 = z_1 C_2 + z_2 \bar{C}_1 \quad . \quad [3-1]$$

For a reversible reaction such as equation (3-1) at chemical equilibrium, one type of exchange selectivity coefficient ( $K_s$ ) can be expressed as

$$K_s = \left[ \frac{\bar{C}_1^*}{C_1} \right]^{z_2} \left[ \frac{C_2}{\bar{C}_2^*} \right]^{z_1} \quad . \quad [3-2]$$

The equivalent fractions ( $\bar{C}_i^*$ ) for cations 1 and 2 in the exchange phase are given by

$$\bar{C}_i^* = \frac{\bar{C}_i}{\bar{C}_i + \bar{C}_j} \quad [3-3]$$

where i and j refers to cations 1 or 2,  $\bar{C}_i$  (or  $\bar{C}_j$ ) is the concentration of exchangeable cation 1 or 2 in moles of positive charge (equivalents per Kg of soil), and  $C_i$  is the solution-phase concentration (mmole(+)  $L^{-1}$ ) of cation 1 or 2. The magnitude of  $K_s$  indicates the relative preference of exchange sites for cation 2 over cation 1. If  $z_1 = z_2$  and  $K_s = 1$  the exchange sites show no preference for either of two ions, whereas  $K_s < 1$  indicates that cation 1 is adsorbed preferentially, and  $K_s > 1$  indicates that cation 2 is preferred by the exchange sites.

#### Effects of Acidification

Continuous addition of acid solution to a soil tends to increase total acidity of the soil and to decrease pH. The extent to which soil pH is decreased by addition of acid is greatly determined by the buffering capacity of a given soil. A number of associated effects are also observed upon addition of acid to soil. One of the more important effects is the loss of basic cations such as  $Ca^{2+}$ ,  $Mg^{2+}$ ,  $K^+$ , and  $Na^+$ . Basic cations are leached with co-anions, such as bicarbonate, chloride, nitrate, sulphate, or organic anions. A second effect is the displacement of cations from weak-acid exchange sites such as occur on humus and on

poorly-ordered aluminosilicates and hydrous oxides. A third effect is a decrease in CEC as the pH drops. Aluminum ions are mobilized by acid dissolution of soil components, and thus strongly compete with other cations for soil exchange sites.

### Materials and Methods

#### Physical and Chemical Properties of the Soil

Cecil soil used in this study was obtained from a forest site located near Clemson University in Clemson, South Carolina. The exact location was reported earlier by Dr. V. L. Quisenberry (Cassel, 1985), Agronomy Department, Clemson University. Reported texture varied from site to site, with the clay content of Ap horizon ranging from 6 to 38 percent depending upon the amount of subsoil mixing which occurred subsequent to soil erosion. Clay content in the B horizon ranged from 42 to 72 percent (Cassel, 1985). In situ values of unsaturated hydraulic conductivity reported (Cassel, 1985) for the 0-30 cm depth ranged from  $1.70 \times 10^{-4}$  to  $4.51 \times 10^{-2}$  ( $\text{cm h}^{-1}$ ), and those for the 30-60 cm depth ranged from  $4.32 \times 10^{-4}$  to  $4.6 \times 10^{-1}$  ( $\text{cm h}^{-1}$ ), respectively. In situ values of soil-water content for the 0-30 cm depth ranged from 0.275 to  $0.495 \text{ cm}^3 \text{ cm}^{-3}$ , and for the 30-60 cm depth ranged from 0.409 to  $0.560 \text{ cm}^3 \text{ cm}^{-3}$  (Cassel, 1985).

The Cecil soil used in this research is classified as a Typic Hapludult. Topsoil and subsoil bulk samples were obtained from depths of 0-30 and 30-60 cm, respectively.

Soil samples were air-dried, passed through a 2-mm sieve, and stored in covered plastic buckets.

Values of pH for the soil samples were determined in soil-water suspensions (1:1 soil:water) using a glass electrode. Organic matter content was determined by the Walkley-Black method (Allison, 1965). Particle-size distribution was estimated by the pipette method (Day, 1965). Exchangeable cations were determined with neutral 1  $\text{M}$   $\text{NH}_4\text{OAc}$ , by placing 5 g of 2-mm air-dried soil in duplicate 50-ml centrifuge tubes, and adding 25 ml of 1  $\text{M}$   $\text{NH}_4\text{OAc}$  to each. All tubes were then stoppered and shaken for 30 min, with the tubes then being placed in a centrifuge and spun at 2000 rpm for 10 min. Number 42 Whatman filter paper was used to collect the supernatant into a 50-ml volumetric flask. The same procedure was repeated, with the volume then brought up to 50 ml with 1  $\text{M}$   $\text{NH}_4\text{OAc}$  (Thomas, 1982).

Exchangeable  $\text{Al}^{3+}$  was determined by 1  $\text{M}$   $\text{KCl}$  extraction of 10-g, air-dried, soil samples in duplicate 50-ml volumetric flasks, with 25 ml of  $\text{KCl}$ . The soil and  $\text{KCl}$  were mixed, allowed to stand for 30 minutes, and then transferred to Buchner funnels fitted with number 42 Whatman filter paper mounted on 250-ml vacuum flasks. An additional 125 ml volume of  $\text{KCl}$  solution was added in 25-ml increments to give a final volume of 150 ml (McClellan, 1965; Thomas, 1982).

#### X-Ray Diffraction

X-ray diffraction analysis of the soil clay was performed for topsoil and subsoil, respectively, by the

method of Whittig (1965). The soil was treated with hypochlorous acid to remove carbonates and organic matter, followed by use of the dithionite method to remove Fe oxides. The clay fraction was separated by alternatively adding pH-10 water followed by centrifuging for different combinations of speed and time. The clay ( $< 2 \mu$ ) fraction was prepared on a ceramic tile such that one was Mg-glycerol saturated and air-dried, and the other was K-saturated and air-dried. The samples were then X-rayed at room temperature ( $25^{\circ} \text{C}$ ). Samples were next heated at  $110^{\circ} \text{C}$  and  $300^{\circ} \text{C}$  by successive treatment and X-rayed after each treatment. As the last step, K-saturated sample was heated at  $550^{\circ} \text{C}$  before being X-rayed.

#### Column Preparation and Displacement Procedure

The column consisted of a stack of 1-cm diameter lathe-cut plexiglass cylinders, with dimensions of 0.10 m length and 0.0375 m inside diameter to give a total internal volume of  $1.105 \times 10^{-4} \text{ m}^3$ . The rings were held together by wrapping water-proof, acid-resistant electrical tape along the circumference in order to give a water-impervious column. Soil was held in the column by placing fine nylon mesh and Whatman number 42 filter paper over a thin plastic disc with small holes distributed on the surface in each of the inflow and outflow endplates. A check for water leaks through the column wall was made prior to packing soil into each column. Each column was then placed in the vertical position and was sequentially packed by slowly adding

increments of air-dry soil until the total quantity of soil required was obtained, the sides of the column being gently tapped during packing to provide the desired bulk density. The whole column was mounted vertically between two wooden support boards and fastened with four threaded steel rods to give mechanical support. After the end of the experiment, the pore volume of each column was obtained from the mass difference between wetted soil columns and oven-dry soil columns, with a correction being made for the amount of solution held inside the endplates. Solutions of HCl were displaced through columns of Cecil topsoil and subsoil with an average Darcy velocity of  $1.06 (\pm 2\%) \text{ cm h}^{-1}$ . Displacing solutions were prepared from a HCl stock solution with pH was adjusted to either 3.9 or 4.9. A Rainin model Rabbit peristaltic pump was calibrated and used to deliver solution to the bottom of each soil column. The soil column was initially air-dry, so transient flow occurred when the experiments were started. Eventually (after displacement of 1 to 2 pore volumes of effluent) steady-state water flow was maintained for each column. Effluent from the top of the column was collected in equal increments of  $11.05 (\pm 2\%) \text{ ml}$ , using a fraction collector. These samples were stored in refrigerator for later analysis.

#### Dissection of Soil Columns, Extraction, and Chemical Analysis

After flow had been terminated, columns were maintained in a vertical position overnight to ensure that

the whole system was of equilibrium. The next day, with the column still in the vertical position, the tape was removed carefully. After removing the outflow endplate, a piece of parafilm was placed over the end of the column and a fine steel thread was forced between consecutive rings in order to slice the column into sections. Resulting sections of soil were carefully removed and placed on a piece of parafilm. Each whole section of soil was then packed into a prenumbered small centrifuge tube which had a predrilled small hole on the closed end. A Whatman number 42 filter paper was placed on top of the hole, inside the tube. Each small centrifuge tube was then placed into a corresponding large-size centrifuge tube along with a glass bead to separate the extracted solution from soil in the small centrifuge tube. Paired tubes were carefully placed in the centrifuge and spun at 4000 rpm for 30 min. Soil samples were then removed from the small centrifuge tubes and placed into a weighing boat, and wet soil weights were recorded. Soil in each weighing boat was air-dried and the soil weight recorded. Exchange-phase concentrations of  $\text{Ca}^{2+}$ ,  $\text{Mg}^{2+}$ ,  $\text{K}^{+}$ , and  $\text{Na}^{+}$  were obtained using a neutral 1 M  $\text{NH}_4\text{OAc}$  extraction method (Thomas, 1982). Correction was made for entrapped equilibrium solution remaining in the exchange phase after centrifuging, by taking differences in equivalents per L for the extractant and the residual solution. Unbuffered 1 M  $\text{KCl}$  (Thomas, 1982) was used in order to obtain exchangeable  $\text{Al}^{3+}$  concentrations. Concentrations of  $\text{Ca}^{2+}$ ,  $\text{Mg}^{2+}$ ,  $\text{K}^{+}$  and

$\text{Na}^+$  in the column effluent, solution and exchange phases of the soil were analyzed using an atomic absorption spectrometer. Total  $\text{Al}^{3+}$  was determined by optical emission spectroscopy (inductively coupled plasma argon ICAP).

### Results and Discussion

Soil parameters used in the leaching experiment are presented in Table 3-1. Clay minerals contained in the Cecil topsoil and subsoil were kaolinite, interlayered-hydroxy vermiculite, quartz, as well as Al and Fe hydrous oxides. In addition, gibbsite was found in the subsoil. Other soil properties, such as particle size distribution and texture are presented in Table 2-2. Concentrations of exchangeable cations in Cecil topsoil and subsoil are presented in Table 3-2.

Table 3-1 Physical and chemical parameters for Cecil topsoil and subsoil columns

Parameter	Topsoil	Topsoil	Subsoil	Subsoil
pH of input solution	3.9	4.9	3.9	4.9
Bulk density <sub>3</sub> ( $\text{mg cm}^{-3}$ )	1.57	1.58	1.37	1.37
Volumetric water content ( $\text{cm}^3 \text{ cm}^{-3}$ )	0.40	0.40	0.49	0.48
Pore velocity ( $\text{cm h}^{-1} \times 10^2$ )	0.027	0.027	0.022	0.023
Column length <sub>2</sub> ( $\text{cm} \times 10^2$ )	0.10	0.10	0.10	0.10
Pore volume ( $\text{L}$ )	0.044	0.045	0.054	0.053
Input total $\text{H}^+$ concentration ( $\text{mmole}(+) \text{ L}^{-1} \times 10^{-3}$ )	125	12.5	125	12.5
Total number of pore volumes collected	37.8	36.9	30	29

Table 3-2 Initial concentrations of exchangeable cations, pH, and CEC for Cecil topsoil and subsoil

Parameter	Topsoil	Subsoil
pH (1:1 water:soil)	4.46	4.86
pH <sub>2</sub> (1:1 KCl: soil)	3.85	3.95
Ca <sup>2+</sup> (NH <sub>4</sub> OAc) (mmole(+) Kg <sup>-1</sup> soil)	1.60 (11%)*	8.80 (41%)
Mg <sup>2+</sup> (NH <sub>4</sub> OAc) (mmole(+) Kg <sup>-1</sup> soil)	2.50 (18%)	2.20 (10%)
K <sup>+</sup> (NH <sub>4</sub> OAc) (mmole(+) Kg <sup>-1</sup> soil)	0.70 ( 5%)	0.80 ( 4%)
Na <sup>+</sup> (NH <sub>4</sub> OAc) (mmole(+) Kg <sup>-1</sup> soil)	2.60 (18%)	2.80 (13%)
Al <sup>3+</sup> (KCl) (mmole(+) Kg <sup>-1</sup> soil)	6.70 (48%)	7.00 (32%)
CEC (NH <sub>4</sub> OAc+KCl) (mmole(+) Kg <sup>-1</sup> soil)	14.10	21.70

\* Numbers enclosed in parentheses represent fractions of each ion in the exchange phase.

From Table 3-2, dominant basic cations in the topsoil in decreasing order of abundance are shown to be Mg<sup>2+</sup>, Ca<sup>2+</sup> and Na<sup>+</sup>, but were Ca<sup>2+</sup>, Na<sup>+</sup> and Mg<sup>2+</sup> in the subsoil. Base saturation was 52% and 68% for topsoil and subsoil, respectively. Soil pH values determined by KCl were less than those determined by distilled water (Table 3-2), indicating that the variable-charge surfaces of the soil particles were predominantly negatively charged. Also, K<sup>+</sup> exchanged with H<sup>+</sup> on the soil surfaces, resulting in the solution becoming even more acid.

### Concentrations and pH of Column Effluent

Figs. 3-1 and 3-2 show breakthrough curves (BTC) for pH and cation concentrations in the effluent from the Cecil topsoil column which received pH 3.9 HCl solution. For the first few effluent samples the pH reading was near pH 4.0 and the concentrations of all reported cations were high. With increasing numbers of pore volumes of effluent, the pH abruptly increased and concentrations of cations sharply declined. From about 10 pore volumes to the end of each run (30 to 37 pore volumes), concentrations of cations and pH values for the effluent were essentially stable and the effluent pH remained higher than that for the input solution. These quasi-stable pH readings for the effluent were also considerably higher than corresponding values for stirred soil-water suspensions (Table 3-2). A similar effect was observed for effluent collected from the topsoil column that received pH 4.9 HCl input solution (data not shown). Effluent pH was lower with the pH 3.9 input solution than when pH 4.9 input solution was applied. Fig. 3-2 shows concentrations of  $\text{Ca}^{2+}$ ,  $\text{Mg}^{2+}$ ,  $\text{K}^{+}$  and  $\text{Na}^{+}$  in effluent from the topsoil column that received pH 3.9 solution. For the first two collected effluent samples (0.14 and 0.28 pore volumes),  $\text{Mg}^{2+}$  and  $\text{Ca}^{2+}$  were the dominant species. Thereafter,  $\text{K}^{+}$  was the dominant species in the effluent until about 16 pore volumes. A similar trend was observed for column effluent of input pH 4.9. Concentrations of  $\text{K}^{+}$  in effluent from topsoil columns

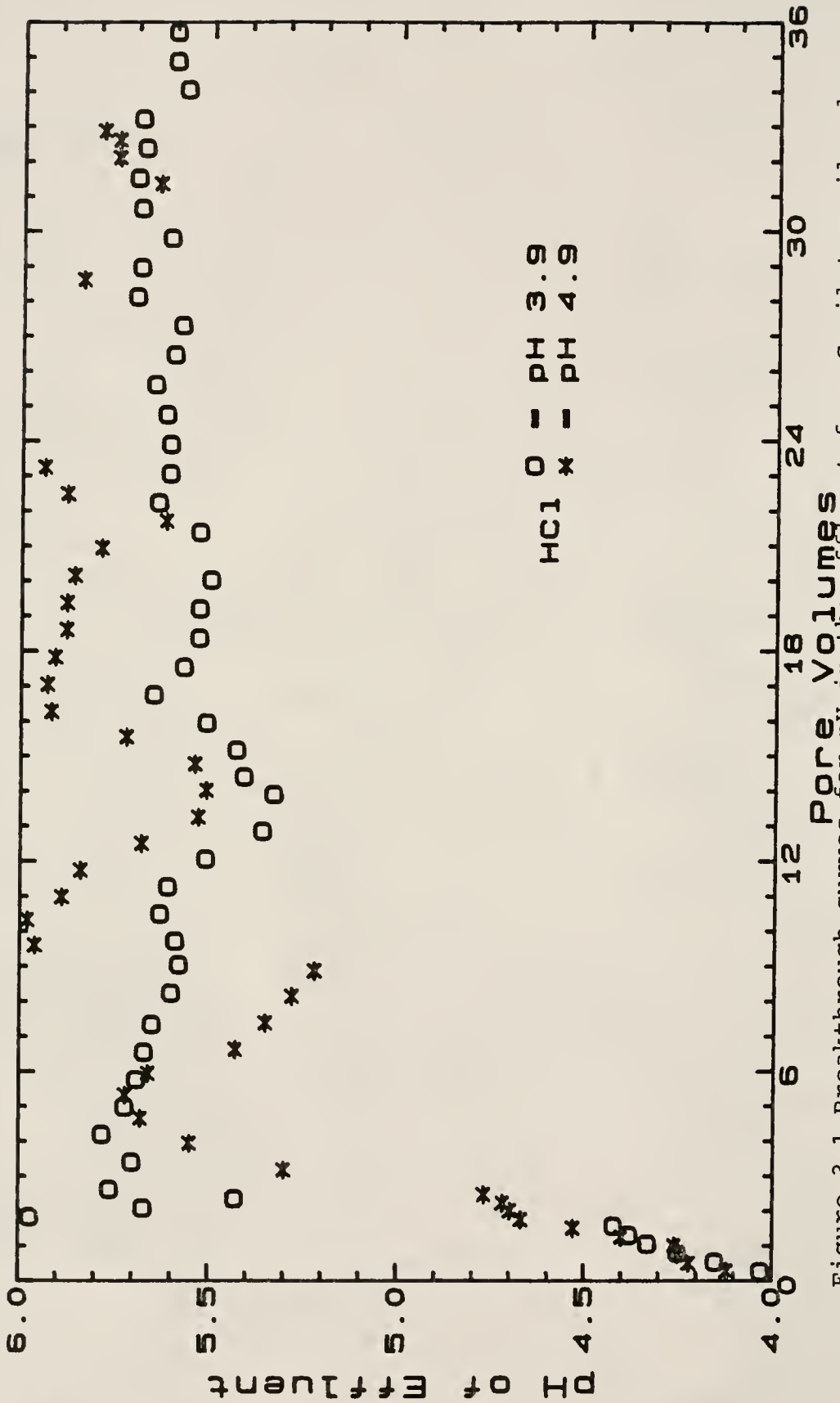


Figure 3-1 Breakthrough curves for pH in the effluent from Cecil topsoil columns which had received two input HCl solutions with different values of pH.

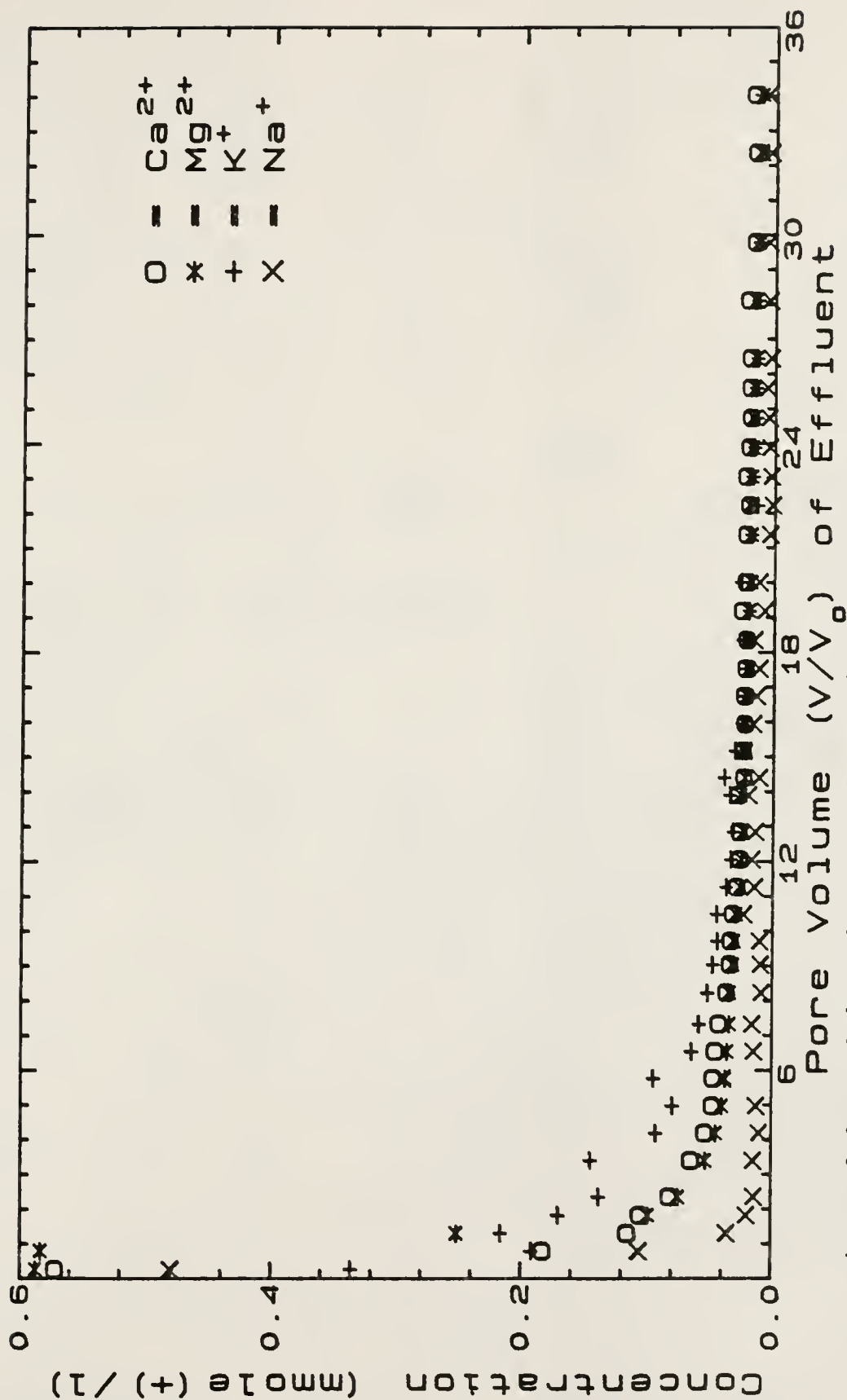


Figure 3-2 Breakthrough curves for cation concentrations in the effluent from Cecil topsoil columns which had received pH 3.9 input HCl solution.

receiving pH 3.9 and 4.9 treatments (Fig. 3-3) were similar. Breakthrough curves for summed concentrations of the  $\text{Ca}^{2+}$ ,  $\text{Mg}^{2+}$ ,  $\text{K}^{+}$ , and  $\text{Na}^{+}$  species of basic cations in the effluent from topsoil columns which received applications of pH 3.9 and 4.9 HCl solutions are presented in Fig. 3-4. Generally, the more acidic the input solution the higher the concentrations of cations observed in the leachate. Breakthrough curves for concentrations of  $\text{Al}^{3+}$  in the effluent are reported in Fig. 3-5 for treatments pH 3.9 and 4.9, respectively. Initial  $\text{Al}^{3+}$  concentrations in the effluent were as high as  $0.25 \text{ mmole(+) L}^{-1}$ , and a second peak in the  $\text{Al}^{3+}$  concentration of about  $0.11 \text{ mmole(+) L}^{-1}$  occurred after about 15 pore volumes elution for input pH 3.9. Corresponding values were  $0.06 \text{ mmole(+) L}^{-1}$  and 24 pore volumes for input pH 4.9. This elution pattern indicates that  $\text{Al}^{3+}$  is much preferred on soil exchange sites over  $\text{Ca}^{2+}$ ,  $\text{Mg}^{2+}$ ,  $\text{K}^{+}$ , and  $\text{Na}^{+}$  which causes the  $\text{Al}^{3+}$  BTC curves to be retarded. The more acidic the input solution, the more  $\text{Al}^{3+}$  which should come into the solution phase. Therefore the  $\text{Al}^{3+}$  BTC for input pH 3.9 should be less retarded than for input pH 4.9, and should also have a higher peak concentration.

Effluent pH from Cecil subsoil columns which received pH 3.9 and 4.9 input solutions, respectively, are presented in Fig. 3-6. Effluent pH initially was 4.2 but abruptly increased to 6.0 after about 2 pore volumes of elution. Thereafter, the effluent pH decreased to a relatively stable

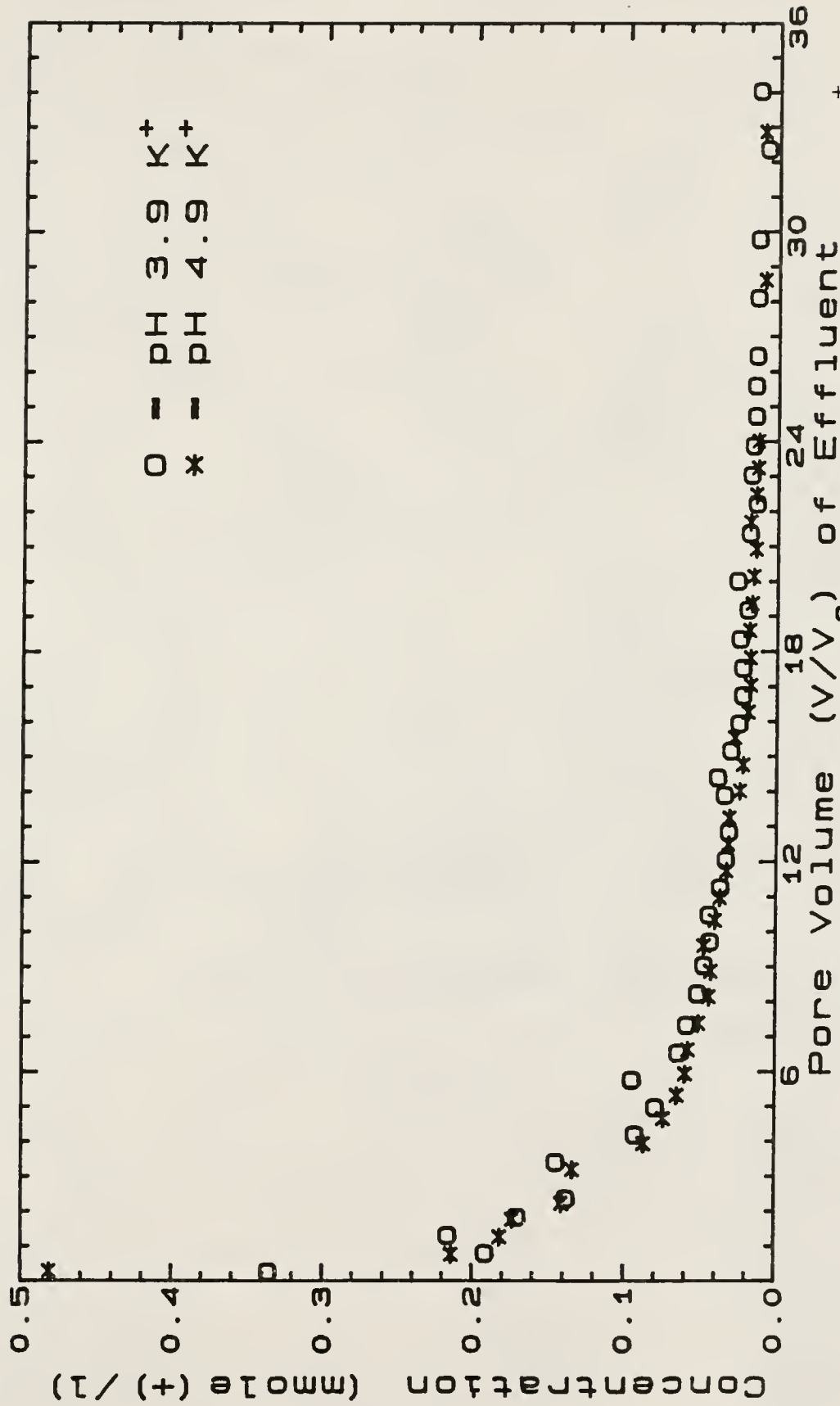


Figure 3-3 The effect of input solution pH upon the breakthrough curves of K<sup>+</sup> from Cecil topsoil columns.

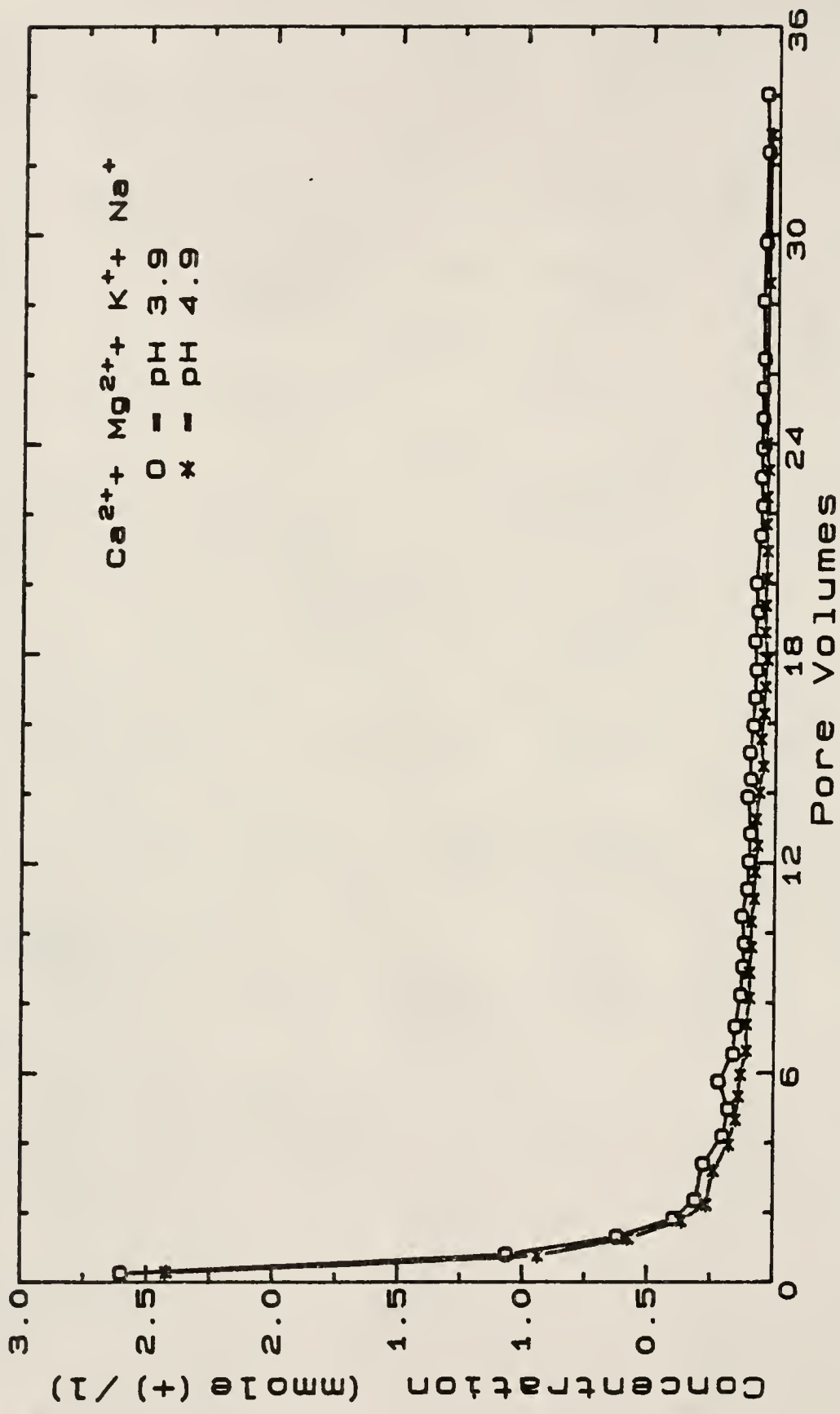


Figure 3-4 The effect of input solution pH upon the breakthrough curves of summed concentrations of Ca<sup>2+</sup>, Mg<sup>2+</sup>, K<sup>+</sup> and Na<sup>+</sup> in effluent from topsoil columns.

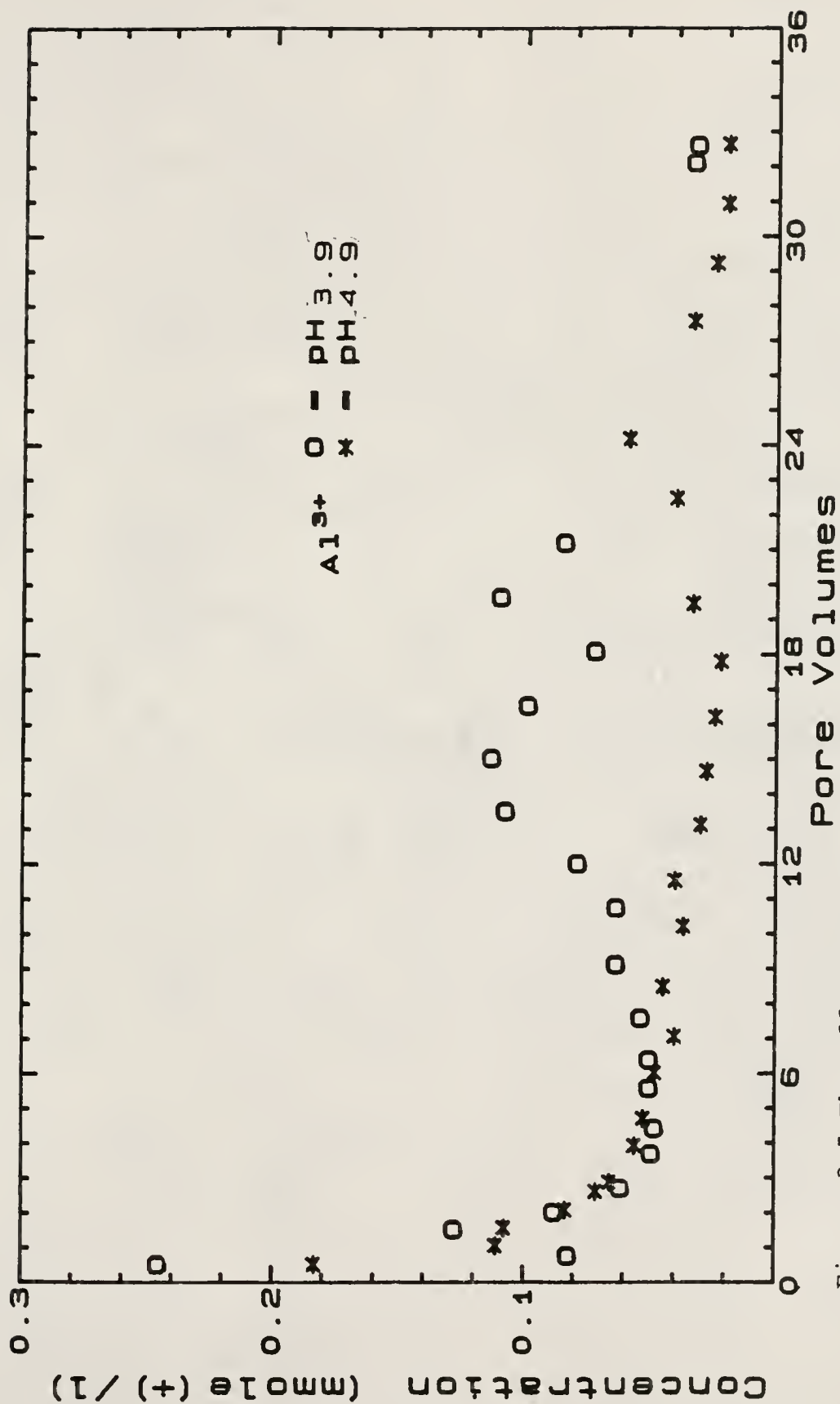


Figure 3-5 The effect of input solution pH upon the breakthrough curves of Al<sup>3+</sup> from Cecil topsoil columns.

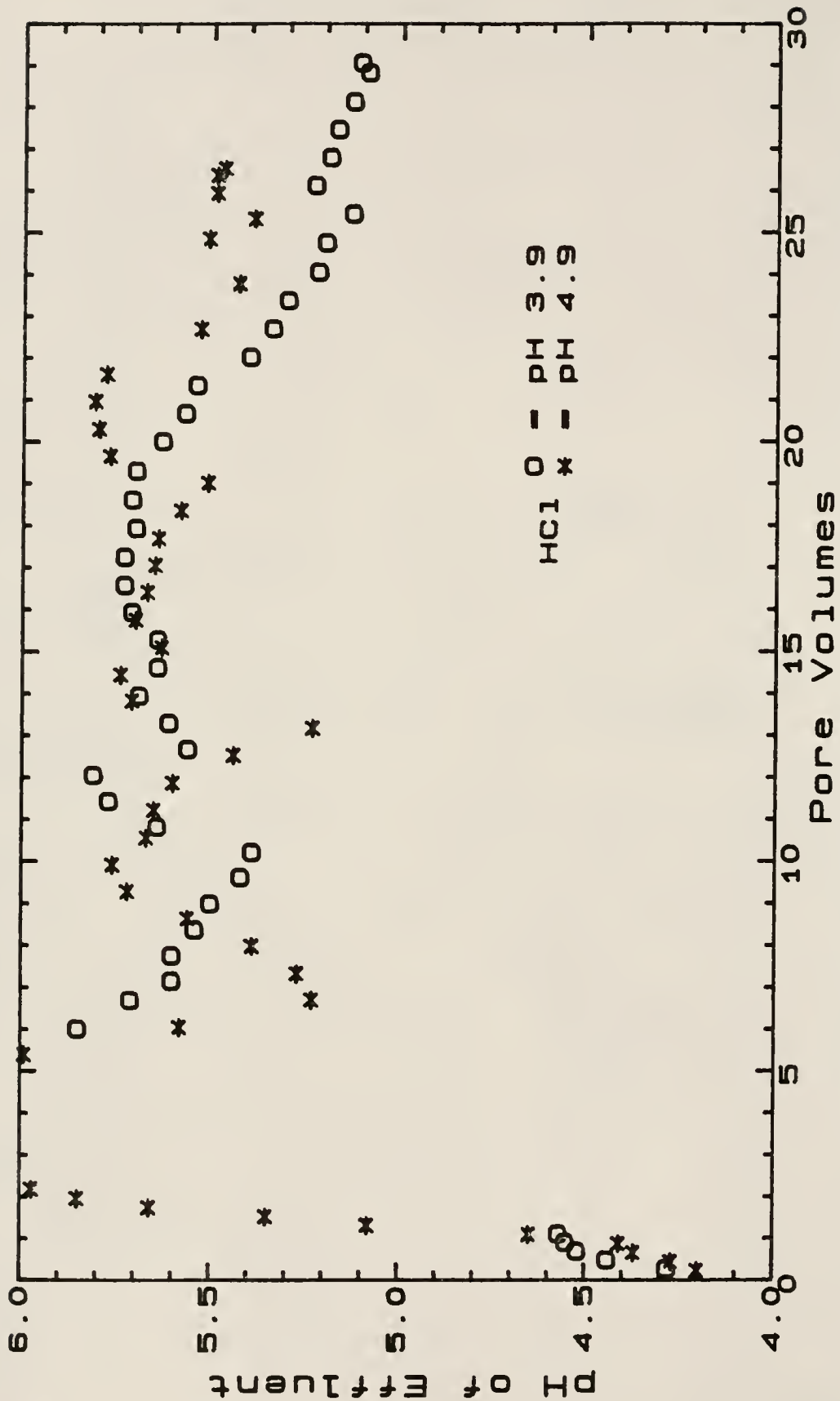


Figure 3-6 Breakthrough curves for pH in the effluent from Cecil subsoil columns which received two input HCl solutions with different values of pH.

value between 7 and 20 pore volumes of effluent. Between 20 and 28 pore volumes the pH gradually decreased once more because the acid-buffering capacity of the soil had by then been exceeded. As expected, effluent from treatment pH 3.9 had slightly lower pH compared to effluent from treatment pH 4.9. Effluent concentrations of  $\text{Ca}^{2+}$ ,  $\text{Mg}^{2+}$ ,  $\text{K}^+$ , and  $\text{Na}^+$  from the subsoil column which received pH 4.9 HCl are presented in Fig. 3-7. Magnitudes of cation concentrations in the effluent from columns treated with either pH 3.9 or 4.9 solutions were in the order  $\text{Ca}^{2+} > \text{Mg}^{2+} > \text{K}^+ > \text{Na}^+$ , which is approximately the same order as quantities of the various ion species initially on the exchange phase of the subsoil (Table 3-2).

The pH effect of input HCl upon concentrations of  $\text{Ca}^{2+}$  in the effluent is shown in Fig. 3-8. More  $\text{Ca}^{2+}$  was leached from the subsoil column receiving treatment pH 3.9 than for input pH 4.9. BTC for summed concentrations of  $\text{Ca}^{2+}$ ,  $\text{Mg}^{2+}$ ,  $\text{K}^+$ , and  $\text{Na}^+$  in the effluent from subsoil columns which received pH 3.9 and 4.9 HCl solutions are presented in Fig. 3-9. The subsoil column (pH 3.9) which received tenfold higher  $\text{H}^+$  concentrations, resulted in leaching of approximately a two-fold greater quantity of basic cations in the effluent. Fig. 3-10 indicates that the concentration of  $\text{Al}^{3+}$  in the effluent from columns of subsoil receiving the two different pH treatments. Higher concentrations of  $\text{Al}^{3+}$  were observed in the effluent for treatment pH 3.9.

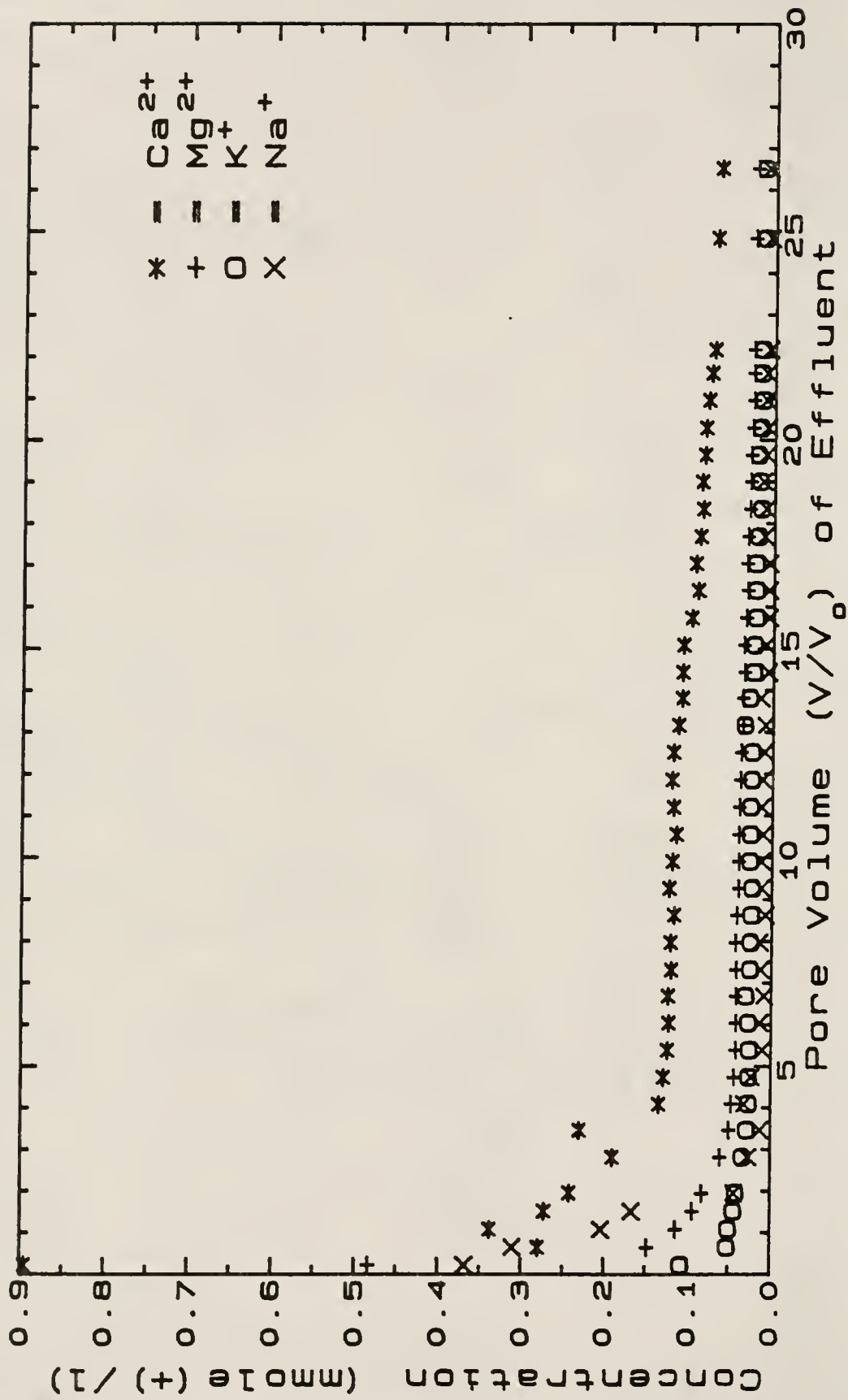


Figure 3-7 Breakthrough curves for cations in the effluent from Cecil subsoil columns which received pH 4.9 input HCl solution.

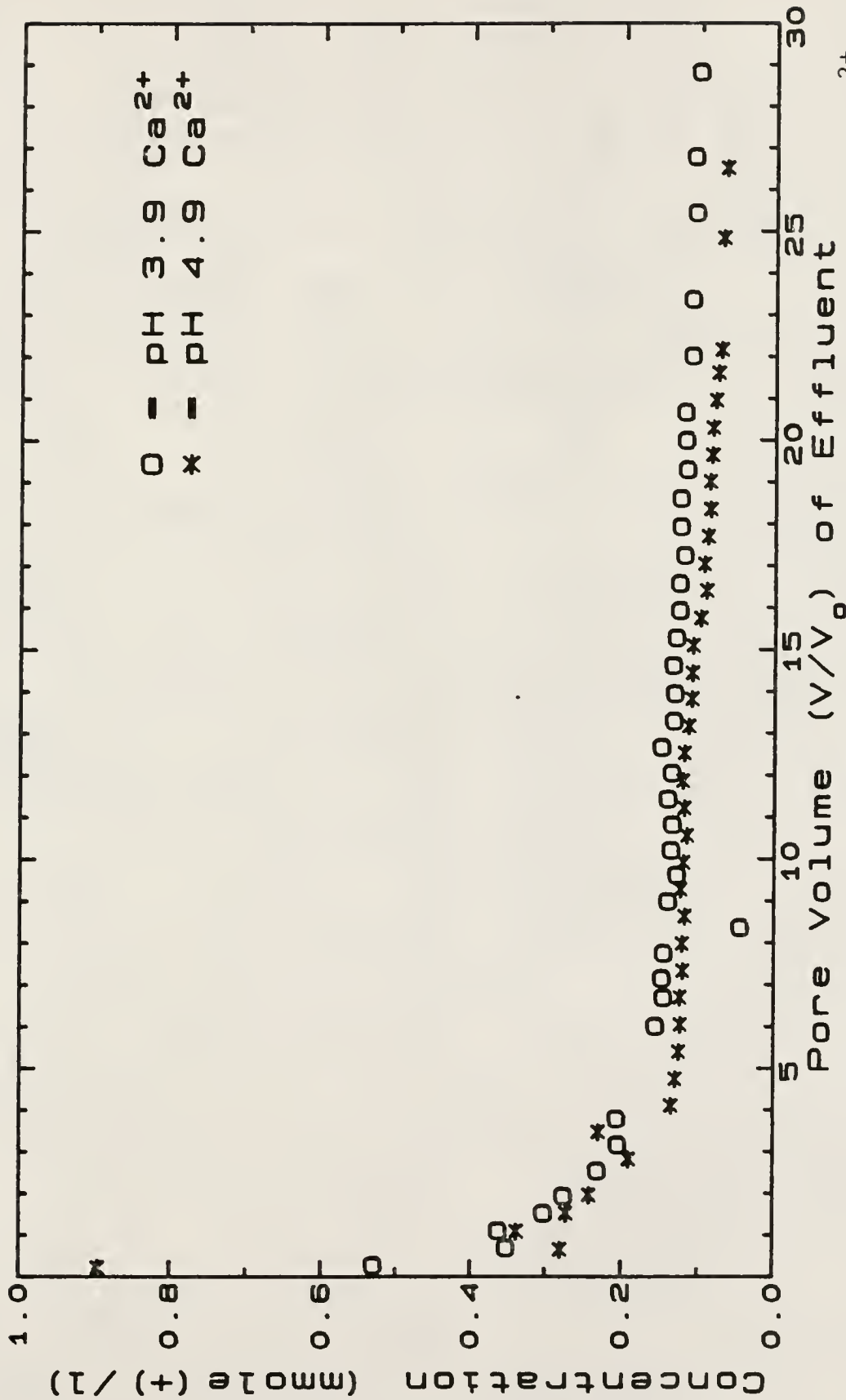


Figure 3-8 The effect of input solution pH upon the breakthrough curves of  $\text{Ca}^{2+}$  from Cecil subsoil columns.

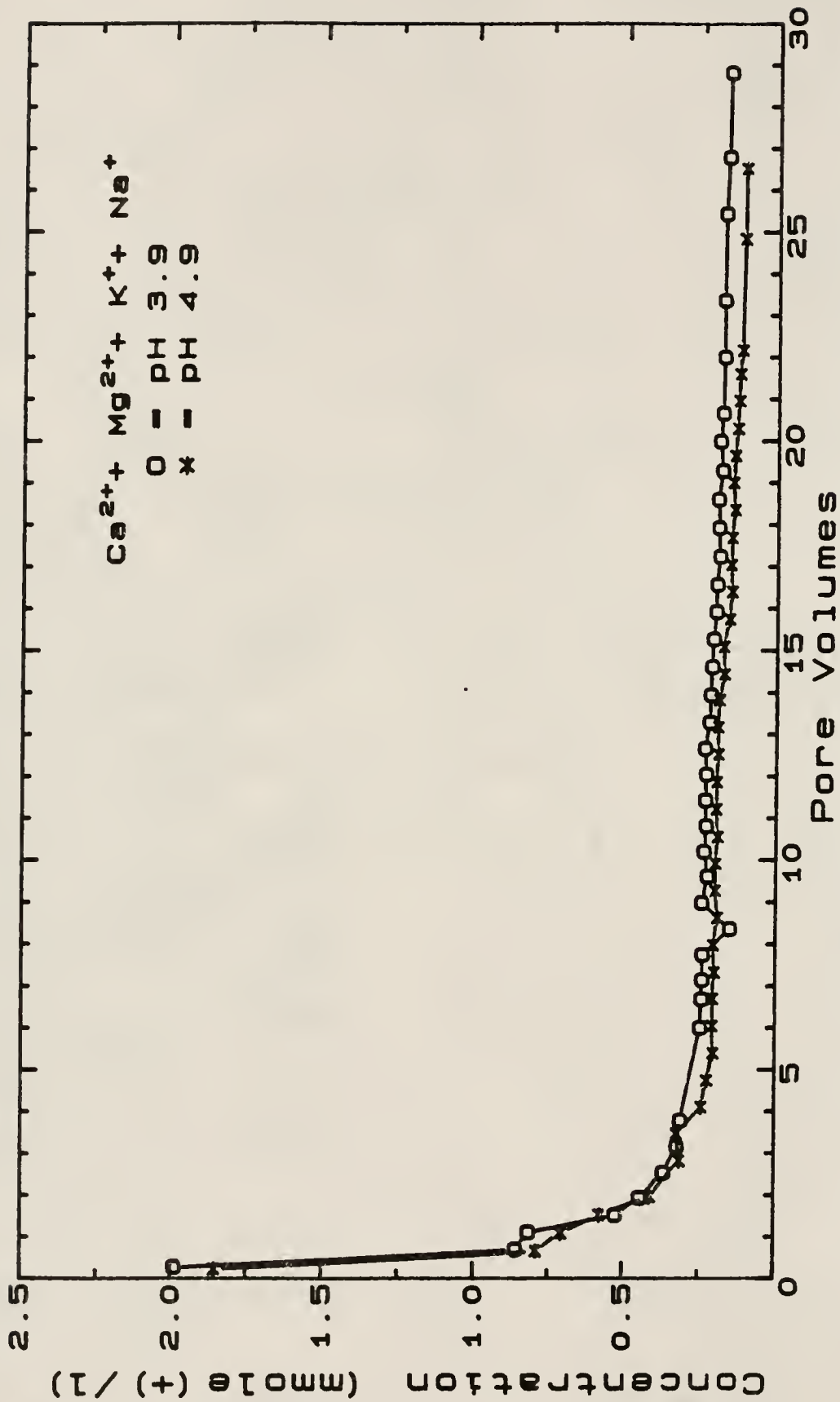


Figure 3-9 The effect of input solution pH upon the breakthrough curves of summed concentrations of Ca<sup>2+</sup>, Mg<sup>2+</sup>, K<sup>+</sup> and Na<sup>+</sup> in effluent from subsoil columns.

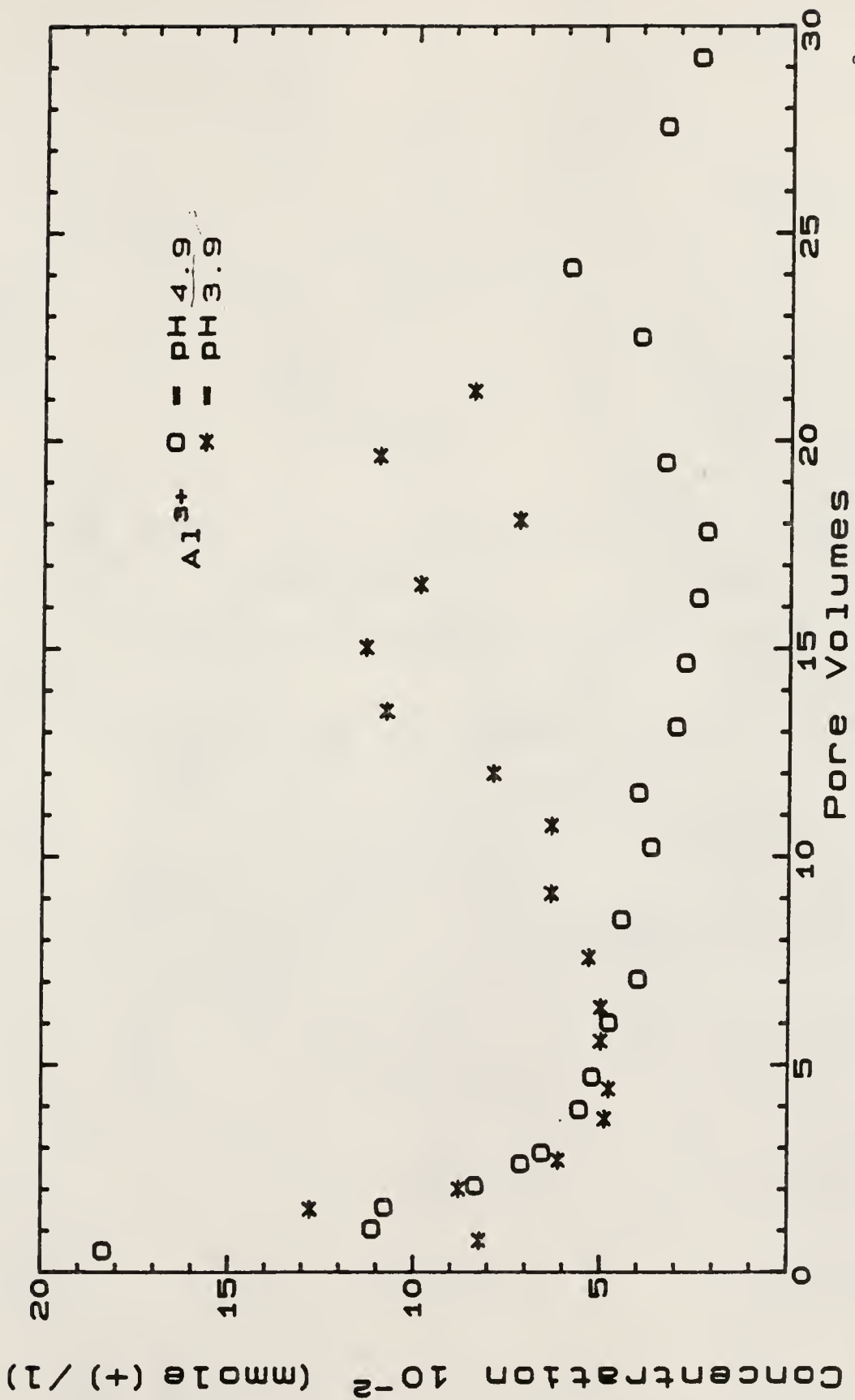


Figure 3-10 The effect of input solution pH upon the breakthrough curves of Al<sup>3+</sup> from Cecil subsoil columns.

The first few samples (within 0.5 pore volume) of column effluent had low pH and high concentrations of cations in each case. This phenomenon can be explained as a salt effect (Wiklander, 1975; Reuss and Johnson, 1985). Topsoil and subsoil columns initially contained 0.6 and 1.0% by volume of water before the leaching experiment was initiated, respectively. As constant-flux infiltration progressed with time and as the wetting front advanced through the soil, soluble salts were accumulated in the moving front. Resulting high concentrations of cations in the wetting front replaced part of the exchangeable  $H^+$  and  $Al^{3+}$ , which decreased the pH of the soil solution. This phenomenon is called a "salt effect". With continuous application of dilute HCl, initially displaced  $H^+$  and  $Al^{3+}$  were subsequently leached resulting in an abrupt rise of effluent pH once more. Another cause for the higher pH of column effluent than of input HCl may have been removal of the solution from contact with soil matrix. As the effluent flowed from soil columns and was exposed to the atmosphere, the  $CO_2$  partial pressure of the solution would decline and the pH of the effluent would increase somewhat. During the elution of 28 pore volumes, effluent pH was always observed to be higher than pH of the input solution. As HCl infiltrated the soil,  $H^+$  ions in the acid input solution underwent cation exchange with basic cations located on soil exchange sites. Larger amounts of displaced  $Al^{3+}$  were found from both topsoil and subsoil columns receiving pH 3.9 HCl

solution as compared to columns receiving pH 4.9 HCl solution. This can be explained by increased solubility and mobility of complex aluminum as acidity increased.

#### Concentrations of Cations in Solution and Exchange Phases

Distributions of  $\text{Ca}^{2+}$ ,  $\text{Mg}^{2+}$ ,  $\text{K}^+$ ,  $\text{Na}^+$  and  $\text{Al}^{3+}$  in solution and exchange phases for columns of Cecil topsoil after leaching with pH 3.9 and 4.9 HCl solutions are presented in Tables 3-3 and 3-4, respectively. When an acid solution is displaced through a soil column, cations with higher affinities for exchange sites would be expected to exchange strongly or tend to displace exchangeable cations with lesser affinities from exchange sites (Helfferich, 1962; Mansell, 1983). For the case where equivalent fractions of cations initially in the exchange phase are approximately equal for all ion species, concentrations in the solution phase of  $\text{K}^+$  and  $\text{Na}^+$  should be higher than those of  $\text{Ca}^{2+}$ , and  $\text{Mg}^{2+}$  and  $\text{Al}^{3+}$ . For the Cecil soil the situation was more complicated since the initial composition of the exchange phase was relatively high in trivalent  $\text{Al}^{3+}$  as well as divalent  $\text{Ca}^{2+}$  and  $\text{Mg}^{2+}$  species. For the exchange phase, concentrations of  $\text{Ca}^{2+}$ ,  $\text{Mg}^{2+}$ ,  $\text{Al}^{3+}$  would be dominant over monovalent species. Results in Tables 3-3 and 3-4 indicate that, in the corresponding solution phase, cation concentrations were in the order  $\text{K}^+ \approx \text{Na}^+ \approx \text{Al}^{3+} > \text{Ca}^{2+} > \text{Mg}^{2+}$ .

Tables 3-5 and 3-6 present distributions of cation concentrations in solution and exchange phases for columns

Table 3-3 Concentrations of cations in solution and exchange phases for topsoil after leaching with pH 3.9 HCl solution

Depth (cm)	Ca	Mg	K	Na	Al	Sum
	Solution phase					
	mmole(+) L <sup>-1</sup>					
1.0	0.062	0.016	0.146	0.174	0.040	0.439
2.0	0.030	0.016	0.176	0.191	0.088	0.501
3.0	0.023	0.016	0.116	0.146	0.155	0.456
4.0	0.042	0.021	0.188	0.200	0.127	0.578
5.0	0.022	0.016	0.102	0.113	0.110	0.363
6.0	0.032	0.023	0.132	0.146	0.400	0.733
7.0	0.042	0.045	0.183	0.193	0.614	1.078
8.0	0.034	0.069	0.172	0.176	1.880	2.331
9.0	0.040	0.118	0.223	0.192	1.720	2.293
10.0	0.080	0.112	0.377	0.310	1.440	2.319

Depth (cm)	Ca	Mg	K	Na	Al	Sum
	Exchange phase					
	mmole(+) Kg <sup>-1</sup> soil					
1.0	0.262	0.021	0.122	0.217	7.850	8.472
2.0	0.412	0.041	0.166	0.239	9.096	9.954
3.0	0.374	0.021	0.141	0.217	16.857	17.610
4.0	0.661	0.041	0.179	0.217	8.451	9.549
5.0	0.786	0.041	0.147	0.065	9.040	10.079
6.0	0.936	0.021	0.122	0.152	8.084	9.314
7.0	1.350	0.062	0.160	0.337	7.639	9.548
8.0	1.530	0.082	0.160	0.326	7.405	9.504
9.0	1.200	0.144	0.166	0.348	6.672	8.530
10.0	1.140	0.288	0.198	0.391	6.916	8.933

Table 3-4 Concentrations of cations in solution and exchange phases for topsoil after leaching with pH 4.9 solution

Depth (cm)	Ca	Mg	K	Na	Al	Sum
			Solution phase			
			mmole (+)	L <sup>-1</sup>		
1.0	0.030	0.021	0.125	0.130	0.172	0.478
2.0	0.032	0.037	0.104	0.113	0.942	1.228
3.0	0.032	0.066	0.122	0.113	1.800	2.133
4.0	0.023	0.058	0.128	0.130	1.300	1.638
5.0	0.040	0.075	0.158	0.139	1.260	1.672
6.0	0.027	0.058	0.164	0.135	1.200	1.584
7.0	0.020	0.074	0.180	0.152	1.570	1.996
8.0	0.025	0.090	0.196	0.141	2.130	2.583
9.0	0.020	0.025	0.156	0.146	0.297	0.644
10.0	0.042	0.054	0.179	0.163	0.724	1.162

Depth (cm)	Ca	Mg	K	Na	Al	Sum
			Exchange phase			
			mmole (+)	Kg <sup>-1</sup>	soil	
1.0	0.714	0.074	0.151	0.178	7.895	9.012
2.0	0.883	0.123	0.123	0.074	7.917	9.120
3.0	0.883	0.173	0.133	0.061	7.984	9.234
4.0	0.883	0.181	0.133	0.087	7.583	8.867
5.0	0.863	0.181	0.136	0.078	8.117	9.375
6.0	0.843	0.214	0.166	0.087	7.828	9.138
7.0	0.973	0.123	0.237	0.054	6.638	8.026
8.0	0.963	0.206	0.225	0.109	7.394	8.897
9.0	0.913	0.197	0.171	0.056	5.715	7.053
10.0	0.893	0.197	0.200	0.165	6.427	7.882

Table 3-5 Concentrations of cations in solution and exchange phases for subsoil after leaching with pH 3.9 HCl solution

Depth (cm)	Ca	Mg	K	Na	Al	Sum
	Solution phase					
	mmole (+) L <sup>-1</sup>					
1.0	0.048	0.013	0.122	0.141	0.008	0.332
2.0	0.055	0.021	0.152	0.154	0.013	0.395
3.0	0.115	0.033	0.247	0.313	0.004	0.712
4.0	0.122	0.033	0.192	0.248	0.004	0.599
5.0	0.085	0.029	0.136	0.239	0.010	0.499
6.0	0.078	0.026	0.125	0.231	0.009	0.469
7.0	0.112	0.037	0.178	0.313	0.006	0.646
8.0	0.092	0.029	0.162	0.267	0.007	0.557
9.0	0.094	0.037	0.290	0.278	0.009	0.708
10.0	0.096	0.040	0.270	0.240	0.007	0.652

Depth (cm)	Ca	Mg	K	Na	Al	Sum
	Exchange phase					
	mmole (+) Kg <sup>-1</sup> soil					
1.0	0.661	0.082	0.243	0.217	12.520	13.723
2.0	3.220	0.514	0.262	0.207	9.785	13.988
3.0	5.610	1.050	0.313	0.207	8.084	15.264
4.0	7.190	1.280	0.320	0.196	6.738	15.724
5.0	6.540	1.360	0.301	0.196	6.850	15.247
6.0	7.420	1.560	0.371	0.174	6.282	15.807
7.0	7.570	1.540	0.390	0.207	6.516	16.223
8.0	7.580	1.540	0.454	0.207	6.505	16.286
9.0	6.560	1.440	0.460	0.217	5.871	14.548
10.0	6.860	1.520	0.576	0.196	5.560	14.712

Table 3-6 Concentrations of cations in solution and exchange phases for subsoil after leaching with pH 4.9 HCl solution

Depth (cm)	Ca	Mg	K	Na	Al	Sum
	Solution phase					
	mmole (+) L <sup>-1</sup>					
1.0	0.084	0.033	0.116	0.551	0.010	0.794
2.0	0.072	0.029	0.087	0.515	0.020	0.723
3.0	0.067	0.029	0.060	0.224	0.016	0.396
4.0	0.080	0.033	0.097	0.365	0.024	0.599
5.0	0.094	0.040	0.084	0.407	0.036	0.660
6.0	0.082	0.037	0.063	0.372	0.031	0.585
7.0	0.107	0.041	0.055	0.350	0.018	0.571
8.0	0.080	0.033	0.061	0.228	0.020	0.422
9.0	0.108	0.043	0.067	0.315	0.016	0.548
10.0	0.126	0.053	0.101	0.393	0.014	0.687

Depth (cm)	Ca	Mg	K	Na	Al	Sum
	Exchange phase					
	mmole (+) Kg <sup>-1</sup> soil					
1.0	2.200	0.913	0.271	0.174	6.883	10.441
2.0	3.590	1.190	0.261	0.157	6.616	11.814
3.0	4.190	1.230	0.281	0.191	6.282	12.174
4.0	4.590	1.330	0.279	0.065	5.671	11.935
5.0	4.640	1.320	0.315	0.122	6.194	12.591
6.0	4.840	1.300	0.330	0.148	5.938	12.556
7.0	4.790	1.370	0.350	0.157	6.093	12.760
8.0	5.190	1.390	0.363	0.178	6.004	13.125
9.0	5.240	1.440	0.427	0.209	6.049	13.365
10.0	4.990	1.370	0.379	0.178	5.871	12.788

of subsoil after leaching with pH 3.9 and 4.9 HCl solutions, respectively. Concentrations of cations in the solution phase were of the order  $\text{Na}^+ > \text{K}^+ \approx \text{Ca}^{2+} > \text{Mg}^{2+} > \text{Al}^{3+}$  and for the exchange phase of the order  $\text{Al}^{3+} > \text{Ca}^{2+} > \text{Mg}^{2+} > \text{Na}^+ \approx \text{K}^+$ . The orders of cation concentration in the solution phase for the topsoil and subsoil were thus dissimilar, but were similar for the respective exchange phases.

A comparison of exchangeable basic cations before and after leaching were made for the topsoil and subsoil and the two different treatments. Comparison of Table 3-2 with Tables 3-3, 3-4, 3-5 and 3-6 revealed leaching losses of basic cations and increased concentrations of  $\text{Al}^{3+}$  for both soils during application of the HCl solutions. Leaching losses of basic cations and  $\text{Al}^{3+}$ , and final amounts of exchangeable  $\text{Al}^{3+}$ , were not strictly proportional to the input  $\text{H}^+$  concentration for either the topsoil or subsoil columns, though greater losses of basic cations were observed for the pH 3.9 treatment. The pH 3.9 treatment resulted in slightly higher magnitudes of  $\text{Al}^{3+}$  than did the pH 4.9 treatment for in the topsoil and subsoil columns.

#### Estimated Selectivity Coefficients for Ion Pairs

Based on information given in Tables 3-3, 3-4, 3-5 and 3-6, binary selectivity coefficients as defined by equation (3-2) were approximated for each pair of ion species. These values are only approximations, since experimental conditions involved multiple species of ions rather than a simple binary system. Estimates of the selectivity

coefficients are presented in Tables 3-7, 3-8, 3-9 and 3-10 for each pair of cations at specific column depths for both topsoil and subsoil after displacement with the two HCl solutions. The average cation exchange capacity for each column was obtained by summing up the 'sums' in the exchange phase that appeared for each depth in Tables 3-3, 3-4, 3-5 and 3-6, respectively, and then averaging them.

Corresponding total solution-phase concentrations for each column were likewise obtained by summing up the 'sums' in the solution phase for each depth. Also, in the calculation of selectivity coefficients, the higher valenced species for any two cations was assumed to pseudo-saturate the soil exchange sites. For example, for the calculated selectivity coefficient  $K_{K \rightarrow Al}$  in Table 3-5 for topsoil, the exchange reaction for these two specific cation species can be described by the equation  $Al-(ads) + 3 K^+ \rightarrow 3 K-(ads) + Al^{3+}$ , with the cation concentrations at specific depths being taken from the table. In the calculation of selectivity coefficients, if two cation species had the same valence, the cation with the greater atomic weight was assumed to pseudo-saturate the soil exchange sites. For example, for the calculated selectivity coefficients  $K_{Mg \rightarrow Ca}$  in Table 3-5 for topsoil, the exchange reaction for these two specific cation species can be described by the equation  $Ca-(ads) + Mg^{2+} \rightarrow Mg-(ads) + Ca^{2+}$ , and cation concentrations in solution and exchange phases for specific depth can be taken from the table. Solution activity

Table 3-7 Topsoil selectivity coefficients as determined  
after leaching with pH 3.9 HCl solution

	Mg-->Ca	K-->Ca	Na-->Ca	Na-->K	K-->Mg
1	0.29335	0.18174E-01	0.40481E-01	1.4925	0.61120E-01
2	0.18077	0.70553E-02	0.12418E-01	1.3267	0.39029E-01
3	0.75109E-01	0.97137E-02	0.14524E-01	1.2228	0.12933
4	0.12798	0.63549E-02	0.82523E-02	1.1396	0.49655E-01
5	0.69720E-01	0.63531E-02	0.10183E-02	0.4004	0.91123E-01
6	0.30525E-01	0.31815E-02	0.40369E-02	1.1264	0.10423
7	0.42872E-01	0.26237E-02	0.10465E-01	1.9971	0.61199E-01
8	0.26389E-01	0.20953E-02	0.83075E-02	1.9912	0.79398E-01
9	0.41085E-01	0.20387E-02	0.12087E-01	2.4349	0.49622E-01
10	0.18000	0.21101E-02	0.12170E-01	2.4015	0.11723E-01
Average selectivity values					
	0.10718	0.59700E-02	0.12376E-01	1.5533	0.67642E-01

	Na-->Mg	Al-->Ca	Mg-->Al	K-->Al	Na-->Al
1	0.13614	4761.6	0.55214E-05	0.35506E-04	0.11803E-03
2	0.68694E-01	37.536	0.15738E-03	0.96728E-04	0.22587E-03
3	0.19337	23.566	0.17981E-04	0.19721E-03	0.36056E-03
4	0.64482E-01	10.694	0.19602E-03	0.15492E-03	0.22925E-03
5	0.14606E-01	1.355	0.25008E-03	0.43499E-03	0.27915E-04
6	0.13225	0.148	0.19225E-03	0.46656E-03	0.66683E-03
7	0.24409	0.044	0.17958E-02	0.64156E-03	0.51104E-02
8	0.31480	0.15444E-02	0.11899E-01	0.24405E-02	0.19267E-01
9	0.29419	0.52535E-02	0.13200E-01	0.12700E-02	0.18333E-01
10	0.06761	0.72402E-01	0.80550E-01	0.36022E-03	0.49893E-02
Average selectivity values					
	0.15302	483.50	0.10826E-01	0.60982E-03	0.49328E-02

Table 3-8 Topsoil selectivity coefficients as determined  
after leaching with pH 4.9 HCl solution

	Mg-->Ca	K-->Ca	Na-->Ca	Na-->K	K-->Ca
1	0.15043	0.10667E-01	0.13705E-01	1.1335	0.70911E-01
2	0.12198	0.89593E-02	0.27394E-02	0.55296	0.73449E-01
3	0.09647	0.76123E-02	0.18604E-02	0.49436	0.78906E-01
4	0.08007	0.48023E-02	0.19921E-02	0.64407	0.59975E-01
5	0.11313	0.60545E-02	0.25930E-02	0.65443	0.53520E-01
6	0.12076	0.58130E-02	0.23563E-02	0.63668	0.48137E-01
7	0.03417	0.62203E-02	0.45791E-03	0.27132	0.18206
8	0.05909	0.59719E-02	0.27082E-02	0.67341	0.10106
9	0.17471	0.45946E-02	0.57266E-03	0.35304	0.26298E-01
10	0.17483	0.10347E-01	0.84928E-02	0.90598	0.59182E-01

Average selectivity values

0.11256	0.71042E-02	0.37478E-02	0.63197	0.75350E-01
---------	-------------	-------------	---------	-------------

	Na-->Mg	Al-->Ca	Mg-->Al	K-->Al	Na-->Al
1	0.91103E-01	0.88631	0.38408E-02	0.11703E-02	0.17042E-02
2	0.22458E-01	0.01999	0.90790E-01	0.59979E-02	0.10141E-02
3	0.19284E-01	0.00557	0.16127	0.89009E-02	0.10754E-02
4	0.24879E-01	0.00323	0.15917	0.58600E-02	0.15657E-02
5	0.22922E-01	0.02439	0.59357E-01	0.30165E-02	0.84548E-03
6	0.19513E-01	0.00837	0.21037	0.48441E-02	0.12502E-02
7	0.13402E-01	0.00089	0.44839E-01	0.16450E-01	0.32855E-03
8	0.45829E-01	0.00121	0.17083	0.13278E-01	0.40550E-02
9	0.32777E-02	0.02230	0.23916	0.20856E-02	0.91769E-04
10	0.48577E-01	0.04832	0.11060	0.47880E-02	0.35605E-02

Average selectivity values

0.31125E-01	0.10206	0.12502	0.66392E-02	0.15491E-02
-------------	---------	---------	-------------	-------------

Table 3-9 Subsoil selectivity coefficients as determined  
after leaching with pH 3.9 HCl solution

	Mg-->Ca	K-->Ca	Na-->Ca	Na-->K	K-->Mg
1	0.45181	0.10565E-01	0.63078E-02	0.77267	0.23385E-01
2	0.42541	0.18616E-02	0.11321E-02	0.77982	0.43760E-02
3	0.65423	0.12097E-02	0.32949E-03	0.52189	0.18491E-02
4	0.66015	0.17322E-02	0.38949E-03	0.47419	0.26239E-02
5	0.61230	0.23342E-02	0.32048E-03	0.37054	0.38122E-02
6	0.62193	0.33944E-02	0.21863E-03	0.25379	0.54578E-02
7	0.61580	0.26102E-02	0.23781E-03	0.30184	0.42387E-02
8	0.65112	0.35146E-02	0.26898E-03	0.27664	0.53978E-02
9	0.55946	0.13292E-02	0.32188E-03	0.49210	0.23759E-02
10	0.53739	0.23357E-02	0.34229E-03	0.38281	0.43464E-02

Average selectivity values

0.57896	0.30887E-02	0.98689E-03	0.46263	0.57862E-02
---------	-------------	-------------	---------	-------------

	Na-->Mg	Al->Ca	Mg-->Al	K-->Al	Na-->Al
1	0.13961E-01	26816.	0.34395E-05	0.66319E-05	0.30593E-05
2	0.26611E-02	72.997	0.10547E-02	0.94013E-05	0.44582E-05
3	0.50364E-03	773.49	0.36202E-03	0.15129E-05	0.21505E-06
4	0.59001E-03	304.80	0.94389E-03	0.41293E-05	0.44030E-06
5	0.52340E-03	27.830	0.82487E-02	0.21377E-04	0.10875E-05
6	0.35153E-03	15.629	0.15392E-01	0.50024E-04	0.81771E-06
7	0.38618E-03	121.03	0.19294E-02	0.12122E-04	0.33335E-06
8	0.41310E-03	46.725	0.59079E-02	0.30482E-04	0.64535E-06
9	0.57535E-03	35.173	0.49785E-02	0.81711E-05	0.97375E-06
10	0.63695E-03	51.489	0.30140E-02	0.15732E-04	0.88254E-06

Average selectivity values

0.20602E-02	2826.5	0.41835E-02	0.15958E-04	0.12913E-05
-------------	--------	-------------	-------------	-------------

Table 3-10 Subsoil selectivity coefficients as determined after leaching with pH 4.9 HCl solution

	Mg->Ca	K-->Ca	Na-->Ca	Na->K	K-->Mg
1	1.0571	0.10071E-01	0.18402E-03	0.13517	0.95277E-02
2	0.83329	0.87928E-02	0.90796E-04	0.10162	0.10552E-01
3	0.68700	0.17035E-01	0.56657E-03	0.18237	0.24796E-01
4	0.70282	0.69391E-02	0.26874E-04	0.06223	0.98732E-02
5	0.67556	0.13804E-01	0.87994E-04	0.07984	0.20434E-01
6	0.59744	0.22818E-01	0.13039E-03	0.07559	0.38194E-01
7	0.74461	0.43823E-01	0.21775E-03	0.07049	0.58853E-01
8	0.64961	0.26035E-01	0.45399E-03	0.13205	0.40077E-01
9	0.69344	0.41166E-01	0.43954E-03	0.10333	0.59365E-01
10	0.65642	0.17224E-01	0.25094E-03	0.12070	0.26240E-01
Average selectivity values					
	0.72973	0.20771E-01	0.24489E-03	0.10634	0.29791E-01
	Na-->Mg	Al->Ca	Mg-->Al	K-->Al	Na-->Al
1	0.17408E-03	540.47	0.21853E-02	0.43475E-04	0.10737E-06
2	0.10896E-03	18.528	0.31230E-01	0.19155E-03	0.20100E-06
3	0.82470E-03	13.935	0.23269E-01	0.59562E-03	0.36127E-05
4	0.38238E-04	5.8117	0.59736E-01	0.23978E-03	0.57790E-07
5	0.13025E-03	5.1617	0.59731E-01	0.71390E-03	0.36332E-06
6	0.21824E-03	3.6995	0.57643E-01	0.17921E-02	0.77406E-06
7	0.29243E-03	26.964	0.15311E-01	0.17667E-02	0.61877E-06
8	0.69886E-03	6.7631	0.40534E-01	0.16153E-02	0.37196E-05
9	0.63386E-03	27.173	0.12271E-01	0.16023E-02	0.17678E-05
10	0.38228E-03	54.483	0.51913E-02	0.30626E-03	0.53854E-06
Average selectivity values					
	0.35019E-03	70.299	0.30710E-01	0.88669E-03	0.11761E-05

coefficients were assumed to be unity for all cations specie in the calculations.

After leaching, exchangeable  $\text{Al}^{3+}$  comprised 75-95% of the total exchangeable cations in topsoil columns for the pH 3.9 HCl treatment and 80-86% for the pH 4.9 treatment. These values greatly exceed the 48% of  $\text{Al}^{3+}$  initially present on the soil exchange phase. The acid leaching processes obviously resulted in more exchangeable  $\text{Al}^{3+}$  as a consequence of acid dissolution of soil clay minerals. Exchangeable  $\text{Al}^{3+}$  comprised about 40-60% of total exchangeable cations in the subsoil after leaching with both treatments of HCl solution, where as  $\text{Al}^{3+}$  initially accounted for only 32% of total exchangeable cations. Hence acid leaching also resulted in forming more exchangeable  $\text{Al}^{3+}$  in the subsoil column. However, the magnitudes were not as large as observed for the topsoil. These observations suggest that, of all the cation species,  $\text{Al}^{3+}$  was the most preferred ion for exchange sites of both topsoil and subsoil, and also dominant in terms of exchangeable and nonexchangeable forms for this acid Cecil soil. Calculated selectivity coefficients for  $\text{Al}^{3+} \rightarrow \text{Ca}^{2+}$  revealed a significant preference of exchange sites for  $\text{Al}^{3+}$  over  $\text{Ca}^{2+}$  in the subsoil but the opposite in the topsoil. Overall, the approximate values of selectivity coefficients for the same ion pair varied from depth to depth, and were highly dependent upon the local concentrations of cations in

solution and on the exchange phase as well as upon cation valence and pH of the applied HCl solution.

If one assumed the input solution concentration for  $H^+$  to be equal to the total solution concentration for all cation species in the soil column and the cation-exchange capacity of the soil column to be invariant with depth and time then, by taking differences between input solution concentrations and the sum of solution-phase concentrations in Tables 3-3, 3-4, 3-5 and 3-6, the solution-phase concentrations of  $H^+$  can be obtained for each treatment and depth of topsoil and subsoil. In the same manner, subtracting the sum of exchangeable cations at each depth in Tables 3-3, 3-4, 3-5 and 3-6 from the appropriate choice of CEC obtained from Table 3-2, gives the exchange-phase concentrations of  $H^+$  for each depth of topsoil and subsoil in the different treatments. Therefore, the selectivity coefficients between basic cations and  $H^+$  can be calculated. Calculations were not performed initially for  $H^+$  versus basic cations, for the reason discussed earlier by Krishnamoorthy and Overstreet (1950) that the exchangeable hydrogen in clays and soil colloids is not completely disassociated. Thus, conventional ion exchange formulations are not valid for calculating these selectivity coefficients. Obtaining such selectivity coefficients for  $H^+$  is especially difficult for Cecil topsoil and subsoil, which contain substantial amounts of Fe and Al hydrous oxides as well as of interlayer-hydroxy vermiculite, which

each have pH-dependent characteristics. Poorly-crystalline clay minerals that are coated with Al compounds act as sinks for  $H^+$  by transforming the soil exchange phase from  $H^+$ - to  $Al^{3+}$ - saturated (Thomas and Hargrove, 1984). Hydrolysis of  $Al^{3+}$  in the soil then causes the formation of  $H^+$  during extraction. This so-called 'exchangeable'  $H^+$  is a result of hydrolysis and really does not exist as such on the exchange sites of soil clay minerals or organic matter (Kissel et al., 1971). Therefore, the ion-exchange behavior of  $H^+$  in acid soil is not easily described in a meaningful way (Thomas and Hargrove, 1984).

#### Charge Balance of Major Cations for Topsoil and Subsoil

The charge balance of major cations in columns of topsoil and subsoil which received two HCl solutions with different pH values are given in Tables 3-11 and 3-12, respectively, with units of mmole(+). The overall charge balance of major cations in each soil column can be described by the following relationship:

$$\begin{array}{l} \text{Total } H^+ \text{ added as HCl} + \text{All cations initially present on} \\ \text{(1)} \qquad \qquad \qquad \text{soil exchange sites} \qquad \qquad \qquad \text{(2)} \end{array}$$

$$\begin{array}{l} = \text{Total } H^+ \text{ exported or leached in the column effluent} \\ \text{(3)} \end{array}$$

$$\begin{array}{l} + \text{Total cation exported or leached in the column effluent} \\ \text{(4)} \end{array}$$

$$\begin{array}{l} + \text{All cations still remaining in the soil columns in the} \\ \text{exchange and solution phases after leaching with the} \\ \text{HCl solutions.} \end{array}$$

(5)

[3-5]

where the first term (1) was obtained from the product of the concentrations of input solution  $H^+$  (mmole(+)  $L^{-1}$ ) and the total volume of input solution (l). The second term (2) was obtained as the cation exchange capacity (mmole(+)  $kg^{-1}$ ) of a given soil times the weight of soil (kg) residing in the column. The third term (3) was obtained by integrating breakthrough curves of effluent pH and converting mmole(+). The fourth term (4) was obtained by integrating breakthrough curves for each cation species and then summing for all species. The last term (5) accounted for remaining cations in the solution and exchange phases. Total charge of cations in the solution phase was taken as the sum of the charge of each individual cation as obtained from the product of its cation concentration, volumetric water content ( $M^3 M^{-3}$ ) of the soil and total volume of soil (L). In the same manner, the total charge of cations in the exchange phase was taken as the sum of the charge of each individual cation on the exchange phase obtained using the concentrations of cations (mmole(+)  $kg^{-1}$ ) as obtained from 1  $M$   $NH_4OAc$  extraction multiplied by the weight of soil in the columns (kg) to give the masses of individual cation species.

Using the previously stated concept of charge balance, the initial charge (total input of  $H^+$  ions and cations initially present in the column) and final charge (total  $H^+$

and cations exported + cations still remaining in the column) were 2.733 mmole(+) and 2.086 mmole(+), respectively, for pH 3.9 input solution and topsoil (Table 3-11). Overall, charge balance error was - 7.5% for the pH 3.9 treatment, indicating a loss of 0.647 mmole(+) of charge during application of the HCl. The corresponding total charge balances were 2.087 mmole(+) and 1.869 mmole(+) for input and output solutions, respectively, for pH 4.9 input solution and topsoil. Overall charge balance error was - 10.5% for treatment pH 4.9, also indicating a loss in charge during application of HCl to the soil.

From Table 3-12 for the subsoil column the total charge balances of major cations for the initial column and after leaching were 3.446 and 2.702 mmole(+) for the pH 3.9 treatment, respectively. The corresponding charge balance error was - 28% indicating a sizeable loss in charge. For pH 4.9 treatment, values of 3.285 and 2.197 mmole(+) were observed for charge balance of major cations, respectively for the initial column and after leaching. The corresponding charge balance error was - 33%, also indicating a substantial loss in charge.

For all of the columns, outputs of cation charge were less than inputs of charge for topsoil and subsoil, indicating a net loss of charge. Sources of charge-balance error can be attributed to the difficulty in precisely determining  $H^+$  in the solution and exchange phases, to the fact that Al analyses were not specific for  $Al^{3+}$  forms, and

Table 3-11 Charge balance of cations for columns of topsoil

Topsoil pH 3.9 (mmole(+))						
	H <sup>+</sup>	Ca <sup>2+</sup>	Mg <sup>2+</sup>	K <sup>+</sup>	Na <sup>+</sup>	Al <sup>3+</sup>
Initial cations		0.278	0.043	0.121	0.451	1.162
Total input	0.202					
Final #		1.820	1.970	7.920	8.040	2.870
solution phase (*10 <sup>-3</sup> )						
Final #		0.150	0.012	0.027	0.044	1.527
exchange phase						
Total	0.07	0.058	0.064	0.069	0.025	0.110
output in effluent						
Topsoil pH 4.9 (mmole(+))						
	H <sup>+</sup>	Ca <sup>2+</sup>	Mg <sup>2+</sup>	K <sup>+</sup>	Na <sup>+</sup>	Al <sup>3+</sup>
Initial cations		0.279	0.044	0.122	0.454	1.170
Total input	0.018					
Final #		1.300	2.460	6.730	6.070	0.051
solution phase (*10 <sup>-3</sup> )						
Final #		0.154	0.029	0.029	0.017	1.275
exchange phase						
Total	0.068	0.040	0.043	0.064	0.023	0.017
output in effluent						

# : undetermined

Table 3-12 Charge balance of cations for columns of subsoil

Subsoil pH 3.9 (mmole(+))						
	H <sup>+</sup>	Ca <sup>2+</sup>	Mg <sup>2+</sup>	K <sup>+</sup>	Na <sup>+</sup>	Al <sup>3+</sup>
Initial cations		1.332	0.331	0.121	0.424	1.060
Total input	0.198					
Final #		4.850	1.610	0.010	0.013	4.160
solution phase (*10 <sup>-3</sup> )						
Final #		0.896	0.180	0.056	0.031	1.131
exchange phase						
Total	0.006	0.230	0.090	0.040	0.030	0.001
output in effluent						
Subsoil pH 4.9 (mmole(+))						
	H <sup>+</sup>	Ca <sup>2+</sup>	Mg <sup>2+</sup>	K <sup>+</sup>	Na <sup>+</sup>	Al <sup>3+</sup>
Initial cations		1.332	0.331	0.121	0.424	1.060
Total input	0.017					
Final #		4.730	1.950	4.150	1.950	1.080
solution phase (*10 <sup>-3</sup> )						
Final #		0.670	0.200	0.049	0.024	0.933
exchange phase						
Total	0.006	0.170	0.061	0.034	0.035	0.001
output in effluent						

#: undetermined

to the fact that not all ion species (i.e.  $\text{NH}_4^+$ ) were included in the analyses. Essentially all of the column effluent and soil-solution phase had a pH of less than 5.6 to 6.0, as shown in Fig. 3-1 and 3-5. Another reason could be due to experimental error to soil chemical reactions that act as sinks for applied  $\text{H}^+$ , and to chemical dissolution of  $\text{Al}^{3+}$  from nonexchangeable form in oxides and clay minerals.

The overall charge balance of major cations in each soil column was described in equation [3-5]. A sixth term would include sinks for  $\text{H}^+$ , and a seventh term would include a source for  $\text{Al}^{3+}$  by acid dissolution of soil oxides and clay minerals. Although these two terms were not measured in this investigation, they are important to the overall balance. The reported charge-balance values are thus in error, but do give apparent charge-balance values.

### Conclusions

Cecil soil is known to be a highly weathered acid soil. The principal soil minerals observed in Cecil topsoil and subsoil were kaolinite, interlayer-hydroxy vermiculite, and quartz. Gibbsite was also observed in the subsoil. A "salt effect" caused the first few effluent samples to be uncommonly low in pH and high in concentrations of several cation species. Application of HCl solutions with two different pH values to the Cecil soil resulted in larger quantities of cations being leached by pH 3.9 solution relative than of pH 4.9. The reverse effect was observed for quantities of  $\text{Al}^{3+}$  exported, however. Concentrations of

basic cations in the exchange phase were decreased and significant hydrolysis of  $\text{Al}^{3+}$  in the soil occurred during leaching with HCl. This effect was more pronounced for topsoil that received pH 3.9 solution. For the subsoil, only the end of the column that received acid input solution showed significant losses of cations and dissolution of  $\text{Al}^{3+}$ . Generally, exchange-phase concentrations of basic cations as determined with  $\text{NH}_4\text{OAc}$  extraction before and after leaching with HCl solutions were decreased for both soils. The percent of base saturation before HCl application was 52%, for the topsoil. After HCl application, base saturation was 0.1% and 1.5% for pH 3.9 and 4.9 treatments, respectively. For the subsoil, base saturation was initially 68%. After acid application, base saturation was 5.4% and 4.4% for the pH 3.9 and 4.9 treatments, respectively.

The distribution of cations in the exchange phase followed the order  $\text{Al}^{3+} > \text{Ca}^{2+} > \text{Mg}^{2+} > \text{K}^+ \approx \text{Na}^+$  for both soils.  $\text{Al}^{3+}$  was the preferred ion on the exchange sites, as expected due to its large valence and large equivalent fraction initially on the exchanger. In the solution phase, the distribution of cation concentrations followed the order  $\text{K}^+ \approx \text{Na} \approx \text{Al}^{3+} > \text{Ca}^{2+} > \text{Mg}^{2+}$  for topsoil and  $\text{Na}^+ > \text{K}^+ \approx \text{Ca}^{2+} > \text{Mg}^{2+} > \text{Al}^{3+}$  for subsoil. The exchange selectivity coefficients for each pair of cations as estimated from distributions of ion concentrations in solution and on exchange phases at specific column depths varied with depth

for both soils and were highly dependent upon the cation concentrations in solution and on the exchange phase as well as upon cation valence and upon the pH of the applied HCl solution.

Greater quantities of basic cations were leached from soil columns that received pH 3.9 solution than of pH 4.9. Specifically, the total losses of divalent  $\text{Ca}^{2+}$ , and  $\text{Mg}^{2+}$  ions from the topsoil were 0.32 and 0.23 mmole(+), respectively, during application of pH 3.9 and 4.9 HCl solutions. For the subsoil these losses were only 0.12 and 0.08 mmole(+) for pH 3.9 and 4.9 HCl treatments, respectively. Application of HCl solution definitely accelerated leaching losses of cation nutrients from the Cecil soil. Charge-balance errors ranged from -10 to -33% and were likely due to undetermined  $\text{H}^+$  in solution and on the exchange phase for the soil, as well as to negatively-charged surfaces of Fe oxides, experimental error, soil chemical reactions that act as sinks for applied  $\text{H}^+$ , and acid dissolution that provides a source for  $\text{Al}^{3+}$  to enter into exchange reactions though the Column of Cecil soil received solution with a ten-fold difference in HCl concentration, the total quantities of basic cations removed differed by less than two-fold. Therefore, leaching by the HCl solution not only involved cation exchange between monovalent, divalent, and trivalent ions, but also apparently involved the dissolution of gibbsite and other Al-bearing compounds (Sardin et al., 1986).

Assuming an annual rainfall of  $120 \text{ cm yr}^{-1}$ , columns of topsoil and subsoil received 1.16 and 1.11 times the annual rainfall equivalent during a period of only 7 days in these study, such laboratory conditions are extreme compared to field conditions, and greatly enhanced leaching of basic soil cations. In nature, rainfall occurs during periodic events separated by sometimes long periods without rain. Such periodical wetting and drying of the soil tends to limit cation exchange and cation transport, and allows time for chemical reactions that inhibit the extent of leaching of basic cations. Under forested conditions, it is possible that Cecil soil could be largely depleted of most of the basic cations ( $\text{Ca}^{2+}$  and  $\text{Mg}^{2+}$ ) on exchange sites of the topsoil if the annual quantity of acid rain was applied continuously over a period of a few weeks to a few months. Under such extreme conditions, application of lime and fertilizer might be necessary in order to maintain the production of forest located on Cecil soil.

CHAPTER IV  
CATION LEACHING DURING CONTINUOUS DISPLACEMENT  
BY HYDROCHLORIC ACID SOLUTION THROUGH COLUMNS OF  
CHEMICALLY-PRETREATED CECIL SOIL

Introduction

Leaching of cations and movement of organic and inorganic anions in response to acid rain deposition in forest soils has been investigated by Mollitor and Raynal (1982) and Ulrich et al. (1980). Cation exchange is recognized as one of the important soil processes which control detrimental effects of acid rain upon the nutrient status of forest soils (Wiklander, 1975; Reuss, 1983; Cosby et al., 1985a, 1985b). Experimental results have shown that neutral salts added to soil-water suspensions or to dilute solutions percolating through soil columns tend to decrease acidification of the soil (Wiklander, 1975).

Very few published papers report investigations of the leaching of soil cations during the displacement of aqueous acid solutions through columns of soil where the exchange sites have initially been saturated with a single specific cation species such as  $K^+$ ,  $Ca^{2+}$ , or  $Mg^{2+}$ . Such an investigation was performed during the research reported in this chapter. The advantage of using chemically-pretreated soil is that the soil system involves fewer species of cations and thus the data are more easily interpreted.

The first objective of this study was to determine the cation exchange capacity for chemically-pretreated Cecil topsoil and subsoil, and a second objective was to determine the influence of input solution pH upon cation leaching during continuous displacement of HCl solution through hand-packed columns of chemically-pretreated Cecil topsoil and subsoil, respectively. A third objective was to determine the distribution of cation concentrations in solution and exchange phases of each pretreated soil column after leaching with HCl.

#### Cation-Exchange Reaction

##### Saturation Mechanisms for Soil Exchange Sites with a Single Cation Species

Most mineral soils contain a mixture of colloids having constant and variable charge-surfaces (Dixon and Weed, 1977), even though one type might tend to dominate over others. Soils located in the Southeastern United States which are highly weathered have properties commonly dominated by sesquioxides of Fe and Al with their pH-dependent charge, by 1:1 kaolinite-type crystalline clay minerals and by 2:1 interlayer-hydroxy vermiculite minerals. Soil organic matter also provides an important contribution to the pH-dependent charge of such soils.

When a neutral-salt solution (examples: KCl,  $\text{MgCl}_2$ , or  $\text{CaCl}_2$ ) is added to a soil it causes a cation-exchange reaction involving the transfer of multiple species of cations between solution and exchange phases. Cation-

exchange sites in the soil result partially from broken edges of the silica-alumina crystalline units, which give rise to unsatisfied electrostatic charge and which is balanced by exchangeable cations. Broken-edge charge is often a source of variable charge. In kaolinite minerals, broken edges are the major source for cation-exchange capacity but, for vermiculite, broken edges account for only a relatively small portion of the CEC. Isomorphous substitutions of  $\text{Al}^{3+}$  for  $\text{Si}^{4+}$ , and of  $\text{Mg}^{2+}$  for  $\text{Al}^{3+}$ , that occur within the crystalline lattice structure of clay minerals result in unbalanced electrostatic charge that is normally balanced by exchangeable cations. Such charge is referred to as permanent (pH-independent) charge.

Exchangeable cations resulting from lattice substitution are found mostly on cleavage surfaces of vermiculitic clay minerals (Grim, 1968). In general, the order of replacement of exchangeable-cation species for soil exchange sites is  $\text{Na}^+ < \text{NH}_4^+ < \text{K}^+ < \text{Mg}^{2+} < \text{Ca}^{2+} < \text{Al}^{3+}$ .

For pH-dependent charge colloids such as hydrous Al and Fe oxides, organic matter and some clay minerals, both active and potential acidic groups occur along with basic groups. Active acid groups are directly equilibrated with soil-solution cations, whereas potential acid groups are activated only by an increase in the soil pH. Basic groups can acquire a positive charge by uptake of  $\text{H}^+$  ions from the soil solution. The positive charge is balanced by anion species such as  $\text{Cl}^-$ ,  $\text{NO}_3^-$ ,  $\text{SO}_4^{2-}$ ,  $\text{H}_2\text{PO}_4^-$  etc. Thus, such

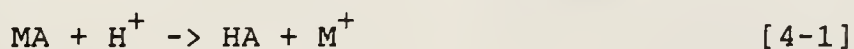
soils are amphoteric, exhibiting both acidic and basic properties and undergoing exchange with cations as well as anions. Also, if neutral salt solution is added to a soil, cations from the salt replace part of the exchangeable  $H^+$  and  $Al^{3+}$  present on the soil exchange phase and thereby increase the base saturation of the soil in proportion to the magnitude of the exchange acidity. The resulting acidity in turn decreases the pH of the soil solution. With continuous addition of salt solution the initial acidity in the solution will gradually be leached, resulting in a corresponding rise of soil pH (Wiklander, 1975). Thus, the higher the normality of the input neutral salt solution, the more complete the saturation of exchange sites with a specific cation species.

#### Mechanisms of $H^+$ Replacement of Exchangeable cations on Soil Exchange Sites

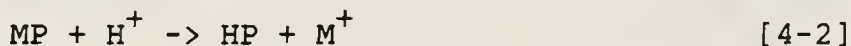
When an acid soil is transformed from (H+Al)-soil to one saturated with a specific cation species (examples:  $K^+$ ,  $Mg^{2+}$ , or  $Ca^{2+}$ ), the acid groups in the soil are successively neutralized and the base saturation of the soil is increased. During subsequent removal of basic cations by leaching with an acid solution, the replacement efficiency of  $H^+$  for basic cations on the soil can be expressed by the ratio  $\delta M / \delta H$  (Wiklander and Andersson, 1972), where  $\delta M$  is the number of equivalents of cations removed and  $\delta H$  is the number of equivalents of  $H^+$  added. A single-species cation-saturated soil always gives a high degree of base

saturation and increases the ratio  $\delta M/\delta H$ . Exchangeable cation nutrients such as  $\text{Ca}^{2+}$ ,  $\text{Mg}^{2+}$  and  $\text{K}^+$  are easily replaced and lost by leaching. Trivalent  $\text{Al}^{3+}$  ions, however, are much more resistant to removal by leaching, with very concentrated salt solutions being required to remove them from the exchange phase of the soil.

With continuous input of acid solution to soil,  $\text{H}^+$  ions have been postulated to successively replace cations from cation-saturated soil in two separate steps (Wiklander and Andersson, 1972); this can be represented as:



where M is a given cation species ( $\text{K}^+$ ,  $\text{Ca}^{2+}$ ,  $\text{Mg}^{2+}$ ), A is the variable charge of the soil, HA is a weak acid group in the soil and MA represents the soil saturated with cation M. Due to the high bonding energy of  $\text{H}^+$  in HA, which produces a high  $\delta M/\delta H$  ratio, the exchange will be practically complete before the beginning of the next step of cation desorption



where P is the permanent charge, MP is from isomorphous substitution, and HP behaves as a strong acid. This means that  $\text{H}^+$  is weakly bound and has a low replacing power for ion species M. Natural occurrence of large quantities of  $\text{Al}^{3+}$  as an exchangeable ion in most acid soils results in a decrease of the replacing efficiency of  $\text{H}^+$  for cation species M. With continuous application of  $\text{H}^+$  ions in solution,  $\text{H}^+$  and  $\text{Al}^{3+}$  concentrations will increase in the

soil solution, will cause more leaching of soil cations, and will lower the content of exchangeable cations.

### Materials and Methods

#### Preparation of Pretreated Soil

Cecil topsoil and subsoil materials used in this study were obtained from the same site as described in chapter two. Cylindrical columns used to house the soil samples were constructed from acrylic plastic with of 0.3 m length and 0.0832 m inside-diameter. The top and bottom endplates obtained from commercially-available Tempe cells (Soil Moisture Equipment Co., Santa Barbara, California) were fitted to each column. Soil was held in each column by a fine nylon mesh and a Whatman no.42 filter paper. Each column was then placed in a vertical position and soil was sequentially packed by adding increments of soil and tapping the side of the column until it was full in order to obtain the desired average bulk density. The endplates were mounted onto ends of the column in order to hold the soil in place. Using the procedure as stated, three soil columns were prepared for topsoil and another three for subsoil. Stock solutions of 10 mmole(+)  $L^{-1}$  KCl,  $MgCl_2$  and  $CaCl_2$  were prepared, respectively. Three topsoil columns were then saturated with 1 mmole(+)  $L^{-1}$  KCl,  $MgCl_2$  and  $CaCl_2$  diluted stock solutions by application to the bottom of each soil column, respectively, in a vertical position. A four-channel peristaltic pump as described in chapter two was used to deliver each of the stock solutions at a rate of

1.10 cm h<sup>-1</sup> ( $\pm$  3%) Darcy velocity to each column. A check for concentrations of cations in the column effluent was made periodically. A conventional way to estimate if the soil exchange sites are saturated with a specific cation is by monitoring concentrations of the specific cation in the effluent with time. If the cation concentration in the effluent becomes equal to that of the input solution then the soil exchange sites are commonly considered to be saturated with that cation species. Such a technique, however, is not without difficulties, particularly if the exchange sites initially contained highly-preferred species of cations. In this investigation concentrations of a specific cation in the effluent reached 99% of the input solution concentration after about 3-4.5 pore volumes of elution, but very small concentrations of other ion species remained even after leaching of the column for a month or more. After the flow was terminated, the columns were leached with 1.5 liters of 95% ethanol to remove all soluble salts. Soil was then removed from each column, air-dried, ground, passed through a 2-mm sieve and stored in large plastic bottles for future use. Three columns of subsoil were prepared similarly to the aforementioned procedure for topsoil columns. Therefore, Ca-saturated, Mg-saturated, K-saturated topsoil and subsoil materials were obtained. Pretreated mixed-topsoil and mixed-subsoil were obtained by carefully mixing equal weight ratios (1:1:1 for Ca:Mg:K) of Ca-saturated, Mg-saturated, and K-saturated soil materials.

Concentrations of exchangeable cations in all of the treated soils were determined by extraction with 1 M neutral  $\text{NH}_4\text{OAc}$  (Thomas, 1982).

#### Soil Column Preparation and Procedure for Displacing HCl Solution Through Columns

Each soil column consisted of a stack of 1-cm thick acrylic plastic (plexiglass) rings with  $3.72 \times 10^{-2}$  m inside-diameter. Water-proof, acid-resistant electrical tape was tightly wrapped around the outside of the rings to insure that lateral leakage of water did not occur during runs. Each column had dimensions of 0.2 m length and 0.0375 m inside diameter, giving a total internal volume of  $2.21 \times 10^{-4}$  m<sup>3</sup>. The soil was held in the columns by a fine nylon mesh and a piece of Whatman no.42 filter paper placed over a thin plastic disc with small holes distributed over its surface in each of the inflow and outflow endplates. A check for water leaks was made prior to packing the soil into a given column. Each column was then placed in a vertical position and sequentially packed by slowly adding incremental quantities of soil and tapping the side of the column until a desired soil bulk density was obtained. After packing, the entire soil column was mounted between two wooden boards for support and fastened with four threaded steel rods to hold the soil and rings in place. Duplicate soil columns were constructed for each chemically pretreated and mixed soil. Columns included Ca-saturated topsoil, Mg-saturated topsoil, K-saturated topsoil,

Ca-saturated topsoil, Mg-saturated subsoil, K-saturated subsoil and mixed subsoil, and mixed topsoil for a total of 16 soil columns. Miscible-displacement experiments were performed for one of the pretreated and mixed soil columns using pH 3.9 displacing HCl solution and for another column using pH 4.9 HCl displacing solution. Darcy velocities ranged from  $1.09 \times 10^{-2}$  to  $1.16 \times 10^{-2}$  ( $\pm 2\%$ )  $\text{m h}^{-1}$ . A four-channel peristaltic pump as described in an earlier chapter was used to deliver the applied solution into the bottom of each soil column. Effluent from the top of the column was collected by the fraction collector described previously and effluent samples were stored in a refrigerator for later analysis. After termination of acid application to a given column, the pore volume was obtained from the mass difference between wetted and air-dried soil columns. Corrections were made to cumulative effluent volume for amounts of solution held inside each of the endplates. Initially the soil was air-dry but water saturation soon was approached. Eventually the soil columns reached steady-state water flow, which was maintained thereafter. Experimental measurements of dispersion coefficient for each column were not conducted, but were assumed using the magnitude of the dispersion coefficients for the topsoil and subsoil as given in chapter two. Since all of the soil columns have the same length, the deviation of bulk density was within  $\pm 3$  and  $\pm 1\%$  for topsoil and subsoil, respectively. Moreover, the deviation for the

Darcy velocity was within  $\pm 3\%$  for most columns. Large differences with regard to the dispersion coefficients between soil columns were assumed absent due to the small variations in bulk density and Darcy flux.

#### Method for Dissection, Extraction and Chemical Analysis of Soil Columns

After liquid flow was terminated, each column was equilibrated overnight to insure that the whole system was at equilibrium. The column was placed in the vertical position, and the tape on the outside of the column was removed carefully. As the outflow endplate was removed, a piece of parafilm was placed over the soil cross section and a small-diameter steel wire was used to slice the consecutive rings of the column. Each section of soil then was carefully placed onto another piece of prepared parafilm before being packed into a prenumbered small centrifuge tube with a predrilled small hole in the bottom. A Whatman no.42 filter paper was cut and placed inside the tube over the hole in the bottom of the tube. Then each small tube was transferred into a large-size centrifuge tube with a glass bead separating the extraction solution from the small centrifuge tube, and spun at 4000 rpm for 30 minutes. The soil sample was then removed from the small centrifuge tube and placed into a plastic weighing boat. The weight of the wet soil was recorded, soil in the weighing boat was air-dried, and the air-dry weight was recorded. The concentrations of basic cations in the exchange phase were

obtained extraction with neutral 1 M  $\text{NH}_4\text{OAc}$  (Thomas, 1982). Unbuffered 1 M  $\text{KCl}$  (Thomas, 1982) was used to obtain exchangeable  $\text{Al}^{3+}$ . Concentrations were corrected for entrapped equilibrium solution near the exchange sites. Concentrations of  $\text{Ca}^{2+}$ ,  $\text{Mg}^{2+}$ ,  $\text{K}^+$ , and  $\text{Na}^+$  in the column effluent, solution and exchange phases of each soil column were analyzed by an atomic absorption spectrometer as described in previous chapters. The  $\text{Al}^{3+}$  was determined by optical emission spectroscopy (inductively coupled argon plasma, ICAP) on a unit located in the Soil Testing Laboratory, Soil Science Department, University of Florida.

### Results and Discussion

Initial exchangeable cations in nontreated topsoil and subsoil are presented in Table 4-1. The soil parameters used for the miscible displacement experiments are presented in Tables 4-2, 4-3 and 4-4 for chemically-pretreated topsoil, pretreated subsoil, and mixed topsoil and subsoil, respectively.

From Tables 4-2 through 4-4, the deviation of the bulk density, volumetric water content and pore-water velocity of hand-packed treated topsoil and subsoil columns were within  $\pm 3 \%$ , respectively. Similar deviations for the bulk density, volumetric water content and pore water velocity were also found for hand-packed mixed subsoil and topsoil columns.

Table 4-1 Concentrations of exchangeable cations for nontreated Cecil topsoil and subsoil

Soil	Exchangeable cations (mmole(+) Kg <sup>-1</sup> soil)					CEC (mmole(+) Kg <sup>-1</sup> soil)
	Ca <sup>2+</sup>	Mg <sup>2+</sup>	K <sup>+</sup>	Na <sup>+</sup>	Al <sup>3+</sup>	
Topsoil	1.60	0.30	0.70	2.60	6.70	11.90
Subsoil	8.80	2.20	0.80	2.80	7.00	21.60

Table 4-2 Soil parameters for chemically pretreated topsoil columns after leaching with HCl solutions

Parameter	Ca-topsoil	Ca-topsoil	Mg-topsoil
Input solution pH	3.9	4.9	3.9
Bulk density (MG M <sup>-3</sup> )	1.61	1.64	1.64
Volumetric water content (M <sup>3</sup> M <sup>-3</sup> )	0.37	0.38	0.37
Dispersion coefficient (M <sup>2</sup> h <sup>-1</sup> )	3.03*10 <sup>-4</sup>	3.03*10 <sup>-4</sup>	3.03*10 <sup>-4</sup>
Pore velocity (M h <sup>-1</sup> )	0.030	0.028	0.030
Pore volume (L)	0.082	0.083	0.082
Column length (M)	0.20	0.20	0.20
Input concentration of H <sup>+</sup> (mmole(+) L <sup>-1</sup> )	0.125	0.0125	0.125
Total amount of H <sup>+</sup> applied (mmole(+) L <sup>-1</sup> )	0.284	0.029	0.277
Total no. of pore volumes collected	26	28	26
Parameter	Mg-topsoil	K-topsoil	K-topsoil
Input solution pH	4.9	3.9	4.9
Bulk density (MG M <sup>-3</sup> )	1.61	1.65	1.64
Volumetric water content (M <sup>3</sup> M <sup>-3</sup> )	0.38	0.37	0.37
Dispersion coefficient (M <sup>2</sup> h <sup>-1</sup> )	3.03*10 <sup>-4</sup>	3.03*10 <sup>-4</sup>	3.03*10 <sup>-4</sup>
Pore velocity (M h <sup>-1</sup> )	0.029	0.034	0.028
Pore volume (L)	0.083	0.081	0.083
Column length (M)	0.20	0.20	0.20
Input concentration of H <sup>+</sup> (mmole(+) L <sup>-1</sup> )	0.0125	0.125	0.0125
Total amount of H <sup>+</sup> applied mmole(+) L <sup>-1</sup>	0.025	0.348	0.029
Total no. of pore volumes collected	27	34	27

Table 4-3 Soil parameters for chemically pretreated subsoil columns after leaching with HCl solutions

Parameter	Ca-subsoil	Ca-subsoil	Mg-subsoil
Input solution pH	3.9	4.9	3.9
Bulk density ( $\text{MG M}^{-3}$ )	1.47	1.47	1.41
Volumetric water content ( $\text{M}^3 \text{ M}^{-3}$ )	0.42	0.42	0.44
Dispersion coefficient ( $\text{M}^2 \text{ h}^{-1}$ )	$1.85 \times 10^{-4}$	$1.85 \times 10^{-4}$	$1.85 \times 10^{-4}$
Pore velocity ( $\text{M h}^{-1}$ )	0.023	0.021	0.024
Pore volume (L)	0.092	0.093	0.098
Column length (M)	0.20	0.20	0.20
Input concentration of $\text{H}^+$ ( $\text{mmole}(+) \text{ L}^{-1}$ )	0.125	0.0125	0.125
Total amount of $\text{H}^+$ applied ( $\text{mmole}(+) \text{ L}^{-1}$ )	0.271	0.024	0.271
Total no. of pore volumes collected	23	23	21

Parameter	Mg-subsoil	K-subsoil	K-subsoil
Input solution pH	4.9	3.9	4.9
Bulk density ( $\text{MG M}^{-3}$ )	1.42	1.39	1.37
Volumetric water content ( $\text{M}^3 \text{ M}^{-3}$ )	0.44	0.47	0.47
Dispersion coefficient ( $\text{M}^2 \text{ h}^{-1}$ )	$1.85 \times 10^{-4}$	$1.85 \times 10^{-4}$	$1.85 \times 10^{-4}$
Pore velocity ( $\text{M h}^{-1}$ )	0.0248	0.0232	0.0228
Pore volume (L)	0.0977	0.1041	0.1034
Column length (M)	0.20	0.20	0.20
Input concentration of $\text{H}^+$ ( $\text{mmole}(+) \text{ L}^{-1}$ )	0.0125	0.125	0.0125
Total amount of $\text{H}^+$ applied ( $\text{mmole}(+) \text{ L}^{-1}$ )	0.024	0.271	0.026
Total no. of pore volumes collected	21.1	19.3	18.3

Table 4-4 Soil parameters for mixed soil columns after leaching with HCl solutions

Parameter	Mixed-cation topsoil	Mixed-cation topsoil
Input solution pH	3.9	4.9
Bulk density ( $\text{MG M}^{-3}$ )	1.68	1.66
Volumetric water content ( $\text{M}^3 \text{ M}^{-3}$ )	0.36	0.36
Dispersion coefficient ( $\text{M}^2 \text{ h}^{-1}$ )	$3.03 \times 10^{-4}$	$3.03 \times 10^{-4}$
Pore velocity ( $\text{M h}^{-1}$ )	0.027	0.030
Pore volume (L)	0.079	0.800
Column length (M)	0.20	0.20
Input concentration of $\text{H}^+$ ( $\text{mmole}(+) \text{ L}^{-1}$ )	0.125	0.0125
Total amount of $\text{H}^+$ applied ( $\text{mmole}(+) \text{ L}^{-1}$ )	0.1253	0.026
Total no. of pore volume collected	23	26
Parameter	Mixed-cation subsoil	Mixed-cation subsoil
Input solution pH	3.9	4.9
Bulk density ( $\text{MG M}^{-3}$ )	1.47	1.47
Volumetric water content ( $\text{M}^3 \text{ M}^{-3}$ )	0.43	0.44
Dispersion coefficient ( $\text{M}^2 \text{ h}^{-1}$ )	$1.85 \times 10^{-4}$	$1.85 \times 10^{-4}$
Pore velocity ( $\text{M h}^{-1}$ )	0.0253	0.0248
Pore volume (L)	0.0951	0.965
Column length (M)	0.20	0.20
Input concentration of $\text{H}^+$ ( $\text{mmole}(+) \text{ L}^{-1}$ )	0.125	0.0125
Total amount of $\text{H}^+$ applied ( $\text{mmole}(+) \text{ L}^{-1}$ )	0.1267	0.024
Total no. of pore volume collected	22.3	22.0

The cation compositions of pretreated and mixed soils are listed in Table 4-4 and concentrations of exchangeable cations for nontreated Cecil topsoil and subsoil are given in Table 4-5.

Table 4-5 Concentrations of exchangeable cations for pretreated and mixed topsoil and subsoil

Soil	Concentrations of exchangeable cations (mmole(+) kg <sup>-1</sup> soil)				
	K <sup>+</sup>	Na <sup>+</sup>	Mg <sup>2+</sup>	Ca <sup>2+</sup>	Al <sup>3+</sup>
K-topsoil	17.20	0.30	0.08	0.60	5.80
Mg-topsoil	0.20	0.30	11.70	0.90	0.50
Ca-topsoil	0.10	0.00	0.02	11.70	2.20
K-subsoil	50.20	0.40	0.10	1.40	0.70
Mg-subsoil	0.30	0.20	96.80	0.30	1.40
Ca-subsoil	0.20	0.00	0.10	54.40	0.20
Mixed-topsoil	6.10	0.60	6.50	5.10	3.00
Mixed-subsoil	16.10	0.50	31.50	26.30	0.80

	CEC mmole(+) kg <sup>-1</sup> soil Al <sup>3+</sup> included	Dominant cation % for this specific CEC with Al <sup>3+</sup> included
K-topsoil	23.68	(K) 72
Mg-topsoil	13.60	(Mg) 86
Ca-topsoil	14.02	(Ca) 84
K-subsoil	52.80	(K) 95
Mg-subsoil	99.00	(Mg) 98
Ca-subsoil	54.90	(Ca) 95
Mixed-topsoil	21.30	*
Mixed-subsoil	75.20	*

	CEC mmole(+) kg <sup>-1</sup> soil Al <sup>3+</sup> not included	Dominant cation % for this specific CEC with Al <sup>3+</sup> not included
K-topsoil	18.18	(K) 95
Mg-topsoil	13.10	(Mg) 89
Ca-topsoil	11.82	(Ca) 99
K-subsoil	52.11	(K) 96
Mg-subsoil	97.60	(Mg) 99
Ca-subsoil	54.70	(Ca) 99.1
Mixed-topsoil	18.30	*
Mixed-subsoil	74.40	*

### Exchange Sites for Chemically Pretreated Soil

Treating the Cecil soil with a specific cation tended to increase the base saturation and CEC (Tables 4-1 and 4-5) of the soil, with the largest effect being found for the subsoil. The pretreated topsoil and subsoil materials were non-homoionic with respect to cations in the exchange phase, indicating that the soil exchange sites were not completely saturated initially with any one specific ion. For example, equivalent fractions of  $K^+$  in K-topsoil were 95 and 72% for cases in which Al was excluded from and included in the CEC calculation, respectively. Equivalent fractions of  $Mg^{2+}$  in Mg-topsoil were 89 and 86% for similar cases, with corresponding values of  $Ca^{2+}$  for Ca-topsoil 99 and 84%, 96 and 95% for K-subsoil, 99 and 98% for Mg-subsoil, and 99 and 95% for Ca-subsoil. Quantities of other basic cations in the exchange phase were small compared with the dominant ion for each of the pretreated soils.

The subsoil had very little exchangeable  $Al^{3+}$  following the cation-saturation procedures. Saturation of topsoil exchange sites was not as complete as it was for the subsoil.

### Effluent pH for Treated Soil Columns

Regardless of pH of the applied HCl solution, effluent pH of all columns of pretreated Cecil topsoil, subsoil, and mixed-cation columns started at about 4.0-4.4 and then quickly increased to about pH 6.7 within two pore volumes of elution. Thereafter, readings fluctuated around pH 6.1-6.8

for the remainder (approximately 25 pore volumes) of each run. Concurrently, high concentrations of basic and acidic cations appeared early in the effluent and then greatly decreased with increasing volumes of effluent. Finally, fairly stable values for concentrations of basic cations in the effluent were maintained. Using input HCl solutions with two different pH values resulted in similar effects upon column effluent. Figs. 4-1 and 4-2 present the effluent pH from Ca-topsoil and Ca-subsoil, respectively. In general, columns that received pH 4.9 solution resulted in higher pH values for the effluent than when pH 3.9 solution was applied.

#### Cation Concentrations in Effluent from Treated Soil Columns

Concentrations of specific basic cations in effluent from pretreated topsoil columns were observed to be very high for each of the first-collected samples (about 0.14-0.17 pore volume). For example, K-topsoil, Ca-topsoil and Mg-topsoil columns that received pH 3.9 HCl solution had initial concentrations of  $K^+$ ,  $Ca^{2+}$  and  $Mg^{2+}$  of 71.63, 164.87, and 249.28 mmole(+)  $L^{-1}$ , respectively. For columns receiving pH 4.9 HCl solution, initial concentrations of 70.13, 101.60, and 204.03 mmole(+)  $L^{-1}$  were observed for  $K^+$ ,  $Ca^{2+}$ , and  $Mg^{2+}$ , respectively. High initial concentrations of specific cations in effluent from correspondingly pretreated subsoil columns were also observed. For K-subsoil, Ca-subsoil, and Mg-subsoil columns that received pH 3.9 HCl solution, concentrations of  $K^+$ ,  $Ca^{2+}$ , and  $Mg^{2+}$

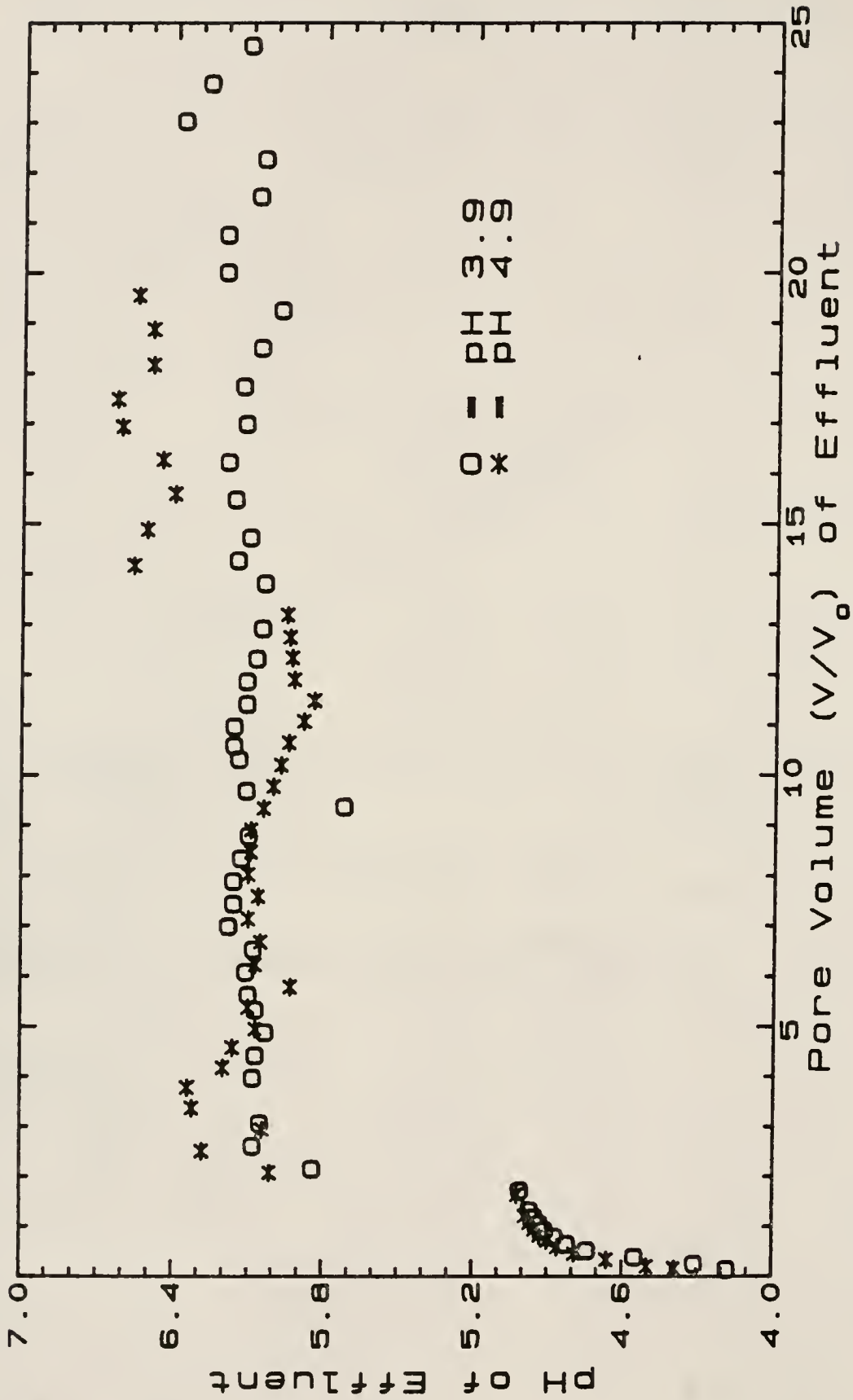


Figure 4-1 Breakthrough curves for pH in the effluent from Ca-topsoil columns which received input HCl solutions with two different pH values.

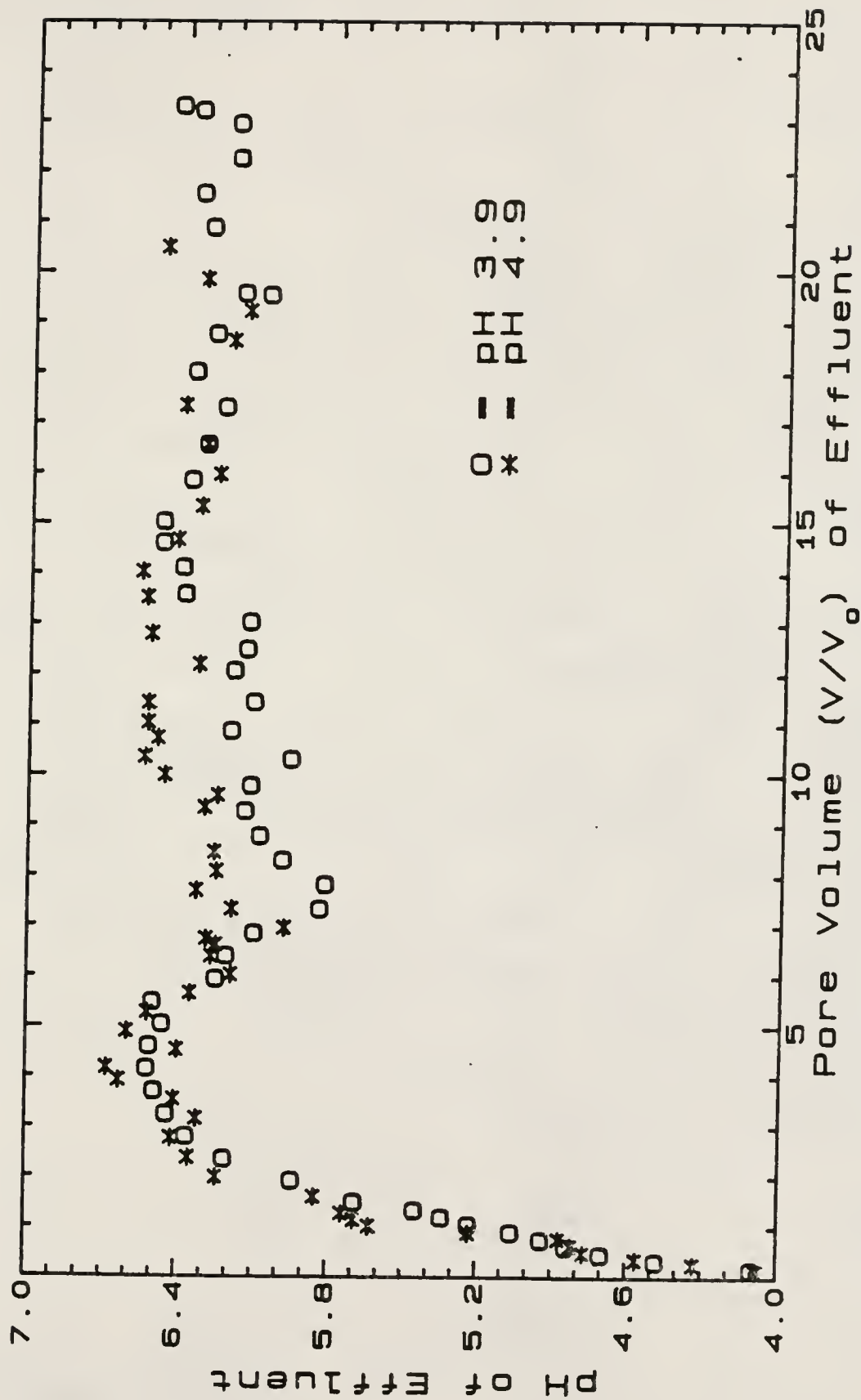


Figure 4-2 Breakthrough curves for pH in the effluent from Ca-subsoil columns which received input HCl solutions with two different pH values.

were 60.89, 94.86 and 186.75 mmole(+) L<sup>-1</sup>, respectively. For columns that received pH 4.9 HCl solution, concentrations of 33.51, 145.62 and 139.72 mmole(+) were observed for K<sup>+</sup>, Ca<sup>2+</sup> and Mg<sup>2+</sup>, respectively. Beginning with the third collected sample (about 0.5 pore volume) of effluent, cation concentrations underwent a drastic decrease to below 10 mmole(+) L<sup>-1</sup> for all of the pretreated topsoil and subsoil columns. Concentrations of other cations for each soil column were detectable but usually so small as to be negligible.

High concentrations of cations that appeared in the first few collected effluent samples from each pretreated soil column can be explained by a "salt effect" and by the replacement efficiency of H<sup>+</sup> for exchangeable cations (Wiklander, 1975; Reuss and Johnson, 1986). All air-dry pretreated topsoil and subsoil contained 0.6 and 1% water content by volume, respectively. Since the soil columns were initially air-dry, as the acid solution infiltrated into each soil column H<sup>+</sup> in the moving wetting front tended to replace cations from variably-charged sites effectively. This resulted in high concentrations of cations in the wetting front. Thus, due to the high ratio of  $\delta M / \delta H$  for the chemically pretreated soil columns, the replacing efficiency of H<sup>+</sup> for basic cations (Wiklander and Andersson, 1972) was enhanced. Thereafter, these high concentrations of cations induced cation exchange with exchangeable (Al<sup>3+</sup> + H<sup>+</sup>), resulting in low pH for the soil solution. This phenomenon

is called a "salt effect" (Wiklander, 1975). As mass flow occurred, the acid displacing solution mixed with the native soil solution by hydrodynamic dispersion. Acidity caused by the salt effect was gradually leached, resulting in increased pH of the soil solution and effluent once more. From about 5 to 25 pore volumes of effluent the pH ranged from about 6.0 to 6.6, indicating strong buffering by the soil. The buffering reflects that  $H^+$  ions which were partially removed from the solution phase either by ion exchange, dissolution of clay minerals, reactions involving aluminum species, or a combination of the three. The initial effluent concentrations of  $Mg^{2+}$  from Mg-topsoil or Mg-subsoil were relatively higher than  $Ca^{2+}$  from Ca-topsoil or Ca-subsoil and than  $K^+$  from K-topsoil and K-subsoil. The cause of these differences was uncertain.

The effect of input solution pH upon concentrations of eluted cations in column effluent showed that the lower pH of input acid solution resulted in approximately the same quantities of cations being leached as obtained at the higher pH. This phenomenon was found for all pretreated topsoil and subsoil columns, but was most obvious for the topsoil (Figs. 4-3, 4-4, and 4-5). Concentrations of cations in the effluent from pretreated subsoil columns are given in Figs. 4-6, 4-7, 4-8 for K-subsoil, Ca-subsoil, and Mg-subsoil columns, respectively. A greater effect of input solution pH upon cation elution was found for pretreated topsoil than for subsoil. This can be explained by the

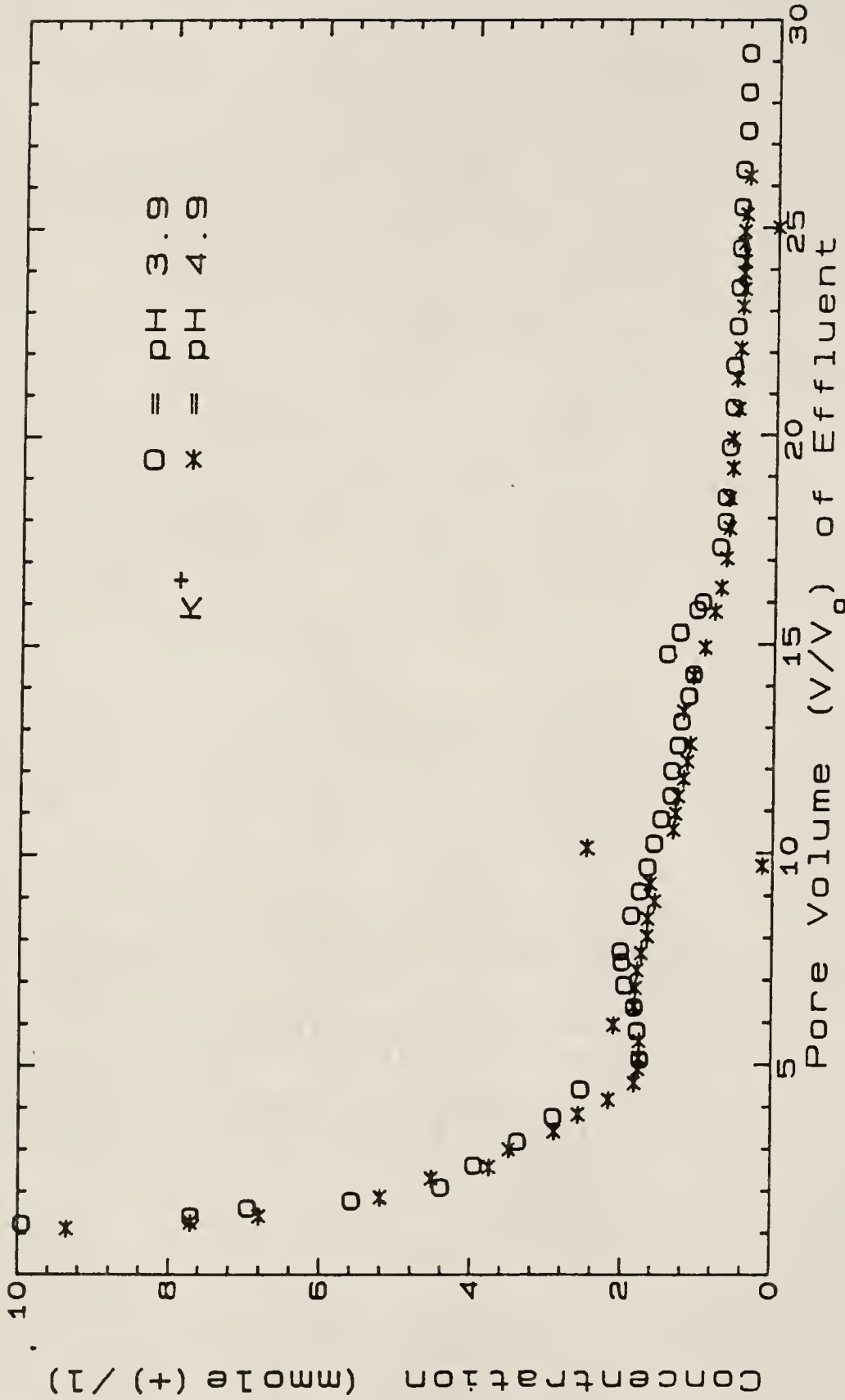


Figure 4-3 Breakthrough curves of  $K^+$  from K-topsoil columns which received input HCl solutions with two different pH values.

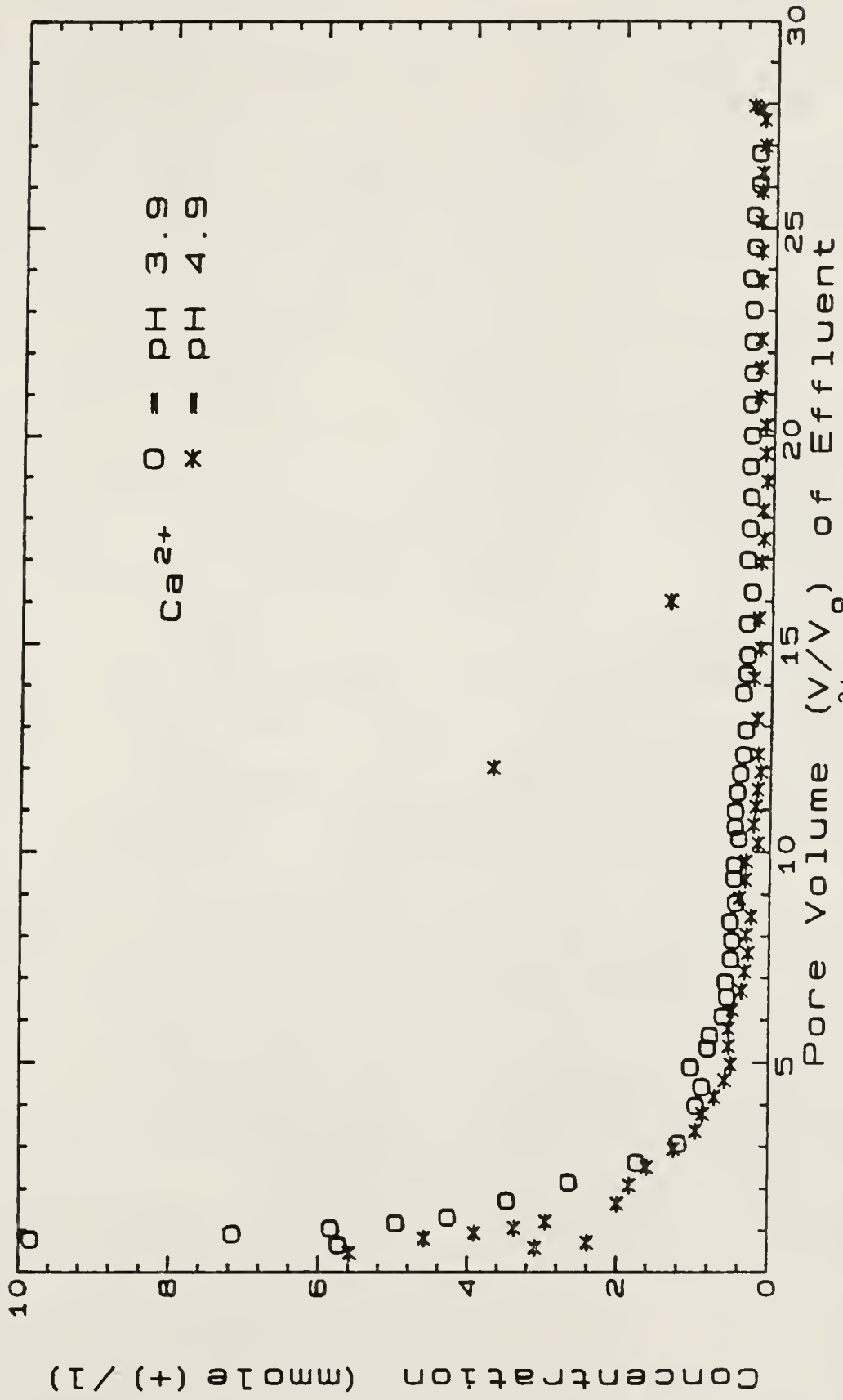


Figure 4-4 Breakthrough curves of Ca<sup>2+</sup> from Ca-topsoil columns which received input HCl solutions with two different pH values.

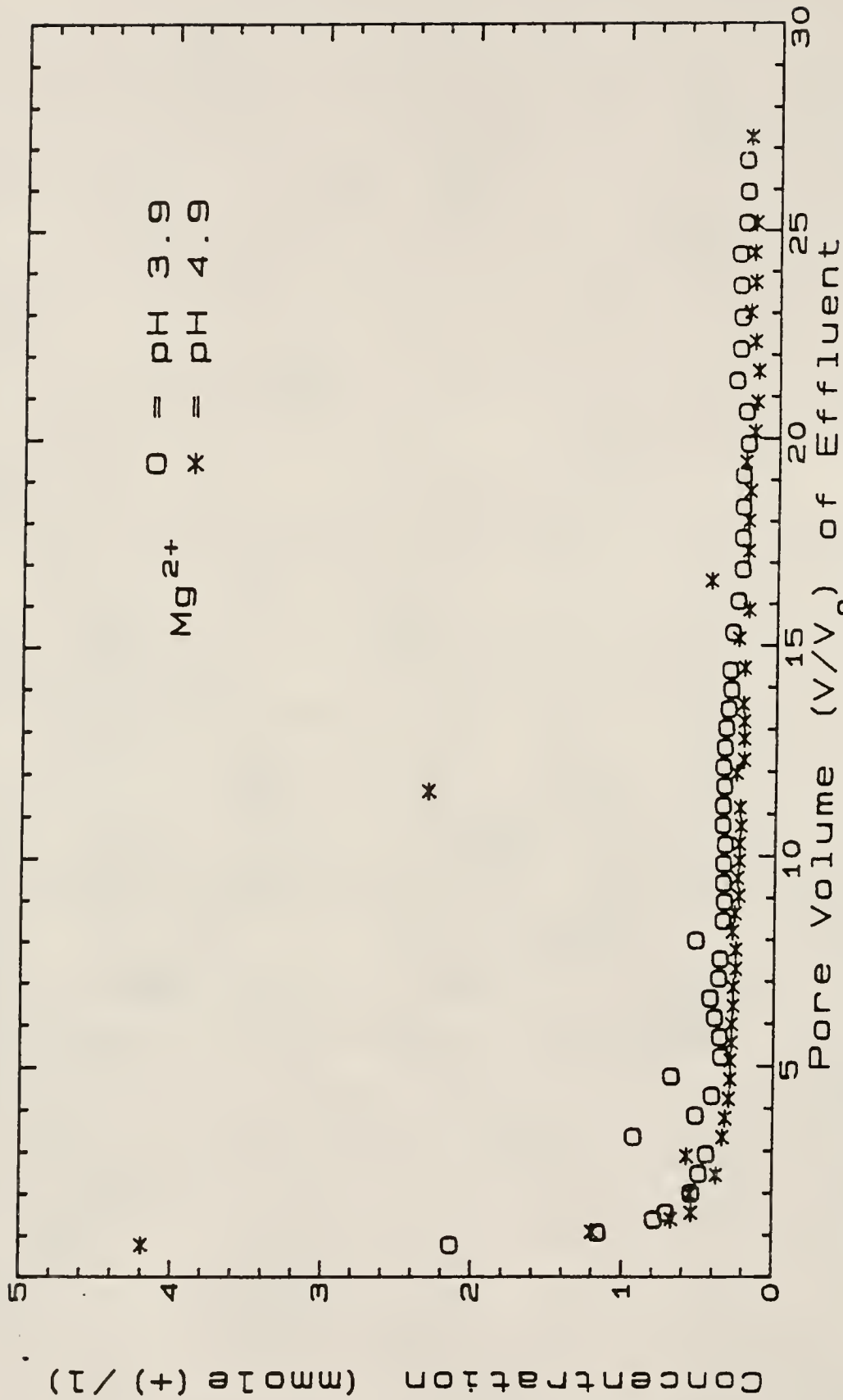


Figure 4-5 Breakthrough curves of  $\text{Mg}^{2+}$  from Mg-topsoil columns which received input HCl solutions with two different pH values.

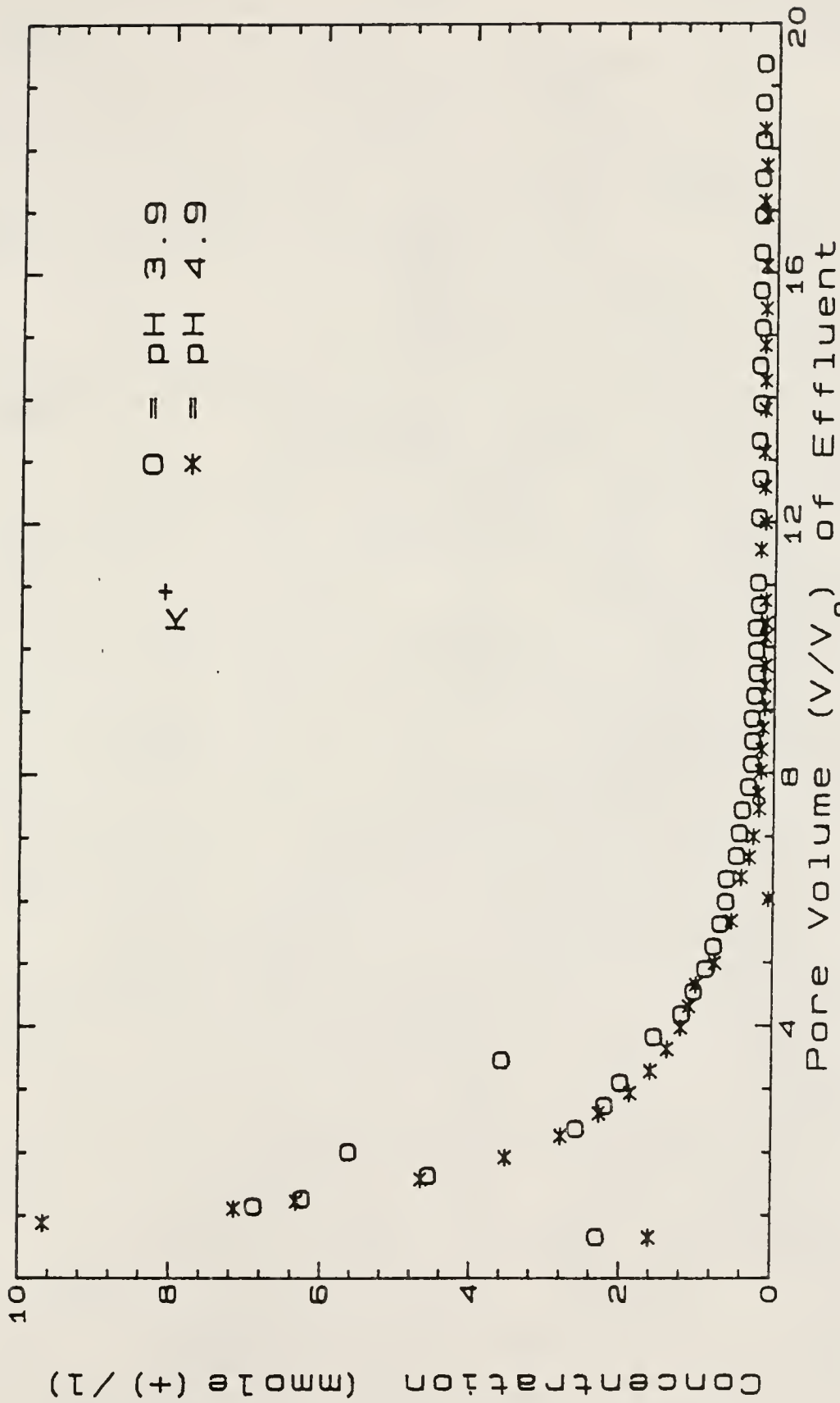


Figure 4-6 Breakthrough curves of  $K^+$  from K-subsoil columns which received input HCl solutions with two different pH values.

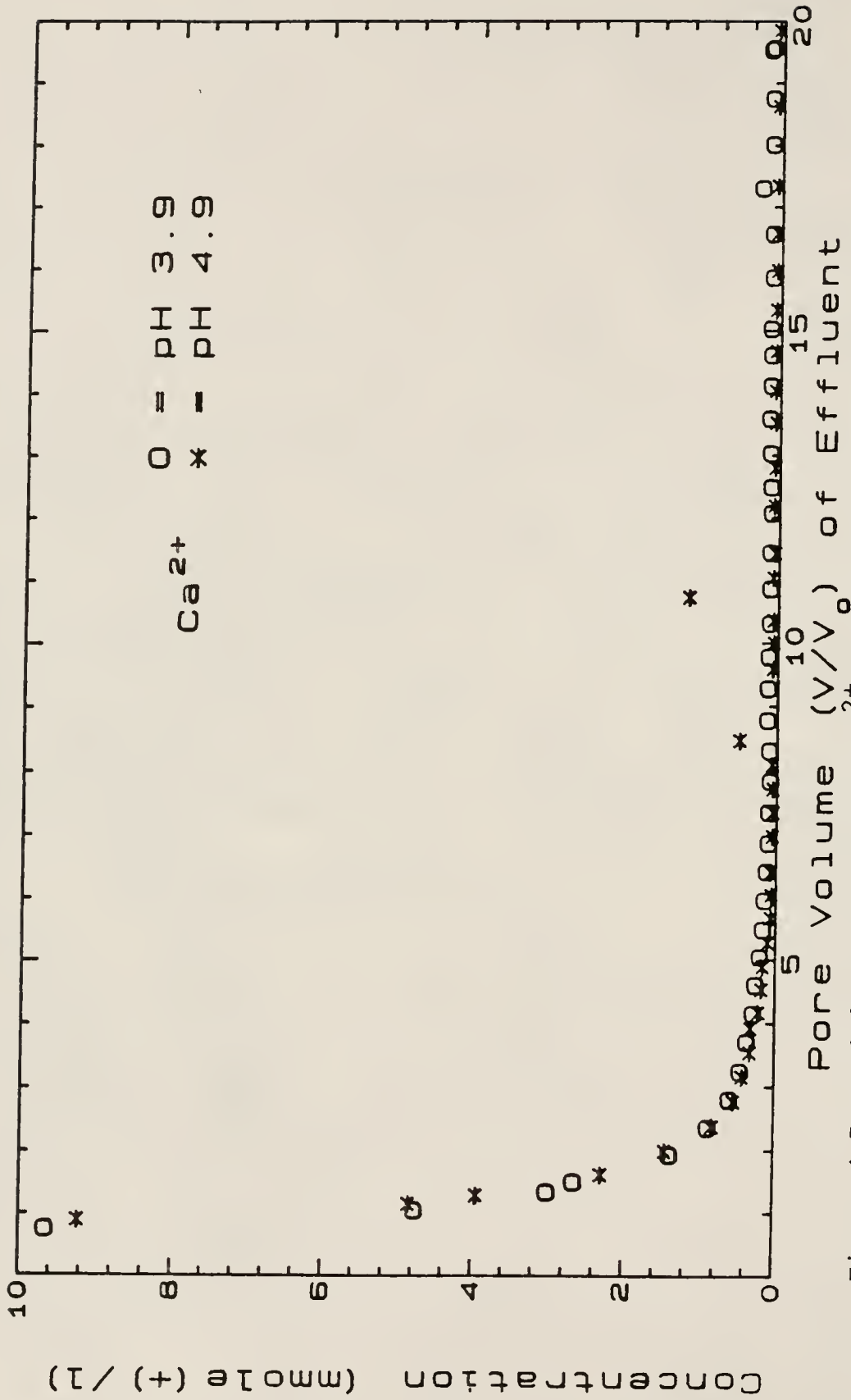


Figure 4-7 Breakthrough curves of  $\text{Ca}^{2+}$  from Ca-subsoil columns which received input HCl solutions with two different pH values.

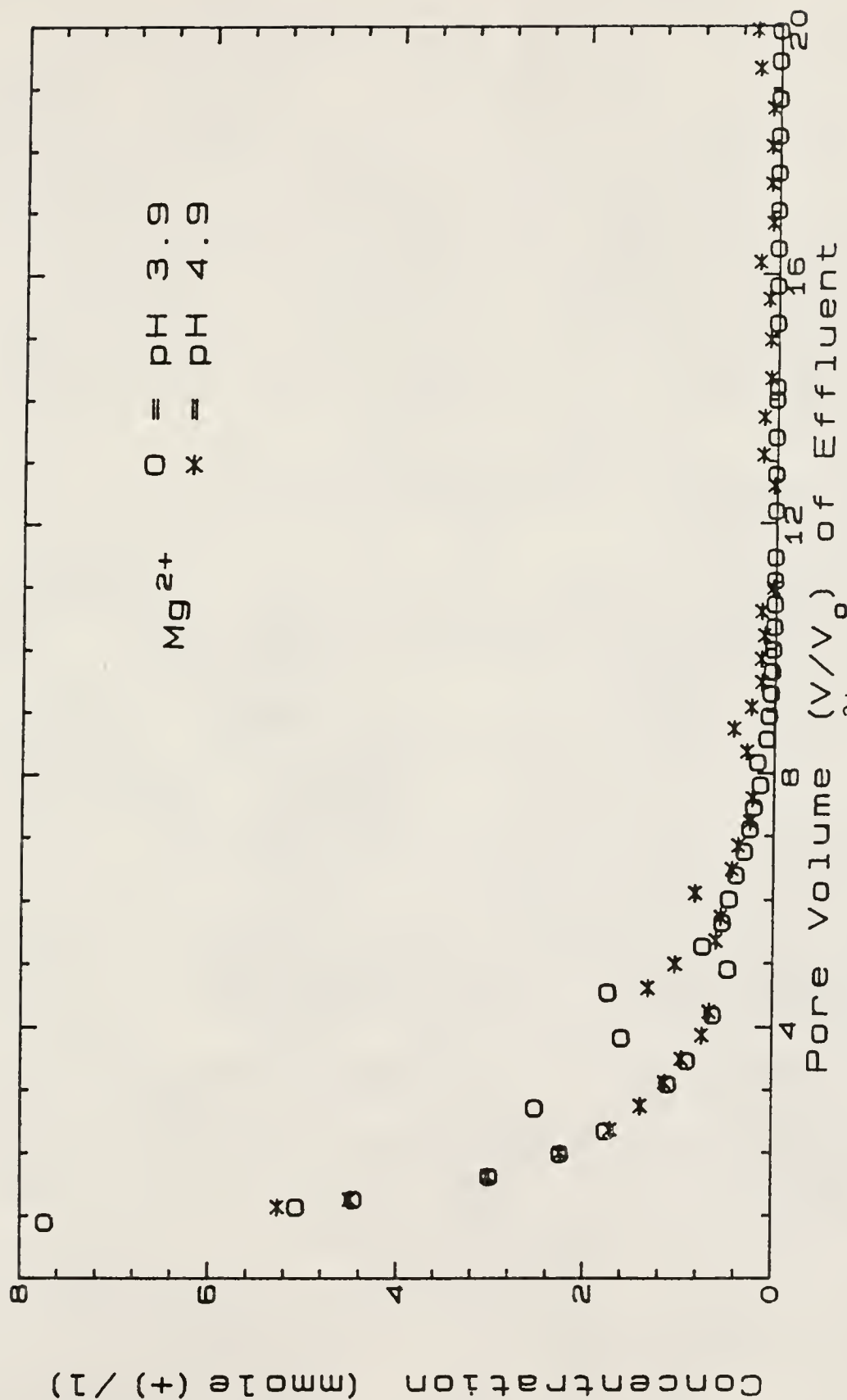


Figure 4-8 Breakthrough curves of  $\text{Mg}^{2+}$  from Mg-subsoil columns which received input HCl solutions with two different pH values.

effect of soil organic matter. Nontreated topsoil contained more organic matter and amorphous material than subsoil (refer to Table 2-2). The variable-charge sites attributable to organic matter or amorphous material tended to saturate with a single basic cation. Therefore, the replacement efficiency of  $H^+$  for cations in the topsoil should have been greater than for subsoil (Chatterjee and Marshall, 1950; Wiklander and Andersson, 1972).

Concentrations of Al determined in the column effluent were assumed to be in the  $Al^{3+}$  form.  $Al^{3+}$  concentrations in the first collected sample of effluent were approximately 1 mmole(+)  $L^{-1}$  for K-subsoil and Ca-subsoil columns. This relatively high effluent concentration was attributed to the salt effect on exchangeable  $Al^{3+}$ . For Mg-subsoil, the  $Al^{3+}$  concentration was as high as 6.67 mmole(+)  $L^{-1}$ . For all columns, concentrations of  $Al^{3+}$  in consecutive effluent samples consistently decreased. Figs. 4-9, 4-10 and 4-11 gave data for K-subsoil, Ca-subsoil and Mg-subsoil columns, respectively. There was no effect of different input solution pH on  $Al^{3+}$  effluent concentration for all pretreated subsoil columns.

Concentrations of  $Al^{3+}$  in the first collected effluent sample for K-topsoil and Ca-topsoil columns were as high as 24.5 and 2.45 mmole(+)  $L^{-1}$ , respectively. These high concentrations were also attributed to the salt effect. The elution of  $Al^{3+}$  was different for Mg-topsoil, in that a concentration peak occurred at about 8.0-8.2 pore volumes.

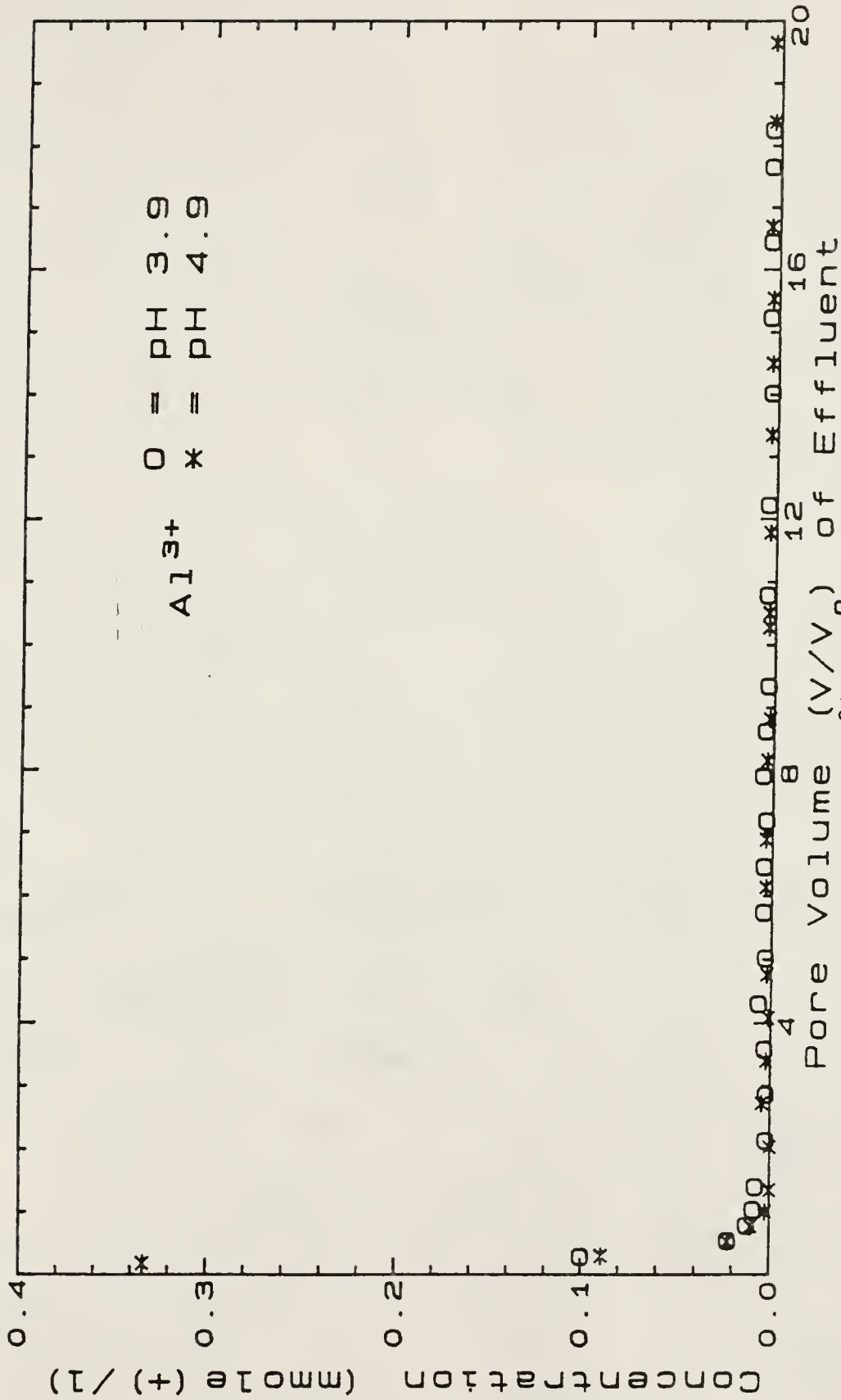


Figure 4-9 Breakthrough curves of  $\text{Al}^{3+}$  from K-subsoil columns which received input HCl solutions with two different pH values.

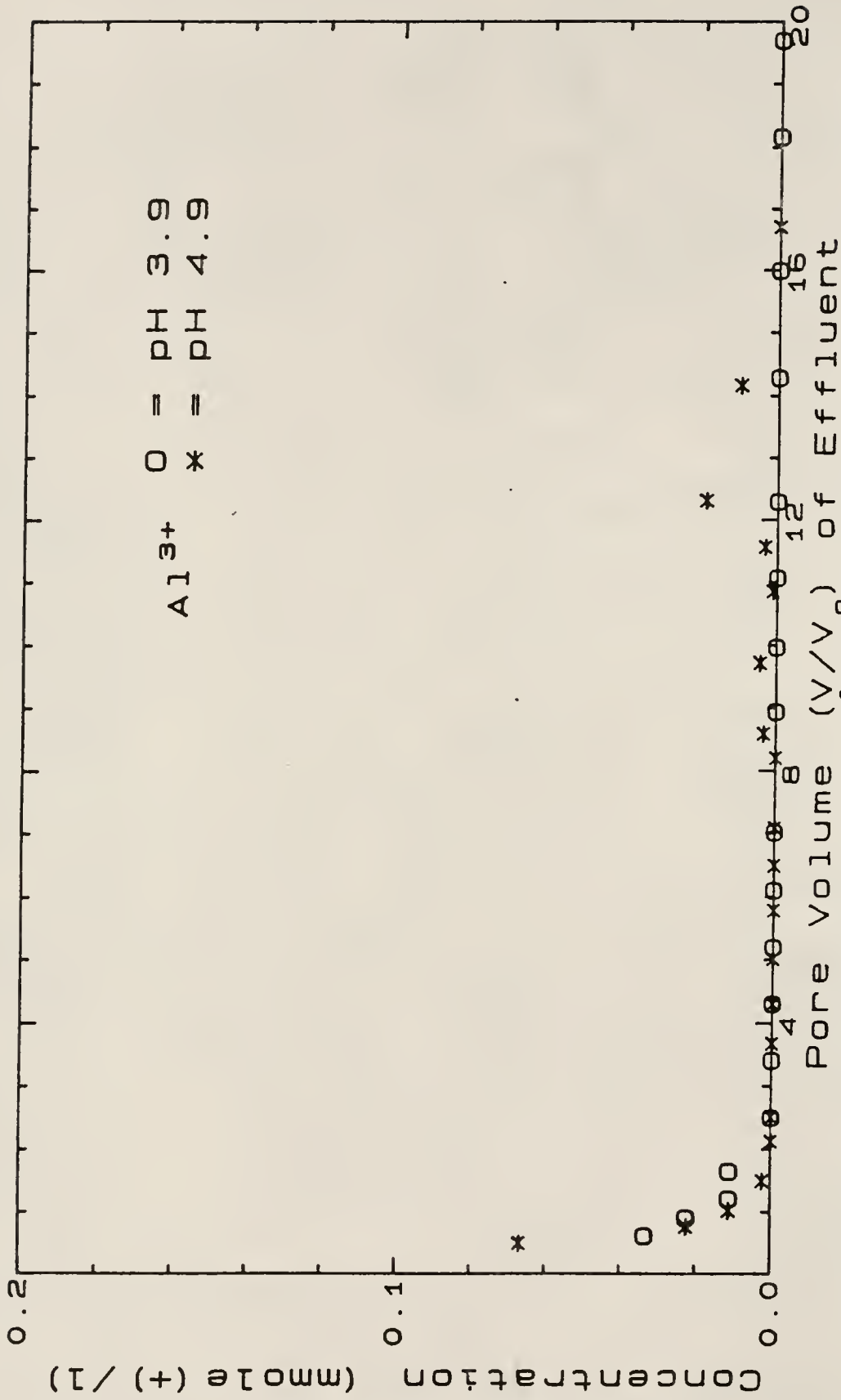


Figure 4-10 Breakthrough curves of  $\text{Al}^{3+}$  from Ca-subsoil columns which received input HCl solutions with two different pH values.

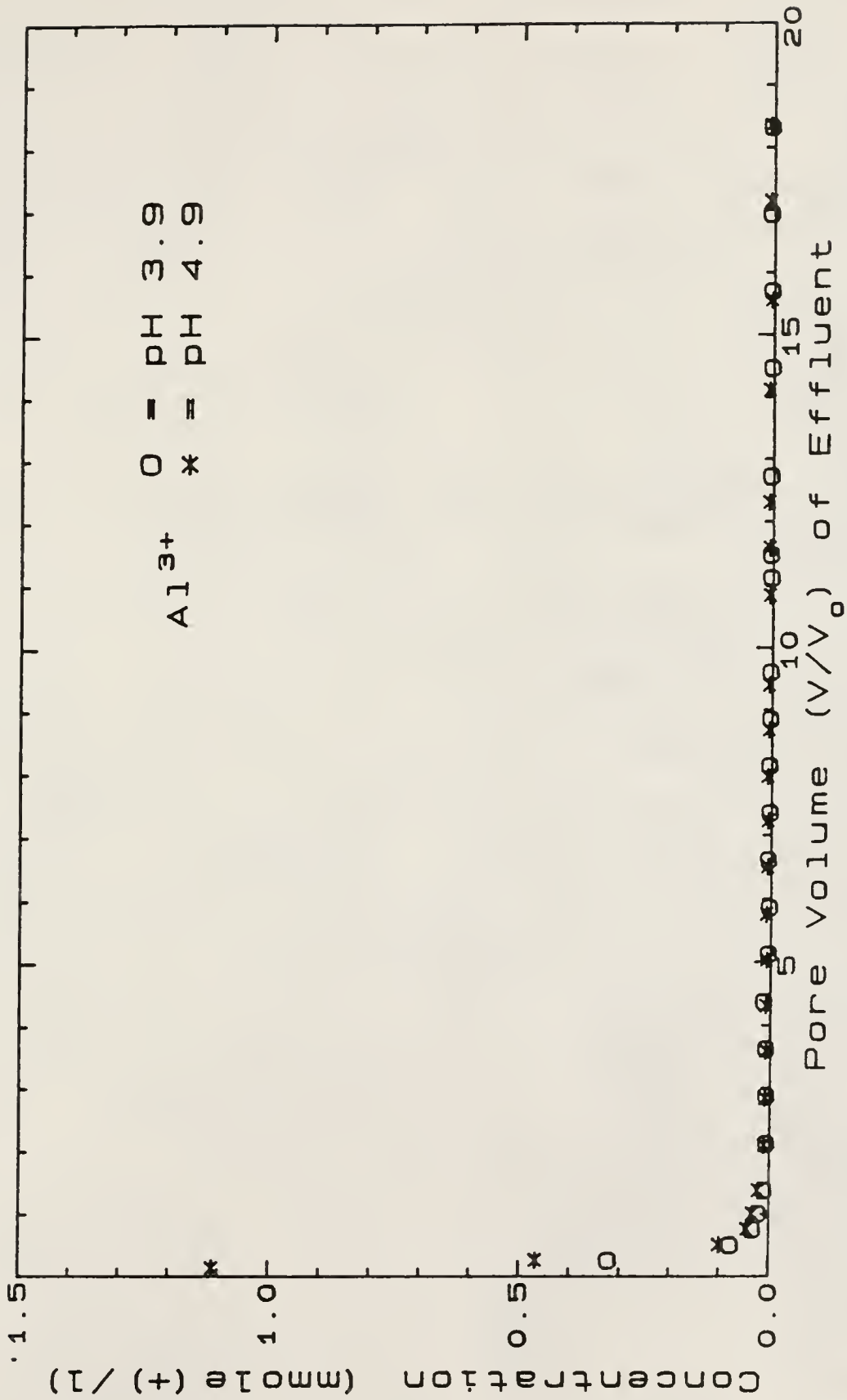


Figure 4-11 Breakthrough curves of Al<sup>3+</sup> from Mg-subsoil columns which received input HCl solutions with two different pH values.

The cause of this is uncertain. Figs. 4-12, 4-13, and 4-14 present  $\text{Al}^{3+}$  concentrations in effluent from columns of K-topsoil, Ca-topsoil and Mg-topsoil, respectively. The effect of input solution pH upon  $\text{Al}^{3+}$  concentration in column effluent was such that, the more acidic the input solution, the more  $\text{Al}^{3+}$  was leached. This effect was not in direct proportion to the  $\text{H}^+$  ion concentration, however.

#### Cation Concentrations in Effluent from Chemically Pretreated Mixed Soil Columns

Figs. 4-15 and 4-16 present concentrations for cations eluted from columns of mixed topsoil and mixed subsoil that received pH 3.9 HCl solution, respectively. Very high concentrations of each cation were observed initially in effluent. For example, for mixed topsoil that received pH 3.9 HCl solution, initial concentrations of  $\text{Ca}^{2+}$ ,  $\text{Mg}^{2+}$ ,  $\text{K}^+$  and  $\text{Na}^+$  were 58.8, 114.36, 24.0 and 0.63 mmole(+)  $\text{L}^{-1}$ , respectively. For effluent from mixed topsoil columns that received pH 4.9 HCl solution, initial concentrations of  $\text{Ca}^{2+}$ ,  $\text{Mg}^{2+}$ ,  $\text{K}^+$  and  $\text{Na}^+$  were 54.8, 115.18, 25.84 and 0.56 mmole(+)  $\text{L}^{-1}$ , respectively. For mixed subsoil that received pH 3.9 HCl, initial concentrations of  $\text{Ca}^{2+}$ ,  $\text{Mg}^{2+}$ ,  $\text{K}^+$  and  $\text{Na}^+$  in column effluent were 788.42, 756.89, 112.30 and 1.2 mmole(+)  $\text{L}^{-1}$ , respectively; and for mixed subsoil that received pH 4.9 HCl solution, initial concentrations of  $\text{Ca}^{2+}$ ,  $\text{Mg}^{2+}$ ,  $\text{K}^+$ ,  $\text{Na}^+$  were 459.08, 699.03, 125.61 and 1.36 mmole(+)  $\text{L}^{-1}$ , respectively. These observations can be explained once more by the salt effect and by the replacing

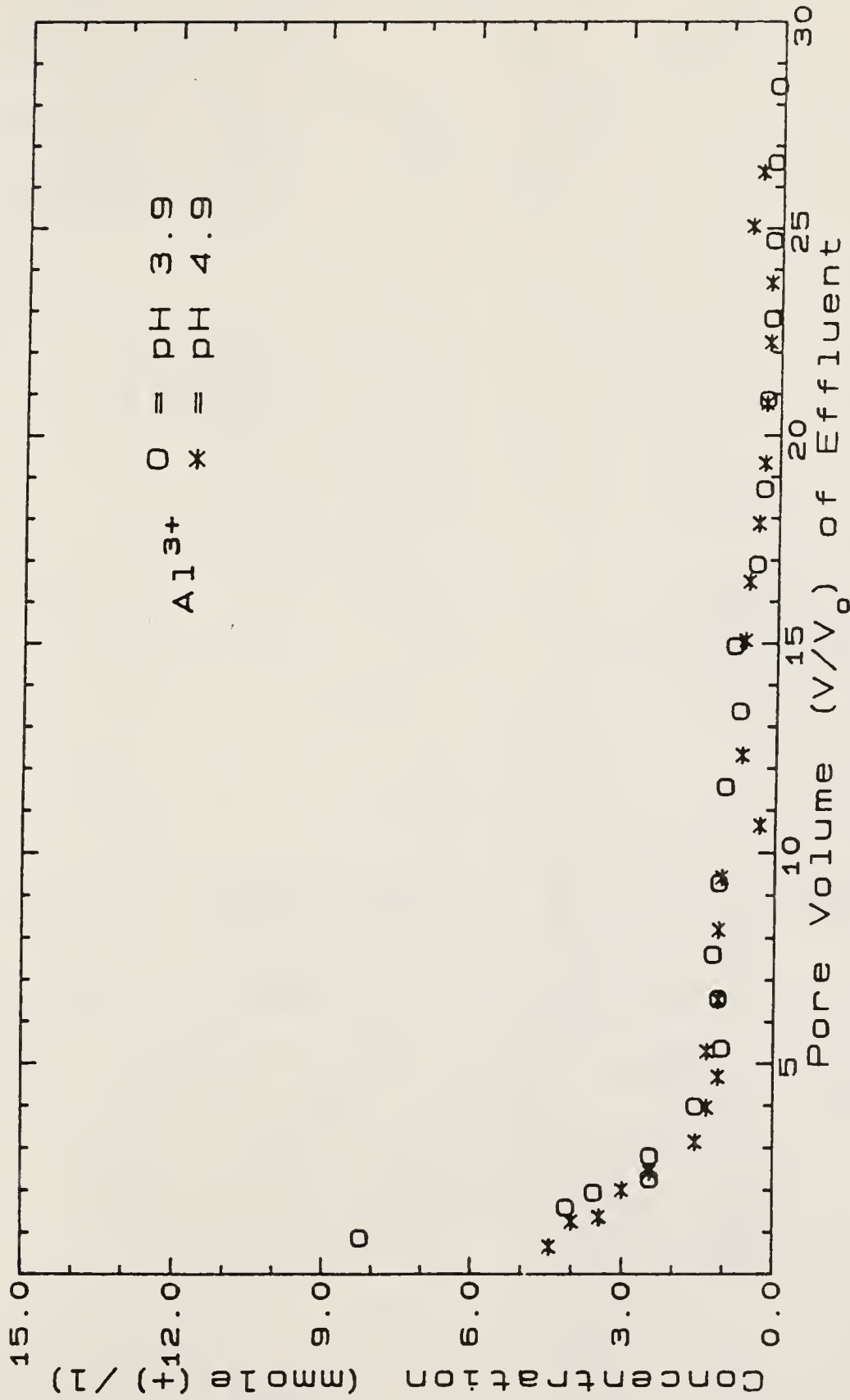


Figure 4-12 Breakthrough curves of  $\text{Al}^{3+}$  from K-topsoil columns which received input HCl solutions with two different pH values.

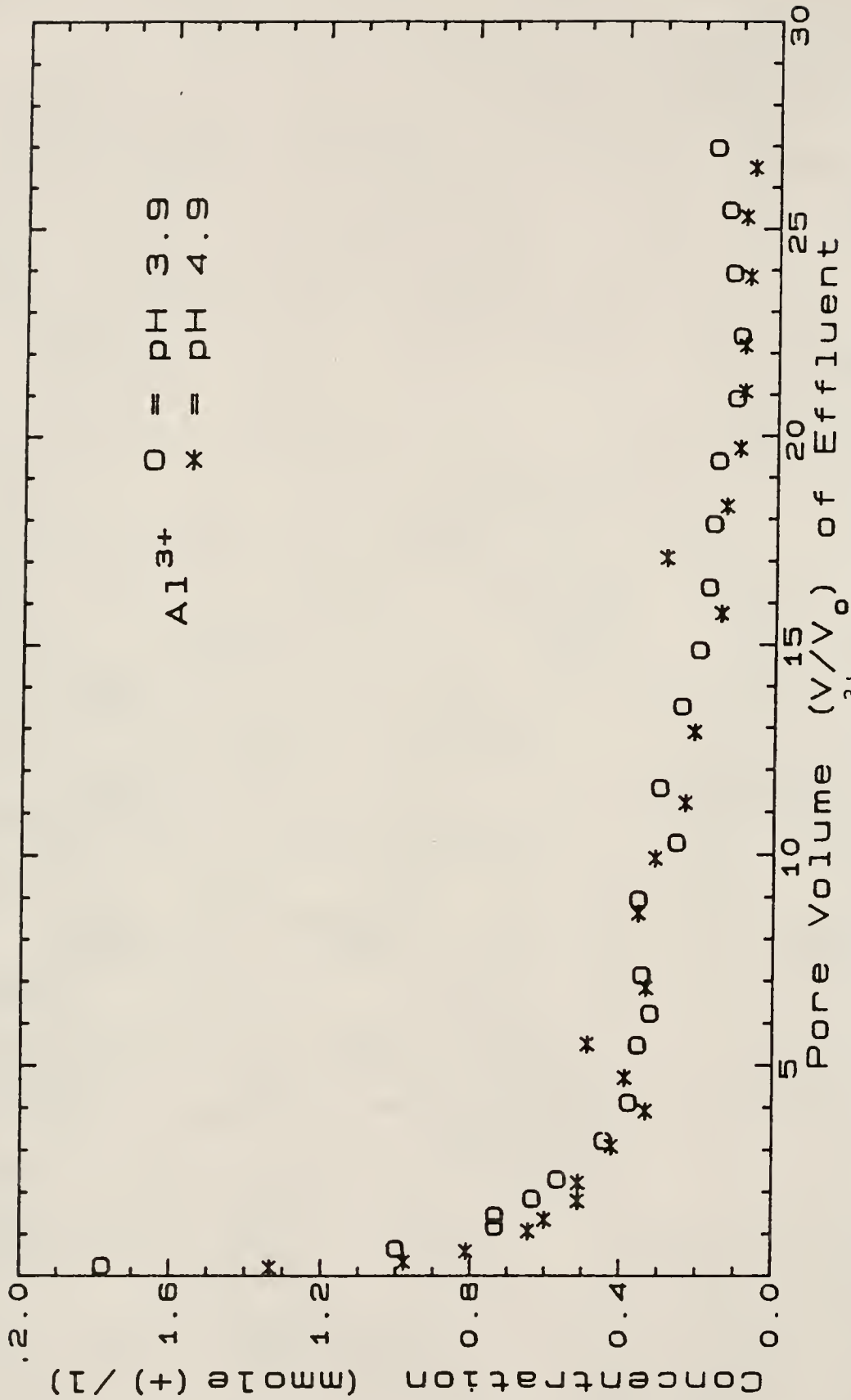


Figure 4-13 Breakthrough curves of  $\text{Al}^{3+}$  from Ca-topsoil columns which received input HCl solutions with two different pH values.

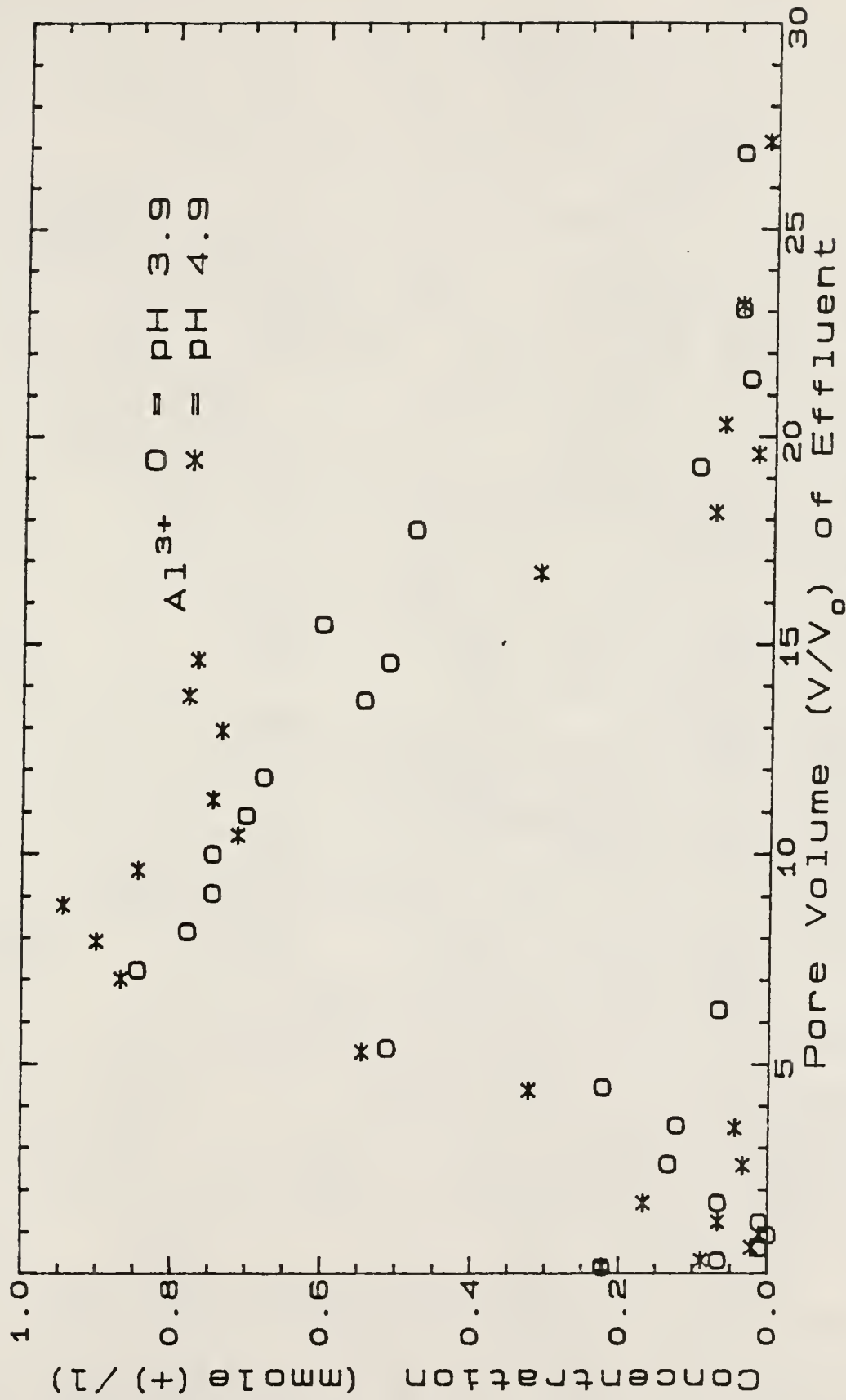


Figure 4-14 Breakthrough curves of  $Al^{3+}$  from Mg-topsoil columns which received input HCl solutions with two different pH values.

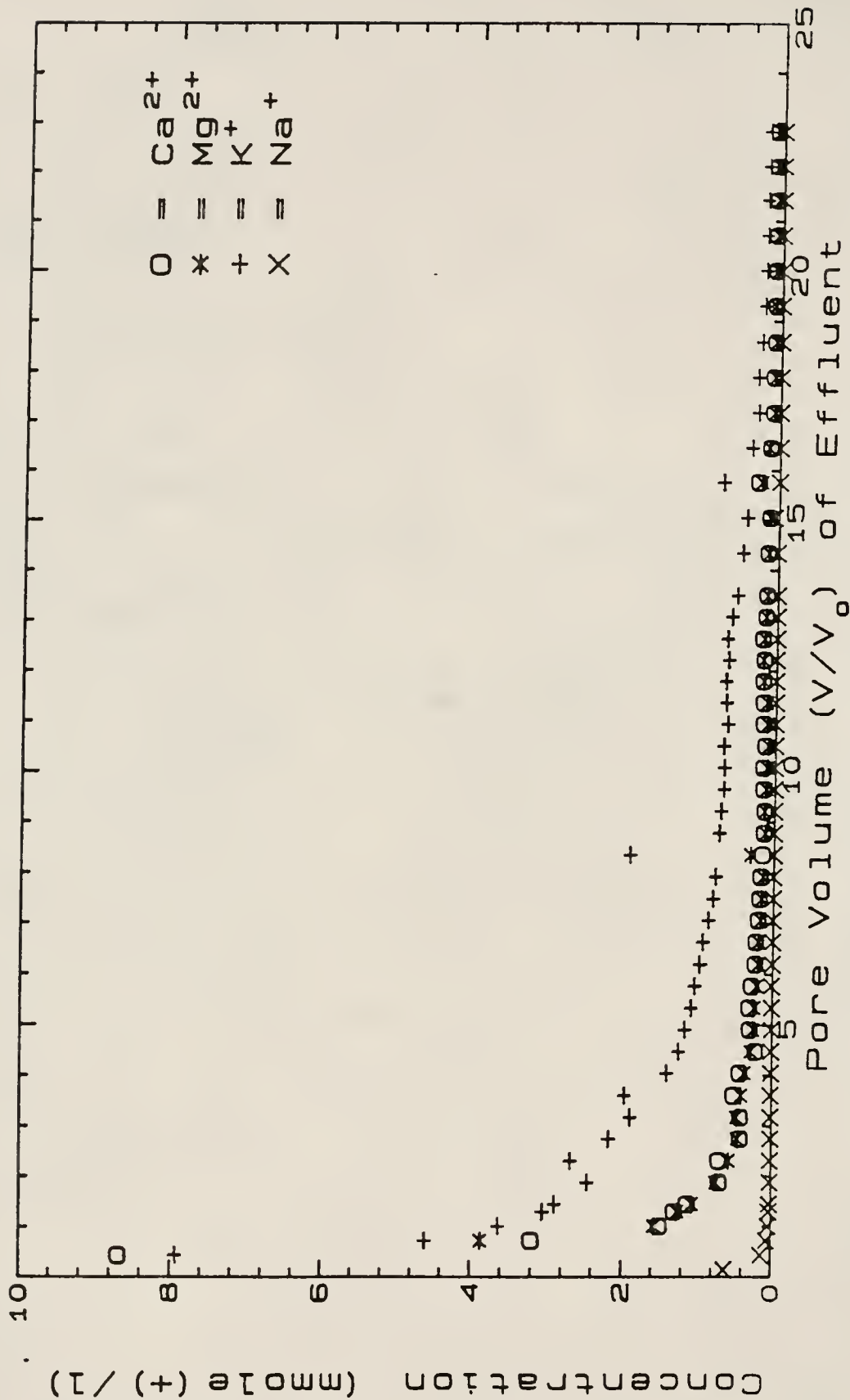


Figure 4-15 Breakthrough curves of cations in the effluent from a mixed-cation topsoil column which received pH 3.9 input HCl solution.

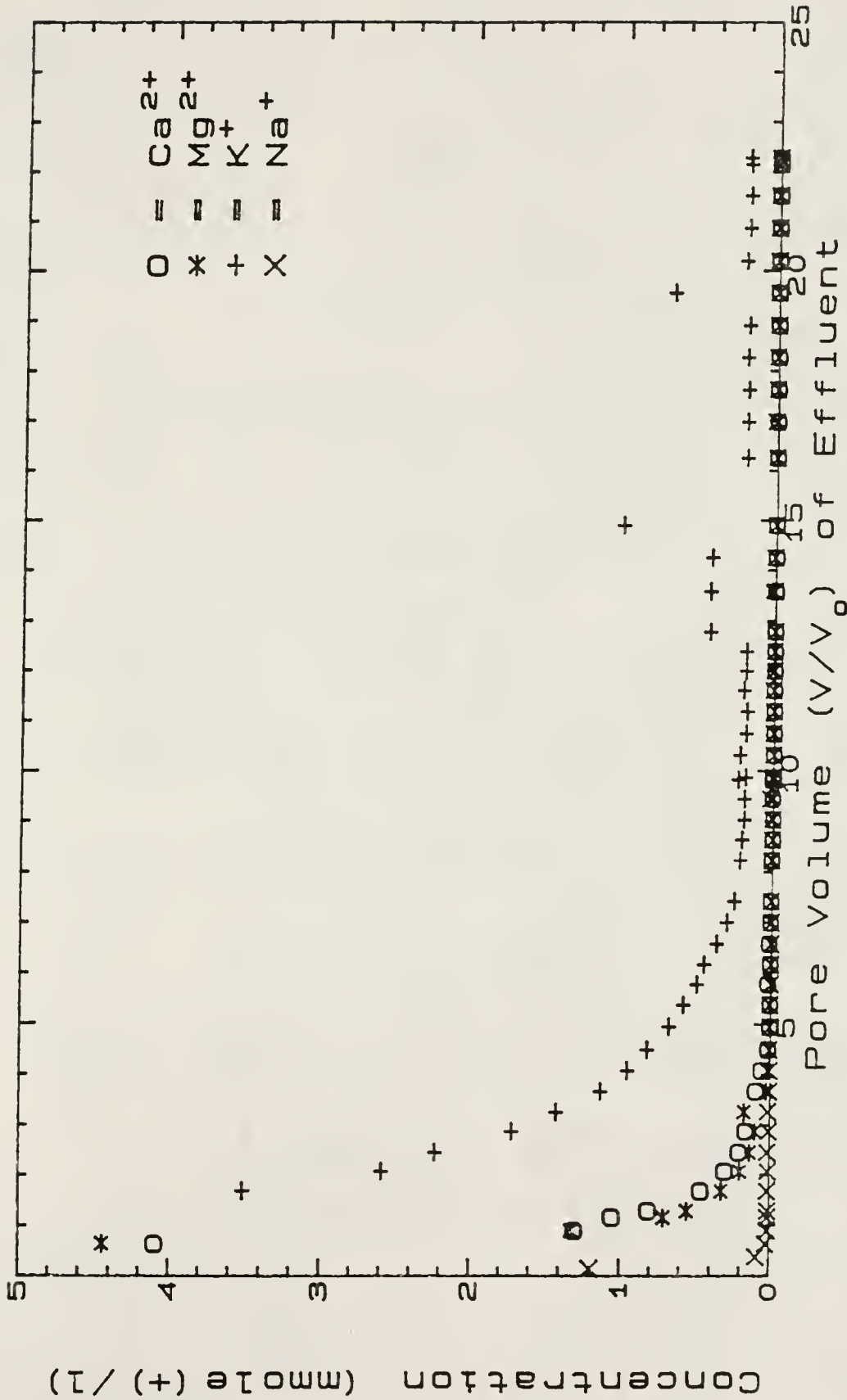


Figure 4-16 Breakthrough curves of cations in the effluent from a mixed-cation subsoil column which received pH 3.9 input HCl solution.

efficiency of  $H^+$  for basic cations described in the aforementioned paragraph. After the first collected sample of effluent, concentrations of cations were observed to decrease drastically in the second or third samples, and then afterwards concentrations gradually decreased with time. The initially larger concentrations for mixed subsoil than for mixed topsoil are attributed to the fact that the CEC of the pretreated mixed subsoil was three-fold greater than for mixed topsoil. For mixed topsoil and subsoil, concentrations of  $K^+$  were the greatest, concentrations of  $Mg^{2+}$  and  $Ca^{2+}$  were less than for  $K^+$ , and concentrations of  $Mg^{2+}$  and  $Ca^{2+}$  were difficult to distinguish from each other. The same concentration behavior was also found when pH 4.9 HCl was applied to columns of mixed topsoil and subsoil, respectively. This occurred because divalent  $Ca^{2+}$  and  $Mg^{2+}$  cations are more preferred than monovalent  $K^+$  and  $Na^+$  cations for the Cecil soil exchange sites.

The effect of pH of the input HCl solutions upon elution of  $K^+$  and  $Ca^{2+}$  from mixed topsoil columns is shown in Figs 4-17 and 4-18, and the effect on  $Mg^{2+}$  and  $K^+$  from mixed subsoil is shown in Figs 4-19 and 4-20. The pH of input HCl solution had a greater effect upon concentrations of  $K^+$  in column effluent than on  $Ca^{2+}$  or  $Mg^{2+}$ . This observation implies that a lower pH (higher  $H^+$  concentration) of input solution enhanced competition of  $H^+$  ions with monovalent cations such as  $K^+$  and  $Na^+$  for soil

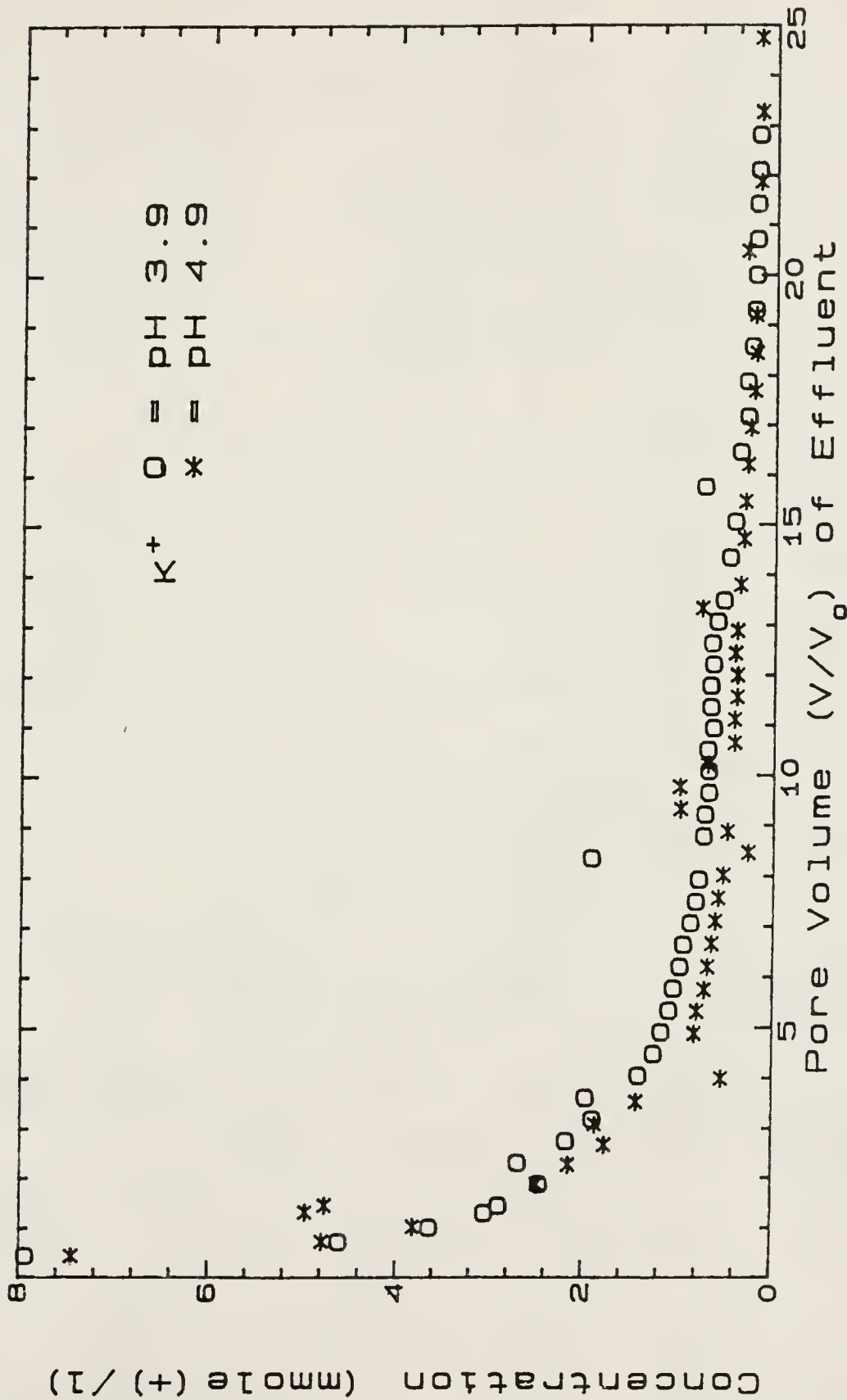


Figure 4-17 Breakthrough curves of  $K^+$  from mixed-cation topsoil columns which received input HCl solutions with two different pH values.

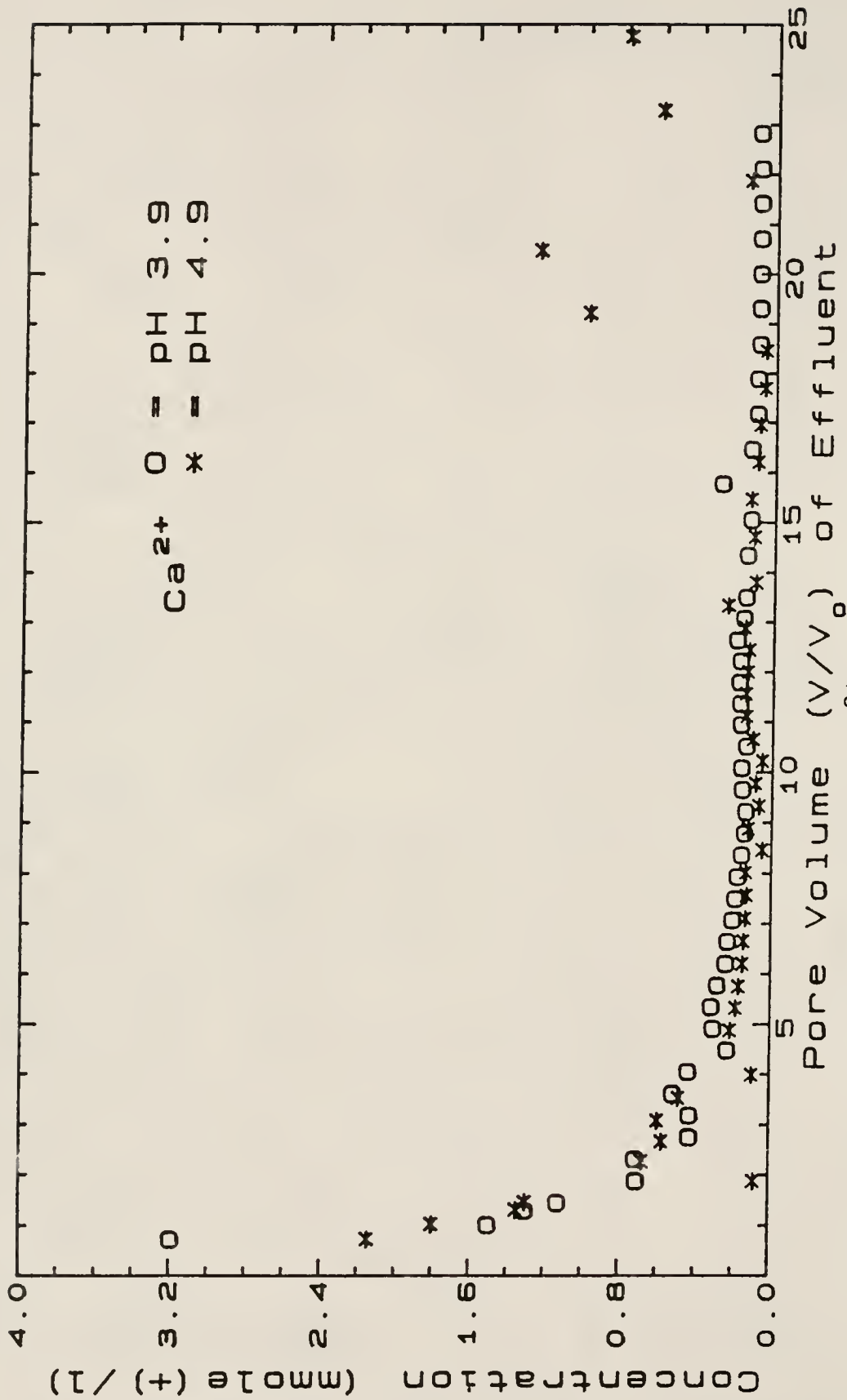


Figure 4-18 Breakthrough curves of Ca<sup>2+</sup> from mixed-cation topsoil columns which received input HCl solutions with two different pH values.

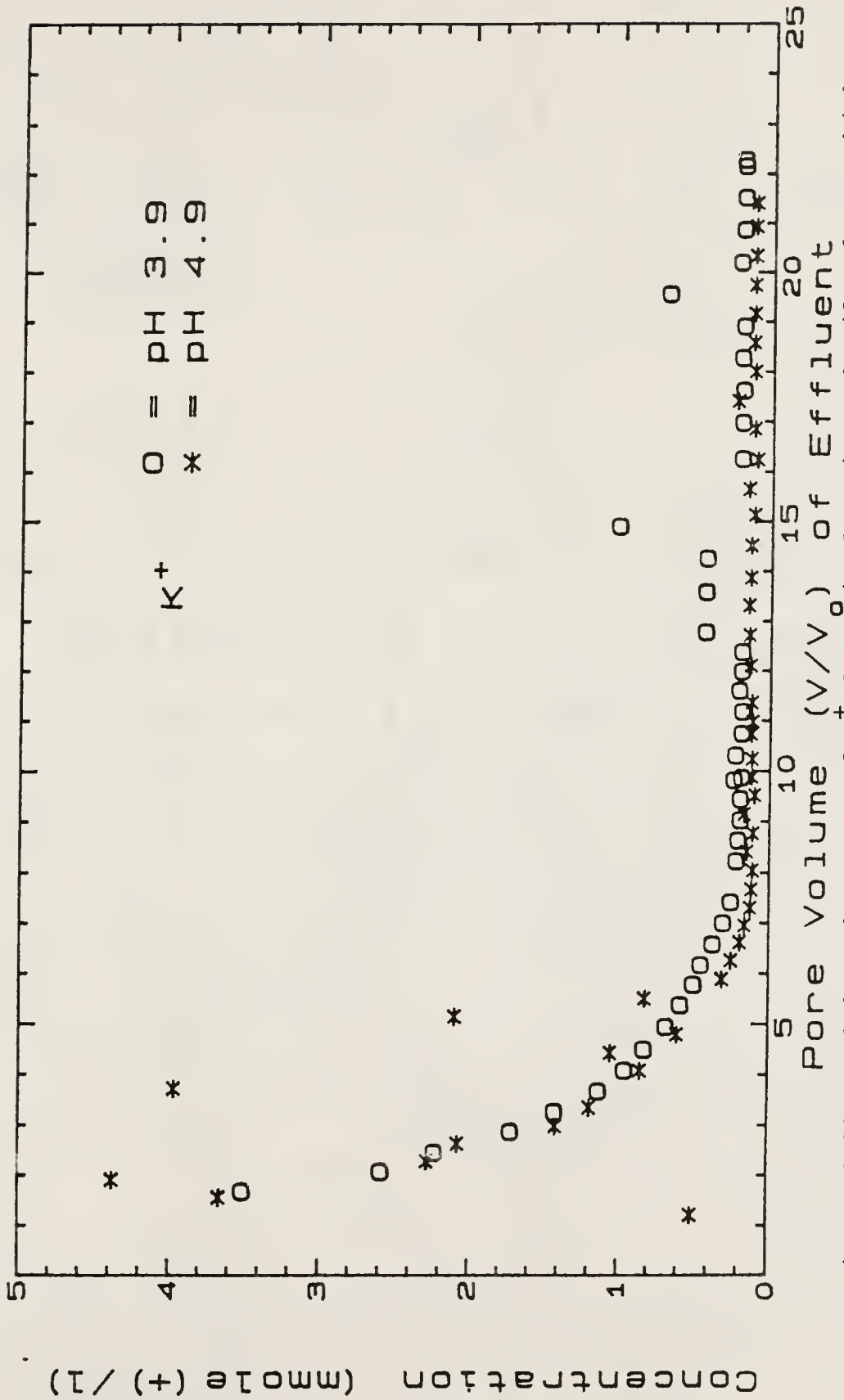


Figure 4-19 Breakthrough curves of  $K^+$  from mixed-cation subsoil columns which received input HCl solutions with two different pH values.

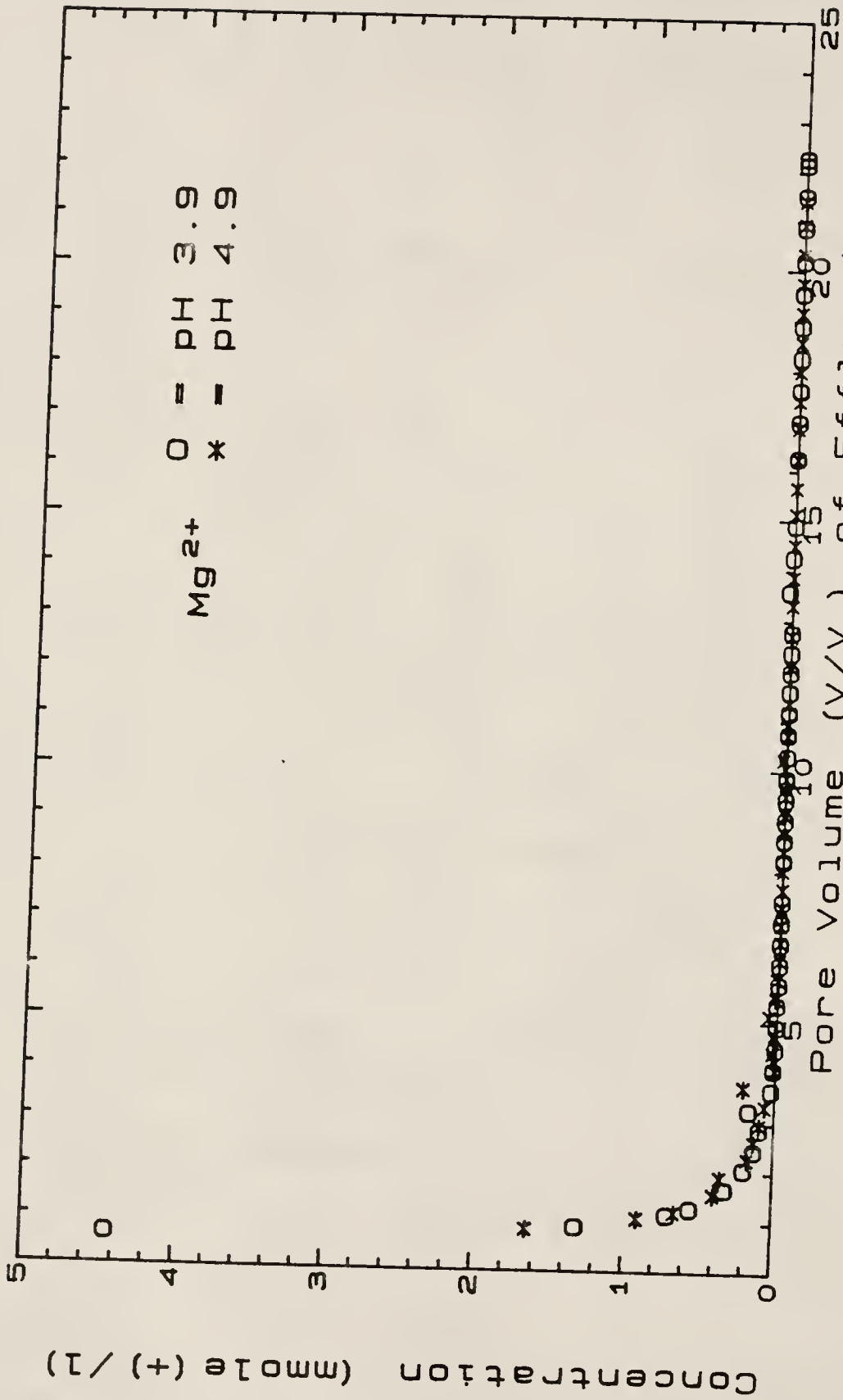


Figure 4-20 Breakthrough curves of  $Mg^{2+}$  from mixed-cation subsoil columns which received input HCl solutions with two different pH values.

exchange sites, but was not as effective in enhancing competition of  $H^+$  ions with divalent cations such as  $Mg^{2+}$  and  $Ca^{2+}$ .

#### Concentrations of $Al^{3+}$ in Effluent from Mixed Soil Columns

Concentrations of  $Al^{3+}$  in effluent from mixed topsoil and subsoil columns that received HCl solutions. are presented in Figs. 4-21 and 4-22, respectively. Initial concentrations of  $Al^{3+}$  were approximately  $2.80 \text{ mmole}(+) \text{ L}^{-1}$ , for effluent from mixed topsoil that received pH 3.9 HCl solution, and  $0.47 \text{ mmole}(+) \text{ L}^{-1}$  from subsoil columns that received pH 4.9 HCl solution. In general, concentrations of eluted  $Al^{3+}$  in the effluent from columns of mixed subsoil were quite low after the first few samples of effluent, and no differences in these values were observed for applied HCl solutions with different pH. For mixed topsoil columns, concentrations of  $Al^{3+}$  decreased gradually and the pH of input HCl solution did effect the concentration of  $Al^{3+}$  in the effluent. Higher concentrations of  $Al^{3+}$  occurred

in initial effluent from columns receiving pH 3.9 solution than at pH 4.9. Total quantities of  $Al^{3+}$  in the effluent from columns receiving pH 3.9 solution were not reasonably greater than for pH 4.9, however. The reason for this observation was uncertain.

#### Concentrations of Cations in Solution and Exchange Phases for Treated and Mixed Soil Columns after Application of 25 Pore Volumes of HCl Solution

Treated Subsoil. Concentrations of cations in solution and exchange phases are presented in Tables 4-6 and 4-7 for

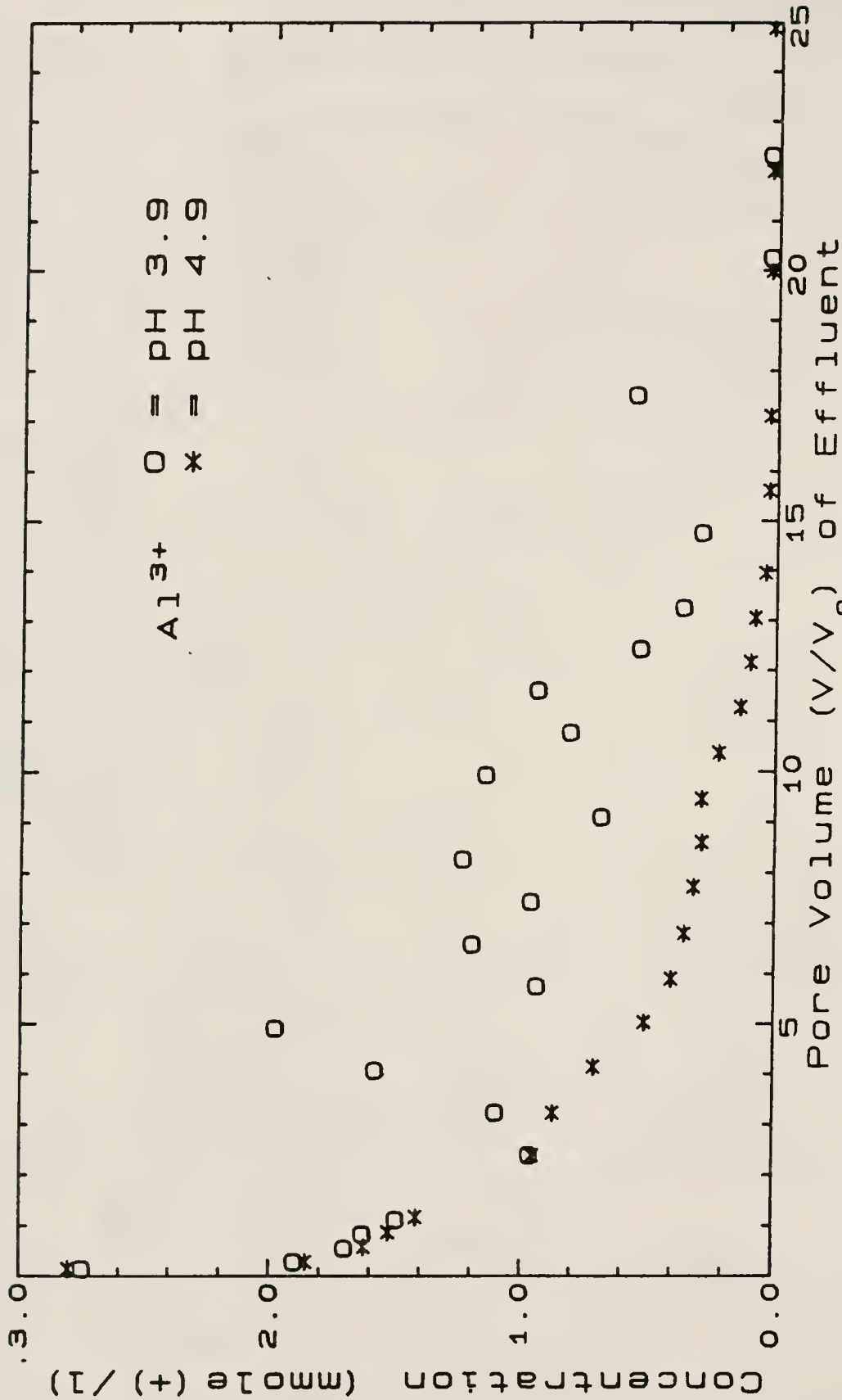


Figure 4-21 Breakthrough curves of Al<sup>3+</sup> from mixed-cation topsoil columns which received input HCl solutions with two different pH values.

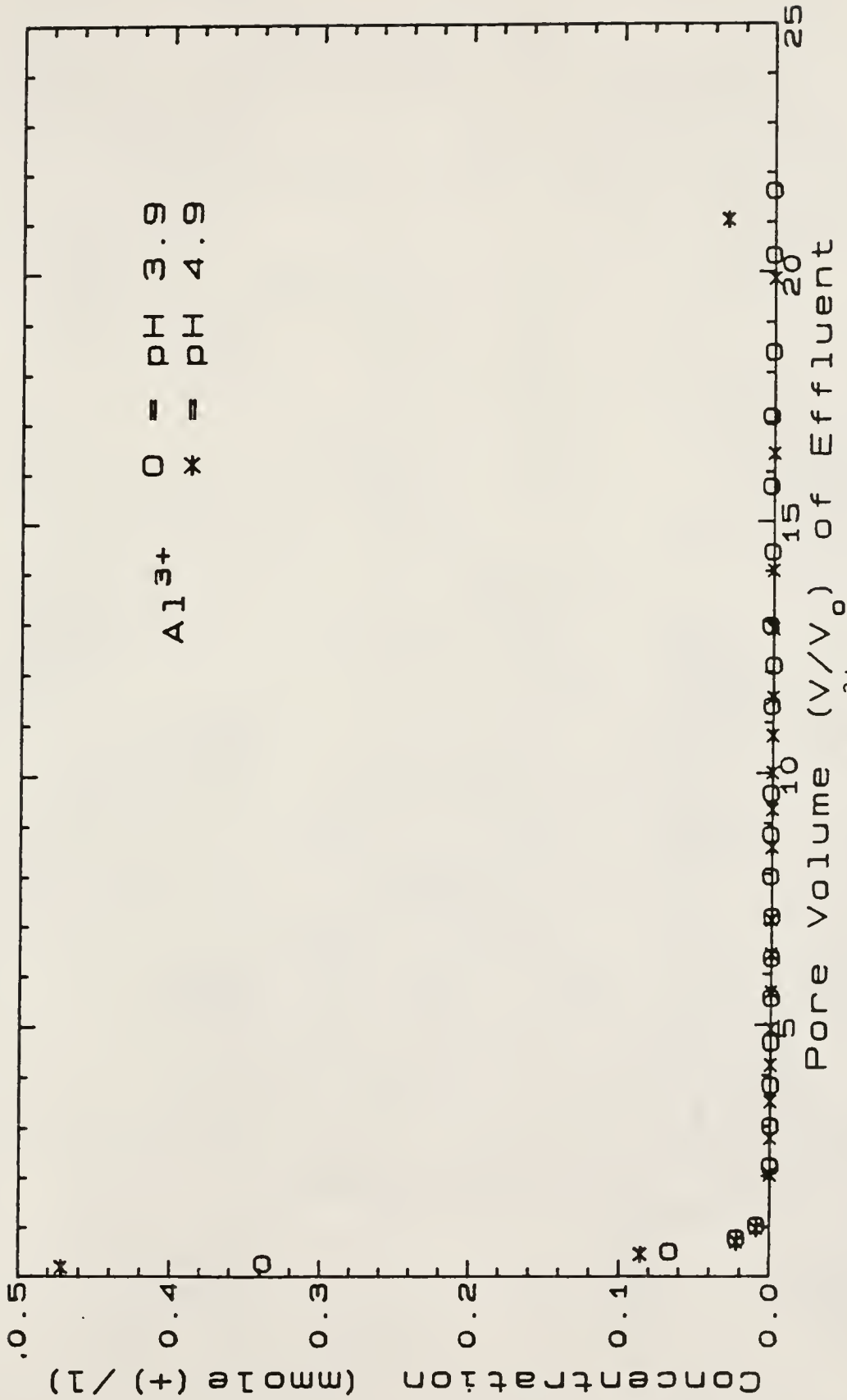


Figure 4-22 Breakthrough curves of  $Al^{3+}$  from mixed-cation subsoil columns which received input HCl solutions with two different pH values.

Table 4-6 Concentrations of cations in solution  
and exchange phases for K-subsoil  
after leaching with pH 3.9 HCl solution

Depth (cm)	Ca	Mg	K	Na	Al	Sum
	Solution phase					
	mmole (+) L <sup>-1</sup>					
1.0	0.354	0.058	0.215	1.130	0.014	1.771
2.0	0.287	0.054	0.413	1.230	0.009	1.992
3.0	0.619	0.107	0.640	2.420	0.014	3.801
4.0	0.372	0.062	0.454	1.480	0.007	2.374
5.0	0.344	0.049	0.370	1.310	0.046	2.119
6.0	0.489	0.099	0.570	3.700	0.008	4.865
7.0	0.564	0.115	0.532	2.680	0.009	3.900
8.0	0.531	0.099	0.350	1.930	0.021	2.931
9.0	0.473	0.064	0.390	1.530	0.008	2.465
10.0	0.459	0.066	0.384	1.220	0.110	2.239
11.0	0.297	0.078	0.480	1.720	0.024	2.600
12.0	0.437	0.084	0.502	2.210	0.009	3.242
13.0	0.312	0.058	0.434	1.200	0.029	2.033
14.0	0.374	0.064	0.454	2.180	0.011	3.083
15.0	0.803	0.140	0.734	2.960	0.009	4.646
16.0	0.713	0.104	0.962	2.680	0.009	4.468
17.0	0.342	0.058	0.315	1.340	0.014	2.069
18.0	0.332	0.069	0.465	1.580	0.028	2.474
19.0	0.743	0.118	0.622	2.990	0.019	4.492
20.0	0.813	0.111	0.458	2.320	0.006	3.708

Depth (cm)	Ca	Mg	K	Na	Al	Sum
	Exchange phase					
	mmole (+) Kg <sup>-1</sup> soil					
1.0	0.661	0.041	1.820	0.652	9.885	13.059
3.0	1.070	0.041	13.400	0.685	0.512	15.708
5.0	1.100	0.123	14.100	0.674	0.701	16.698
7.0	1.520	0.103	14.800	0.739	0.467	17.629
9.0	1.250	0.041	15.100	0.652	0.789	17.832
11.0	1.380	0.082	13.000	0.674	0.556	15.692
13.0	1.330	0.062	14.300	0.652	0.441	16.785
16.0	1.470	0.062	14.100	0.685	0.311	16.628
18.0	1.170	0.062	14.400	0.652	0.523	16.807
20.0	1.160	0.062	14.100	0.696	0.478	16.496

Table 4-7 Concentrations of cations in solution and exchange phases for K-subsoil after leaching with pH 4.9 HCl solution

Depth (cm)	Ca	Mg	K Solution phase mmole (+) L <sup>-1</sup>	Na phase L <sup>-1</sup>	Al	Sum
1.0	0.027	0.008	0.318	0.448	0.007	0.808
2.0	0.027	0.010	0.441	0.368	0.000	0.846
3.0	0.207	0.030	0.187	0.921	0.021	1.366
4.0	0.267	0.029	0.161	1.150	0.000	1.607
5.0	0.031	0.012	0.496	0.965	0.004	1.508
6.0	0.257	0.040	0.344	1.300	0.003	1.944
7.0	0.437	0.049	0.424	1.600	0.000	2.510
8.0	0.398	0.046	0.365	1.410	0.004	2.224
9.0	0.317	0.049	0.394	1.530	0.037	2.327
10.0	0.308	0.054	0.408	1.750	0.000	2.520
11.0	0.428	0.059	0.464	1.790	0.004	2.746
12.0	0.459	0.082	0.496	2.400	0.000	3.437
13.0	0.424	0.054	0.403	1.690	0.002	2.573
14.0	0.608	0.079	0.465	2.250	0.011	3.413
15.0	0.828	0.099	0.454	2.790	0.000	4.171
16.0	0.571	0.062	0.263	1.690	0.000	2.586
17.0	0.689	0.079	0.427	2.420	0.000	3.615
18.0	0.889	0.099	0.562	2.880	0.000	4.430
19.0	0.629	0.079	0.546	2.030	0.000	3.284
20.0	0.790	0.118	0.556	2.680	0.000	4.144

Depth (cm)	Ca	Mg	K Exchange phase mmole(+) Kg <sup>-1</sup> soil	Na phase Kg <sup>-1</sup> soil	Al	Sum
1.0	1.280	0.226	9.790	0.739	3.614	15.649
3.0	1.200	0.165	13.900	0.772	0.901	16.938
5.0	1.150	0.062	13.700	0.652	0.678	16.242
7.0	1.410	0.062	15.500	0.696	0.812	18.480
9.0	1.330	0.041	14.100	0.685	0.756	16.912
11.0	1.360	0.062	13.600	0.707	0.645	16.374
14.0	1.270	0.062	14.500	0.652	0.623	17.107
16.0	1.410	0.062	15.100	0.696	0.645	17.913
18.0	1.240	0.062	14.000	0.717	0.689	16.708
20.0	1.330	0.062	14.800	0.739	0.645	17.576

K-subsoil columns after application with pH 3.9 and 4.9 input HCl solutions, respectively. In the solution phase, cation concentrations were in the order  $\text{Na}^+ > \text{K}^+ \approx \text{Ca}^{2+} > \text{Mg}^{2+} > \text{Al}^{3+}$ , while for the exchange phase cation concentrations were in the order  $\text{K}^+ > \text{Ca}^{2+} \approx \text{Al}^{3+} \approx \text{Na}^+ > \text{Mg}^{2+}$  for both pH treatments. If one compared concentrations of cations in the exchange phase in Tables 4-6 and 4-7 with values in Table 4-4 for the initial K-subsoil, leaching loss of K was significant, while leaching losses for  $\text{Ca}^{2+}$ ,  $\text{Mg}^{2+}$ ,  $\text{Na}^+$  and  $\text{Al}^{3+}$  were small. A similar trend was observed for both pH treatments.

Tables 4-8 and 4-9 present concentrations of cations in solution and exchange phases for Ca-subsoil columns after application of pH 3.9 and 4.9 HCl solutions, respectively. Solution-phase concentrations of cations were of the order  $\text{Na}^+ > \text{Ca}^{2+} > \text{Al}^{3+} \approx \text{K}^+ > \text{Mg}^{2+}$  and, for the exchange phase, concentrations of cations were  $\text{Ca}^{2+} > \text{Al}^{3+} > \text{K}^+ \approx \text{Na}^+ > \text{Mg}^{2+}$  for both pH treatments. If one compared cation concentrations in the exchange phase in Tables 4-8 and 4-9 with values in Table 4-4 for the initial Ca-subsoil, the concentrations of  $\text{Ca}^{2+}$  were dramatically decreased by leaching, but concentrations of other species such as  $\text{Na}^+$  and  $\text{Al}^{3+}$  were actually somewhat increased.  $\text{Mg}^{2+}$  was slightly decreased for both pH treatments, and  $\text{K}^+$  was increased for the pH 3.9 treatment but not for the pH 4.9 case. The explanation for increased concentrations of certain species in the exchange phase is that  $\text{K}^+$ ,  $\text{Na}^+$  and

Table 4-8 Concentrations of cations in solution and exchange phases for Ca-subsoil after leaching with pH 3.9 HCl solution

Depth (cm)	Ca	Mg	K	Na	Al	Sum
	Solution phase					
	mmole (+) L <sup>-1</sup>					
1.0	0.385	0.053	0.161	0.918	0.013	1.530
2.0	0.385	0.043	0.210	1.240	0.391	2.269
3.0	0.417	0.063	0.214	1.300	0.018	2.011
4.0	0.349	0.056	0.191	0.835	0.374	1.805
5.0	0.313	0.043	0.214	1.260	0.125	1.955
6.0	0.531	0.045	0.137	1.580	0.172	2.465
7.0	0.442	0.066	0.152	1.120	1.230	3.010
8.0	0.858	0.095	0.243	1.960	0.022	3.178
9.0	0.359	0.045	0.320	0.978	0.578	2.280
10.0	0.409	0.058	0.165	1.420	0.856	2.908
11.0	0.339	0.049	0.107	0.861	5.130	6.486
12.0	0.404	0.037	0.334	0.939	0.450	2.164
13.0	0.344	0.054	0.265	0.874	1.630	3.167
14.0	0.806	0.078	0.148	1.360	0.045	2.437
15.0	0.489	0.058	0.141	1.230	0.178	2.096
16.0	0.614	0.058	0.171	1.280	0.767	2.890
17.0	0.430	0.067	0.125	1.330	0.465	2.417
18.0	1.190	0.099	0.637	3.150	0.027	5.102
19.0	0.851	0.103	0.246	1.430	0.061	2.691
20.0	0.873	0.115	0.217	2.280	0.022	3.507

Depth (cm)	Ca	Mg	K	Na	Al	Sum
	Exchange phase					
	mmole (+) Kg <sup>-1</sup> soil					
1.0	2.820	0.021	0.185	0.239	6.961	10.226
3.0	10.200	0.021	0.205	0.217	0.267	10.910
5.0	11.900	0.041	0.205	0.239	0.334	12.719
7.0	12.800	0.062	0.301	0.359	0.300	13.822
9.0	11.700	0.021	0.198	0.228	0.323	12.470
11.0	11.600	0.021	0.230	0.207	0.278	12.336
14.0	11.400	0.021	0.205	0.196	0.300	12.122
16.0	12.100	0.021	0.269	0.228	0.467	13.085
18.0	12.500	0.082	0.646	0.348	0.256	13.832
20.0	11.700	0.021	0.217	0.217	0.267	12.422

Table 4-9 Concentrations of cations in solution and exchange phases for Ca-subsoil after leaching with pH 4.9 HCl solution

Depth (cm)	Ca	Mg	K	Na	Al	Sum
	Solution phase					
	mmole (+) L <sup>-1</sup>					
1.0	0.503	0.066	0.178	1.910	0.129	2.786
2.0	0.826	0.092	0.257	2.440	0.018	3.633
3.0	0.479	0.046	0.137	1.140	0.765	2.567
4.0	0.523	0.056	0.192	1.310	0.369	2.450
5.0	0.575	0.053	0.192	1.610	0.080	2.510
6.0	0.659	0.066	0.235	2.310	0.167	3.437
7.0	0.665	0.069	0.135	1.660	0.013	2.542
8.0	0.555	0.056	0.108	1.250	0.129	2.098
9.0	0.645	0.072	0.143	1.660	0.125	2.645
10.0	0.659	0.053	0.171	1.380	0.156	2.419
11.0	0.681	0.066	0.221	1.650	0.040	2.658
12.0	1.220	0.094	0.327	3.900	0.040	5.581
13.0	0.840	0.072	0.193	1.940	0.031	3.077
14.0	0.831	0.082	0.132	2.200	0.067	3.312
15.0	0.495	0.049	0.085	1.380	0.018	2.027
16.0	0.575	0.049	0.151	1.230	0.031	2.036
17.0	0.816	0.095	0.204	2.030	0.027	3.172
18.0	0.551	0.076	0.171	1.570	0.142	2.510
19.0	0.591	0.072	0.153	1.460	0.169	2.445
20.0	0.399	0.059	0.099	1.060	3.180	4.798

Depth (cm)	Ca	Mg	K	Na	Al	Sum
	Exchange phase					
	mmole (+) Kg <sup>-1</sup> soil					
1.0	8.980	0.123	0.205	0.261	0.979	10.548
3.0	10.400	0.041	0.173	0.304	0.289	11.207
5.0	11.600	0.041	0.256	0.283	0.300	12.480
7.0	10.500	0.041	0.198	0.326	0.289	11.354
9.0	11.000	0.041	0.147	0.370	0.322	11.880
11.0	11.500	0.041	0.160	0.391	0.334	12.426
12.0	9.610	0.041	0.192	0.348	0.311	10.502
15.0	10.500	0.021	0.179	0.174	0.311	11.185
17.0	10.500	0.041	0.166	0.196	0.300	11.203
19.0	11.600	0.041	0.179	0.380	0.322	12.522

$\text{Ca}^{2+}$  occur in nonexchangeable forms such as between lattices or interlayers of interlayer-hydroxy vermiculite ( $\text{M}^+(\text{Mg}, \text{Fe})_3(\text{Si}, \text{Al})_4\text{O}_{10}(\text{OH})_2$ ), where  $\text{M}^+$  denotes cation species located between lattices or interlayers (Dixon and Weed, 1977; Bohn et al., 1985). A long period of leaching with acid solutions will result in weathering of the minerals, releasing nonexchangeable cations from within the lattices or interlayers.

Tables 4-10 and 4-11 present concentrations of cations in solution and exchange phases for Mg-subsoil columns after application of pH 3.9 and 4.9 HCl solutions, respectively. In the solution phase, concentrations of cations were of the order  $\text{Na}^+ > \text{Ca}^{2+} > \text{K}^+ \approx \text{Mg}^{2+} > \text{Al}^{3+}$  but, for the exchanger phase, concentrations of cations were  $\text{Mg}^{2+} > \text{Al}^{3+} > \text{Ca}^{2+} > \text{Na}^+ > \text{K}^+$  for both pH treatments. If we compare concentrations of cations in the exchange phase in Tables 4-10 and 4-11 with values in Table 4-4 for initial Mg-subsoil, the concentrations of  $\text{Mg}^{2+}$  were greatly decreased by leaching but  $\text{Al}^{3+}$  concentrations were changed only slightly,  $\text{Ca}^{2+}$  and  $\text{Na}^+$  concentrations were increased and  $\text{K}^+$  was decreased. This change in cation concentrations was found both for pH treatments 3.9 and 4.9. Usually, cation species with the higher valence have a higher affinity for exchange sites. Therefore, high concentrations of divalent and trivalent species were observed in the exchange phase compared to  $\text{Na}^+$  and  $\text{K}^+$ . Cations with low valence demonstrated lower affinity for exchange sites, such

Table 4-10 Concentrations of cations in solution  
and exchange phases for Mg-subsoil after  
leaching with pH 3.9 HCl solution

Depth (cm)	Ca	Mg	K Solution mmole(+)	Na phase L <sup>-1</sup>	Al	Sum
1.0	0.362	0.078	0.187	1.130	0.003	1.761
2.0	0.472	0.119	0.243	1.800	0.001	2.635
3.0	0.267	0.103	0.139	0.785	0.002	1.296
4.0	0.364	0.144	0.164	1.280	0.003	1.955
5.0	0.327	0.115	0.114	0.991	0.008	1.555
6.0	0.359	0.123	0.159	1.110	0.003	1.754
7.0	0.377	0.123	0.079	1.330	0.002	1.912
8.0	0.349	0.140	0.113	1.510	0.003	2.115
9.0	0.324	0.128	0.132	1.390	0.004	1.978
10.0	0.487	0.152	0.132	1.770	0.000	2.541
11.0	0.514	0.144	0.104	1.680	0.000	2.442
12.0	0.589	0.136	0.212	2.410	0.002	3.349
13.0	0.509	0.148	0.169	1.680	0.002	2.508
14.0	0.589	0.156	0.180	1.520	0.002	2.447
15.0	0.574	0.169	0.182	1.980	0.001	2.906
16.0	0.444	0.111	0.157	1.440	0.004	2.156
17.0	0.576	0.136	0.175	1.690	0.004	2.581
18.0	0.556	0.111	0.155	1.720	0.002	2.544
19.0	0.474	0.136	0.153	1.480	0.010	2.253
20.0	0.464	0.132	0.088	1.610	0.001	2.295

Depth (cm)	Ca	Mg	K Exchange mmole(+)	Na phase Kg <sup>-1</sup> soil	Al	Sum
2.0	1.210	5.550	0.179	0.391	9.329	16.659
4.0	0.861	8.020	0.179	0.337	3.269	12.666
5.0	0.724	8.640	0.192	0.228	1.390	11.174
7.0	0.624	7.820	0.185	0.217	1.401	10.247
9.0	0.636	8.230	0.217	0.239	1.301	10.623
11.0	0.761	8.840	0.205	0.304	1.379	11.489
13.0	0.736	8.840	0.441	0.457	1.379	11.853
15.0	0.686	8.840	0.230	0.283	1.223	11.262
18.0	0.699	8.020	0.281	0.326	1.223	10.549
20.0	0.674	8.020	0.365	0.391	1.368	10.818

Table 4-11 Concentrations of cations in solution and exchange phases for Mg-subsoil after leaching with pH 4.9 HCl solution

Depth (cm)	Ca	Mg	K	Na	Al	Sum
	Solution phase			mmole(+) L <sup>-1</sup>		
1.0	0.419	0.090	0.184	1.000	0.022	1.716
2.0	0.294	0.086	0.139	0.935	0.022	1.477
3.0	0.259	0.086	0.134	0.804	0.041	1.325
4.0	0.511	0.119	0.243	1.110	0.017	2.000
5.0	0.205	0.090	0.105	0.676	0.203	1.280
6.0	0.302	0.074	0.134	0.817	0.001	1.328
7.0	0.264	0.078	0.114	0.809	0.029	1.294
8.0	0.419	0.090	0.152	0.965	0.002	1.629
9.0	0.432	0.103	0.136	1.360	0.016	2.047
10.0	0.319	0.103	0.164	1.110	0.130	1.826
11.0	0.479	0.109	0.526	1.140	0.003	2.257
12.0	0.356	0.079	0.330	0.939	0.003	1.707
13.0	0.050	0.099	0.243	1.290	0.002	1.684
14.0	0.389	0.082	0.243	1.190	0.004	1.909
15.0	0.269	0.084	0.235	0.916	0.048	1.552
16.0	0.557	0.099	0.152	1.270	0.003	2.081
17.0	0.434	0.165	0.148	1.710	0.001	2.458
18.0	0.452	0.107	0.171	1.280	0.010	2.020
19.0	0.467	0.128	0.321	1.570	0.017	2.503
20.0	0.392	0.107	0.129	1.200	0.014	1.843

Depth (cm)	Ca	Mg	K	Na	Al	Sum
	Exchange phase			mmole (+) Kg <sup>-1</sup> soil		
2.0	0.823	9.050	0.192	0.359	3.514	13.938
4.0	0.749	9.870	0.211	0.370	2.113	13.313
5.0	0.786	9.670	0.230	0.348	1.968	13.002
7.0	0.811	9.460	0.217	0.435	1.868	12.791
9.0	0.674	9.670	0.243	0.337	1.935	12.859
12.0	0.699	9.050	0.211	0.283	1.334	11.577
14.0	0.724	8.840	0.230	0.326	1.301	11.421
16.0	1.620	9.260	0.294	0.326	1.190	12.690
18.0	0.773	9.460	0.301	0.391	1.801	12.726
20.0	0.711	9.870	0.249	0.348	2.168	13.346

that the concentration of monovalent cations tended to be higher in the solution phase. After leaching pretreated subsoil with HCl solution for about 20 pore volumes, the initial cation species which had saturated the exchange sites were observed to still be the most dominant exchangeable cation in the soil as shown in Tables 4-6 through 4-11. The resultant CEC of the pretreated soil was quite stable and had approximately the same quantity of cations, but less than that for the nontreated soil, as given in Table 4-5. Base saturation was greatly decreased by continuous acid leaching from 90% initially to 55% after application of acid for all cases. In the section of each column which received acid input solution a high concentration of exchangeable  $\text{Al}^{3+}$  was generally observed and was attributed to poorly crystalline vermiculite or hydrous oxides of Al being exposed as exchange sites.

Treated Topsoil. Tables 4-12 and 4-13 present concentrations of cations in solution and exchange phases for Ca-topsoil columns which received input HCl solutions of pH 3.9 and 4.9, respectively. Concentrations of cations in the solution phase were in the order  $\text{Na}^+ > \text{Ca}^{2+} > \text{Mg}^{2+} > \text{K}^+ > \text{Al}^{3+}$  and for the exchange phase were  $\text{Ca}^{2+} > \text{Al}^{3+} > \text{K}^+ \approx \text{Na}^+ > \text{Mg}^{2+}$  for both treatments. If concentrations of cations in the exchange phase for Tables 4-12 and 4-13 are compared with values in Table 4-4 for original Ca-topsoil, the cation concentrations for  $\text{Mg}^{2+}$ ,  $\text{K}^+$ , and  $\text{Na}^+$  tended to increase during acid leaching but  $\text{Ca}^{2+}$  and  $\text{Al}^{3+}$

Table 4-12 Concentrations of cations in solution  
and exchange phases for Ca-topsoil after  
leaching with pH 3.9 HCl solution

Depth (cm)	Ca	Mg	K Solution mmole(+) L <sup>-1</sup>	Na phase L <sup>-1</sup>	Al	Sum
1.0	0.799	0.726	0.184	1.210	0.002	2.921
2.0	1.260	0.792	0.490	1.780	0.017	4.339
3.0	0.948	1.120	0.127	0.939	0.060	3.194
4.0	0.741	1.330	0.122	0.998	0.022	3.213
5.0	0.633	0.437	0.134	1.430	0.066	2.700
6.0	0.723	0.318	0.166	1.390	0.217	2.814
7.0	0.804	0.207	0.364	2.410	0.009	3.794
8.0	0.656	1.220	0.136	1.350	0.009	3.371
9.0	0.838	0.592	0.350	2.320	0.007	4.107
10.0	1.320	1.000	0.364	2.110	0.004	4.798
11.0	0.912	0.918	0.200	1.130	0.012	3.172
12.0	1.320	0.067	0.219	1.410	0.038	3.053
13.0	1.190	0.481	0.127	1.370	0.012	3.180
14.0	0.858	1.670	0.274	3.990	0.407	7.199
15.0	0.705	0.489	0.076	0.743	0.054	2.067
16.0	0.907	1.550	0.246	1.860	0.046	4.609
17.0	0.880	0.141	0.087	10.200	0.018	11.326
18.0	0.979	0.896	0.186	1.530	0.008	3.599
19.0	1.010	0.444	0.269	1.260	0.007	2.990
20.0	0.859	0.222	0.158	1.680	0.006	2.925

Depth (cm)	Ca	Mg	K Exchange mmole (+) Kg <sup>-1</sup>	Na phase Kg <sup>-1</sup>	Al soil	Sum
1.0	3.620	0.041	0.192	0.337	5.182	9.372
3.0	10.500	0.041	0.294	0.304	1.511	12.650
5.0	10.400	0.021	0.237	0.283	1.156	12.097
7.0	9.360	0.021	0.211	0.261	1.023	10.876
10.0	11.700	0.041	0.301	0.337	1.012	13.391
11.0	12.700	0.041	0.269	0.359	1.201	14.570
14.0	10.600	0.041	0.269	0.283	0.867	12.060
16.0	11.700	0.062	0.326	0.370	0.845	13.303
18.0	12.000	0.082	0.499	0.413	0.978	13.972
20.0	10.900	0.082	0.288	0.304	0.789	12.363

Table 4-13 Concentrations of cations in solution  
and exchange phases for Ca-topsoil  
after leaching with pH 4.9 HCl solution

Depth (cm)	Ca	Mg	K Solution mmole(+)	Na phase L <sup>-1</sup>	Al	Sum
1.0	1.330	0.204	0.565	0.268	0.006	2.373
2.0	0.913	0.103	0.453	1.090	0.012	2.571
3.0	0.606	0.086	0.413	0.891	0.016	2.012
4.0	0.718	0.174	0.632	1.020	0.016	2.560
5.0	0.731	0.197	0.577	0.939	0.014	2.459
6.0	0.521	0.089	0.445	0.646	0.018	1.719
7.0	0.687	0.215	0.465	1.100	0.016	2.483
8.0	0.599	0.148	0.256	0.630	0.019	1.652
9.0	0.695	0.109	0.200	0.522	0.009	1.535
10.0	0.692	0.207	0.387	0.770	0.018	2.074
11.0	0.674	0.070	0.224	0.500	0.012	1.480
12.0	0.958	0.074	0.216	0.600	0.012	1.860
13.0	0.852	0.194	0.401	0.852	0.011	2.310
14.0	0.888	0.140	0.380	0.826	0.012	2.246
15.0	0.946	0.156	0.299	0.750	0.014	2.166
16.0	0.727	0.046	0.176	0.496	0.023	1.469
17.0	0.862	0.099	0.259	0.665	0.022	1.907
18.0	1.080	0.155	0.186	0.565	0.076	2.062
19.0	1.230	0.270	0.265	0.609	0.020	2.394
20.0	1.010	0.165	0.164	0.435	0.039	1.813

Depth (cm)	Ca	Mg	K Exchange mmole (+)	Na phase Kg <sup>-1</sup>	Al soil	Sum
1.0	6.610	0.082	0.249	0.130	6.249	13.320
3.0	10.500	0.082	0.288	0.174	5.393	16.437
6.0	9.480	0.062	0.160	0.272	5.526	15.500
8.0	10.100	0.062	0.205	0.217	5.582	16.166
10.0	10.900	0.062	0.275	0.283	5.582	17.102
12.0	11.100	0.021	0.230	0.261	5.315	16.927
14.0	10.500	0.021	0.179	0.283	5.404	16.387
16.0	11.500	0.000	0.217	0.304	5.010	17.031
18.0	13.000	0.103	0.294	0.326	4.759	18.482
20.0	11.400	0.103	0.480	0.370	6.416	18.769

concentrations tended to decrease. Increased concentrations of cations in the exchange phase during acid leaching are explained by the argument given in the section on treated subsoil, since  $K^+$ ,  $Na^+$  and  $Ca^{2+}$  occur naturally between the lattices or interlayers of interlayer-hydroxy vermiculite (Dixon and Weed, 1977; Bohn et al., 1985). Due to the dissolution or weathering of such minerals and of carbonates, the release of cations from nonexchangeable forms tends to offset leaching losses of cations due to acid deposition. Calcium was not decreased greatly due to leaching for either of the acid treatments, since  $Ca^{2+}$  was more preferred on soil exchange sites.

Tables 4-14 and 4-15 provide concentrations of cations in solution and exchange phases for K-topsoil columns which received input HCl solutions with pH 3.9 and 4.9, respectively. The concentrations of cations in the solution phase were in the order  $Na^+ > Mg^{2+} \approx K^+ > Ca^{2+} > Al^{3+}$ , and for the exchange phase the concentrations were in order  $Al^{3+} > K^+ > Ca^{2+} > Na^+ > Mg^{2+}$ . If one compared the concentrations of cations in exchanger phase for Tables 4-14 and 4-15 with values in Table 4-4 for original K-topsoil, concentrations of exchangeable  $K^+$  were significantly less. Concentrations of other cations such as  $Ca^{2+}$ ,  $Mg^{2+}$ ,  $Na^+$  and  $Al^{3+}$  tended to increase for both treatments, however. Reasons similar to those mentioned earlier were used to explain the increased concentrations of specific cations in the exchange phase. The column that received pH 4.9 HCl

Table 4-14 Concentrations of cations in solution and exchange phases for K-topsoil after leaching with pH 3.9 HCl solution

Depth (cm)	Ca	Mg	K	Na	Al	Sum
	Solution phase					
	mmole (+) L <sup>-1</sup>					
1.0	0.296	0.622	0.090	0.587	0.004	1.599
2.0	0.844	0.874	0.583	1.370	0.004	3.675
3.0	0.449	0.852	0.205	0.783	0.006	2.295
4.0	0.130	1.220	0.246	0.593	0.002	2.191
5.0	0.817	1.110	0.592	1.240	0.006	3.765
6.0	0.692	0.666	0.638	1.130	0.006	3.132
7.0	1.190	8.400	1.600	4.370	0.048	15.608
8.0	0.110	1.660	0.652	1.470	1.140	5.032
9.0	0.221	1.250	0.725	0.061	0.681	2.938
10.0	0.298	1.110	0.905	1.160	0.006	3.479
11.0	0.850	1.500	1.450	2.540	0.003	6.343
12.0	0.435	0.406	1.030	1.670	0.003	3.544
13.0	0.259	0.118	1.060	1.610	0.004	3.051
14.0	0.220	1.160	1.360	0.765	0.033	3.538
15.0	0.229	1.760	1.110	1.660	0.007	4.766
16.0	0.269	0.526	0.999	0.900	0.016	2.710
17.0	0.184	1.180	1.200	1.350	0.036	3.950
18.0	0.153	1.250	1.080	1.510	0.014	4.008
19.0	0.404	0.940	0.960	2.780	0.011	5.095
20.0	0.856	2.410	1.970	2.400	0.150	7.786

Depth (cm)	Ca	Mg	K	Na	Al	Sum
	Exchange phase					
	mmole(+) Kg <sup>-1</sup> soil					
1.0	0.499	0.082	0.761	0.543	7.583	9.468
4.0	0.923	0.123	1.400	0.652	6.794	9.892
6.0	0.986	0.123	1.540	0.554	5.660	8.863
8.0	0.948	0.123	2.220	0.565	5.838	9.694
10.0	1.010	0.144	2.850	0.446	5.860	10.310
12.0	0.848	0.123	2.790	0.435	6.271	10.467
14.0	1.040	0.165	3.270	0.630	5.982	11.087
16.0	1.050	0.123	3.180	0.478	5.504	10.335
18.0	0.823	0.123	3.000	0.663	6.038	10.647
20.0	1.060	0.185	3.470	0.707	5.104	10.526

Table 4-15 Concentrations of cations in solution and exchange phases for K-topsoil after leaching with pH 4.9 HCl solution

Depth (cm)	Ca	Mg	K Solution mmole(+) L <sup>-1</sup>	Na phase L <sup>-1</sup>	Al	Sum
1.0	0.407	1.330	0.426	2.050	0.006	4.219
2.0	0.292	1.620	0.463	0.761	0.012	3.148
3.0	0.182	1.420	0.478	0.946	0.016	3.042
4.0	0.139	0.259	0.511	0.528	0.016	1.453
5.0	0.135	2.120	0.744	1.150	0.014	4.163
6.0	0.212	2.710	0.700	1.230	0.018	4.870
7.0	0.355	1.050	0.565	0.487	0.016	2.473
8.0	0.208	0.449	1.140	1.580	0.019	3.396
9.0	0.164	2.420	0.770	0.661	0.009	4.024
10.0	1.150	1.460	0.919	1.500	0.018	5.047
11.0	1.380	0.518	1.170	1.720	0.012	4.800
12.0	0.436	0.992	1.080	0.763	0.012	3.283
13.0	0.120	0.062	0.721	0.380	0.011	1.294
14.0	0.092	0.045	0.733	0.283	0.012	1.166
15.0	0.144	0.089	1.040	0.430	0.014	1.717
16.0	0.103	0.037	0.967	0.274	0.023	1.404
17.0	0.045	0.052	1.040	0.215	0.022	1.374
18.0	0.076	0.059	1.110	0.215	0.076	1.536
19.0	0.112	0.089	1.170	0.313	0.020	1.704
20.0	0.501	2.100	0.944	1.050	0.039	4.634

Depth (cm)	Ca	Mg	K Exchange mmole (+) Kg <sup>-1</sup>	Na phase Kg <sup>-1</sup>	Al soil	Sum
1.0	0.561	0.041	0.582	0.217	2.891	4.292
3.0	0.599	0.062	1.300	0.239	1.768	3.968
5.0	0.674	0.082	1.920	0.261	1.568	4.505
7.0	0.699	0.082	2.620	0.207	1.423	5.031
9.0	0.561	0.062	2.290	0.196	1.579	4.688
11.0	0.649	0.103	2.650	0.239	1.501	5.142
13.0	0.674	0.082	3.200	0.217	1.390	5.563
15.0	0.836	0.082	3.010	0.239	1.446	5.613
17.0	0.836	0.103	3.480	0.217	1.357	5.993
20.0	1.500	0.391	6.270	0.087	1.201	9.449

solution showed that very little exchangeable  $\text{Al}^{3+}$  existed initially, however.

Tables 4-16 and 4-17 present concentrations of cations in solution and exchange phases for Mg-topsoil columns which received input HCl solutions of pH 3.9 and 4.9, respectively. Concentrations of cations in the solution phase were in the order  $\text{Al}^{3+} > \text{Na}^+ > \text{Ca}^{2+} > \text{Mg}^{2+} > \text{K}^+$ , but for the exchange phase were in the order  $\text{Mg}^{2+} > \text{Ca}^{2+} > \text{Al}^{3+} > \text{Na}^+ > \text{K}^+$ . Abnormally high solution concentrations of  $\text{Al}^{3+}$  were observed for both treatments. Comparison of concentrations of cations in the exchange phase with values in Table 4-4 for original exchangeable cations in Mg-topsoil showed that the concentration of  $\text{Mg}^{2+}$  decreased but the other cations such as  $\text{Ca}^{2+}$ ,  $\text{K}^+$ ,  $\text{Na}^+$  and  $\text{Al}^{3+}$  increased after leaching with acid. This may be explained by decomposition of the minerals due to the effect the input acid solutions.

A comparison of the CEC after leaching with the CEC of initial pretreated topsoil showed a significant decrease but if one compared the CEC that resulted after leaching with the CEC of the original untreated topsoil (Table 4-5), good agreement occurred. A small decrease in CEC was found only for the section of the soil column that received input acid solution. Large concentrations of exchangeable  $\text{Al}^{3+}$  were found at the end of the columns receiving input acid solution.

Mixed subsoil. Tables 4-18 and 4-19 present concentrations of cations in solution and exchange phases

Table 4-16 Concentrations of cations in solution and exchange phases for Mg-topsoil after leaching with pH 3.9 HCl solution

Depth (cm)	Ca	Mg	K	Na	Al	Sum
	Solution phase					
	mmole (+) L <sup>-1</sup>					
1.0	0.587	0.115	0.142	1.340	0.213	2.397
2.0	0.322	0.584	0.161	0.164	0.024	1.256
3.0	0.067	0.387	0.106	0.848	7.860	9.268
4.0	0.569	0.370	0.215	0.861	0.078	2.093
5.0	0.192	0.704	0.115	1.410	0.053	2.474
6.0	0.215	0.629	0.299	1.280	0.367	2.790
7.0	0.657	0.398	0.197	2.260	0.178	3.690
8.0	0.354	0.432	0.141	1.680	1.350	3.957
9.0	0.399	0.388	0.186	1.890	1.860	4.723
10.0	0.491	0.372	0.075	1.660	0.173	2.771
11.0	0.595	0.652	0.179	4.050	0.053	5.529
12.0	0.539	0.559	0.197	2.300	1.630	5.225
13.0	0.437	0.580	0.230	2.490	4.170	7.907
14.0	0.503	0.991	0.321	3.310	21.200	26.325
15.0	0.439	0.457	0.127	1.530	0.058	2.611
16.0	0.255	0.431	0.117	1.570	0.138	2.511
17.0	0.403	0.536	0.216	1.620	10.900	13.675
18.0	0.411	0.497	0.106	1.640	3.750	6.404
19.0	0.527	0.454	0.157	1.730	5.570	8.438
20.0	0.517	0.872	0.199	1.870	21.000	24.458

Depth (cm)	Ca	Mg	K	Na	Al	Sum
	Exchange phase					
	mmole (+) Kg <sup>-1</sup> soil					
1.0	1.320	0.473	0.230	0.391	6.772	9.186
2.0	2.880	4.110	0.281	0.478	1.001	8.750
3.0	2.060	7.200	0.153	0.435	0.767	10.615
5.0	2.540	8.640	0.326	0.467	0.890	12.863
7.0	1.950	9.260	0.166	0.348	0.801	12.525
10.0	1.850	9.460	0.198	0.304	0.767	12.579
13.0	1.920	9.460	0.185	0.348	0.745	12.658
16.0	2.160	8.840	0.166	0.283	0.645	12.094
18.0	1.980	10.100	0.205	0.337	0.601	13.223
20.0	2.210	10.700	0.230	0.500	0.556	14.196

Table 4-17 Concentrations of cations in solution and exchange phases for Mg-topsoil after leaching with pH 4.9 HCl solution

Depth (cm)	Ca	Mg	K	Na	Al	Sum
			Solution	phase		
			mmole(+) L <sup>-1</sup>	mmole(+) L <sup>-1</sup>		
1.0	0.737	0.349	0.234	1.740	2.080	5.140
2.0	0.413	0.494	0.150	2.350	11.700	15.107
3.0	0.626	0.415	0.183	1.550	1.410	4.184
4.0	0.596	0.329	0.230	2.000	3.740	6.895
5.0	0.631	0.698	0.357	2.070	1.670	5.426
6.0	0.701	0.434	0.363	2.490	2.860	6.848
7.0	0.180	0.681	0.225	1.680	32.600	35.366
8.0	0.695	0.527	0.358	1.970	10.600	14.150
9.0	0.293	0.528	0.178	1.940	13.600	16.539
10.0	0.607	0.372	0.166	1.380	2.740	5.265
11.0	0.418	0.588	0.160	1.720	11.900	14.786
12.0	1.000	0.666	0.577	3.990	0.183	6.416
13.0	0.363	0.553	0.302	2.440	8.480	12.138
14.0	0.152	0.502	0.175	1.100	17.700	19.629
15.0	0.134	0.543	0.187	1.280	17.300	19.444
16.0	0.087	0.605	0.171	0.848	19.600	21.311
17.0	0.120	0.647	0.310	1.520	22.800	25.397
18.0	0.031	0.518	0.213	1.210	17.100	19.072
19.0	0.132	0.592	0.190	1.270	21.900	24.084
20.0	0.134	0.513	0.189	0.751	12.900	14.487

Depth (cm)	Ca	Mg	K	Na	Al	Sum
			Exchange	phase		
			mmole (+) Kg <sup>-1</sup>	mmole(+) Kg <sup>-1</sup>	soil	
1.0	2.070	5.550	0.416	0.500	2.335	10.871
3.0	1.920	8.640	0.160	0.391	0.956	12.067
5.0	1.710	8.840	0.141	0.304	0.923	11.918
7.0	1.860	8.840	0.294	0.446	0.767	12.207
9.0	1.630	9.460	0.147	0.228	0.812	12.277
11.0	1.670	9.050	0.115	0.239	0.689	11.763
14.0	1.720	9.460	0.160	0.370	0.634	12.344
16.0	1.770	9.670	0.173	0.359	0.712	12.684
18.0	1.770	8.640	0.365	0.489	0.623	11.887
20.0	1.970	10.100	0.294	0.565	0.656	13.585

for mixed subsoil columns that received input HCl solutions of pH 3.9 and 4.9, respectively. Concentrations of cations throughout the column for the solution phase were generally in the order  $K^+ > Na^+ > Ca^{2+} > Mg^{2+} > Al^{3+}$  but, for the exchange phase the order was  $K^+ > Ca^{2+} > Mg^{2+} > Al^{3+} > Na^+$ . If one only examines the shallowest depth for the column receiving the pH 3.9 input acid solution, the exchange-phase concentrations were in the order  $Al^{3+} > Ca^{2+} > Mg^{2+} > K^+ > Na^+$  and for pH treatment 4.9 in the order  $Ca^{2+} > Mg^{2+} > Al^{3+} > K^+ > Na^+$ . Concentrations of the basic cations  $Ca^{2+}$ ,  $Mg^{2+}$ ,  $K^+$  and  $Na^+$  were much less than the  $Al^{3+}$  concentration for the pH 3.9 case. The pH 4.9 treatment had a reverse effect. A comparison of concentrations on the exchange phase in Tables 4-18 and 4-19 with values in Table 4-4 for the original exchangeable cations in mixed subsoil showed that concentrations of the basic cation  $Mg^{2+}$ ,  $Ca^{2+}$ ,  $K^+$  and  $Na^+$  were decreased but those  $Al^{3+}$  remained fairly stable. The base-cation saturation was remarkably decreased by leaching.

Mixed topsoil. Tables 4-20 and 4-21 present concentrations of cations in the solution and exchange phases for mixed topsoil columns after receiving pH 3.9 and 4.9 input HCl solutions, respectively. Concentrations of cations through the soil columns for the solution phase were generally in the order  $Al^{3+} > Ca^{2+} > Mg^{2+} > K^+ > Na^+$  for pH treatment 3.9 and in the order  $Al^{3+} > Mg^{2+} > K^+ > Ca^{2+} > Na^+$  for pH treatment 4.9. The exchange phase was in the order  $Ca^{2+} > Al^{3+} > Mg^{2+} > K^+ > Na^+$  for both treatments.

Table 4-18 Concentrations of cations in solution and exchange phases for mixed-cation subsoil after leaching with pH 3.9 HCl solution

Depth (cm)	Ca	Mg	K	Na	Al	Sum
	Solution phase					
	mmole (+) L <sup>-1</sup>					
1.0	0.050	0.016	0.142	0.178	0.017	0.403
2.0	0.082	0.037	0.151	0.165	0.011	0.446
3.0	0.085	0.062	0.205	0.167	0.011	0.530
4.0	0.062	0.058	0.129	0.100	0.011	0.360
5.0	0.040	0.021	0.288	0.139	0.000	0.487
6.0	0.032	0.016	0.260	0.115	0.006	0.429
7.0	0.015	0.025	0.285	0.133	0.013	0.471
8.0	0.027	0.021	0.326	0.148	0.022	0.544
9.0	0.060	0.037	0.365	0.202	0.006	0.669
10.0	0.000	0.000	2.530	0.154	0.000	2.684
11.0	0.078	0.035	0.523	0.334	0.060	1.029
12.0	0.057	0.021	0.386	0.243	0.050	0.757
13.0	0.035	0.016	0.362	0.189	0.000	0.602
14.0	0.015	0.012	0.365	0.165	0.000	0.557
15.0	0.042	0.020	0.375	0.219	0.033	0.689
16.0	0.023	0.005	0.324	0.236	0.014	0.602
17.0	0.012	0.015	0.301	0.130	0.007	0.464
18.0	0.027	0.010	0.335	0.157	0.027	0.555
19.0	0.033	0.015	0.275	0.193	0.020	0.536
20.0	0.045	0.020	0.410	0.237	0.060	0.772

Depth (cm)	Ca	Mg	K	Na	Al	Sum
	Exchange phase					
	mmole(+) Kg <sup>-1</sup> soil					
1.0	2.990	0.716	0.491	0.222	8.117	12.536
2.0	4.640	3.040	1.010	0.183	0.912	9.785
3.0	5.240	3.130	1.370	0.191	1.007	10.938
5.0	4.940	2.960	3.500	0.196	0.845	12.441
7.0	4.690	2.710	4.450	0.174	0.790	12.814
9.0	4.790	2.630	5.650	0.191	0.899	14.160
12.0	4.790	2.140	6.270	0.200	0.723	14.123
15.0	4.140	2.330	6.040	0.226	0.801	13.537
18.0	4.890	2.410	6.500	0.217	0.634	14.651
20.0	4.240	2.350	6.340	0.252	0.656	13.838

Table 4-19 Concentrations of cations in solution and exchange phases for mixed-cation subsoil after leaching with pH 4.9 HCl solution

Depth (cm)	Ca	Mg	K	Na	Al	Sum
	Solution phase					
	mmole (+) L <sup>-1</sup>					
1.0	0.062	0.041	0.414	0.120	0.006	0.643
2.0	0.047	0.033	0.267	0.122	0.011	0.480
3.0	0.027	0.013	0.354	0.086	0.018	0.498
4.0	0.035	0.008	0.247	0.107	0.011	0.408
5.0	0.057	0.016	0.421	0.183	0.017	0.695
6.0	0.032	0.008	0.656	0.087	0.000	0.784
7.0	0.030	0.016	0.344	0.124	0.022	0.537
8.0	0.025	0.008	0.342	0.126	0.011	0.512
9.0	0.092	0.021	0.384	0.217	0.011	0.725
10.0	0.025	0.008	0.265	0.122	0.006	0.426
11.0	0.027	0.008	0.307	0.130	0.006	0.478
12.0	0.027	0.004	0.288	0.098	0.006	0.423
13.0	0.020	0.008	0.434	0.135	0.028	0.625
14.0	0.037	0.012	0.404	0.167	0.017	0.637
15.0	0.027	0.012	0.377	0.133	0.011	0.561
16.0	0.077	0.037	0.794	0.128	0.022	1.059
17.0	0.007	0.008	0.287	0.104	0.028	0.435
18.0	0.020	0.008	0.411	0.200	0.028	0.667
19.0	0.075	0.025	0.625	0.170	0.020	0.915
20.0	0.018	0.008	0.375	0.091	0.028	0.520

Depth (cm)	Ca	Mg	K	Na	Al	Sum
	Exchange phase					
	mmole (+) Kg <sup>-1</sup> soil					
1.0	3.590	3.620	1.430	0.313	2.635	11.588
3.0	4.540	2.960	3.480	0.196	1.190	12.366
5.0	4.490	2.630	4.550	0.200	0.956	12.826
7.0	4.690	2.300	4.940	0.196	1.012	13.138
9.0	4.040	2.570	5.350	0.200	0.878	13.038
11.0	3.940	2.500	5.550	0.183	0.756	12.929
14.0	4.040	2.390	5.830	0.130	0.812	13.202
16.0	4.190	2.330	6.060	0.191	0.701	13.472
18.0	4.090	2.220	5.940	0.235	0.689	13.174
20.0	4.240	2.100	6.640	0.243	0.767	13.990

Table 4-20 Concentrations of cations in solution and exchange phases for mixed-cation topsoil after leaching with pH 3.9 HCl solution

Depth (cm)	Ca	Mg	K	Na	Al	Sum
	Solution phase					
	mmole (+) L <sup>-1</sup>					
1.0	0.202	0.078	0.151	0.115	0.100	0.646
2.0	0.167	0.062	0.155	0.183	0.139	0.706
3.0	0.205	0.074	0.182	0.159	0.094	0.715
4.0	0.227	0.128	0.208	0.193	0.295	1.051
5.0	0.279	0.152	0.223	0.196	1.070	1.920
6.0	0.319	0.267	0.313	0.198	13.800	14.897
7.0	0.277	0.197	0.228	0.154	2.300	3.156
8.0	0.342	0.276	0.205	0.124	9.060	10.007
9.0	0.317	0.230	0.220	0.150	1.530	2.447
10.0	0.414	0.415	0.292	0.152	23.000	24.273
11.0	0.409	0.341	0.290	0.157	10.800	11.997
12.0	0.392	0.317	0.385	0.148	7.800	9.042
13.0	0.384	0.247	0.294	0.187	1.150	2.262
14.0	0.359	0.346	0.278	0.141	14.000	15.124
15.0	0.387	0.354	0.504	0.152	13.400	14.797
16.0	0.334	0.235	0.340	0.182	0.757	1.848
17.0	0.374	0.420	0.336	0.117	23.100	24.347
18.0	0.394	0.337	0.344	0.159	12.100	13.334
19.0	0.334	0.296	0.267	0.100	10.000	10.997
20.0	0.357	0.284	0.331	0.109	9.440	10.521

Depth (cm)	Ca	Mg	K	Na	Al	Sum
	Exchange phase					
	mmole (+) Kg <sup>-1</sup> soil					
1.0	3.340	0.946	0.379	0.252	4.770	9.687
3.0	4.040	0.872	0.358	0.239	2.320	7.829
6.0	5.440	1.650	0.489	0.226	2.210	10.015
8.0	5.290	1.890	0.650	0.217	2.430	10.477
10.0	5.490	1.890	0.650	0.209	2.420	10.659
12.0	5.640	2.040	0.744	0.174	2.160	10.758
14.0	6.040	2.020	0.837	0.226	2.350	11.473
17.0	6.040	2.000	0.929	0.130	2.040	11.139
18.0	6.790	2.050	1.030	0.109	1.630	11.609
20.0	6.420	2.130	1.150	0.109	1.460	11.269

Table 4-21 Concentrations of cations in solution and exchange phases for mixed-cation topsoil after leaching with pH 4.9 HCl solution

Depth (cm)	Ca	Mg	K Solution mmole(+) L <sup>-1</sup>	Na phase mmole(+) L <sup>-1</sup>	Al	Sum
1.0	0.413	0.173	0.138	0.170	11.300	12.194
2.0	0.382	0.111	0.137	0.096	0.600	1.326
3.0	0.497	0.459	0.305	0.136	41.800	43.197
4.0	0.491	0.326	0.295	0.146	20.800	22.058
5.0	0.281	0.420	0.325	0.073	30.500	31.599
6.0	0.272	0.485	0.353	0.067	32.600	33.777
7.0	0.311	0.474	0.427	0.162	38.500	39.874
8.0	0.252	0.403	0.321	0.089	31.400	32.465
9.0	0.217	0.276	0.257	0.150	17.300	18.200
10.0	0.254	0.378	0.257	0.074	3.270	4.233
11.0	0.245	0.119	0.283	0.122	1.350	2.119
12.0	0.232	0.218	0.217	0.080	10.200	10.947
13.0	0.249	0.385	0.272	0.055	33.100	34.061
14.0	0.202	0.292	0.223	0.089	29.800	30.606
15.0	0.309	0.601	0.389	0.083	64.400	65.782
16.0	0.225	0.257	0.315	0.123	16.300	17.220
17.0	0.263	0.449	0.364	0.086	33.100	34.262
18.0	0.269	0.548	0.413	0.112	66.000	67.342
19.0	0.344	0.563	0.328	0.112	69.300	70.647
20.0	0.326	0.360	0.431	0.271	18.900	20.288

Depth (cm)	Ca	Mg	K Exchange mmole (+) Kg <sup>-1</sup>	Na phase mmole (+) Kg <sup>-1</sup>	Al soil	Sum
2.0	5.140	1.760	0.647	0.217	3.847	11.611
3.0	6.040	1.910	0.729	0.200	2.913	11.792
6.0	5.190	1.790	0.998	0.209	2.780	10.967
8.0	5.990	1.970	1.110	0.200	2.769	12.039
10.0	5.840	1.790	1.040	0.191	2.680	11.541
12.0	5.240	1.810	1.030	0.235	2.713	11.028
13.0	4.740	1.720	0.941	0.130	2.646	10.177
16.0	5.040	1.710	1.120	0.226	2.402	10.498
18.0	4.690	1.780	1.190	0.209	2.858	10.727
19.0	6.190	1.950	1.220	0.217	2.558	12.135

Concentrations of  $\text{Al}^{3+}$  in the solution phase were relatively high for both treatments. If one examined only the shallowest depth (at the end of the column receiving acid input solution), cation concentrations in the exchange phase were in the order  $\text{Ca}^{2+} > \text{Al}^{3+} > \text{Mg}^{2+} > \text{K}^+ > \text{Na}^+$  for pH treatment 4.9 and in the order  $\text{Al}^{3+} > \text{Ca}^{2+} > \text{Mg}^{2+} > \text{K}^+ > \text{Na}^+$  for pH treatment 3.9. Higher  $\text{Al}^{3+}$  concentrations but lower concentrations of the basic cations  $\text{Ca}^{2+}$ ,  $\text{Mg}^{2+}$ ,  $\text{K}^+$ , and  $\text{Na}^+$  were found at the input end of the soil column for the pH 3.9 case.

#### Charge Balance Using All Major Cations for Treated and Mixed Soil Columns

The charge balance of all major cations for pretreated and mixed topsoil and subsoil are given in Tables 4-22 through 4-27. The theoretical charge balance of major cations in each soil column can be described by the following relationship

$$\begin{aligned}
 &\text{Total } \text{H}^+ \text{ (mmole(+)) added + Exchangeable cations (mmole(+))} \\
 &\quad \quad \quad \text{(includes exchangeable } \text{H}^+ \text{)} \\
 &\quad \quad \quad \text{initially present on soil} \\
 &\quad \quad \quad \text{exchange sites} \\
 &= \text{Total } \text{H}^+ \text{ (mmole(+)) and cations (mmole(+))} \\
 &\quad \quad \quad \text{exported from the soil column} \\
 &+ \text{Exchangeable cations (mmole(+)) (includes } \text{H}^+ \text{ ions)} \\
 &\quad \quad \quad \text{remaining in the soil column. [4-3]}
 \end{aligned}$$

Details for the calculation procedure are the same as stated in chapter three. In the following text the

Table 4-22 Charge balance of cations for columns of Ca-topsoil

Ca-topsoil pH 3.9 (mmole(+))						
	H <sup>+</sup>	Ca <sup>2+</sup>	Mg <sup>2+</sup>	K <sup>+</sup>	Na <sup>+</sup>	Al <sup>3+</sup>
Initial cations		4.163	0.007	0.036	0.000	0.783
Total input	0.284					
Final #		0.075	0.060	0.017	0.169	0.004
solution phase						
Final #		3.682	0.017	0.103	0.116	0.518
exchange phase						
Total	0.004	4.060	0.016	0.024	0.100	0.116
output in effluent						
Ca-topsoil pH 4.9 (mmole(+))						
	H <sup>+</sup>	Ca <sup>2+</sup>	Mg <sup>2+</sup>	K <sup>+</sup>	Na <sup>+</sup>	Al <sup>3+</sup>
Initial cations		4.240	0.007	0.036	0.000	0.800
Total input	0.029					
Final #		0.070	0.012	0.029	0.059	0.002
solution phase						
Final #		3.810	0.022	0.093	0.095	2.000
exchange phase						
Total	0.003	2.120	0.042	0.019	0.023	0.193
output in effluent						

#: undetermined

Table 4-23 Charge balance of cations for columns of K-topsoil

K-topsoil pH 3.9 (mmole(+))						
	H <sup>+</sup>	Ca <sup>2+</sup>	Mg <sup>2+</sup>	K <sup>+</sup>	Na <sup>+</sup>	Al <sup>3+</sup>
Initial cations		0.219	0.030	6.272	0.109	2.115
Total input	0.348					
Final #		0.036	0.117	0.075	0.121	0.009
solution phase						
Final #		0.335	0.048	0.893	0.081	2.210
exchange phase						
Total	0.009	0.001	0.001	5.144	0.042	2.910
output in effluent						
K-topsoil pH 4.9 (mmole(+))						
	H <sup>+</sup>	Ca <sup>2+</sup>	Mg <sup>2+</sup>	K <sup>+</sup>	Na <sup>+</sup>	Al <sup>3+</sup>
Initial cations		0.217	0.029	6.233	0.108	2.102
Total input	0.029					
Final #		0.026	0.078	0.069	0.068	0.002
solution phase						
Final #		0.275	0.040	0.990	0.077	0.584
exchange phase						
Total	0.008	0.233	0.044	5.167	0.098	2.518
output in effluent						

#: undetermined

Table 4-24 Charge balance of cations for columns of Mg-topsoil

Mg-topsoil pH 3.9 (mmole(+))						
	H <sup>+</sup>	Ca <sup>2+</sup>	Mg <sup>2+</sup>	K <sup>+</sup>	Na <sup>+</sup>	Al <sup>3+</sup>
Initial cations		0.326	4.241	0.072	0.109	0.181
Total input	0.277					
Final #		0.030	0.043	0.016	0.145	0.330
solution phase						
Final #		0.756	2.836	0.776	0.141	0.491
exchange phase						
Total	0.001	0.033	9.840	0.022	0.021	0.739
output in effluent						
Mg-topsoil pH 4.9 (mmole(+))						
	H <sup>+</sup>	Ca <sup>2+</sup>	Mg <sup>2+</sup>	K <sup>+</sup>	Na <sup>+</sup>	Al <sup>3+</sup>
Initial cations		0.326	4.241	0.072	0.109	0.181
Total input	0.025					
Final #		0.033	0.044	0.020	0.146	1.341
solution phase						
Final #		0.656	0.320	0.082	0.141	0.330
exchange phase						
Total	0.001	0.035	4.128	0.040	0.017	0.849
output in effluent						

# : undetermined

Table 4-25 Charge balance of cations for columns of Ca-subsoil

Ca-subsoil pH 3.9 (mmole(+))						
	H <sup>+</sup>	Ca <sup>2+</sup>	Mg <sup>2+</sup>	K <sup>+</sup>	Na <sup>+</sup>	Al <sup>3+</sup>
Initial cations		17.900	0.033	0.066	0.000	0.066
Total input	0.271					
Final #		0.050	0.006	0.020	0.126	0.058
solution phase						
Final #		3.580	0.011	0.088	0.086	0.321
exchange phase						
Total	0.003	14.926	0.029	0.026	0.023	0.012
output in effluent						
Ca-subsoil pH 4.9 (mmole(+))						
	H <sup>+</sup>	Ca <sup>2+</sup>	Mg <sup>2+</sup>	K <sup>+</sup>	Na <sup>+</sup>	Al <sup>3+</sup>
Initial cations		17.900	0.033	0.066	0.000	0.066
Total input	0.024					
Final #		0.060	0.006	0.016	0.162	0.026
solution phase						
Final #		3.500	0.016	0.061	0.100	0.124
exchange phase						
Total	0.003	14.167	0.020	0.045	0.038	0.071
output in effluent						

#: undetermined

Table 4-26 Charge balance of cations for columns of K-subsoil

K-subsoil pH 3.9 (mmole(+))						
	H <sup>+</sup>	Ca <sup>2+</sup>	Mg <sup>2+</sup>	K <sup>+</sup>	Na <sup>+</sup>	Al <sup>3+</sup>
Initial cations		0.430	0.031	15.421	0.123	0.215
Total input	0.271					
Final #		0.050	0.008	0.051	0.207	0.002
solution phase						
Final #		0.372	0.021	3.721	0.208	0.450
exchange phase						
Total	0.009	0.151	0.030	11.140	0.030	0.015
output in effluent						
K-subsoil pH 4.9 (mmole(+))						
	H <sup>+</sup>	Ca <sup>2+</sup>	Mg <sup>2+</sup>	K <sup>+</sup>	Na <sup>+</sup>	Al <sup>3+</sup>
Initial cations		0.424	0.030	15.199	0.121	0.212
Total input	0.026					
Final #		0.044	0.006	0.042	0.176	0.001
solution phase						
Final #		0.393	0.026	4.208	0.214	0.303
exchange phase						
Total	0.008	0.082	0.019	6.872	0.021	0.010
output in effluent						

#: undetermined

Table 4-27 Charge balance of cations for columns of Mg-subsoil

Mg-subsoil pH 3.9 (mmole(+))						
	H <sup>+</sup>	Ca <sup>2+</sup>	Mg <sup>2+</sup>	K <sup>+</sup>	Na <sup>+</sup>	Al <sup>3+</sup>
Initial cations		0.093	30.164	0.093	0.006	0.436
Total input	0.125					
Final #		0.044	0.013	0.015	0.148	0.001
solution phase						
Final #		0.237	2.518	0.077	0.099	0.725
exchange phase						
Total	0.021	0.041	22.959	0.043	0.041	0.062
output in effluent						
Mg-subsoil pH 4.9 (mmole(+))						
	H <sup>+</sup>	Ca <sup>2+</sup>	Mg <sup>2+</sup>	K <sup>+</sup>	Na <sup>+</sup>	Al <sup>3+</sup>
Initial cations		0.094	30.380	0.094	0.063	0.044
Total input	0.026					
Final #		0.037	0.010	0.020	0.108	0.029
solution phase						
Final #		0.263	2.956	0.075	0.111	0.602
exchange phase						
Total	0.01	0.154	22.438	0.035	0.039	0.035
output in effluent						

#: undetermined

terminology of "input" and "output" refers to the left- and right- hand sides of equation [4-3], respectively.

Treated Topsoil. Tables 4-22 through 4-24 present the charge balance of Ca-topsoil, K-topsoil and Mg-topsoil, respectively. Inputs were 5.272 and 5.112 mmole(+) and outputs were 8.893 and 8.590 mmole(+) for Ca-topsoil that received treatment pH 3.9 and 4.9 HCl solutions, respectively. Therefore, very large charge-balance errors, of + 69 and + 68%, were observed for Ca-topsoil for treatments of pH 3.9 and 4.9, respectively. From Table 4-22 the sum of concentrations of  $\text{Ca}^{2+}$  in the exchange phase and effluent exceeded the initial quantities of  $\text{Ca}^{2+}$  in the Ca-topsoil, indicating that soil minerals underwent dissolution during leaching with the HCl solutions. Inputs were 9.353 and 8.718 mmole(+) and outputs were 12.031 and 10.275 mmole(+) for K-topsoil that received pH 3.9 and 4.9 HCl solutions, respectively. Charge-balance errors for K-topsoil were + 29 and + 15% for the pH 3.9 and 4.9 treatments, respectively. Inputs were 5.206 and 4.954 mmole(+), and outputs were 15.734 and 8.183 mmole(+) for Mg-topsoil that received pH 3.9 and 4.9 HCl solutions, respectively. Charge-balance errors were + 202 and + 8% for treatments of pH 3.9 and 4.9 respectively. The extremely large error observed for the pH 3.9 treatment with Mg-topsoil can possibly be explained by the effect of mineral dissolution, since concentrations of  $\text{Mg}^{2+}$  in the exchange phase and effluent were 3-fold greater than the

initial quantities for Mg-topsoil. For all of the pretreated topsoil, quantities of all cations leached were not directly proportional to the  $H^+$  concentration of the applied solution, but larger quantities of major cations were leached from columns receiving pH 3.9 HCl than for pH 4.9 HCl. For example, for Ca-topsoil that received pH 3.9 HCl, 4.06 mole(+) of  $Ca^{2+}$  were leached but only 2.12 mmole(+) were leached when pH 4.9 HCl was applied. Mineral dissolution was implied from concentrations of cations in the leachate and on exchange sites. For example for Ca-topsoil,  $K^+$  and  $Na^+$  were initially 0.036 and 0.0 mmole(+) in the exchange phase but became 0.103 and 0.116 mmole(+) after leaching with pH 3.9 HCl. Similar results were observed for all treated topsoil columns of all cations species examined. The increase of exchangeable-cation concentration was most dramatic for  $Al^{3+}$ . Output from the treated topsoil was observed to be greater than input, and the resulting positive-charge-balance errors can be attributed to the dissolution or decomposition of interlayer-hydroxy vermiculite, as well as to other mineral-weathering processes in this soil.

Treated subsoil. Tables 4-25 through 4-27 present the charge balance for Ca-subsoil, K-subsoil and Mg-subsoil, respectively. Inputs were 18.336 and 18.089 mmole(+) and outputs were 19.473 and 18.418 mmole(+) for Ca-subsoil that received pH 3.9 and 4.9 HCl solutions, respectively. Ca-subsoil gave charge-balance errors of + 6 and + 2 % for

pH 3.9 and 4.9 HCl solutions, respectively. Inputs were 16.491 and 16.012 mmole(+) and outputs were 16.465 and 12.425 mmole(+) for K-subsoil receiving pH 3.9 and 4.9 HCl solutions, respectively. K-subsoil thus gave + 4 and + 22 % charge-balance errors for treatments of pH 3.9 and 4.9, respectively. Inputs were 30.917 and 30.701 mmole(+), and outputs were 27.020 and 26.931 mmole(+) for Mg-subsoil that received pH 3.9 and 4.9 HCl solutions, respectively. Mg-subsoil thus gave - 13 and - 12% charge-balance errors for treatments of pH 3.9 and 4.9, respectively. For all of the pretreated subsoil, quantities of cations leached were not directly proportional to  $H^+$  concentration of the applied HCl solution for the major saturating cation. For example for K-subsoil that received pH 3.9 solution, 11.140 mmole(+) of  $K^+$  was leached, but only 6.872 mmole(+) was leached when pH 4.9 acid was applied. The leaching of other cations was also less than proportional to the applied solution pH. The result of mineral dissolution was evident from the concentrations of cations in the leachate and an exchange phases, but was not as much as for the topsoil. For Mg-subsoil, for example, concentrations of  $Na^+$  and  $Al^{3+}$  initially on the exchange sites were 0.006 and 0.436 mmole(+) but, after leaching with pH 3.9 HCl solution, these concentrations became 0.041 and 0.725 mmole(+), respectively. For all of the treated Cecil subsoil columns the outputs were much less than were inputs, and negative charge-balance errors occurred. This can be explained by

the red-orange color of the treated Cecil subsoil, which is due to substantial amounts of Fe oxides. pH-Dependent sites for these oxides tend to develop a negatively charged surface at moderate to high pH ( $\text{pH} > 5.0$ ). The stable pH readings for the samples of effluent and of soil solution were near 6.5. Therefore, some of the exchangeable cations were adsorbed for charge-balance purpose, resulting in a decrease in the quantity of exchangeable cations or cations exported.

Mixed soil. Tables 4-28 and 4-29 present the charge balance for mixed subsoil and topsoil, respectively. Inputs were 8.161 and 7.841 mmole(+) and outputs were 11.576 and 12.656 mmole(+) for mixed topsoil that received pH 3.9 and 4.9 HCl solution, respectively. Charge-balance errors for mixed topsoil were + 42 and + 61% for treatments pH 3.9 and 4.9, respectively. The large charge-balance error was explained by mineral dissolution. Inputs were 24.825 and 24.582 mmole(+) and outputs were 26.889 and 30.360 mmole(+) for mixed subsoil that received pH 3.9 and 4.9 acid, respectively. Charge-balance errors for mixed subsoil were 8% and 23% for treatments of pH 3.9 and 4.9, respectively. Mixed soils obtained by mixing the three pretreated soils in a 1: 1: 1 weight ratio resulted in  $\text{Mg}^{2+}$  domination of exchange sites. Concentrations of cations in the leachate were also dominated by  $\text{Mg}^{2+}$ . Thus leaching losses of  $\text{Mg}^{2+}$  were greater than for all other cations. Total concentrations of each cation in the effluent were not

Table 4-28 Charge balance of cations for columns of mixed-cation subsoil

Mixed-cation subsoil pH 3.9 (mmole(+))					
H <sup>+</sup>	Ca <sup>2+</sup>	Mg <sup>2+</sup>	K <sup>+</sup>	Na <sup>+</sup>	Al <sup>3+</sup>
Initial cations	8.544	10.233	5.360	0.162	0.260
Total input	0.267				
Final #	0.004	0.002	0.040	0.017	0.002
solution phase					
Final #	1.473	0.793	1.352	0.067	0.500
exchange phase					
Total	0.008	9.900	8.970	3.720	0.028
output in effluent					0.017

Mixed-cation subsoil pH 4.9 (mmole(+))					
H <sup>+</sup>	Ca <sup>2+</sup>	Mg <sup>2+</sup>	K <sup>+</sup>	Na <sup>+</sup>	Al <sup>3+</sup>
Initial cations	8.544	10.233	5.360	0.162	0.260
Total input	0.024				
Final #	0.003	0.002	0.039	0.013	0.002
solution phase					
Final #	1.360	0.832	1.617	0.068	0.338
exchange phase					
Total	0.007	8.183	8.000	4.640	0.036
output in effluent					0.020

#: undetermined

Table 4-29 Charge balance of cations for columns of mixed-cation topsoil

Mixed topsoil pH 3.9 (mmole(+))						
	H <sup>+</sup>	Ca <sup>2+</sup>	Mg <sup>2+</sup>	K <sup>+</sup>	Na <sup>+</sup>	Al <sup>3+</sup>
Initial cations		1.894	2.413	2.265	0.222	1.114
Total input	0.253					
Final	#	0.026	0.020	0.022	0.012	0.607
solution phase						
Final	#	2.025	0.650	0.268	0.070	0.883
exchange phase						
Total	0.03	1.357	2.147	2.058	0.029	1.372
output in effluent						
Mixed topsoil pH 4.9 (mmole(+))						
	H <sup>+</sup>	Ca <sup>2+</sup>	Mg <sup>2+</sup>	K <sup>+</sup>	Na <sup>+</sup>	Al <sup>3+</sup>
Initial cations		1.871	2.385	2.238	0.220	1.101
Total input	0.026					
Final	#	0.024	0.029	0.024	0.009	2.282
solution phase						
Final	#	1.985	0.667	0.368	0.075	1.033
exchange phase						
Total	0.033	1.548	2.030	1.905	0.023	0.621
output in effluent						

#: undetermined

proportional to the  $H^+$  concentration of the applied solution for the mixed soil, but the application of pH 3.9 acid solution did increase the quantities of cations leached compared to the case where pH 4.9 solution was applied. Base saturation of cations was apparently decreased by acid application to the soil columns.

### Conclusions

The clay content of treated subsoil was 2.7-fold greater than for treated topsoil, but organic matter content was 1.6-fold greater for the topsoil than for the subsoil.

Exchange sites of pretreated Cecil subsoil gave equivalent fractions of 95 and 99 % saturation with respect to the major cation of saturation ( $K^+$ ,  $Ca^+$ , or  $Mg^{2+}$ ) in the cases of where exchangeable  $Al^{3+}$  was considered or not in the calculation of cation exchange capacity. For pretreated Cecil topsoil, however, equivalent fractions totalled 85 and 95% saturation with respect to the major cation of saturation ( $K^+$ ,  $Ca^{2+}$ , or  $Mg^{2+}$ ). Leaching of Cecil soil with unbuffered salt solution resulted in an increase in the cation exchange capacity of the soil.

All of the first few samples of effluent from soil columns that received HCl solutions were observed to have low pH but high concentrations of cations. This observation could be explained by the replacement efficiency of  $H^+$  for the cation-saturated sites as well as by a salt effect. Soil chemically pretreated with a given cation was observed to be more sensitive to the pH effect of the input solution

than untreated soil. Concentrations of the major saturating cation in the column effluent usually were not proportional to the  $H^+$  concentration of the applied input solution, though concentrations of major cations were usually higher in the effluent from columns receiving pH 3.9 solution as compared to columns receiving pH 4.9 solution. Cation concentrations in the solution and exchange phases of soil columns were in general as expected, with cation concentrations in the solution phase being in the order  $Na^+ > K^+ > Mg^{2+} > Ca^{2+}$ , whereas concentrations in the exchange phase were in the order  $Al^{3+} > Ca^{2+} > Mg^{2+} > K^+ > Na^+$ . Exceptions to these orders, however, were observed for some columns.

Although pretreatment of the soil eliminated much uncertainty with respect to chemical analysis, observed charge balances were larger between inputs and outputs for all of the pretreated and mixed soils. As HCl acid solutions were applied to the columns, several complicated soil chemical reactions occurred between the pH-independent exchange sites as well as between newly formed exchange sites and pH-dependent charge-surface sites. Further investigation of the effects of acid upon Cecil soil is needed in the future, in order to understand the mechanism and dissolution rate of interlayer vermiculite upon acid application. Addition of neutral salt during chemical treatment of the soil increased the exchange capacity of the soil, and subsequent application of HCl acid solution to the

treated soil tended to accelerate the leaching loss of nutrient cations ( $\text{Ca}^{2+}$ ,  $\text{Mg}^{2+}$ ) and induced the transformation of nonexchangeable Al to exchangeable  $\text{Al}^{3+}$ .

Acid deposition tended to adversely effect Cecil soil by decreasing its fertility status. Therefore, under forest conditions, fertilizer and lime application might be needed in the future to replace  $\text{Ca}^{2+}$  and  $\text{Mg}^{2+}$  leached from Cecil soil if prolonged acid precipitation occurs.

## CHAPTER V SUMMARY AND CONCLUSIONS

### Summary

Cecil (Typic Hapludult) soil was used in investigations of cation movement during steady displacement of electrolyte solution and of cation leaching during application of acid solutions under constant-flux conditions. Cecil soil was characterized as a highly weathered soil. The principal clay minerals in topsoil (0-30 cm depth) and subsoil (30-60 cm depth) were interstratified or interlayered vermiculite, kaolinite, and quartz. Gibbsite was found only in the subsoil. Topsoil and subsoil textures were classified as sandy loam and sandy clay loam, respectively. Organic matter (O.M) contents for topsoil and subsoil were 1.60 and 1.04%, respectively.

Studies of cation transport were conducted using columns filled with water-saturated Cecil topsoil or subsoil. Using a steady liquid flux of  $1 \text{ cm h}^{-1}$ , soil columns were initially saturated with  $\text{Ca}^{2+}$ , using  $0.005 \text{ M}$   $\text{CaCl}_2$ , and then miscibly displaced by  $0.005 \text{ M}$   $\text{MgCl}_2$  solution. After displacing 4.5 and 3.6 pore volumes of  $\text{MgCl}_2$  solution for topsoil and subsoil columns, respectively, the flow was terminated. Soil columns were equilibrated overnight, before dissection into sections the next day. Cations in the solution and exchange phases were

separated by a centrifuge method. In the solution and exchange phases, distributions of cation species and CEC varied with depth in the columns.  $\text{Al}^{3+}$  comprised about 25 and 50% of the total exchangeable cations in subsoil and topsoil columns, respectively. The large aluminum contents of the Cecil soil are possibly due to dissolution of interlayered vermiculite ( $\text{M}^+ (\text{Mg}, \text{Fe})_3 (\text{Si}, \text{Al})_4 \text{O}_{10} (\text{OH})_2$ ), and of hydrous Al oxides.

The  $\text{Mg}^{2+}$  exchange isotherm curve for the binary  $\text{Mg}^{2+} \rightarrow \text{Ca}^{2+}$  reaction was concave in shape and indicated that exchange sites in both the topsoil and subsoil preferred  $\text{Ca}^{2+}$  over  $\text{Mg}^{2+}$ . Average magnitudes of selectivity coefficients for the topsoil and subsoil were 0.225 and 0.798, respectively. Hydrodynamic dispersion coefficients obtained from experimental  $\text{Cl}^-$  breakthrough curves were  $1.85 \times 10^{-4}$  and  $3.03 \times 10^{-4} \text{ m}^2 \text{ h}^{-1}$ , respectively, for subsoil and topsoil columns.

A computer model was developed for predicting the transport and exchange of two cation species in Cecil soil columns. The model is based upon a Galerkin finite-element numerical solution of the convective-dispersive partial differential equation. The governing equation describes one-dimensional transport and binary exchange of cations under steady water flow through soil. The exchange term in the transport equation is treated as an explicit function of total solution concentration, cation exchange capacity, valence and cation concentrations in the solution phase.

The use of cubic spline functions as shape functions enabled employment of a Galerkin finite-element formulation over the spatial and time domain. The resulting ordinary differential equations were solved by a method based on backward differentiation formulation (Gear, 1969).

Verification of the numerical model was performed using an analytical model for nonreactive solute transport during miscible displacement, where the retardation factor ( $R$ ) is assumed to be unity. Verification was also performed for the case of non-preferential ion exchange with a selectivity coefficient equal to unity and cation-transport retardation  $R = 1 + [(\sigma \bar{C}_T)/(\theta C_T)]$ .

Sensitivity analyses for dispersion coefficient, volumetric water content, bulk density, selectivity coefficient and cation exchange capacity parameters were performed for the numerical model with respect to the experimental data from the columns of Cecil soil. Sensitivity analysis showed cation exchange capacity to be the most critical parameter in the model. Relatively small values of CEC gave the best simulations for measured cation-concentration distributions with depth in the solution and exchange phases. Use of CEC values obtained from 1  $\underline{M}$   $\text{NH}_4\text{OAc}$  extraction resulted in discrepancies between observed and predicted cation distributions within the columns.

Leaching of soil cations was investigated during displacement of acid solutions under constant liquid flux through columns of initially air-dry Cecil topsoil and

subsoil. Samples of Cecil topsoil and subsoil were treated with electrolyte solutions in order to saturate exchange sites with a single ( $K^+$ ,  $Ca^{2+}$ , or  $Mg^{2+}$ ) cation (treated soil). Mixed soils were obtained by mixing equal masses of  $K^+$ -,  $Ca^{2+}$ -, and  $Mg^{2+}$ - saturated soils. Packed soil columns used in these experiments were 10-cm long for nontreated soil, and 20-cm long for treated and mixed soils. Dilute aqueous HCl solutions of pH 3.9 or 4.9 were applied at  $1.0 \text{ cm h}^{-1}$  Darcy flux to separate air-dry soil columns, until approximately 30 pore volumes of effluent had been collected. Initially, liquid flow into the soil was transient as the wetting front moved through the unsaturated soil, and effluent outflow did not occur until the wetting front had reached the end of the column. Steady flow occurred after a short transition period.

For all columns, regardless of applied-solution pH, initial samples of effluent were characterized by low pH and high concentrations of basic ( $Ca^{2+}$ ,  $Mg^{2+}$ ,  $K^+$ ,  $Na^+$ ) and acidic ( $Al^{3+}$ ) cation species. These observations were attributed primarily to miscible displacement of soil solution originally present within small pores, and secondarily to the combined effects of removal of exchangeable cations by ion exchange with  $H^+$  ions, and release of cations by mineral hydrolysis, as the acid wetting front penetrated the initially air-dry soil column. With increasing volume of column effluent, cation concentrations dramatically decreased and pH increased up to

about 5 pore volumes of effluent for nontreated soil, 3 pore volumes for treated soil, and 3.5 pore volumes for mixed soils. Between 5 to 30 pore volumes, effluent pH was in the range of 6.0 - 6.5, but cation concentrations decreased in a gradual manner. The  $H^+$  ions were obviously removed from the soil solution at a fairly constant rate during the last 25 pore volumes of effluent as exchangeable cations were leached from the soil.

During application of pH 3.9 and 4.9 HCl solutions, the total quantities of basic cation eluted in effluent were 0.286 and 0.238 mmole(+), respectively, from columns of nontreated topsoil; 0.395 and 0.306 mmole(+), respectively, from nontreated subsoil; 4.204 and 2.207 mmole(+), respectively, from Ca-topsoil; 5.697 and 5.55 mmole(+), respectively, from K-topsoil; 9.917 and 4.221 mmole(+), respectively, from Mg-topsoil; 15.007 and 14.273 mmole(+), respectively, from Ca-subsoil; 11.360 and 7.002 mmole(+), respectively, from K-subsoil; 23.105 and 22.676 mmole(+), respectively, from Mg-subsoil; 22.626 and 21.066 mmole(+), respectively, from mixed subsoil; and 5.621 and 5.519 mmole(+), respectively, from mixed topsoil. Also, during application of pH 3.9 and 4.9 HCl solutions, total quantities of aluminum were 0.110 and 0.017 mmole(+), respectively, from nontreated topsoil; 0.001 and 0.001 mmole(+), respectively, from nontreated subsoil; 0.116 and 0.193 mmole(+), respectively, from Ca-topsoil; 2.910 and 2.518 mmole(+), respectively, from K-topsoil; 0.739 and

mmole(+), respectively, from Mg-topsoil; 0.012 and 0.071 mmole(+), respectively, from Ca-subsoil; 0.062 and 0.035 mmole(+), respectively, from Mg-subsoil; 0.015 and 0.010 mmole(+), respectively, from K-subsoil; 1.372 and 0.621 mmole(+) from mixed topsoil; and 0.017 and 0.020 mmole(+), respectively, from mixed subsoil. Therefore, the total leaching of basic cations in the effluent from the soil columns that received ten-fold different  $H^+$  concentrations differed by less than two-fold, indicating that, in addition to ion exchange, chemical reactions such as acid dissolution of soil minerals were important during the leaching process. Higher concentrations of  $Al^{3+}$  were observed in column effluent from nontreated topsoil than from nontreated subsoil, but the concentrations of  $Al^{3+}$  were very low for all chemically pretreated and mixed subsoil columns.

Distributions of cation concentrations on the exchange sites revealed that, during displacement of pH 3.9 acid solutions through the soil columns, base saturation decreased from 52 to 11% for nontreated topsoil; from 68 to 29% for nontreated subsoil; from 99 to 27% for K-subsoil; from 99 to 10% for Mg-subsoil; from 99 to 21% for Ca-subsoil; from 85 to 79% for Ca-topsoil; from 76 to 15% for K-topsoil; from 96 to 24% for Mg-topsoil; from 99 to 15% for mixed subsoil, and from 86 to 38% for mixed topsoil. During the period of pH 4.9 acid solution application, base saturation decreased from 52 to 12 % for nontreated topsoil;

from 68 to 35% for nontreated subsoil; from 99 to 31% for K-subsoil; from 99 to 11% for Mg-subsoil; from 99 to 21% for Ca-subsoil; from 85 to 80% for Ca-topsoil; from 76 to 16% for K-topsoil, 96 to 91% for Mg-topsoil, 99 to 16 % for mixed subsoil; from 86 to 40% for mixed topsoil. As expected, the distribution of cations on soil exchange sites followed the order  $\text{Al}^{3+} > \text{Mg}^{2+} > \text{Ca}^{2+} > \text{Mg}^{2+} > \text{K}^+ \approx \text{Na}^+$ , while for the solution phase the order was  $\text{Na}^+ > \text{K}^+ \approx \text{Ca}^{2+} > \text{Mg}^{2+} > \text{Al}^{3+}$ . The most significant response to input HCl solution occurred at the receiving end of the soil columns, where larger values of exchangeable  $\text{Al}^{3+}$  were observed. Base saturation drastically decreased for columns of soil which received pH 3.9 input acid solution. Columns of soil which were chemically pretreated showed a greater decrease in base saturation than did nontreated soil.

### Conclusions

In general, the numerical model for binary cation transport during steady liquid flow agreed very well with analytical solutions for simple cases. Experiments were performed to generate data for evaluating the predictive capacity of the numerical model. During steady liquid flow through water-saturated columns of Ca-saturated Cecil topsoil and subsoil, aqueous  $\text{MgCl}_2$  solutions were displaced through the columns. When the overall measured CEC values in the column were used as the input for the model, simulated results overestimated the distributions of cation concentrations in the columns. When the measured sum of

dominant basic cations was used as input CEC for the model, however, the numerical simulation result gave a reasonable prediction of the experimental data. The model proposed in this study was shown to approximate the cation transport and exchange processes during one-dimensional steady displacement through columns of Cecil soil.

A ten-fold difference in  $H^+$  concentrations of HCl solutions applied at constant flux to columns of nontreated, treated, and mixed Cecil soil resulted in a less than proportional difference in quantities of cations removed in the effluent. This difference was noted from  $H^+$  and cations added and recovered as a result of  $H^+$  interactions with and dissolution of soil minerals. Therefore, further investigation of effects of acid upon Cecil soil is needed to determine dissolution rates for interlayered vermiculite as well as for Al hydrous oxide, and for gibbsite.

Leaching of cations during acid application to Cecil soil columns under laboratory condition presents an extreme case compared to field conditions when periodic wetting and drying of soil during rainfall events limit cation exchange and transport with the water, and where cations released by the dynamic weathering of soil minerals tends to offset cation-leaching losses. The most deleterious effects of acid deposition on the soil would be those cases where the soil is of low CEC and of medium to high base saturation.

For most acid agricultural soils where lime and fertilizer are applied with relatively high frequency, the

effects of acid deposition are likely to go unnoticed. However, for certain forest soils, periodical fertilizer application may be needed in the future to minimize adverse effects of acid deposition upon soil fertility.

## REFERENCES

- Abrahamsen, G. 1980. Acid precipitation, plant nutrients and forest growths. p.58-63. In Ecology Impact of Acid Precipitation. D. Drablos and A. Tollan (eds.). The Norwegian Interdisciplinary Research Programme: Acid Precipitation-Effects on Forest and Fish, Oslo-As, Norway.
- Ahlberg, J.H., E.N. Nilson, and J.L. Walsh. 1967. Theory of Splines and Their Application. Academic Press., New York.
- Allison, L.E. 1965. Walkley-Black method. p.1372-1376. In Methods of Soil Analysis. Part 2. C.A. Black (ed.). American Society of Agronomy, Madison, WI.
- Babcock, K.L., and R.K. Schulz. 1963. Effect of anion on the sodium-calcium exchange in soil. Soil Sci. Soc. Am. Proc. 27:630-632.
- Bohn. H.L., B.L. McNeal, and G.A. O'Connor. 1985. Soil Chemistry, 2nd edition. Wiley-Interscience. New York.
- Bolt, G.H. 1967. Cation exchange equations in soil science: A review. Neth. J. Agric. Sci. 15:81-103.
- Brenner, H. 1962. The diffusion model of longitudinal mixing in beds of finite length: Numerical values. Chem. Eng. Sci. 17:229-243.
- Cassel, D.K. 1985. Physical characteristics of soils of the southern region: Summary of in-situ unsaturated hydraulic conductivity. Southern Cooperative Series, Bulletin 303, Regional Research Project S-124. North Carolina State University, Raleigh.
- Chatterjee, B., and C.E. Marshall. 1950. Studies in the ionization of magnesium, calcium and barium clay. J. Phys. Colloid. Chem. 54:671-681.
- Cho, C.M. 1985. Ionic transport in soil with ion-exchange reaction. Soil Sci. Soc. Am. J. 49:1379-1386.
- Cosby, B.J., R.F. Wright, G.M. Hornberger, and J. N. Galloway. 1985a. Modeling the effects of acid deposition: Assessment of a lumped-parameter model of soil water and streamwater chemistry. Water Resour. Res. 21:51-63.

- Cosby, B.J., R.F. Wright, G.M. Hornberger, and J.N. Galloway. 1985b. Modeling the effects of acid deposition: Estimation of long-term water quality responses in a small forested catchment. *Water Resour. Res.* 21:1591-1601.
- Day, P.R. 1965. Particle fraction and particle size analysis. p.552-562. *In* *Methods of Soil Analysis. Part 1.* C.A. Black (ed.). American Society of Agronomy, Madison, WI.
- Dixon, J.B., and S.B. Weed. 1977. *Minerals in the Soil Environment.* Soil Sci. Soc. Am, Madison, WI.
- Gaines, G.L., and H.C. Thomas. 1953. Adsorption studies on clay minerals: A formulation of thermodynamics of exchange-adsorption. *J. Chem. Phys.* 21:714-718.
- Gast, R.G. 1977. Surface and colloid chemistry. p.27-70. *In* *Minerals in the Soil Environment.* J.B. Dixon (ed.). Soil Sci. Soc. Am, Madison, WI.
- Gear, C.W. 1969. The automatic integration of stiff ordinary differential equations. p.187-193. *In* *Information Process.* A.J.H. Morrel. (ed.). North Holland Publishing Co., Amsterdam.
- Grim, R.E. 1968. *Clay Mineralogy.* McGraw-Hill, New York.
- Helferich, F.G. 1962. *Ion Exchange.* McGraw-Hill, New York.
- Helferich, F.G., and G. Klein. 1970. *Multicomponent Chromatography.* Marcel Dekker, Inc., New York.
- Hindmarsh, A.C. 1980. LSODE and LSODI, Two new initial value ordinary differential equation solvers. *ACM-SIGNUM Newsletter* 15:10-11.
- Hindmarsh, A.C. 1981. ODE solver for use with the method of lines. *In* *Advances in Computer Methods for Partial Differential Equations-IV.* R. Vichnevetsky, and R.S. Stepleman (eds.). IMASC. New Brunswick, N J
- Hindmarsh, A.C. 1983. ODEPACK. A systematized collection of ODE solvers. p.55-63. *In* *Scientific Computing.* R.S. Stepleman and M. Carver (eds.). IMACS. North-Holland Publishing Co., Amsterdam.
- Hsu, C.C. 1976. The use of splines for the solution of boundary-layer equations. Tech. Rep. AFFDL-TR-75-158. Air Force Wright Aeronautical Laboratories, WPAFB.
- Hsu, C.C., and A. Liakopoulos. 1981. A finite element-differential method for a class of compressible

- laminar boundary-layer flow. p.497-504. In Numerical Methods in Laminar and Turbulent Flow. C. Taylor and B.A. Schrefler (eds.). Pineridge Press, Swansea, UK.
- Hutchinson, T.C., and M. Havas. (eds.). 1980. Effects of Acid Precipitation on Terrestrial Ecosystems. Plenum, New York.
- Jennings, A.A., D.J. Kirkner, and T.L. Theis. 1982. Multicomponent equilibrium chemistry in groundwater quality models. Water Resour. Res. 18:1089-1096.
- Johnson, D.W., and D.W. Cole. 1980. Anion mobility in soil: Relevance to nutrient transport from forest ecology. Environ. Internat. 3:79-80.
- Johnson, D.W., J. Turner, and J.M. Kelly. 1982. The effects of acid rain on forest nutrient status. Water Resour. Res. 18:449-461.
- Keng, J.C.W., and G. Uehara. 1974. Chemistry, mineralogy and taxonomy of oxisols and ultisols. Soil Crop Sci. Soc. Fl. Proc. 33:119-126.
- Kissel, D.E., E.P. Gentzsch, and G.W. Thomas. 1971. Hydrogen of nonexchangeable acidity in soils during soil extractions of exchangeable acidity. Soil Sci. 111:293-297.
- Krishnamoorthy, C., and R. Overstreet. 1950. Behavior of hydrogen in ion-exchange reactions. Soil Science 69:87-93.
- Krug, E.C., and C.R. Frink. 1983. Acid rain on acid soil: A new perspective. Science 221:520-525.
- Krylov, V.I. 1962. Approximation calculation of integrals. Macmillan, New York.
- Lai, S.H., and J.J. Jurinak. 1971. Numerical approximation of cation exchange in miscible displacement through soil columns. Soil Sci. Soc. Am. Proc. 35:849-899.
- Lapidus, L., and N.R. Amundson. 1952. Mathematics of adsorption in beds: VI. The effect of longitudinal diffusion in ion exchange and chromatographic columns. J. Phys. Chem. 56:984-988.
- Mansell, R.S. 1983. Ion exchange coupled with convective-dispersive transport of cations during acid rain infiltration in soil: A review. p.256-264. In Acid Deposition: Causes and Effects. A.E.S. Green and W.H. Smith (eds.). Government Institute, Inc., Rockville, MD.

- Mansell, R.S., S.A. Bloom, H.M. Selim, and R.D. Rhue. 1986. Multispecies cation leaching during continuous displacement of electrolyte solutions through soil columns. *Geoderma* 38:61-75.
- McLean, E.O. 1965. Aluminum. p.978-998. *In* *Methods of Soil Analysis*. Part 1. C.A. Black (ed.). American Society of Agronomy, Madison, WI.
- McFee, W.W. 1980. Sensitivity of soil regions to long term acid precipitation. p.495-505. *In* *Atmospheric Sulfur Deposition: Environmental Impact and Health Effects*. D.S. Shriner, C.R. Richmond, and S.E. Linberg (eds.). Ann Arbor Science Publishers, Ann Arbor, MI.
- Mollitor, A.V., and D.J. Raynal, 1982. Acid precipitation and ionic movements in Adirondack forest soil. *Soil Sci. Soc. Am. J.* 46:137-141.
- Persaud, N., and P.J. Wierenga. 1982. A differential model for one-dimensional cation transport in discrete homoionic ion exchange media. *Soil Sci. Soc. Am. J.* 46:482-490.
- Pinder, G.F. 1973. A Galerkin finite-element simulation of ground-water contamination on Long Island, New York. *Water Resour. Res.* 9:1657-1670.
- Pinder, G.F. and W.G. Gray. 1977. *Finite Element Simulation in Surface and Subsurface Hydrology*. Academic Press, New York.
- Price, H.S., C.J. Cavendish, and R.S. Vangar. 1968. Numerical methods of higher order accuracy for diffusion-convection equations. *Soc. Petroleum Eng. Jour.* 8:293-303.
- Reiniger, P., and G.H. Bolt. 1972. Theory of chromatography and its application to cation exchange in soil. *Neth. J. Agric. Sci.* 20:301-313.
- Reuss, J.O. 1983. Implication of the calcium-aluminum exchange system for the effect of acid precipitation on soil. *J. Environ. Qual.* 12:591-595.
- Reuss, J.O., and D.W. Johnson. 1985. Effect of soil processes on the acidification of water by acid deposition. *J. Environ. Qual.* 14:26-31.
- Reuss, J.O., and D.W. Johnson. 1986. *Acid Deposition and Acidification of Soil and Water*. Springer-Verlag, New York.

- Rible, J.M., and L.E. Davis. 1955. Ion exchange in soil columns. *Soil Sci.* 79:41-47.
- Rubin, J., and R.V. James. 1973. Dispersion-affected transport of reacting solutes in saturated porous media: Galerkin methods applied to equilibrium-controlled exchange in unidirectional steady water flow. *Water Resour. Res.* 9:1332-1356.
- Sardin, M., R. Krebs, and D. Schweich. 1986. Transient mass-transport in the presence of non-linear physico-chemical interaction law: Progressive modeling and appropriate experimental procedures. *Geoderma* 38:115-130.
- Sposito, G. 1981. *The Thermodynamics of Soil Solutions.* Oxford University Press, New York.
- Thomas, G.W. 1982. Exchangeable cations. p.159-165. *In* *Methods of Soil Analysis. Part 2.* A.L. Page, R.H. Miller, and D.R. Keeney (eds.). American Society of Agronomy, Madison, WI.
- Thomas, G.W., and W.L. Hargrove. 1984. The chemistry of soil acidity. p.3-57. *In* *Soil Acidity and Liming.* F. Adams (ed.). American Society of Agronomy, Madison, WI.
- Thomas, H.C. 1944. Heterogeneous ion exchange in a flow system. *J. Am. Chem. Soc.* 66:1664-1666.
- Ulrich, B., R. Mayer, and P.K. Khanna. 1980. Chemical changes due to acid precipitation in a loess-derived soil in central Europe. *Soil Sci.* 130:193-199.
- Valocchi, A.J., R.L. Street, and P.V. Rolberts. 1981. Transport of ion-exchanging solutes in groundwater: Chromatographic theory and field simulation. *Water Resour. Res.* 17:1517-1527.
- van Beek, G.G.E.M., and G.H. Bolt. 1973. The relationship between the composition of the exchange complex and the composition of the soil solution. p.379-388. *In* *Physical Aspects of Soil Water and Salts in Ecosystems.* A. Hadas, D. Swartzendruber, P.E. Rijtema, M. Fuchs and B. Yaron (eds.). Springer-Verlag, New York.
- van Genuchten, M.Th. 1981. Non-equilibrium transport parameters from miscible displacement experiments. USDA Res. Report No. 119. U.S. Salinity Laboratory. Riverside, CA
- van Genuchten, M.Th., and W.J. Alves. 1982. Analytical solution of the one-dimensional convective-dispersive

solute transport equation. USDA Tech. Bull. 1661. U.S. Salinity Laboratory. Riverside, CA

van Genuchten, M.Th., and P.J. Wierenga. 1976. Mass transfer studies in sorbing porous media, I. Analytical solution. Soil Sci. Soc. Am. J. 40:473-480.

Whittig, L.D. 1965. X-ray diffraction techniques for mineral identification and mineralogical composition. p.671-698. In Methods of Soil Analysis. Part 1. C.A. Black (ed.). American Society of Agronomy, Madison, WI.

Wiklander, L. 1975. The role of neutral salts in the ion exchange between acid precipitation and soil. Geoderma 14:93-105.

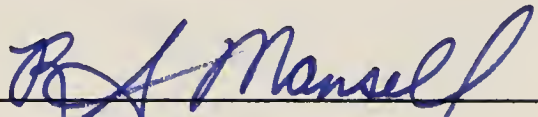
Wiklander, L., and A. Andersson. 1972. The replacing efficiency of hydrogen ion in relation to base saturation and pH. Geoderma 7:159-165.

## BIOGRAPHICAL SKETCH

Ko-Hui Liu was born on November 5, 1951, in Taichung, Taiwan, Republic of China. After graduating from high school she entered National Chung-Hsing University, Taichung, Taiwan, where she received her Bachelor of Science degree in 1974. She then taught high school in the city of Taipei. In the fall of 1979 she enrolled as a graduate student in the Department of Soil Science at the University of Florida. After receiving her Master of Science degree in 1982, she remained to perform graduate study toward the Ph.D. degree.

She is married to Ming-Hsinug Chen. She is a member of Gamma Sigma Delta, the Honor Society of Agriculture, and is also an associate member of Sigma Xi.

I certify that I have read this study and that in my opinion it conforms to acceptable standards of scholarly presentation and is fully adequate, in scope and quality, as a dissertation for the degree of Doctor of Philosophy.

A handwritten signature in blue ink, reading "R. S. Mansell", written over a horizontal line.

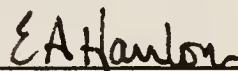
R. S. Mansell, Chairman  
Professor of Soil Science

I certify that I have read this study and that in my opinion it conforms to acceptable standards of scholarly presentation and is fully adequate, in scope and quality, as a dissertation for the degree of Doctor of Philosophy.

A handwritten signature in blue ink, reading "R. D. Rhue", written over a horizontal line.

R. D. Rhue  
Associate Professor  
of Soil Science

I certify that I have read this study and that in my opinion it conforms to acceptable standards of scholarly presentation and is fully adequate, in scope and quality, as a dissertation for the degree of Doctor of Philosophy.

A handwritten signature in blue ink, reading "E. A. Hanlon", written over a horizontal line.

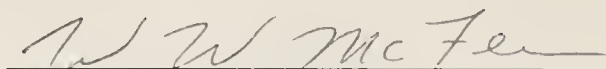
E. A. Hanlon  
Assistant Professor  
of Soil Science

I certify that I have read this study and that in my opinion it conforms to acceptable standards of scholarly presentation and is fully adequate, in scope and quality, as a dissertation for the degree of Doctor of Philosophy.

A handwritten signature in blue ink, reading "C. C. Hsu", written over a horizontal line.

C. C. Hsu  
Professor of  
Engineering Sciences

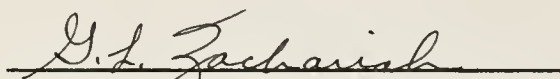
I certify that I have read this study and that in my opinion it conforms to acceptable standards of scholarly presentation and is fully adequate, in scope and quality, as a dissertation for the degree of Doctor of Philosophy.



W. W. McFee  
Professor of Soil Science

This dissertation was submitted to the Graduate Faculty of the College of Agriculture and to the Graduate School and was accepted as partial fulfillment of the requirements for the degree of Doctor of Philosophy.

August, 1987

  
Dean, College of Agriculture

---

Dean, Graduate School

UNIVERSITY OF FLORIDA



3 1262 08554 1612